Department of Medicine, Hematology

CENTRO DE INVESTIGACIÓN DEL CÁNCER – IBMCC

(USAL – CSIC)

VNiVERSiDAD D SALAMANCA

CAMPUS OF INTERNATIONAL EXCELLENCE

**DOCTORAL DISSERTATION**

# Characterization of novel genes and variants involved in Congenital Platelet Disorders: from the genomic data to the functional studies.

With the approval of the University of Salamanca, Department of Medicine, this thesis will be defended on 16th September 2022, in the Lecture Hall,

Centro de Investigación del Cáncer – IBMCC, Salamanca

Supervisors

Dr. José María Bastida Bermejo

Dr. José Ramón González Porras

Dr. Ignacio García-Tuñón Llanio

Tutor

Dr. Jesús María Hernández Rivas

**Ana Marín Quílez**

**2022**

CIC Centro de Investigación del Cáncer · VNiVERSiDAD D SALAMANCA · IBSAL Instituto de Investigación Biomédica de Salamanca · Hematología Hospital Universitario Salamanca

This doctoral thesis corresponds to a compendium of publications, consisting of the following articles:

Paper I: **Marín-Quílez A**, García-Tuñón I, Fernández-Infante C, Hernández-Cano L, Palma-Barqueros V, Vuelta E, Sánchez-Martín M, González-Porras JR, Guerrero C, Benito R, Rivera J, Hernández-Rivas JM, Bastida JM. Characterization of the Platelet Phenotype Caused by a Germline *RUNX1* Variant in a CRISPR/Cas9-Generated Murine Model. *Thrombosis and Haemostasis*. 2021;121(9):1193-1205. doi: 10.1055/s-0041-1723987. PMID: 33626581.

Paper II: **Marín-Quílez A**, Sanz D, del Rey M, Ordoñez JL, Diaz-Ajenjo L, González-Porras JR, Guerrero C, Pérez-Losada J, Rivera J, Hernández-Rivas JM, Benito R García-Tuñón I, Bastida JM. Expanding the role of germline *RUNX1* variants in leukemogenesis in a murine model generated by CRISPR/Cas9. *Manuscript in preparation.*

Paper III: **Marín-Quílez A**, Vuelta E, Díaz-Ajenjo L, Fernández-Infante C, García-Tuñón I, Benito R, Palma-Barqueros V, Hernández-Rivas JM, González-Porras JR, Rivera J, Bastida JM. A novel nonsense variant in *TPM4* caused dominant macrothrombocytopenia, mild bleeding tendency and disrupted cytoskeleton remodeling. *Journal of Thrombosis and Haemostasis.* 2022;20(5):1248-1255. doi: 10.1111/jth.15672. PMID: 35170221

Paper IV: **Marín-Quílez A**, Di Buduo CA, Díaz-Ajenjo L, Abbonante V, Vuelta E, Soprano P, Miguel-García C, Santos-Mínguez S, Serramito-Gómez I, Ruiz-Sala P, Peñarrubia MJ, Pardal E, Hernández-Rivas JM, González-Porras JR, García-Tuñón I, Benito R, Rivera J, Balduini A, Bastida JM. Novel variants in *GALE* cause syndromic macrothrombocytopenia by disrupting glycosylation and thrombopoiesis. *Blood, second revision.*

Scientific contribution during the thesis performed by Ana Marín Quílez:

1. Bastida JM, Morais S, Palma-Barqueros V, Benito R, Bermejo N, Karkucak M, Trapero-Marugan M, Bohdan N, Pereira M, **Marin-Quilez A,** Oliveira J, Yucel Y, Santos R, Padilla J, Janusz K, Lau C, Martin-Izquierdo M, Couto E, Ruiz-Pividal JF, Vicente V, Hernandez-Rivas JM, Gonzalez-Porras JR, Lozano ML, Lima M, Rivera J. Identification of novel variants in ten patients with Hermansky-Pudlak syndrome by high-throughput sequencing. *Annals of Medicine*. 2019;51(2):141-148. doi: 10.1080/07853890.2019.1587498

2. Bastida JM, Benito R, Lozano ML, **Marin-Quilez A,** Janusz K, Martin-Izquierdo M, Hernandez-Sanchez J, Palma-Barqueros V, Hernandez-Rivas JM, Rivera J, Gonzalez-Porras JR. Molecular diagnosis of inherited coagulation and bleeding disorders. *Seminars in Thrombosis and Hemostasis*. 2019;45(7):695-707. doi: 10.1055/s-0039-1687889

3. Palma-Barqueros V, Crescente M, de la Morena ME, Chan MV, Almarza E, Revilla N, Bohdan N, Miñano A, Padilla J, Allan HE, Maffucci T, Edin ML, Zeldin DC, Mesa-Nuñez C, Damian C, **Marín-Quilez A**, Benito R, Martínez-Martínez I, Bermejo N, Casas-Aviles I, Rodríguez-Alen A, González-Porras JR, Hernández-Rivas JM, Vicente V, Corral J, Lozano ML, Warner TD, Bastida JM, Rivera J. A novel genetic variant in *PTGS1* affects N-glycosylation of cyclooxygenase-1 causing a dominant-negative effect on platelet function and bleeding diathesis. *American Journal of Hematology*. 2021;96(3):E83-E88. doi: 10.1002/ajh.26076

4. Palma-Barqueros V, Revilla N, Sánchez A, Zamora-Cánovas A, Rodriguez-Alén A, **Marín-Quílez A,** González-Porras JR, Vicente V, Lozano ML, Bastida JM, Rivera J. Inherited Platelet Disorders: An Updated Overview. *International Journal of Molecular Sciences*. 2021;22(9):4521-4552. doi: 10.3390/ijms22094521

5. Palma-Barqueros V, Bury L, Kunishima S, Lozano ML, Rodriguez-Alen A, Revilla N, Bohdan N, Padilla J, Fernández-Pérez MP, de la Morena-Barrio ME, **Marín-Quílez A**, Benito R, López-Fernández MF, Marcellini S, Zamora-Cánovas A, Vicente V, Martínez C, Gresele P, Bastida JM, Rivera J. Expanding the genetic spectrum of *TUBB1*-related thrombocytopenia. *Blood Advances*. 2021;5(24): 5453-5467. doi: 10.1182/bloodadvances.2020004057

6. Palma-Baqueros V, Revilla N, Zaninnetti C, Galera AM, Sánchez-Fuentes A, Zamora-Cánovas A, Bohdan N, Padilla J, **Marín-Quilez A**, Rodriguez-Alen A, Fuster J, Greinacher A, Vicente V, Bastida JM, Rivera J, Lozano ML. Src-related thrombocytopenia - a fine line between a megakaryocyte dysfunction and an

immune-mediated disease. *Blood Advances*. 2022. doi: 10.1182/bloodadvances.2021005446

7. Fernández-González JF, García-Pedraza JA, **Marín-Quílez A**, Bastida JM, Martín ML, Morán A, García-Domingo M. Effect of sarpogrelate treatment on 5-HT modulation of vascular sympathetic innervation and platelet activity in diabetic rats. *Biomedicine & Pharmacotherapy.* 2022. doi: 10.1016/j.biopha.2022.113276

D. **José María Bastida Bermejo**, Doctor en Medicina por la Universidad de Salamanca, Médico Adjunto del Servicio de Hematología del Hospital Clínico Universitario de Salamanca e Investigador del Instituto de Investigación Biomédica de Salamanca

D. **José Ramón González Porras**, Doctor en Medicina por la Universidad de Salamanca, Médico Adjunto del Servicio de Hematología del Hospital Clínico Universitario de Salamanca e Investigador del Instituto de Investigación Biomédica de Salamanca

D. **Ignacio García-Tuñón Llanio**, Doctor en Biología por la Universidad de Alcalá e Investigador del Centro de Investigación del Cancer y del Departamento de Medicina de la Universidad de Salamanca

D. **Jesús María Hernández Rivas**, Doctor en Medicina, Catedrático del Departamento de Medicina de la Universidad de Salamanca, Médico Adjunto del Servicio de Hematología del Hospital Clínico Universitario de Salamanca, e Investigador del Centro de Investigación del Cáncer de Salamanca, **como tutor**

**CERTIFICAN**

Que **D.ª Ana Marín Quílez**, graduada en Bioquímica por la Universidad de Murcia, ha realizado bajo nuestra dirección el trabajo de Tesis Doctoral titulado "**Characterization of novel genes and variants involved in Congenital Platelet Disorders: from the genomic data to the functional studies**", y que reúne, a nuestro juicio, las condiciones de originalidad y calidad científica requeridas para su presentación y defensa ante el tribunal correspondiente para optar al grado de Doctor, con mención "Doctor Internacional" por la Universidad de Salamanca.

Y para que así conste a los efectos oportunos, firmamos el presente certificado en Salamanca, a 29 de junio de 2022.

Fdo:

Dr. José María Bastida Bermejo

Dr. José Ramón González Porras

Dr. Ignacio García-Tuñón Llanio

Dr. Jesús María Hernández Rivas

This thesis was performed being Ana Marín Quílez supported by “Ayudas para tesis doctorales en los grupos de investigación del Instituto de Investigación Biomédica de Salamanca 2018” (February 2019 – June 2019) and “Contratos predoctorales de la Junta de Castilla y León”, Fondo Social Europeo (JCYL- EDU/556/2019, Orden de 29 de octubre de 2018) (June 2019 – January 2023).

---

Acknowledgements:

- Fondo de Investigaciones Sanitarias (FIS) PI17/01966 and PI20/00926, Instituto de Salud Carlos III, European Regional Development Fund (ERDF) “Una manera de hacer Europa”.
- Proyectos de Investigación en Salud de la Fundación Mutua Madrileña (FMM) AP172142019.
- Proyectos de Investigación en biomedicina, gestión sanitaria y atención sociosanitaria del Instituto de Investigación Biosanitaria de Salamanca (IBSAL). IBY17/00006
- Proyectos de Investigación de la Consejería de Sanidad y Gerencia Regional de Salud de la Junta de Castilla y León (SACYL) GRS 1647/A/17, GRS 2061A/19, GRS 2135/A/2020 and GRS 2314/A/2021.
- Premio López Borrasca 2019 & Ayuda a Grupos de Trabajo en Patología Hemorrágica 2020-2021, Sociedad Española de Trombosis y Hemostasia (SETH-FETH).
- Ayudas para Breves Estancias Formativas 2021 Sociedad Española de Trombosis y Hemostasia (SETH-FETH).
- Ayuda Económica para Innovación Tecnológica 2021, Sociedad Española de Hematología y Hemoterapia (SEHH-FEHH).

---

# TABLE OF CONTENTS

**LIST OF ABBREVIATIONS** **1**

**LIST OF TABLES AND FIGURES** **3**

**INTRODUCTION** **5**

1. PLATELET FORMATION AND FUNCTION……..……..... 7

    1.1. Megakaryopoiesis and thrombopoiesis…….....…… 7

    1.2. Glycosylation and platelet clearance……..…….. 11

    1.3. Platelet function……...……...…….. 13

2. CONGENITAL PLATELET DISORDERS ……..……..…..… 15

3. MOLECULAR AND CLINICAL ASPECTS OF CONGENITAL PLATELET DISORDERS..……...……..……..…… 17

    3.1. Congenital Platelet Disorders associated to increased risk of bleeding…….……..…….…….. 17

    3.2. Congenital Platelet Disorders with neoplasm predisposition……. 19

    3.3. Syndromic Congenital Platelet Disorders...…….. 19

4. DIAGNOSIS OF CONGENITAL PLATELET DISORDERS……..… ……..22

    4.1. Platelet phenotyping assays……... 25

    4.2. Molecular diagnosis in the genomic era ..……...……. 27

        *4.2.1. Sanger Sequencing*……...…….. 27

        *4.2.2. Targeted-gene Sequencing*……..... 27

        *4.2.3. Whole Exome Sequencing*……..……..... 28

        *4.2.4. Whole Genome Sequencing*……..…… 29

        *4.2.5. Variant interpretation*…… ..……...……. 29

5. FUNCTIONAL CHARACTERIZATION OF CONGENITAL PLATELET DISORDERS…… 30

    5.1. *In vitro* approaches……... 31

5.2. *Ex vivo* approaches……33

5.3. *In vivo* approaches……35

5.4. Genome-editing technologies…… 36

**HYPOTHESIS** **39**

**AIMS** **43**

**RESULTS** **47**

- **CHAPTER 1.** **51**

  Characterization of the Platelet Phenotype Caused by a Germline *RUNX1* Variant in a CRISPR/Cas9-Generated Murine Model.

- **CHAPTER 2.** **71**

  Expanding the role of germline RUNX1 variants in leukemogenesis in a murine model generated by CRISPR/Cas9.

- **CHAPTER 3.** **93**

  A novel nonsense variant in *TPM4* caused dominant macrothrombocytopenia, mild bleeding tendency and disrupted cytoskeleton remodeling.

- **CHAPTER 4.** **103**

  Novel variants in *GALE* cause syndromic macrothrombocytopenia By disrupting glycosylation and thrombopoiesis.

**GENERAL DISCUSSION** **149**

**CONCLUDING REMARKS** **161**

**RESUMEN EN CASTELLANO** **167**

**REFERENCES** **261**

**SUPPLEMENTARY INFORMATION** **287**

# LIST OF ABBREVIATIONS

| | |
|---|---|
| **AA** | Arachidonic Acid |
| **ACMG/AMP** | American College of Medical Genetics and Genomics and the Association for Molecular Pathology |
| **ADP** | Adenosine diphosphate |
| **ALL** | Acute Lymphoblastic Leukemia |
| **AML** | Acute Myeloid Leukemia |
| **ClinGen** | Clinical Genome Resource |
| **CML** | Chronic Myeloid Leukemia |
| **CMP** | Cytidine-5'-monophosphate |
| **CNV** | Copy Number Variations |
| **CPDs** | Congenital Platelet Disorders |
| **CRISPR** | Clustered Regularly Interspaced Short Palindromic Repeats |
| **CRP** | Collagen-related peptide |
| **DSB** | Double Strand Break |
| **ESC** | Embryonic stem Cells |
| **FPD/AML** | Familial Platelet Disorder with predisposition to Acute Myelogenous Leukemia |
| **GP** | Glycoprotein |
| **HR** | Homologous Recombination |
| **HSC** | Human Stem Cell |
| **IL** | Interleukin |
| **HTS** | High-Throughput Sequencing |
| **IPFD** | Inherited Platelet Function Disorder |
| **iPSC** | Induced Pluripotent Stem Cell |
| **ISTH** | International Society on Thrombosis and Haemostasis |
| **ISTH-BAT** | ISTH bleeding assessment tool |
| **IT** | Inherited Thrombocytopenia |
| **KI** | *Knock-in* |
| **KO** | *Knock-out* |
| **LTA** | Light Transmission Aggregometry |
| **MAF** | Minor Allele Frequency |
| **MDS** | Myelodysplastic Syndrome |
| **Mk** | Megakaryocyte |
| **MPV** | Mean Platelet Volume |

| | |
|---|---|
| **NHEJ** | Non-Homologous End-Joining |
| **NMHC-II** | Nonmuscle myosin heavy chain II |
| **PF4** | Platelet Factor 4 |
| **Plt** | Platelet |
| **PMA** | Phorbol-12-myristate-13-acetate |
| **RD** | Related disorder |
| **RT** | Related thrombocytopenia |
| **sgRNA** | Single-guide RNA |
| **SS** | Sanger Sequencing |
| **SSC-GinTH** | Scientific and Standardization Committee on Genomics in Thrombosis and Hemostasis |
| **TALEN** | Transcription Activator-Like Effector Nucleases |
| **$TBXA_2$** | Thromboxane $A_2$ |
| **TPO** | Thrombopoietin |
| **UDP** | Uridine diphosphate |
| **VUS** | Variant of uncertain significance |
| **vWF** | Von Willebrand Factor |
| **WAS** | Wiskott-Aldrich syndrome |
| **WES** | Whole-exome Sequencing |
| **WGS** | Whole-genome Sequencing |
| **ZFN** | Zinc Finger Nucleases |

# LIST OF TABLES AND FIGURES

## INTRODUCTION

Table 1. General characteristics of the human cell lines that express megakaryocytic features..……32
Figure 1. Megakaryocyte differentiation and maturation ……..…… 8
Figure 2. Proteins involved in the megakaryocyte actomyosin cytoskeleton…...……10
Figure 3. Platelet O-linked and N-linked glycosylation and sialylation ..…….....12
Figure 4. Platelet adhesion and activation mechanisms……...……...……....14
Figure 5. Genes involved in Congenital Platelet Disorders…..……..16
Figure 6. Workflow algorithm for the diagnosis of Congenital Platelet Disorders ……..…….……...……24
Figure 7. The main types of DNA-sequencing used for the diagnosis of Congenital Platelet Disorders …..……29
Figure 8. *Ex vivo* megakaryopoiesis approaches……..…….…34
Figure 9. The nuclease genome editing technologies…….…37

## CHAPTER 1

Figure 1. Generation of the RUNX1 p.Leu56Ser murine model by the CRISPR/Cas9 genome editing system…….57
Figure 2. The RUNX1 p.Leu43Ser variant alters platelet hemostasis in mice.…….58
Figure 3. RUNX1 p.Leu43Ser variant impairs platelet activation of integrin αIIbβ3 and α-granule secretion……..58
Figure 4. RUNX1 p.Leu43Ser variant mice display impaired platelet aggregation with several agonists……...59
Figure 5. The deleterious effect of the RUNX1 p.Leu43Ser variant on platelet function is related to impaired PKC phosphorylation…….……..60
Figure 6. Platelets of RUNX1 p.Leu43Ser variant mice show impaired spreading……..61
Figure 7. The RUNX1 p.Leu43Ser variant displays normal collagen–platelet adhesion, but impaired fibrinogen binding……...……...62
Supplemental Tables and Figures……...……...……...…67

## CHAPTER 2

Figure 1. Characterization of hematopoietic cells in peripheral blood of RUNX1$^{WT/WT}$, RUNX1$^{WT/L43S}$, and RUNX1$^{L43S/L43S}$ mice……...78

Figure 2. Characterization of the aberrant cell population in bone marrow from Het#1, Hom#1, and Hom#2 mice ……..……...80
Figure 3. Characterization of the aberrant cell population in spleen from Het#1, Hom#1, and Hom#2 mice.…….81
Figure 4. RNA-seq revealed disrupted pathways related to changes in protein binding and immune system regulation, and the overexpression of Rapgef1 in the three affected mice with Mac1+ Sca1+ aberrant cells.…….....83
Supplemental Tables ……...……..……...…….....…91

**CHAPTER 3**

Figure 1. Molecular alteration and clinical and laboratory parameters of a family with tropomyosin-4 related macrothrombocytopenia (*TPM4*-RT)……..97
Figure 2. Platelet functional phenotyping performed by light transmission aggregometry and flow cytometry (propositus) and immunoblotting (all family members)……...98
Figure 3. Deleterious effect of p.Gln108* TPM4 variant in cytoskeleton remodeling…..99

**CHAPTER 4**

Table 1. Clinical and laboratory characteristics of 3 patients from the 2 unrelated families…….110
Figure 1. Patients carrying *GALE* variants showed giant and/or grey platelets in blood films and impaired granules secretion……..111
Figure 2. *GALE* variants associated with reduced GALE protein levels, impaired enzymatic activity, platelet hypoglycosylation, and increased apoptosis……..……...113
Figure 3. Immunoblotting of platelet lysates revealed severely reduced levels of GPIbα and glycosylated β1 integrin…….…..…….115
Figure 4. Characterization of *GALE* expression among the megakaryopoiesis…….117
Figure 5. Megakaryocyte culture from proband carrying GALE p.Val128Met and p.Leu223Pro variants showed normal polyploidization and maturation but impaired proplatelet formation…...……..…….118
Figure 6. Carrier of GALE p.Val128Met and p.Leu223Pro variant displayed vWF delocalization within the megakaryocyte membrane……..……120
Figure 7. Megakaryocytes from proband carrying p.Val128Met and p.Leu223Pro variant show impaired GPIbα and β1 glycosylation and externalization…….121
Supplemental Tables and Figures……....…….……...……...139

# INTRODUCTION

# 1. PLATELET FORMATION AND FUNCTION

## 1.1 Megakaryopoiesis and thrombopoiesis

Megakaryopoiesis is the process in which human stem cells [HSCs] differentiate and proliferate, giving rise to mature megakaryocytes [Mks].[1] According to the classical model of hematopoiesis, HSC sequentially transition through multipotent progenitors will give rise to immature Mks or megakaryoblasts, which undergo endomitosis to increase their size and DNA content, during the process called polyploidization, but also increasing their reservoir of granules and cytoskeletal proteins to develop the demarcation membrane system.[2,3] Therefore, mature Mks start to shed their cytoplasm, a complex process that requires the formation of elongated structures called proplatelets, which lead to the platelet formation and the release intro bloodstream. This terminal process is known as thrombopoiesis (Figure 1A).[4]

The processes of HSCs differentiation, Mk maturation and proplatelet formation are regulated at multiple levels by many different cytokines and environmental factors.[5] Thrombopoietin [TPO] is the major regulator of megakaryopoiesis and thrombopoiesis and, in combination with other cytokines, such as IL-3 or IL-11, modulates all stages of Mk development (Figure 1A).[6,7]

Several surface glycoproteins [GP] appeared at different stages of the megakaryopoiesis, and they are commonly used as lineage specific markers, such GPIIb/IIIa (CD41-CD61 markers) or GPIb-IX-V (CD42a-d).[8] CD34 is express only in HSC and multipotential progenitors, being nearly absent in the immature Mks. CD41-CD61 are express since early megakaryopoiesis, as well as CD29, the β1 integrin marker, while CD42a-d or GPVI appear during late-megakaryopoiesis (Figure 1A).[9,10]

However, recent studies have begun to redefine this hierarchy, which has traditionally been determined by the surface markers, highlighting alternative routes by which HSCs are differentiated into Mks (Figure 1B).[1,5] First, the multipotential population has been further characterized to include several subsets of lineage progenitors. It has also been defined that late HSCs are capable of unilaterally differentiating into Mks. Finally, the existence of a common progenitor capable of producing erythroblasts and megakaryoblast is

controversial, and new technologies have shown that this multipotent progenitor is transient and difficult to detect in native hematopoiesis.[11–14]

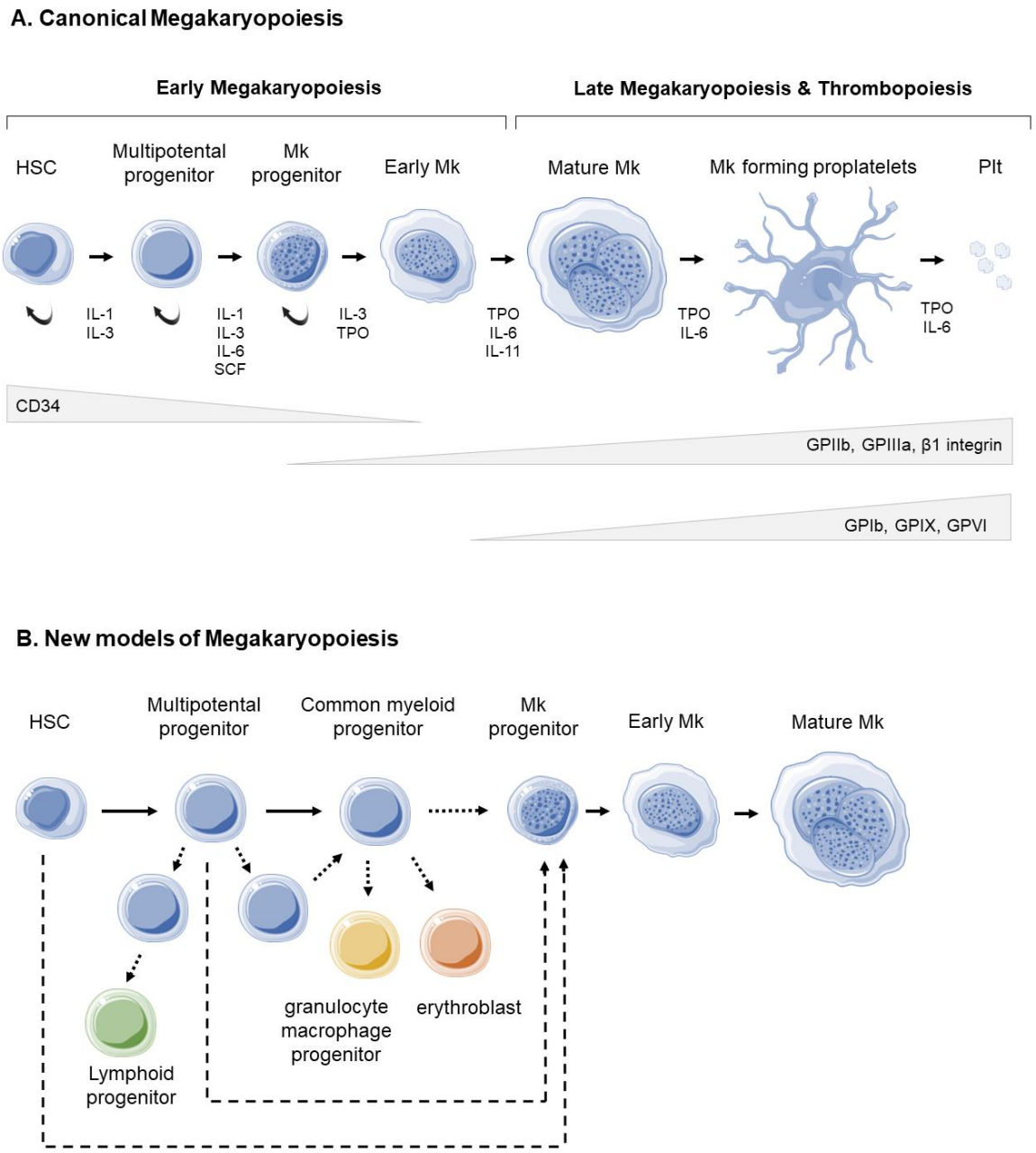


**Figure 1. Megakaryocyte differentiation and maturation. A.** Canonical model of megakaryopoiesis. Expression of the most relevant surface markers and growth factors and cytokines involved in each stage. **B**. New models proposed for megakaryopoiesis, pointing out alternative routes by which HSCs differentiate into Mks. Adapted from:[1,15] Created with Servier Medical Art (https://smart.servier.com/).

The proper development of hematopoiesis, and Mk differentiation and maturation is under control of crucial transcriptional factors, which bind to the promoters, acting either as repressors or activators depending on their association with other transcriptional factors. *GATA1* controls the expression of GPIIb, while *FLI1* regulates GPIbα and GPIX.[1,16–18] Moreover, *RUNX1* regulates embryonic and definitive human hematopoiesis through CBFβ dimerization,[19] and plays an essential role in the maturation and differentiation of myeloid, lymphoid, and megakaryocytic lineage.[20,21] In fact, RUNX1 biallelic loss of function results in embryonic lethality due to the failure of hematopoiesis.[22]

Cytoskeleton proteins have a crucial role in the late-megakaryopoiesis and proplatelet formation.[23,24] During the initial stages of proplatelet formation, Mks remodel their cytoplasm into pseudopodia by a process based on microtubules, specially β1 tubulin (encoded by *TUBB1* gene),[25,26] and the actomyosin cytoskeleton.[27,28] The actin cytoskeleton is critical for the demarcation membrane system formation, as it provides mechanical forces that drive invaginations at the plasma membrane, leading to the formation of proplatelets,[29] while the tubulin cytoskeleton guides proplatelet shaft initiation and elongation.[30]

The actomyosin cytoskeleton comprise multiple proteins that establish a link between different cytoskeleton-driven cellular responses.[31] Association of filamentous β-actin with the demarcation membrane system is crucial before proplatelet emission.[24,29] Actin polymerization is powered by the actin-related protein 2/3 (Arp2/3). The Arp2/3 complex displays low intrinsic actin nucleation activity and needs to be activated by proteins such as Wiskott–Aldrich syndrome protein (WASP) (Figure 2).[32]

Several actin-binding proteins are critical regulators of the Mk function, and most of them are involved in the complex generation of the proplatelets.[33] α-Actinin is a member of the actin-crosslinking protein superfamily that contributes to this process by crosslinking actin filaments into bundles.[34] Tropomyosin-4, encoded by *TPM4*, is a coiled-coil dimer protein that lies end-to-end in the actin groove, and provides structural stability to actin filaments and regulates the access of other proteins that bind to actin.[35] Tropomyosins are implicated in the regulation of cell morphology, adhesion, migration, granule trafficking, cell division, and apoptosis.[27] Meanwhile, filamin-A is a multidomain cytoskeletal

protein that stabilizes the membranes subjected to shear stress and promotes the cellular adhesion by linking membrane glycoproteins, mainly the GPIb-V-IX receptor, to the actin cytoskeleton (Figure 2).[36]

Mk migration depends on the interaction of nonmuscle myosin II with the actin cytoskeleton. Two types are expressed in Mks: nonmuscle myosin heavy chain II-A (NMHC-IIA, *MYH9*) and nonmuscle myosin heavy chain II-B (NMHC-IIB, *MYH10*).[37] NMHC-IIA is required for maintaining cell shape and organizing cell cytoplasm, linking to the filamentous actin to help actin turnover during proplatelet formation (Figure 2).[24,38] On the other hand, NMHC-IIB is expressed in immature Mks, where it accumulates on the contractile ring in endomitosis transition. NMHC-IIB expression is downregulated by RUNX1 through *MHY10* gene silencing during Mk polyploidization. This process is essential for switching from mitosis to endomitosis to increase the ploidy level during Mk differentiation.[39,40] In fact, RUNX1 has also been described as a direct regulator of *MYL9*, which codifies for the myosin light chain, playing a crucial role in the regulation of the NMHC-IIA activity by reversible phosphorylation of specific amino acids.[41]

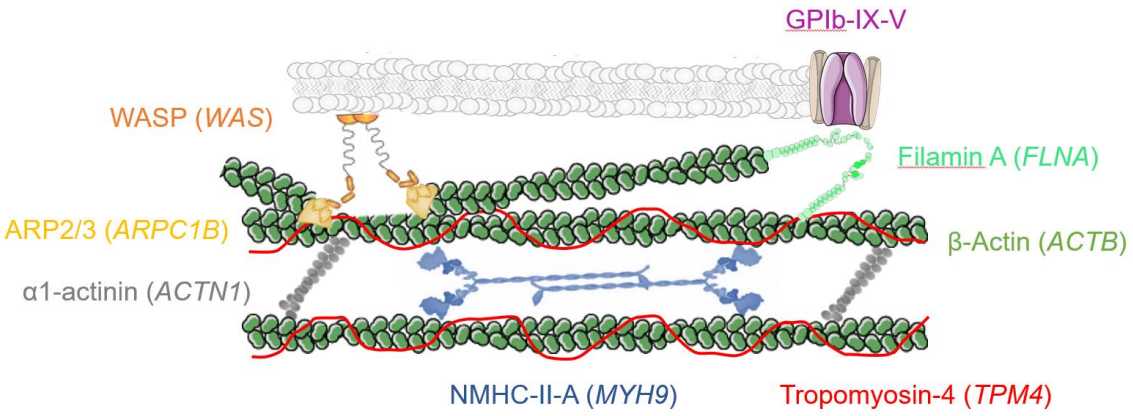


**Figure 2. Proteins involved in the megakaryocyte actomyosin cytoskeleton.** Filamentous β-actin is organized in a branched network. The ARP2/3 complex, controlled by the WASP, among other proteins, initiates branching of actin filaments. Tropomyosin-4, α1-actinin 4 and myosin II filaments bind along F-actin, controlling the tension generated by the actomyosin network and the structural organization. Filamin-A links membrane glycoproteins to the actin cytoskeleton. Created with Servier Medical Art (https://smart.servier.com/).

### 1.2 Glycosylation and platelet clearance

Protein glycosylation, and the linked sialylation, are common and complex post-translational modifications, with a critical role in different biological processes such as protein clearance.[42] The conjugation of carbohydrate moieties onto specific molecules and receptors is critical for normal hematopoiesis, since it favor proliferation and clearance of hematopoietic precursors. Through this mechanism, circulating platelet counts are under control by the dual balance of platelet production rate by Mks and the removal kinetics.[43,44]

Platelets have a half-life in blood ranging from 8 to 11 days, after which they lose the final sialic acid, and they turned apoptotic and subsequent phagocyted by macrophages.[45] Those platelet without sialic acid are recognized by receptors in the liver, thus acting as a signal to increase TPO levels, which induce megakaryopoiesis to produce new platelets.[46] In fact, it has been described that mice with genetic deficiencies in sialylation presented low platelet counts in bloodstream,[47,48] demonstrating that platelets without sialic acid are prone to clearance.[49]

Several enzymes are responsible for the proper glycosylation and sialylation. *GALE* gene encodes the uridine diphosphate [UDP]-galactose-4-epimerase, which catalyzes the bidirectional interconversion of UDP-glucose to UDP-galactose, and UDP-N-acetyl-glucosamine to UDP-N-acetyl-galactosamine (Figure 3). In this way, *GALE* balances, through reversible epimerization, the pools of the four sugars essential during the biosynthesis of glycoproteins and glycolipids.[50,51] Conversely, *GNE* gene codifies for the UDP-N-acetylglucosamine 2-epimerase, involved in the sialic acid biosynthesis. This bifunctional enzyme regulates the total levels of N-acetylneuraminic acid, a precursor of sialic acids, while *SLC35A1* encodes the cytidine-5'-monophosphate [CMP]-sialic acid transporter that transports CMP-sialic acid from the nucleus into the Golgi apparatus for sialylation (Figure 3).[44,52,53]

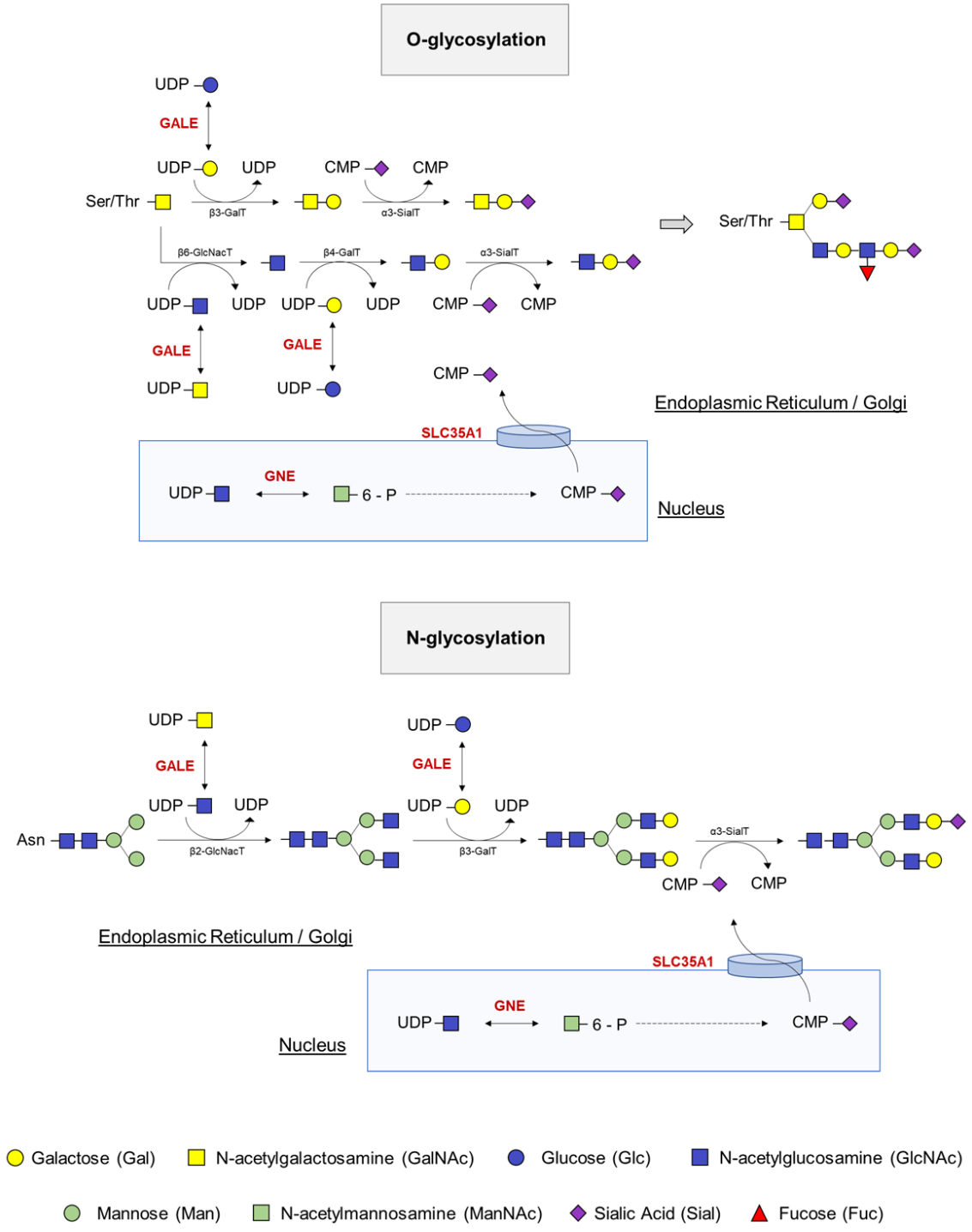


**Figure 3. Platelet O-linked and N-linked glycosylation and sialylation.** GALE protein allows the interconversion of four molecules essential in the glycosylation process, by serving as substrates for other enzymes incorporating the carbohydrates of interest and releasing UDP. Branches of carbohydrates are produced during glycosylation. A final sialic acid cleavage prevents platelet for clearance. GNE and SLC35A1 are involved in pathway that allows the incorporation of this sialic acid into the platelet.

### 1.3 Platelet function

Under physiological conditions, platelets circulate in blood in quiescence without interacting with the endothelium. After an injury that compromise the integrity of the vessel wall, platelets interact with extracellular matrix components, during a process called adhesion.[54,55] The adhesion mainly involves integrin-like membrane receptor, or glycoproteins that specifically binds to matrix components such fibrinogen, collagen, fibronectin, laminin, and/or von Willebrand Factor [vWF], which activate downstream signaling pathways linked to Src kinases.[56,57]

GPVI immunoglobulin and the α2β1 integrin are the two mainly receptors in the platelet surface that bind directly to collagen after damage.[58,59] vWF, which is found soluble in blood in the normal circulation to prevent aggregation, changes its affinity, interacting thus with the GPIb-IX-V complex.[60–62] Meanwhile, α5β1 and α6β1 integrins binds to fibronectin and laminin, respectively, which are also exposure after vessel damage (Figure 4).[63,64]

After a platelet monolayer binding over the exposed matrices, the next step required for thrombus formation is the recruitment of additional platelets. Activated platelets secrete soluble agonists, such as thromboxane $A_2$ [$TBXA_2$] or adenosine diphosphate [ADP], into the circulation,[56,65] which stimulate adjacent platelets, triggering their activation by specific binding of the molecules into their specific receptor (mainly G-protein coupled transmembrane receptors) such as ADP binding to $P2Y_1$ and $P2Y_{12}$ receptors, or thrombin that binds to PAR1 and PAR4, among others (Figure 4).[66–68]

Soluble components such as ADP or vWF are mainly stored in platelet granules. The α-granules are rich in peptides and proteins, like PF4, P-selectin, vWF or fibrinogen, while δ-granules are rich in soluble molecules such as ADP, ATP, $Ca^{2+}$, or serotonin.[69–71] The final step is the activation of the GPIIb/IIIa, also known as αIIbβ3 integrin. The conformational change produced after the activation lead to the fibrinogen-binding, allowing the formation of stable bridges between platelets (Figure 4). The interaction of platelet-fibrinogen-platelet initiates the process of platelet aggregation.[72–74]

The agonist-stimulation lead to the sequential activation of one or more PLC isoforms, activating PKC and yielding a rise in cytosolic $Ca^{2+}$, which activates the

CalDAG-GEF1 signaling pathway, leading to the reorganization and activation of cytoskeletal platelet proteins, and promoting a shift in the platelet shape. Activation of both PKC and CalDAG-GEF1 signaling pathways lead to final activation of RAP1. These processes are group in the outside-in signaling pathway.[75,76] The last step is the activation of αIIbβ3 integrin by RAP1, known as inside-out signaling, which trigger essential events for thrombus growth and stabilization, such as cytoskeletal reorganization, formation and stabilization of large platelet aggregates, and the final clot retraction (Figure 4).[70,77]

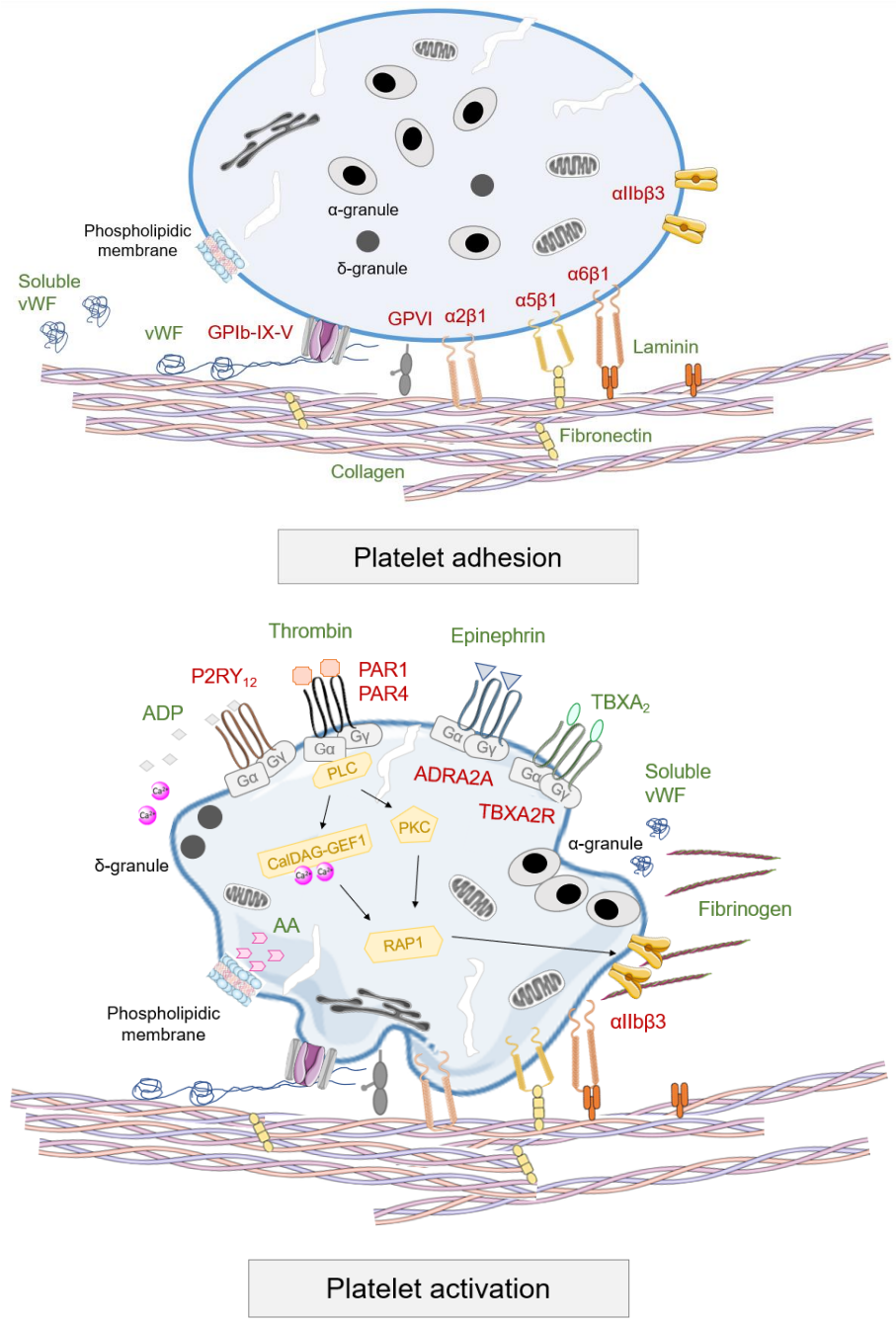

**Figure 4. Platelet adhesion and activation mechanisms.** During platelet adhesion, the main extracellular matrix components, such as collagen, fibronectin, laminin and vWF (green) bind to their corresponding platelet membrane receptors (red). During platelet activation, the main soluble agonists (green) bind to the relative receptors (red). Granule's secretion and the crucial proteins involved in the platelet activation pathway are shown. Created with Servier Medical Art (https://smart.servier.com/).

## 2. CONGENITAL PLATELET DISORDERS

Congenital Platelet Disorders [CPDs] comprise an heterogenous group of rare diseases caused by molecular alterations in genes that are essential for platelet formation and/or function.[78] The prevalence of CPDs is unknown, but it is estimate to affect 1 individual between 1.000-100.00, being recognized more frequently in the last few years.[79,80] To date, the International Society on Thrombosis and Haemostasis [ISTH] stablished that CPDs are caused by molecular alterations in 66 different genes, which are classified as Tier1 genes (Figure 5).[81,82] Genes are considered Tier1 for CDPs whether the gene-disease association had been reported in at least three independent pedigrees, or less than three pedigrees but supported by linkage analysis in large pedigrees, and specific functional data or a murine model. Indeed, 7 genes are consider as Tier2, recently discovered in small single pedigrees, and still requiring confirmation studies (Figure 5).[81,83]

In general terms, CPDs are classified as:

- Inherited Thrombocytopenias [ITs]: disorders related with low platelet counts (< 150 x $10^9$ plt/L) in bloodstream. ITs could be associated with decreased, normal, or enlarged platelet size, measure as the mean platelet volume [MPV], which lead to microthrombocytopenia (MPV < 7.2 fL), thrombocytopenia (MPV: 7.2-11.1 fL), or macrothrombocytopenia (MPV > 11.1 fL), respectively. ITs are mainly caused by alterations in genes involved in megakaryopoiesis, thrombopoiesis, and platelet release and clearance.[84–86]

- Inherited Platelet Function Disorders [IPFDs]: disorders characterized by impaired platelet functionality due to defects in membrane receptors, signaling proteins, alpha (α) and/or dense (δ) granules, maintenance of the platelet

ultrastructure, or other alterations in the platelet activation mechanisms after agonist stimulation.[87,88]

Several disorders display a combination of thrombocytopenia with variable platelet dysfuction.[85] Increased risk of bleeding is the major and common characteristic of these disorders, and its relevance depends on the degree of thrombocytopenia and the concomitant association of significant platelet dysfunction.[89] The relevance of clinical complications is highly variable, even for the same disorder, ranging from almost negligible to life-threatening bleeding.[90] Moreover, it is currently well established that many CPDs evolve with the development of other serious congenital defects affecting different organs or additional diseases, including hematological malignancies, bone marrow failure, or non-hematological defects (Figure 5).[91,92]

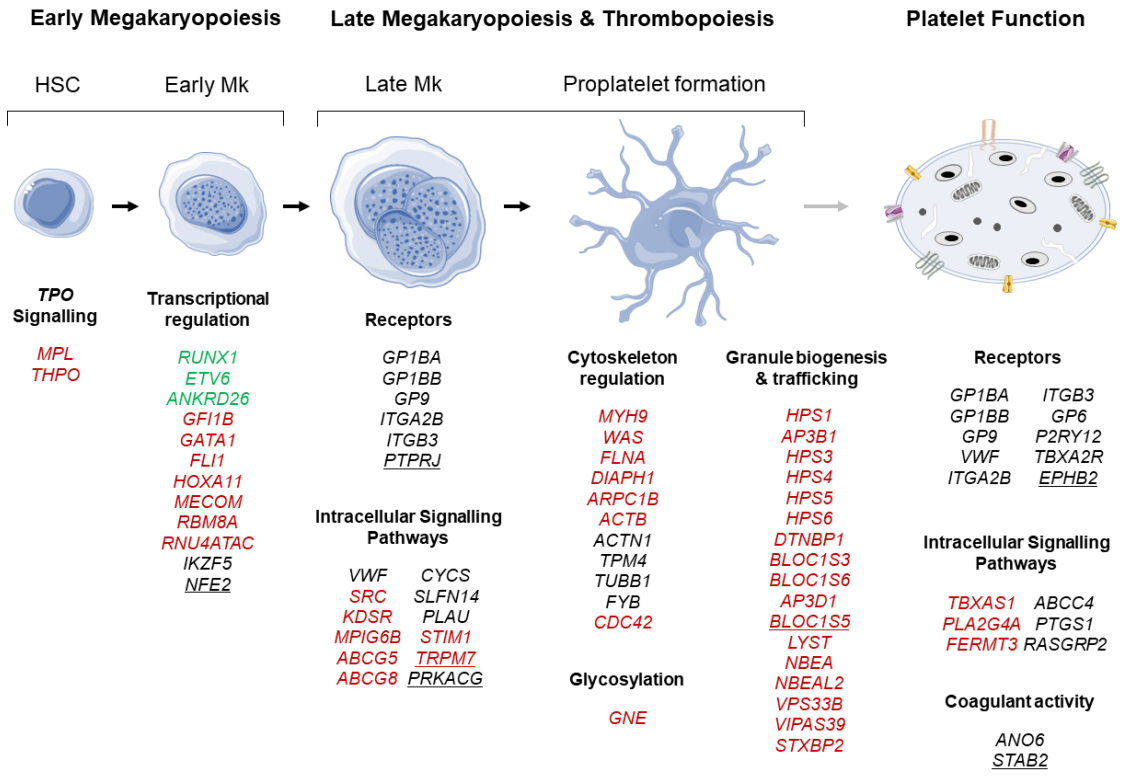


**Figure 5. Genes involved in Congenital Platelet Disorders.** Classification of Tier1 and Tier2 (underlined) genes according to the gene function during megakaryopoiesis, thrombopoiesis, or platelets in bloodstream. Green indicates genes with predisposition to develop leukemias. Red indicates genes associated to syndromic manifestations. Adapted from:[82,93] Created with Servier Medical Art (https://smart.servier.com/).

## 3. MOLECULAR AND CLINICAL ASPECTS OF CONGENITAL PLATELET DISORDERS

Congenital Platelet Disorders [CPDs] associates with a wide heterogeneity of clinical phenotypes, since patients with alterations in different genes could exhibit the same phenotype, while other individuals with molecular alterations in the same gene can displayed different phenotype.[89] CPDs usually associate with mild to moderate mucocutaneous bleeding, such as epistaxis or menorrhagia, and excessive blood loss after trauma, surgery, pharmacological treatments, or delivery. In severe cases, significant diathesis can be diagnosed in the central nervous system or gastrointestinal bleeding.[94–96] Although alterations in several genes are only associated with increased bleeding, other CDPs predispose to hematological malignancies, or multisystem disorders, such as sensorineural deafness, renal failure, or cataracts, among others (Figure 5).[92,93,97]

Some CPDs of clinical relevance are next briefly described, including disorders with a high bleeding degree and several syndromic disorders. General clinical aspects associated with disorders caused by variants in all Tier1 genes (ISTH-SSC 2021) can be found in the supplementary material.

### 3.1. Congenital Platelet Disorders associated to increased risk of bleeding

- Glanzmann Thrombasthenia

Glanzmann Thrombasthenia is an autosomal recessive disorder caused by pathogenic variants affecting *ITGA2B* or *ITGB3* genes, abrogating the GPIIb/IIIa complex (αIIbβ3 integrin). The disorder is rarely associated with thrombocytopenia, but patients display severe to life-threatening bleeding. Platelet function is usually affected due to impaired αIIbβ3 integrin activation, leading to severely reduced fibrinogen-binding and aggregation.[98,99]

Monoallelic variants in these genes caused the *ITGA2B* / *ITGB3*-related thrombocytopenia [RT], a disorder characterized by slight-mild thrombocytopenia and mild bleeding tendency. Platelet function is rarely affected.[100]

- Bernard Soulier Syndrome

Bernard Soulier Syndrome is related with pathogenic variants affecting *GP1BA, GP1BB* or *GP9,* disrupting the formation of the GPIb-IX-V complex. General forms of the disorder are related with biallelic abrogation of the genes, and the phenotype is characterized by severe bleeding tendency and moderate thrombocytopenia with giant platelets. Platelet function is impaired after stimulation with vWF, as well as platelet and Mk adhesion to this matrix.[101–103]

Heterozygous variants of *GP1BA* and *GP1BB* cause a mild form of the disease, known as Mediterranean thrombocytopenia, and it used to be associated with slight thrombocytopenia and nearly absent to mild bleeding diathesis.[104,105]

- Cytoskeleton proteins alterations

*ACTN1*, *TUBB1*, and *TPM4*-related thrombocytopenias are autosomal dominant disorders with similar phenotypes. They usually present mild thrombocytopenia with enlarged platelets, and moderate to nearly absent bleeding tendency. Platelet dysfunction is not commonly found but they used to be associated with alterations in the platelet cytoskeleton remodeling after activation with several agonists.[26,34,106–109]

- Platelet signaling pathway defects

*P2RY12, TBXA2R* and *GP6* genetic variants associates with normal platelet count and morphology, and mild to moderate bleeding tendency, usually after the administration of anticoagulants. *P2RY12* and *TBXA2R* variants could be inherited both as an autosomal dominant and recessive manner, while *GP6* deficiency had an autosomal recessive pattern. Platelet function is impaired after stimulation with ADP, $TBXA_2$ and collagen, respectively.[110–112]

*RASGPR2* codifies for CalDAG-GEF1, involved in the RAP1-signaling pathway during platelet activation (Figure 4). Disease-causing variants in homozygosis associates with severe bleeding due to impaired activation of the αIIbβ3 integrin.[113]

### 3.2. Congenital Platelet Disorders with neoplasm predisposition

The World Health Organization (WHO) 2016 classification incorporated the germline monoallelic variants in the transcriptional factors *RUNX1, ETV6* and *ANKRD26* as a new entitle subgroup: Inherited Myeloid Neoplasm associated with platelet disorder.[114,115]

*RUNX1-r*elated disorder [RD], or familial platelet disorder with predisposition to acute myelogenous leukemia [FPD/AML] has been associated with slight to moderate bleeding disorder, variable thrombocytopenia with normal platelet size, impaired platelet function, and increased risk to develop leukemias: 45% of risk to acute myeloid leukemia [AML] or myelodysplastic syndrome [MDS], and 1-3% to develop T-acute lymphoblastic leukemia [ALL]. The average age is 33 years old (range; 6-76 years old).[116,117]

Patients with *ETV6*-RD and *ANKRD26*-RD displayed a slight-mild bleeding diathesis, variable thrombocytopenia with normal platelet morphology, and usually normal platelet function. Around the 25% of patients with *ETV6*-pathogenic variants develop ALL during the childhood, while 5-10% of patients suffer from AML, MDS, multiple myeloma, or polycythemia vera. Patients with *ANKRD26*-RD develop AML or MDS at the average age of 35 years old (range; 6-93) in the 5-10% of the cases.[118,119] Pathogenic variants in *ANKRD26* are mostly found in the 5'UTR region.[120]

### 3.3 Syndromic Congenital Platelet Disorders

- Congenital amegakaryocytic thrombocytopenia

The autosomal recessive disorder is caused by biallelic variants in the gene *MPL*, which codifies for the receptor of the TPO. Patients with this disorder displayed lifelong hypomegakaryocytic thrombocytopenia, progressing from cytopenia during the first years of life to medullar aplasia. Patients suffer frequently from severe bleeding diathesis.[121,122] Currently, treatment with TPO analogues has been demonstrated as a promising therapy for the patients.[123,124]

- Transcriptional factors defects

In general, syndromic Congenital Platelet Disorders associate with transcriptional factors with essential roles during the differentiation of HSC to progenitors, and genes involved in early megakaryopoiesis, such as *GATA1* or *FLI1.*[85]

*GATA1*-RD is an X-linked disease characterized by mild-moderate thrombocytopenia with dysplastic Mks, with variable degree of anemia, and frequent β-thalassemia, neutropenia, and or congenital erythropoietic porphyria. Bleeding diathesis is moderate, associated with impaired platelet function and defects in platelet granules.[125,126]

*FLI1*-RD could have an autosomal dominant or recessive inheritance patter. Patients display mild to moderate thrombocytopenia and bleeding tendency, and facial, cardiac, and neurological malformations.[127]

- Cytoskeleton proteins alterations

*MYH9* codifies for the nonmuscle myosin heavy chain II-A. *MYH9*-related disorder is the most common inherited thrombocytopenia, since more than 300 families and up to 100 different pathogenic variants in the *MYH9* gene have been described. *MYH9*-RD is inherited in an autosomal dominant manner, but approximately 35% of probands have a *de novo* pathogenic variant during gestation in utero.[128] Clinical phenotype associates with mild to moderate bleeding, severe macrothrombocytopenia, and neutrophilic inclusions, known as Döhle bodies. Moreover, half percent of patients present neurosensorial deafness, and the 20-25% develop nephropathies and/or cataracts.[129,130]

Wiskott-Aldrich syndrome [WAS] is caused by pathogenic variants is *WAS*, which codifies for the WASP. More than 400 different variants in *WAS* have been described in the literature, uncovering a relationship between clinical course and the genotype. This X-linked disorder associate with moderate microthrombocytopenia, mild to moderate bleeding, eczema, and recurrent infections. Besides, autoimmune syndromes have been observed in ~40% of the patients, which have an increased risk of developing tumors at any age.[131,132]

Alteration in *FLNA, ACTB* or *ARPC1B* proteins are less frequent disorders. *FLNA*-RD is inherited as X-linked disorder and associate with mild bleeding tendency, and mild to moderate macrothrombocytopenia. Syndromic manifestations could include nodular periventricular heterotopia, skeletal malformations, mental retardation, heart valve dystrophy, intestinal obstruction, or medullar dysplasia.[133,134] *ACTB*-RD is an autosomal dominant disorder characterized by mild-moderate macrothrombocytopenia, nearly absent bleeding diathesis, frequent leucopenia or leukocytosis with eosinophilia, microcephalia with developmental delay, and mild intellectual disability.[135] *ARPC1B*-RD is caused by biallelic loss of function in ARP2/3, and the clinical manifestations include mild-moderate bleeding and thrombocytopenia, usually with small platelets, and frequent eosinophilia, immune-mediated inflammatory disease, eczema, lymphadenopathy, and hepatosplenomegaly.[136]

- <u>Glycosylation and sialylation defects</u>

Until recently, defects in glycosylation were not linked to Congenital Platelet Disorders.[44] In fact, only *GNE* is consider a Tier1 gene in the last revision of the ISTH 2021 (Figure 1).[83]

*GNE*-related disorder is inherited in an autosomal recessive manner, and it is associated with severe macrothrombocytopenia and bleeding tendency. Patients with biallelic loss of function of the UDP-N-acetylglucosamine 2-epimerase present myopathy since childhood and increased platelet clearance from bloodstream.[137,138]

Biallelic variants in the sialic transporter gene *SLC35A1* have also been related with mild to moderate thrombocytopenia and bleeding.[47] However, the bleeding diathesis found in these patients is less aggressive than in patients with *GNE*-RD, since the truncation of *SLC35A1* is not involved in a defective megakaryopoiesis, and the platelet reduction in blood is only caused by increased clearance.[139] Moreover, these patients suffer from impaired psychomotor development, epilepsy, ataxia, microcephaly.

Finally*, GALE*-related disorder present an autosomal recessive inheritance pattern and it is commonly associated with galactosemia. Peripheral

galactosemia generally associates with non-generalized forms or even asymptomatic presentations,[140,141] while classical galactosemia may be related with complications such as severe thrombocytopenia, febrile neutropenia, learning difficulties, developmental delay, cardiac failure, or dysmorphic features.[142–145]

## 4. DIAGNOSIS OF CONGENITAL PLATELET DISORDERS

The diagnosis of patients with Congenital Platelet Disorders [CPDs] is challenging due to the clinical and laboratory heterogeneity, the limited understanding about the biological role of many genes implicated in CPDs, and the poor reproducibility and specificity of platelet function tests.[146,147] Consequently, many CPDs remain underdiagnosed, waning the quality of life of patients and increasing the risk of new bleeding episodes; or misdiagnosis, receiving inappropriate management, even harmful and unnecessarily invasive treatment, such as splenectomy, among others.[148,149] In addition, it trigger a great economic challenge, due to the use of time-consuming and costly diagnostic methods, and the need of re-treatment of those patients.[150]

Many inherited thrombocytopenia associate with a moderate reduction of platelet counts, mildly platelet dysfunction and slight bleeding tendency.[79] It is hence common for asymptomatic thrombocytopenia to be incidental found in adulthood, in the context of routine health examination or when undergoing surgery or other hemostatic challenges.[95,151]

In general, the diagnosis of Congenital Platelet Disorders is based on a combination of: (Figure 6)

- Clinical symptoms, based on a family history of bleeding, hematological malignancies, solid tumors, and/or systemic manifestations, such as renal failure, myopathies, among other. For the clinical evaluation of the bleeding assessment, the use of standardized questionnaires, such as the ISTH-BAT, is recommended.[152] The ISTH-BAT could be useful for patients who require further functional studies to identify their bleeding disorder. In general, abnormal

bleeding diathesis is stablished when ISTH-BAT>3 in men, and >5 in women, and >2 points in children.[152,153]

- Standard laboratory analysis, including coagulation and biochemical routine diagnosis, hemogram, being particularly important the platelet count and the MPV for the diagnosis of inherited thrombocytopenia, and finally the morphology evaluation using blood films with or without immunofluorescence staining.[154,155]

- Platelet phenotyping. These analyses are limited and usually performed in highly specialized laboratories, where specific platelets studies, such as light transmission aggregometry and flow cytometry, are conducted.[149,156] Additionally, platelet functional screening should be performed within a limited time after blood collection, with standard conditions, such as reagents, methods, equipment, and data interpretation, which makes the diagnosis difficult.[157]

- Diagnostic confirmation by molecular analysis of the affected gene. The inclusion criteria consisted of at least ≥1 clinical and ≥1 laboratory criteria.[158] Until recent years, Sanger sequencing [SS] of candidate genes has been used as a diagnostic tool. However, the approach is, at present, costly, time-consuming, and not applicable to disorders whose phenotype-based diagnosis is not straightforward and for which there is no obvious candidate gene. The implementation of high throughput sequencing [HTS], either targeted pre-specified gene sequencing, whole-exome sequencing [WES], or whole-genome sequencing [WGS], has revolutionized the field of genetic diagnosis, and has being rapidly established for clinical practice.[97,159] Despite their undoubted importance, until recently, molecular studies of CPDs have been performed as the last step in the workflow of the diagnosis of these diseases.[160,161] The main limitation of the molecular analysis is the classification of the genetic variants found, since most of them are novel or of uncertain significance. For that reason, international standard recommendations from the ACMG / AMP have been established to classify the pathogenicity of genetic variants found in patients.[162] Nevertheless, despite these guidelines, there is a large variability in the classification of variants among laboratories. The appearance of the GoldVariant project has enabled the data sharing of variants from different research groups worldwide,[83] which are curated by expert panels from the Clinical Genome

Resource [ClinGen] to determine the gene´s role and the variant effect in a specific disease, enabling the development of specific recommendation.[163–166]

- Functional approaches. Validation of potential novel or unknown significant variants should be accompanied by functional testing, when possible, in cell lines models, primary cells from patients' samples, induced pluripotent stem cells [iPSC] and/or, ultimately, animal models.[93]

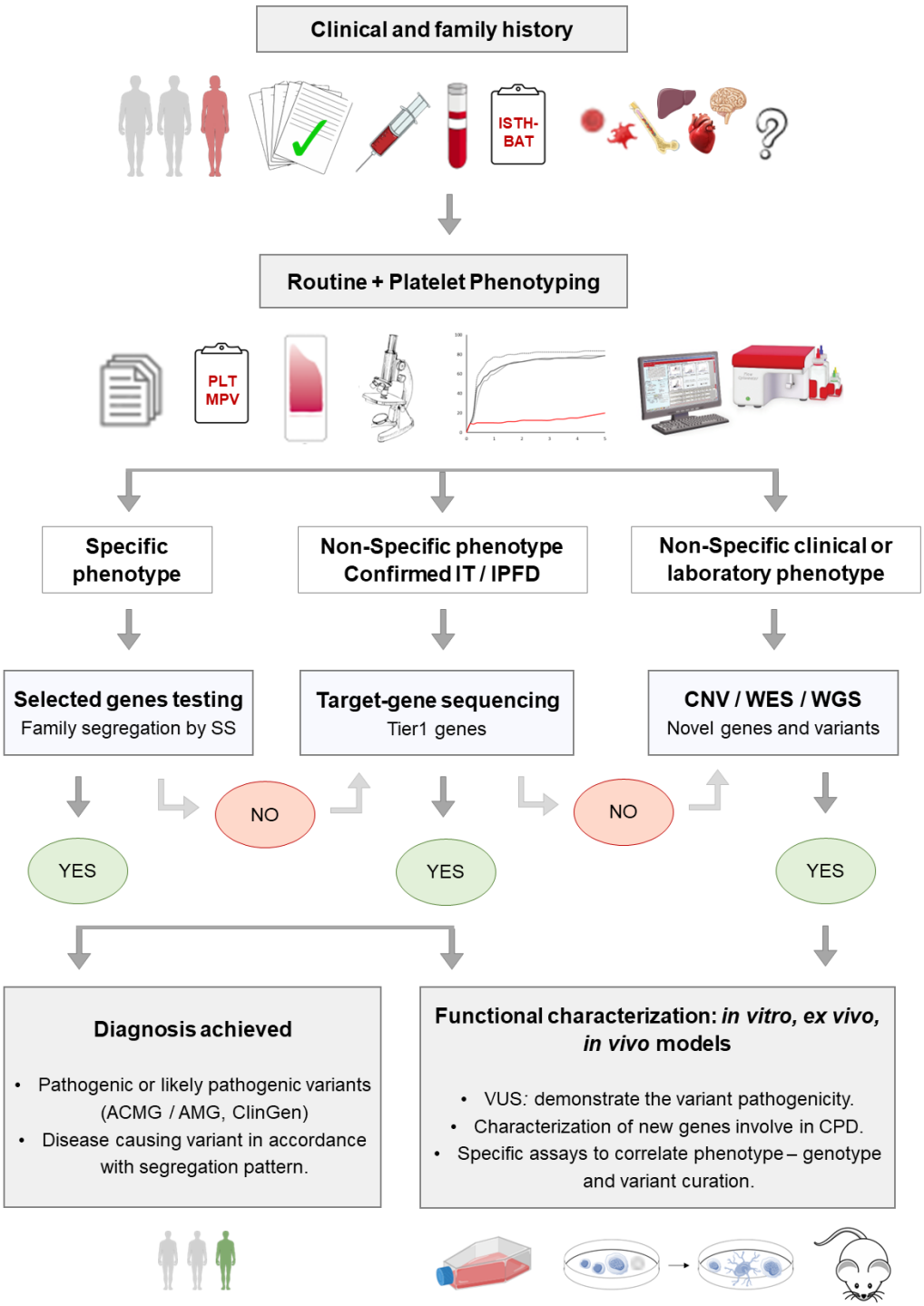

**Figure 6. Workflow algorithm for the diagnosis of Congenital Platelet Disorders.** Adapted from: [97,167]

### 4.1 Platelet phenotyping assays

Initial testing should include a complete blood count and the evaluation of a peripheral blood film: these assays help to detect abnormalities in platelet number and structure that could guide further laboratory investigations.[147,154] Normal platelet counts will exclude inherited thrombocytopenia [IT] as the cause of bleeding, suggesting a platelet function disorder. However, reduced platelet number does not exclude further platelet function testing because several ITs are associated with platelet dysfunction. MPV evaluation is also an important diagnostic parameter because ITs are often characterized by abnormal platelet size.[78,88,168–170] Thrombocytopenia associated with altered MPV can guide the diagnosis of several ITs, specially, those associated with cytoskeleton protein alterations.[169,171] However, it is important to point that we could observe unusual features, such as WAS associated to macrothrombocytopenia instead of the common microthrombocytopenia.[172]

Examination of the peripheral blood film allows to evaluate platelet size, complementary to MPV values, but also platelet clumping, morphology, and granularity, or white and/or red cell abnormalities.[147] Pale and enlarged platelets focus the diagnosis on the absence/ reduction of platelet granules, characteristic of *NBEAL2* variants;[173] reduced and very large granulated platelets are characteristic of the Bernard Soulier Syndrom;[174] leukocyte inclusions (Döhle - like bodies) suggest the *MYH9*-RD,[175,176] large platelets with stomatocytes orients towards molecular alterations in *ABCG5* and *ABCG8*,[177,178] while abnormal red blood cell morphology focus the diagnosis on *GATA1* gene.[179] Besides, a recent approach based on the blood smear staining with fluorescent antibodies against specific platelet proteins has increased the diagnosis rate in an easy and fast way.[154,155]

Conversely, the most used screening test for primary hemostasis is the platelet function analyzer (PFA-100®). Even its widely used in laboratories, PFA-100® is not recommended for initial laboratory screening due to its low specificity,

sensitivity, and reproducibility. However, it could guide the diagnosis of an impaired hemostasis.[180,181]

The *gold standard* method for the diagnosis of platelet function is the light-transmission aggregometry [LTA].[182] Upon the addition of an agonist, platelets aggregate, so the platelet-rich plasma loses turbidity and becomes clearer, increasing the light transmission detected by the photocell. The time required to get this shift is recorded and represented as the aggregation over time.[183,184] Common agonists for LTA diagnostic screening include ADP, collagen, arachidonic acid [AA], or epinephrine at standardized concentrations (Figure 4). α-thrombin mediated-activation is analyzed by using specific peptides, such as thrombin receptor activating peptides TRAP-6, PAR-4 and/or PAR-1. To evaluate the GPIb-IX-V complex, it is widely used the antibiotic ristocetin, which cause the binding of vWF to the complex. Specific agonists such as collagen-related peptide [CRP] convulxin or phorbol-12-myristate-13-acetate [PMA] could be optionally used when there is a suspected alteration in these specific pathways.[183,185,186]

Platelet aggregation could be also evaluated by impedance aggregometry in whole blood. This method is based on the measurement of the resistance to the electricity between two platinum electrodes. When platelets aggregates, they bind to the electrodes producing changes in electrical impedance, which are then transformed in an aggregation tracing. However, this method is less frequently used nowadays since it is poorly sensitive to detect mild platelet function defects.[187,188]

Otherwise, flow cytometry allows the evaluation of several structural and functional platelet parameters, like the expression of surface receptors, ligand binding, or secretion of granule contents, by using specific antibodies. Indeed, the technique requires low amounts of blood, which represents a very useful assay for patients with severe thrombocytopenia or pediatrics. Common routine assessment includes the antibodies towards GPIIb (anti-CD41), GPIIIa (anti-CD61), GPIbα (anti-CD42b) and GPIX (anti-CD42a), and less frequently or as a second step, GPIa/IIa (CD31 and CD49b), GPIV (CD36), and GPVI. Flow cytometry also allows the evaluation of platelet function defects measuring the surface expression of activation markers, like CD62P (α-granules), CD63 (δ-granules) or PAC-1 (active αIIbβ3 integrin), upon stimulation with agonists.[189–191]

## 4.2 Molecular diagnosis in the genomic era

Until early 2010, DNA sequencing had been largely restricted to the analysis of candidate genes by Sanger Sequencing. Diagnosis based on this technique was limited due to the selection of the candidate genes, which required a well-defined clinical and laboratory phenotype. For that reason, less than 40% of patients were diagnosed. The recent application of the high throughput sequencing [HTS], specially using target panels of variable number of known genes involved in bleeding disorders, has revolutionized the molecular diagnosis of Congenital Platelet Disorders, improving the diagnostic efficiency by 70%, and up to 90% in cases with a clear diagnostic suspicion or with a specific phenotype.[97,158,192–195] Finally, the increasingly economical cost-reduction and the progression in the interpretation of whole exomes and genomes has allowed the discovery of new genes involved in the pathology.[108,142,196,197]

### *4.2.1 Sanger Sequencing*

Sanger Sequencing [SS] allowed the mapped of the entirety human genome,[198] being the *gold standard* method for molecular diagnosis of the bleeding disorders since the early 1990s.[149,192] It is useful in Congenital Platelet Disorders with a well-defined clinical and laboratory phenotype, such as Bernard Soulier Syndrome or Glanzmann Thrombasthenia. Moreover, SS associated with other techniques such as genome-wide linkage analysis made it possible to identify *MYH9* or *RUNX1* genes, among others.[97] However, its major limitation is the reduced diagnostic efficiency for disorders whose phenotype-genotype relation is uncertain and for which no obvious candidate gene can be selected. Indeed, the fact that many diseases are caused by many culprit genes, such as Hermansky-Pudlak Syndrome [HPS], or a gene with many exons, makes diagnostic by SS costly and time-consuming. Nowadays, SS is used when there is a strong phenotype-genotype evidence, for genetic confirmation of the diagnosis, and for familial segregation (Figure 7).[97,158,192,199,200]

### *4.2.2 Targeted-gene Sequencing*

In the last decade, HTS has revolutionized DNA sequencing and the diagnosis of human diseases, allowing the simultaneous exploration of multiple genes in a rapid and economical way. The use of target-gene panels simplifies and speeds

up the overall diagnosis, allowing the sequencing of target regions of interest from a panel of prespecified candidate genes (Figure 7).[97,201,202]

Several research groups have already introduced gene panels into the clinical practice for managing and diagnosis of patients with Congenital Platelet Disorders. First, the Genotyping and Phenotyping of Platelets Project (GAPP) examined up to 329 genes, characterizing novel variants in genes likes *FLI1* or *RUNX1*,[193,203] or the ThromboGenomics consortium, which emerged from the BRIDGE-BPD consortium, developing an HTS platform to sequence a panel of 63 genes involved in inherited bleeding, thrombotic, and platelet disorders.[194,204] Otherwise, an Australian group used a Custom Amplicon panel of 27 candidate genes causing inherited thrombocytopenia to investigate a large cohort of patients with macrothrombocytopenia.[175,205]

Regarding the “Grupo Español de Alteraciones Plaquetarias Congénitas”, a targeted panel of 72 genes was used for the clinical practice, uncovering novel variants in infrequent genes, such as *DIAPH1, RASGRP2* or *PTGS1*.[158,113,206]

The used of target-gene sequencing has improved the genetic diagnosis of patients up to 70%, by using different custom panels in different laboratories worldwide.[158,193,204,207] However, current limitations persist, such as a substantial proportion of patients that cannot be diagnosed.[208] It remains difficult to identify large structural chromosomal variants, inversions, translocations, aneuploidies, and copy number variations [CNVs] using this approach, in addition to the fact that several processes of megakaryopoiesis and platelet function are not well characterized, will explain that a substantial number of disorders are caused by genes not described so far.[97,161]

### *4.2.3 Whole Exome Sequencing*

WES enables the sequencing of all protein-coding regions (exons), which represents ~1.5% of the human genome, and involves the 85% of the Mendelian disorders (Figure 7).[209] In the last few years, the use of WES allowed the identification of novel genes in Congenital Platelet Disorders, such as *DIAPH1, GNE* or *TPM4*.[108,138,197] Besides, CNV could be detected with this approach. However, the main limitation of the technique is the time-consuming, the vast amount of data generated, and the difficulties regarding the gene-interpretation.[97]

### *4.2.4. Whole Genome Sequencing*

WGS can provide complete genomic information, since all coding and noncoding sequences are analyzed (Figure 7). This method is increasing importance among the years, and the cost of this technology has progressively dropped.[210] However, and similarly to WES, it provides a large amount of data, which requires an extensive and complex bioinformatic workflow and expert interpretation to identify the disease-causing variants.[211] In addition, the interpretation of noncoding variants has proved to be extremely challenging and is not yet routinely performed in most research projects.[212,213]


**Figure 7. The main types of DNA-sequencing used for the diagnosis of Congenital Platelet Disorders.**

### *4.2.5. Variant Interpretation*

Genetic diagnosis of Congenital Platelet Disorders helps to achieve an accurate diagnosis, providing better clinical care, prognosis, preventive treatments, and enabling genetic counseling. This last step is essential for patients with high risk of malignancy and another predisposition to serious conditions.[195] In this context, high-throughput sequencing [HTS] provides, in a rapid and increasingly economical way, a large amount of genetic information, facilitating the identification of genetic variants, being established as the gold standard for identifying the molecular pathology underlying monogenic diseases.[97,211] However, despite the diagnostic advantages of HTS, ethical dilemmas persist in the use of genetic screening and the identification of variants of uncertain significance [VUS].[208,214]

To categorize the large amount of genetic information obtained from HTS, standards guidelines for the interpretation of sequence variants have been established by the ACMG / AMP.[162] However, these rules are not universally applicable to different genes or disorders, which give rise to different interpretation of the same variant by different laboratories worldwide and, therefore, not reaching a definitive and uniform classification. To achieve an accurate diagnosis of patients, it has recently been created the GoldVariant project, which facilitates data sharing among different laboratories from all over the world, specifically, 30 expert centers in 14 countries.[83] This vast amount of genetic information is rapidly and easily submitted to ClinVar, and these variants will be re-classified and evaluated by small working groups of experts, the ClinGen variant curation expert panels, providing gene-specific modification to the general ACMG / AMP variant classification rules, based on the published literature and databases regarding the clinical and laboratory phenotype found in patients with a specific disorder, cellular or animal models, or population databases. This approach will allow the determination of the variant role in a disease (disease association) and provide information on the mode of inheritance and mutational disease mechanism, discarding incidental variants in disease-causing genes that are unrelated to the original rationale for testing.[163–166]

## 5. FUNCTIONAL CHARACTERIZATION OF CONGENITAL PLATELET DISORDERS

The final step for the curation of a variant of uncertain significance is the demonstration of the pathogenesis and the mechanism underlying the variant, especially when no evidence of disease association reviewing the bibliography is found.[215] In fact, the increasing application of WES and WGS in the clinical routine practice has allowed the identification of novel genes involved in the pathogenesis of Congenital Platelet Disorders, which require functional studies to uncover its role and implication in the disease. Therefore, the final confirmation of a variant as disease-causing should be bound to the performance of an experimental model to demonstrate the causality.[97,162,167]

### 5.1 *In vitro* approaches

Human megakaryocytic cell lines, derived from the peripheral blood or the bone marrow of patients with leukemia, are powerful tools to evaluate the proliferation, differentiation, and maturation of Mks. The availability of homogeneous populations of hematopoietic progenitor cells has facilitated the understanding of the biological and molecular mechanism of genes crucial in megakaryopoiesis.[216–218]

To date, at least 18 human cell lines with some megakaryocytic properties have been reported in the literature.[219] These cell lines in undifferentiated conditions expressed specific markers of Mks or erythrocytes (Table 1). Treatment with PMA or TPO stimulate megakaryocytic differentiation, allowing the study of the signaling pathways involved in the process. Commonly, cells are treated with PMA, since the induce-differentiation is accompanied by changes in cell morphology, cell growth arrest, endomitosis and acquisition of specific Mk markers, mimicking the physiological process that takes place in the bone marrow. Besides, PMA-treatment do not require a specific receptor, since it directly activates the PKC protein.[218,220,221] Treatment with TPO is physiologically more similar to the nature megakaryopoiesis that takes places in the human bone marrow, however, only UT7 cell line presents *MPL* gene. Indeed, UT7 is the unique hematopoietic factor-dependent cell line, so this cell line can provide an important new model for the study of the TPO-induced differentiation of Mks (Table 1).[222,223]

K562, HEL, MEG-01 and Dami are the most frequently cell lines used for *in vitro* characterization of the megakaryopoiesis, because after the treatment with low-dose of PMA (10-30 nM), cells increase their size and show cytoplasmic maturation. Therefore, polyploidy can be easily measure by flow cytometry. Indeed, they also increase surface expression of various megakaryocyte-platelet-associated proteins such as GPIIb-IIIa, GPIb, vWF and PF4. In fact, GPIb expression in K562 and MEG-01 lines in basal conditions is absent, so the appearance of the expression could be considered as a direct measure of PMA-induced maturation.[219,224–227]

| Cell line | Source | GPIIb-IIIa (CD41-61) expres. | GPIb (CD42b) expres. | vWF expres. | Differentiation with PMA / TPO | Ref |
|---|---|---|---|---|---|---|
| **K562** | CML blast crisis | +/- | - | - | PMA | [224] |
| **HEL** | AML M6 | + | + | - | PMA | [225] |
| **MEG-01** | CML blast crisis | + | +/- | + | PMA | [226] |
| **EST-IU** | Germ cell tumor | + | N/A | + | PMA | [228] |
| **LAMA-84** | CML blast crisis | + | - | - | PMA | [229] |
| **Dami** | AML M7 | + | + | + | PMA | [227] |
| **KOPM-28** | CML blast crisis | + | N/A | N/A | PMA | [230] |
| **T-33** | CML blast crisis | + | + | + | PMA | [231] |
| **M-07** | AML M7 | + | + | N/A | N/A | [232] |
| **OCIM1/ OCIM2** | AML M6 | +/- | - | - | PMA | [233] |
| **KU812** | CML blast crisis | +/- | - | N/A | PMA | [234] |
| **CMK** | AML M7 | + | + | - | PMA | [235] |
| **CHRF-288-11** | AML M7 | + | N/A | + | PMA | [236] |
| **UT7** | AML M7 | + | + | N/A | PMA / TPO | [222, 223] |
| **MOLM-1** | CML blast crisis | + | N/A | N/A | N/A | [237] |
| **MKPL-1** | AML M7 | + | - | - | N/A | [238] |
| **ELF-153** | AML M7 | + | + | + | PMA | [239] |
| **MEG-A2** | CML blast crisis | + | - | - | PMA | [240] |

**Table 1. General characteristics of the human cell lines that express megakaryocytic features.** GPIIa, IIIa, Ib and vWF expression is referred to

undifferentiated conditions. + means positive expression, +/- very weak positive, - negative, N/A specifies not evaluated features in the cell line. Adapted from:[219]

### 5.2 *Ex vivo* approaches

Mk differentiation and maturation is highly dependent on the microenvironment and cytokines.[5] Even *in vitro* approaches are useful for the characterization of signaling pathways involved in the megakaryopoiesis, they do not reproduce the biological processes. In the last years, the *ex vivo* generation of platelets from HSC has improved the understanding of the heterogeneity underlying human Mk development.[241] Mks cultures' from HSC and human embryonic stem cells [ESCs] or human induced pluripotent stem cells [iPSCs] have emerged as an effective model for the study of megakaryopoiesis in patients with inherited thrombocytopenia or platelet dysfunction, and it is a promising alternative source to meet the ever-increasing demand for platelet therapy.[241–243]

- Megakaryocytes cultured from HSC and progenitors

Human megakaryocytes [Mks] and platelets could be generated *in vitro* after isolation of $CD34^+$ progenitor cells derived either from peripheral blood, umbilical cord blood, fetal liver, or bone marrow. Cells must be culture for 14 days in the presence of TPO or human plasma (Figure 8). Additional supplementation with cytokines has been proved to increase the differentiation rates in the culture. Indeed, as the hematopoietic microenvironment relies on stromal cells to provide many of the signals for HSC self-renewal and proliferation, stromal cell-based cultures could be of major interest.[4,244,245]

Characterization of Mk from primary cells is a technology-limiting approach, since the number of cells obtained at the end of the culture is quite reduced and no longer in time.[246]

- Human embryonic stem cells and induced pluripotent stem cells

In comparation with primary Mks, ESCs and iPSCs can be immortal cells and could provide a limitless number of $CD34^+$ cells after manipulation of C-MYC, and one of the four Yamanaka factors used to induce pluripotency in somatic cells (*SOX2, REX1, NANOG* and *OCT4*) (Figure 8).[247,248]

However, those Mks are quite different from the physiological ones since they do not exceed a ploidy of 32n, and only around a 15% of these Mks are $CD41^+$ $CD42b^+$. In fact, the main limitation is the low number of platelets shed by Mks.[241,247]

One of the main reasons of these differences is related with the fact that *ex vivo* generation is carried out in static culture, and therefore, not mimicking blood flow conditions. One emerging strategy to gain insight into the fundamental role of the bone marrow microenvironment in the regulation of the hematopoiesis is through the use of three-dimensional (3D) models of human tissues via tissue engineering. The most recent models are made of biocompatible materials supporting Mk function. Once in contact with the biomaterial, Mks extend proplatelets into the perfused culture medium mimicking blood shear stress. Promising advances have been achieved in the last 20 years on platelet production *ex vivo,* suggesting that in the near future this technique to fully differentiate functional Mks could be commonly used for research.[4,246,249–251]

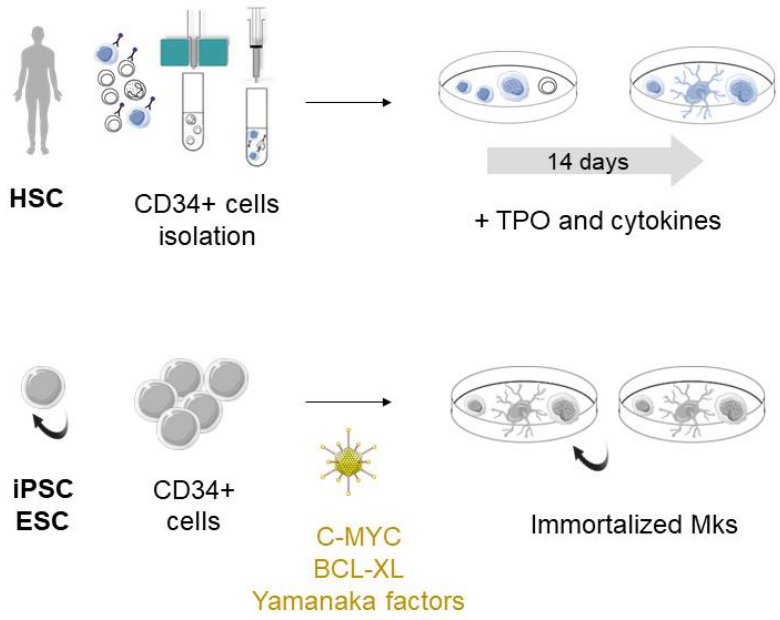


**Figure 8. *Ex vivo* megakaryopoiesis approaches.** In the top figure, the isolation and expansion of $CD34^+$ cells into Mks are represented. In the bottom, induced pluripotent stem cells (iPSCs) and embryonic stem cells (ESCs) generation by the activation of transgenes provides a source of immortalized Mks. Created with Servier Medical Art (https://smart.servier.com/).

### 5.3 *In vivo* approaches

The development of the genetic reprogramming of iPSC or Mk differentiation has enabled some progress, but these *in vitro* systems are imperfect and do not faithfully reproduce all the steps leading to the formation of platelets. The improvement of tools to study mice genetically modified has allowed the generation of *in vivo* models mimicking the pathologies and enabling the assessment of the impact of genetic variants on platelet production and function. Even is less used, zebrafish models have also been demonstrated to be a potentially useful animal model reproducing human platelet disorders.[252–254]

Targeted mutagenesis and transgenesis now offer a wide range of genetically modified models. *Knock-out* [KO] are generated by the inactivation of the gene in the whole organism. Given the germline condition of Congenital Platelet Disorders, those animal models are potentially useful. Conditional *knock-out* mice allow the inactivation of a gene in a particular tissue, or at a specific stage of development under the control of the promoter of interest. Finally, *knock-in* [KI] mice are generated by the point mutation or insertions/deletions through homologous recombination at the locus of interest. These models faithfully reproduce the missense variants presented in humans and represent the best approach to mimic the pathology.[255,256] To date, mice models have been generated for the study of *MYH9*-RD, Bernard Soulier Syndrome, Wiskott Aldrich Syndrome, Congenital amegakaryocytic thrombocytopenia o *RUNX1*-RD, among others.[22,257–260]

The recent advances in the generation of iPSC now permits the production of mutated HSC from fibroblasts of patients.[255] Xenotransplantation of these stem cells into immunodeficient mice may be expected to mimic or reproduce the human pathology. This strategy is commonly used for hematological malignancies, but for now the approach in Mks and platelets to study the physio pathological mechanisms and to evaluate new therapeutic approaches is not well standardized.[261–264]

### 5.4 Genome-editing technologies

In the last few years, the development of genome editing technologies has revolutionized the field of genetic engineering, enabling genome modification in a fast, specific, and straightforward way.[265,266]

The genome editing systems implemented so far included Zinc Finger Nucleases [ZFN], Transcription Activator-Like Effector Nucleases [TALEN] and Clustered Regularly Interspaced Short Palindromic Repeats [CRISPR] / Cas9. The ZFN and TALENs methodologies are based on the engineering of proteins consisting of a recognition region of the target sequence to be edited a and catalytic region responsible for generating double strand breaks [DSB] in the DNA (Figure 9). Both methodologies have some limitations, as it is necessary to generate a different protein for each region of the genome to be edited and, in addition, both systems are difficult to introduce into cells due to their large size, thus reducing editing efficiencies and compromising the ability to generate simultaneous edits of several genomic regions in the same cell.[267,268] Nevertheless, the CRISPR/Cas9 system is able to overcome these limitations, allowing the editing of DNA sequences in a simpler and more efficient form.[269]

To induce targeted cleavages in human cells using this system, it is necessary to express two essential components; the Cas9 protein, and an RNA sequence, consisting of 20 nucleotides complementary to the target genomic region and the Cas9 protein-binding region,which acts as a guide. This specific sequence is named single-guide RNA [sgRNA]. The only requirement to edit the genomic region by the CRISPR/Cas9 tool is that the 20-nucleotide sequence should be followed by a three-nucleotide sequence, -NGG-, called PAM. These components are introduced into mammalian cells via plasmids, lentiviruses, or ribonucleoproteins. Once the system is introduced into the cell, a double-stranded DNA cleavage mediated by Cas9 nuclease will occur in the region complementary to the guide, between nucleotide 17 and 18 of the complementary sequence upstream of the PAM.[270,271] Subsequently, endogenous double-strand break repair mechanisms will be activated in the cell, consisting of two main mechanisms. In most cases, the break is corrected through the non-homologous end-joining [NHEJ] mechanism, based on the joining of blunt ends by incorporation or deletion of random nucleotides, generating insertions or

deletions. These alterations can result in a frameshift, leading to a stop codon that can truncate the target protein, thus generating a KO.[272,273] On the other hand, the homologous recombination [HR] mechanism uses a homologous sequence as a template [ssODN] for targeted repair. In this way, it is possible to generate or correct point mutations in a genomic region of interest by integrating a specific repair template together with the components of the CRISPR/Cas9 system (Figure 9).[274,275]

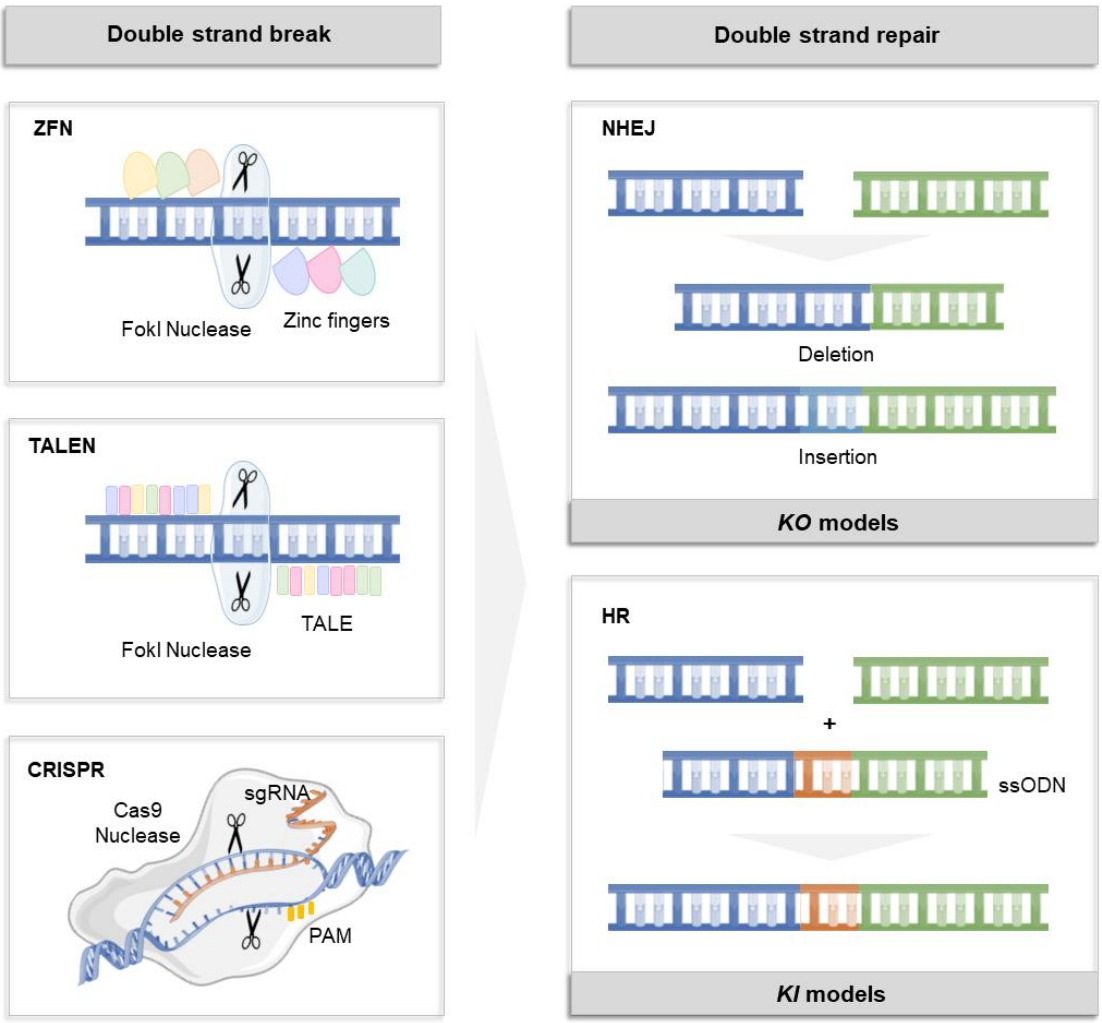


**Figure 9. The nuclease genome editing technologies.** The three most used types of nucleases include ZFNs, TALENs and CRISPR systems, which can induce double-strand breaks [DSBs] in the target region followed by the activation of DNA repair mechanisms. These DSB can be repair either by NHEJ or HR. NHEJ is an error prone repair mechanism, which generally results in heterogeneous indels (deletions and insertions) whereas HR is a precise repair method in which homologous donor template DNA, called ssODN, is being used in repair DNA damage target site. Created with Servier Medical Art (https://smart.servier.com/).

Since the application of CRISPR/Cas9 for human cell editing is relatively recent, there are still several limitations associated with the use of this methodology. One of the major weaknesses is the occurrence of "off-target" effects, this is, mutations in non-targeted regions of the genome mediated by the active Cas9 nuclease. The ongoing progress and improvement of the CRISPR system includes the use of the Cas9 nickase (Cas9n) instead of the Cas9, which has allowed the reduction of the off-targets since this nuclease produces single-strand breaks very close to each other, mimicking a double strand break.[253,276]

The use of CRISPR/Cas9 for point mutation correction in patient cells also presents a major challenge because most cell types preferentially repair the double-strand break by NHEJ rather than HR, which is required for mutation correction. Numerous strategies are currently being investigated to improve the efficiency of HR by modifying the template required for repair, transiently inhibiting one of the components of the NHEJ mechanism to promote HR, or improving transfection methods.[277–279]

To date, several strategies in the field of Congenital Platelet Disorders have emerged. Several groups have used this genome editing technique to generate specific mutations to study the underlying mechanisms of pathogenesis, such as a *KO* model of *PTPRJ,*[254] which allowed to determine its role in megakaryopoiesis, or a *KI* mouse carrying the ITGA2B c.2659C > T variant to stablish its effect on Glanzmann's thrombasthenia.[280] Moreover, a recent approach of CRISPR-edited Mks has been developed for rapid screening of platelet gene functions, emerging as a potential tool for the study of variants detected in patients.[281]

Finally, this potential strategy is not only being used to reproduce and characterize the pathophysiological mechanisms of variants detected in patients, but it is also already being used as a promising strategy for targeting monogenic diseases. Recently, the correction of endogenous pathogenic microduplication alleles for Hermansky-Pudlak Syndrome 1 (HPS1) to wild-type sequence in primary patient-derived fibroblasts has been developed,[282] which provides a promising future for the gene therapy in the field of Congenital Platelet Disorders.

# HYPOTHESIS

Congenital Platelet Disorders [CPDs] comprise a wide and heterogeneous group of rare diseases that predispose patients to thrombocytopenia and/or bleeding but also, in some cases, to other complications, such as hematological malignancies or syndromic manifestations. Diagnosis is challenging and requires multiple laboratory tests as well as a final molecular confirmation. The introduction of High Throughput Sequencing [HTS] tools into the clinical practice has significantly improved and streamlined patients' diagnosis. However, despite the substantial improvement that HTS tools have brought, two major challenges still persist.

Firstly, the interpretation of the variants found by HTS and their classification according to ACMG / AMP. Thus, data sharing is extremely encouraged. For that reason, the ISTH SSC-GinTH developed the GoldVariant project to identify most of the variants reported in platelet disorders for a rapid and easy submission to ClinVar. Therefore, these variants will be re-classified and adequately curated by small working groups of experts. In that context, ClinGen Variant Curation Expert Panels have developed specific adapted ACMG / AMP rules for *ITGA2B* / *ITGB3* and *RUNX1* genes. Nonetheless, for the curation of the variants, especially for novel or uncertain significance, it is encouraging the development of functional models to formally demonstrate its role in the pathogenesis and the mechanism underlying the disease.

The previously described missense variant c.167T>C; p.Leu56Ser in the transcriptional factor *RUNX1* has thrown up great controversy about whether it is a leukemia-predisposing allele or a benign polymorphism. This variant has been found in some patients with clinical and laboratory suspicion of Familial Platelet Disorder with predisposition to Acute Myelogenous Leukemia [FPD/AML]. Furthermore, this variant has been reported to be associated with impaired transcriptional activation of several targeted genes. However, it is also a relatively frequent variant in the general population, which leads to its classification as benign by the ClinGen. Hence, the final confirmation of the biological and functional role of RUNX1 p.Leu56Ser in FPD/AML requires the generation of an experimental model reproducing the human alteration, to unveil the potential mechanisms of pathogenesis.

The second challenge to be faced is the fact that, regardless of the success in the diagnosis and phenotypic characterization by an integrative approach using targeted sequencing panels and functional studies, there are still patients and families without a final diagnosis. Considering the unknown prevalence and the underdiagnosis of the CPDs, in addition to the fact that several physiological processes of the megakaryopoiesis and platelet function are not well understood, it is highly possible that a substantial number of disorders are caused by variants in genes that have not been described or characterized so far.

Over the last few years, novel genes related to CPDs have been described using WES and WGS. In fact, the first description in the world of thrombocytopenia associated with genetic variants in *TPM4* was made by using these technologies. *TPM4* encodes the tropomyosin-4, a protein involved in the actin cytoskeleton, which alteration cause macrothrombocytopenia. Nevertheless, deepen characterization of the phenotype associated to *TPM4* variants is required, as well as further investigations to assess the role of this crucial protein in the megakaryocyte and platelet remodeling.

Similarly, the first evidence of molecular alterations in *GALE* triggering hematological disorders has been described by using WGS. The UDP-Galactose-4-Epimerase protein is involved in both galactose metabolism and protein glycosylation. Despite several patients carrying *GALE* missense variants have been described displaying thrombocytopenia, the mechanisms of pathogenicity remain unveiled. Therefore, an in-depth study of the role of this enzyme in the megakaryopoiesis and thrombopoiesis processes, and the correlation with the glycosylation reactions triggered during both processes (which are essential for the correct formation and function of the platelets) will shed light on the molecular mechanisms underlying this phenotype.

Therefore, the integration of genomic analysis by different High Throughput Sequencing methodologies, together with the *in vitro, ex vivo* or *in vivo* functional approaches, will be useful to characterize and curate variants of uncertain significance in the transcriptional factor *RUNX1*, and to assess its role in platelet disorders and leukemia progression, as well as to provide novel insights into the biological and physio-pathological processes triggered by variants in two novel genes involved in Congenital Platelet Disorders: *TPM4* and *GALE*.

AIMS

## General aims

To characterize the clinical and platelet phenotype associated with the molecular alterations found by high throughput sequencing tools in genes involved in Congenital Platelet Disorders, and to demonstrate the pathogenicity-related mechanism using *in vitro* and *ex vivo* megakaryocyte cultures, and *in vivo* disease models generated by the CRISPR/Cas9 technology.

## Specific aims

- Functional characterization of RUNX1 p.Leu56Ser variant, previously found by a custom gene panel, using an *in vivo* approach.
    - To generate a *knock-in* murine model carrying the RUNX1 p.Leu43Ser variant (mimicking the human germline variant p.Leu56Ser) by CRISPR/Cas9*,* to settle down its implication in the platelet disorder.
    - To gain knowledge into the signaling pathways and biological determinants underlying the leukemia progression associated with *RUNX1* variants.

- Application of whole-exome sequencing for the identification of novel genes involved in Congenital Platelet Disorders, and assessment of the physiopathological mechanisms driving the disease through *in vivo* and *ex vivo* functional models.
    - To explore the clinical and laboratory phenotype of the third family worldwide with thrombocytopenia associated with *TPM4* variants, and to deeply-characterized its role in the platelet cytoskeleton remodeling.
    - To assess the clinical and platelet phenotype of three patients from two unrelated families with syndromic macrothrombocytopenia associated to compound heterozygous variants in *GALE.*
    - To investigate the functional effect of the genetic variants identified in *GALE* during megakaryopoiesis and thrombopoiesis, and its role in megakaryocyte and platelet glycosylation using an *in vitro* overexpression model and *ex vivo* culture of patients' megakaryocytes.

# RESULTS

This section includes the experimental work performed on this thesis, including Material and Methods, Results and Discussion. This section has been divided into four chapters:

**Chapter 1.** Marín-Quílez A, García-Tuñón I, Fernández-Infante C, Hernández-Cano L, Palma-Barqueros V, Vuelta E, Sánchez-Martín M, González-Porras JR, Guerrero C, Benito R, Rivera J, Hernández-Rivas JM, Bastida JM. **Characterization of the Platelet Phenotype Caused by a Germline *RUNX1* Variant in a CRISPR/Cas9-Generated Murine Model.** *Thrombosis and Haemostasis*. 2021;121(9):1193-1205. doi: 10.1055/s-0041-1723987. PMID: 33626581.

**Chapter 2.** Marin-Quilez A, Sanz D, del Rey M, Ordoñez JL, Diaz-Ajenjo L, González-Porras JR, Guerrero C, Pérez-Losada J, Rivera J, Hernández-Rivas JM, Benito R, García-Tuñón I, Bastida JM. **Expanding the role of germline *RUNX1* variants in leukemogenesis in a murine model generated by CRISPR/Cas9.** *Manuscript in preparation.*

**Chapter 3.** Marín-Quílez A, Vuelta E, Díaz-Ajenjo L, Fernández-Infante C, García-Tuñón I, Benito R, Palma-Barqueros V, Hernández-Rivas JM, González-Porras JR, Rivera J, Bastida JM**. A novel nonsense variant in *TPM4* caused dominant macrothrombocytopenia, mild bleeding tendency and disrupted cytoskeleton remodeling.** *Journal of Thrombosis and Haemostasis.* 2022;20(5):1248-1255. doi: 10.1111/jth.15672. PMID: 35170221

**Chapter 4.** Marín-Quílez A, Di Buduo CA, Díaz-Ajenjo L, Abbonante V, Vuelta E, Soprano P, Miguel-García C, Santos-Mínguez S, Serramito-Gómez I, Ruiz-Sala P, Peñarrubia MJ, Pardal E, Hernández-Rivas JM, González-Porras JR, García-Tuñón I, Benito R, Rivera J, Balduini A, Bastida JM. **Novel variants in *GALE* cause syndromic macrothrombocytopenia by disrupting glycosylation and thrombopoiesis.** *Blood. Second revision.*

All of them have been developed to accomplish the general aim of this work and give the title to this doctoral disertation: **“Characterization of novel genes and variants involved in Congenital Platelet Disorders: from the genomic data to the functional studies.”**

The supplementary material corresponding to each sections indicated above is included at the end of each chapter.

In addition, a General Discussion, with additional data and which comprises all research, is addressed in a separate section of this thesis.

# CHAPTER 1

## Characterization of the Platelet Phenotype Caused by a Germline *RUNX1* Variant in a CRISPR/Cas9-Generated Murine Model.

Ana Marín-Quílez[1], Ignacio García-Tuñón[1], Cristina Fernández-Infante[1], Luis Hernández-Cano[1], Verónica Palma-Barqueros[2], Elena Vuelta[1,3], Manuel Sánchez-Martín[1,3], José Ramón González-Porras[4], Carmen Guerrero[1], Rocío Benito[1], José Rivera[2,5*], Jesús María Hernández-Rivas[1,4*] and José María Bastida[4,5*].

[1] Cancer Research Center - CSIC, University of Salamanca, Instituto de Investigación Biomédica de Salamanca (IBSAL), Spain; [2] Servicio de Hematología y Oncología Médica, Hospital Universitario Morales Meseguer, Centro Regional de Hemodonación, University of Murcia, IMIB - Arrixaca, CIBERER-U765, Murcia, Spain; [3] Transgenic Facility, Nucleus, University of Salamanca, Spain; [4] Department of Hematology - University Hospital of Salamanca - IBSAL, Spain; [5] On behalf of the "Grupo Español de Alteraciones Plaquetarias Congénitas, (GEAPC)"; Hemorrhagic Diathesis Working Group, SETH. *These authors share senior authorship.

*Thrombosis & Haemostasis*. 2021 Sep;121(9):1193-1205. doi: 10.1055/s-0041-1723987. PMID: 33626581

Cellular Haemostasis and Platelets

# Characterization of the Platelet Phenotype Caused by a Germline *RUNX1* Variant in a CRISPR/Cas9-Generated Murine Model

Ana Marín-Quílez[1] Ignacio García-Tuñón[1] Cristina Fernández-Infante[1] Luis Hernández-Cano[1] Verónica Palma-Barqueros[2] Elena Vuelta[1,3] Manuel Sánchez-Martín[1,3,4] José Ramón González-Porras[4,5] Carmen Guerrero[1,4] Rocío Benito[1] José Rivera[2,6,*] Jesús María Hernández-Rivas[1,4,5,*] José María Bastida[4,5,6,*]

[1]Cancer Research Center - CSIC, Instituto de Investigación Biomédica de Salamanca, University of Salamanca, Salamanca, Spain
[2]Servicio de Hematología y Oncología Médica, Hospital Universitario Morales Meseguer, Centro Regional de Hemodonación, University of Murcia, Murcia, Spain
[3]Transgenic Facility, Nucleus, University of Salamanca, Salamanca, Spain
[4]Department of Medicine, University of Salamanca, Salamanca, Spain
[5]Department of Hematology, University Hospital of Salamanca - IBSAL, Salamanca, Spain
[6]On behalf of the "Grupo Español de Alteraciones Plaquetarias Congénitas (GEAPC)", Hemorrhagic Diathesis Working Group, SETH

**Address for correspondence** Rocío Benito, PhD, Centro de Investigación del Cáncer - CSIC, Universidad de Salamanca, Campus Miguel de Unamuno, S/N, 37007, Salamanca, Spain (e-mail: beniroc@usal.es).

Thromb Haemost

## Abstract

*RUNX1*-related disorder (*RUNX1*-RD) is caused by germline variants affecting the *RUNX1* gene. This rare, heterogeneous disorder has no specific clinical or laboratory phenotype, making genetic diagnosis necessary. Although international recommendations have been established to classify the pathogenicity of variants, identifying the causative alteration remains a challenge in *RUNX1*-RD. Murine models may be useful not only for definitively settling the controversy about the pathogenicity of certain *RUNX1* variants, but also for elucidating the mechanisms of molecular pathogenesis. Therefore, we developed a *knock-in* murine model, using the CRISPR/Cas9 system, carrying the RUNX1 p.Leu43Ser variant (mimicking human p.Leu56Ser) to study its pathogenic potential and mechanisms of platelet dysfunction. A total number of 75 mice were generated; 25 per genotype ($RUNX1^{WT/WT}$, $RUNX1^{WT/L43S}$, and $RUNX1^{L43S/L43S}$). Platelet phenotype was assessed by flow cytometry and confocal microscopy. On average, $RUNX1^{L43S/L43S}$ and $RUNX1^{WT/L43S}$ mice had a significantly longer tail-bleeding time than $RUNX1^{WT/WT}$ mice, indicating the variant's involvement in hemostasis. However, only homozygous mice displayed mild thrombocytopenia. $RUNX1^{L43S/L43S}$ and $RUNX1^{WT/L43S}$ displayed impaired agonist-induced spreading and α-granule release, with no differences in δ-granule secretion. Levels of integrin $\alpha_{IIb}\beta_3$ activation, fibrinogen binding, and aggregation were significantly lower in platelets from $RUNX1^{L43S/L43S}$ and $RUNX1^{WT/L43S}$ using phorbol 12-myristate 13-acetate

**Keywords**
- RUNX1
- inherited platelet disorders
- platelet function
- mouse model
- CRISPR/Cas9

**received**
July 29, 2020
**accepted after revision**
December 28, 2020



**DOI** https://doi.org/10.1055/s-0041-1723987.
**ISSN** 0340-6245.

(PMA), adenosine diphosphate (ADP), and high thrombin doses. Lower levels of PKC phosphorylation in RUNX1$^{L43S/L43S}$ and RUNX1$^{WT/L43S}$ suggested that the PKC-signaling pathway was impaired. Overall, we demonstrated the deleterious effect of the RUNX1 p.Leu56Ser variant in mice via the impairment of integrin $\alpha_{IIb}\beta_3$ activation, aggregation, α-granule secretion, and platelet spreading, mimicking the phenotype associated with *RUNX1* variants in the clinical setting.

## Introduction

RUNX1/AML1, encoded by RUNX1, is a key transcriptional factor (TF) that regulates embryonic and definitive human hematopoiesis through CBFβ dimerization,[1] and plays an essential role in the maturation and differentiation of myeloid, lymphoid, and megakaryocytic lineages.[2,3] RUNX1 biallelic loss of function results in embryonic lethality because of intracranial bleeding.[4]

Germline monoallelic alterations in *RUNX1* have been incorporated into the World Health Organization 2016 classification of inherited myeloid neoplasms, as familial platelet disorder with predisposition to acute myelogenous leukemia (FPD/AML) (OMIM 601399).[5] This autosomal dominant disorder is characterized by variable thrombocytopenia and platelet dysfunction, associated with an increased risk of developing hematological malignancies, especially AML and myelodysplastic syndrome (MDS).[6]

As in most inherited platelet disorders (IPDs), *RUNX1*-related disorder (*RUNX1*-RD) lacks a specific clinical and laboratory phenotype, which makes genetic diagnosis essential.[7] The introduction of high-throughput sequencing (HTS) techniques into mainstream genetic diagnostic practice for IPDs has shown that molecular variations in TFs are far more frequent than previously believed.[8–10] To date, more than 130 families with *RUNX1* variants have been reported.[11]

Although international recommendations have been established to classify the pathogenicity of genetic variants found in patients,[12] the application of these recommendations is still challenging, and there may be alternative interpretations for many genetic variants. This is the case of the previously described missense variant c.167T > C [p.Leu56Ser] (rs8131520), which occurs in the N-terminal region of RUNX1.[13] This variant is relatively frequent in the general population (MAF 0.012 in GnomAD), and has a discrepant pathogenicity classification in several databases (COSMIC: Pathogenic; dbSNP: Likely Benign; ClinVar: Benign), according to its in silico prediction (MutationTaster: Causing disease; PROVEAN: Neutral; SIFT: Tolerated) and previous reports.[13–18] Therefore, murine and/or induced pluripotent stem cell (iPSC) models may be useful not only for settling definitively the controversy about the pathogenicity of certain *RUNX1* variants, but also for elucidating the mechanisms of molecular pathogenesis.[18,19]

In this study, we have used the CRISPR/Cas9 genome editing technology to create a knock-in murine model of the RUNX1 p.Leu56Ser variant. Detailed platelet and hemostasis phenotyping suggests that this relatively common RUNX1 variant has a deleterious effect in our murine model.

## Methods

Further details of the experimental procedures are available in the online Supplementary Material.

### Generation of RUNX1 p.Leu56Ser Murine Model

Two complementary RNA guides (single-guide RNAs, sgRNAs) targeting *Runx1* exon 2, Cas9 nickase mRNA, and a single-strand DNA oligonucleotide (ssODN) (Integrated DNA Technologies, IDT, Iowa, United States), carrying the c.127–128CT > TC alteration, were microinjected into the pronucleus of one-cell-stage embryos from superovulated C57BL/6J females, and transferred to foster CD1 females. Littermates were genotyped by polymerase chain reaction (PCR) target amplification and Sanger sequencing (►**Supplementary Tables S1** and **S2**, available in the online version).

Mice were housed in the Servicio de Experimentación Animal (SEA), Salamanca (Spain), a temperature-controlled specific-pathogen-free animal house facility. In total, 75 mice were analyzed, 25 of each of three genotypes (RUNX1$^{WT/WT}$, RUNX1$^{WT/L43S}$, and RUNX1$^{L43S/L43S}$), in the functional studies, except where otherwise indicated. All experiments were performed at least in duplicate.

### Platelet Phenotyping of the RUNX1 p.Leu56Ser Mouse Model

#### Tail Bleeding

Mouse tail-bleeding time and volume were measured as previously described.[20,21] Briefly, a 5-mm incision was made in the tip of the tail of 3-week-old mice that had been previously anesthetized with 2.5% isoflurane. Time to cessation of blood flow and bleeding volume were recorded. Tests were stopped if the bleeding time reached 8 minutes.

#### Platelet Count

Blood (15 µL) was collected from the submandibular vein of adult mice and anticoagulated with EDTA. Whole blood was diluted in 800 µL of Tyrode's-HEPES buffer; 30 µL of diluted blood was stained with rat anti-mouse CD41–APC antibody (Thermo Fisher) for 15 minutes in the dark at room temperature (RT), and suspended in 500 µL of Tyrode's-HEPES

buffer. The number of platelets was determined in 50 µL volumes of blood using an Accuri C6 cytometer (BD Biosciences, California, United States).[21]

### Analysis of Platelet Structure and Receptor Levels

Platelet sizes, as well as glycoprotein VI (GPVI), GPIb, and integrin $\alpha_{IIb}\beta_3$ levels on the platelet surface, were evaluated by flow cytometry, as previously described.[22,23]

### Platelet Function Tests

Mouse platelet function was assessed by flow cytometry procedures.[24] Blood (100 µL) was collected from the submandibular vein of adult mice into tubes containing 400 µL of TBS/heparin 20 U/mL. Whole blood was diluted (1:8) in Tyrode's HEPES buffer. Samples were incubated (15 minutes at RT) with selected agonists at various doses (α-thrombin [0.1–1.0 U/mL], phorbol 12-myristate 13-acetate [PMA; 3 µM], adenosine diphosphate [ADP; 30 µM; Sigma-Aldrich, Missouri, United States], and C-reactive protein [CRP; 10 µg/mL; Stago, France]), in the presence of fluorophore-conjugated monoclonal antibodies. Rat anti-mouse JON/A–PE antibody (Emfret Analytics, Germany) or AlexaFluor-488 labeled fibrinogen (Molecular Probes, Oregon, United States) was used to evaluate conformational activation of integrin $\alpha_{IIb}\beta_3$, rat anti-mouse CD62P–FITC antibody (BD Pharmingen, California, United States) was used to evaluate P-selectin secretion from α-granules, and/or rat anti-mouse CD63–APC antibody (Biolegend, California, United States) was used to assess δ-granule secretion. Results were represented as the percentage of positive platelets for each antibody upon acquisition of 30,000 CD41–APC platelets.

To evaluate platelet aggregation by flow cytometry,[25] separate blood samples were incubated with fluorescein isothiocyanate (FITC)- and PE-labeled rat anti-mouse CD9 antibody (Biolegend), then mixed (30 µL:30 µL) and incubated with the selected agonist for different times (0, 1, 5, 10, and 15 minutes) at 37°C with mild shaking. Results were represented as the percentage of double-positive FITC and PE CD9 platelets.

Reactions were stopped by dilution, and samples were run in an Accuri C6 cytometer (BD Biosciences, California, United States). The platelet population was analyzed using FlowJo V10 (Tree Star, Inc., Oregon, United States) software.

Platelet aggregation was validated with a light transmission aggregometry (LTA) assay, and ATP release was evaluated after 10 minutes of aggregation.

### Platelet Adhesion and Spreading Assays

Blood from groups of four mice/genotype ($1 \times 10^8$ platelets) were obtained by cardiac puncture into trisodium citrate microtubes, and then pooled. Washed platelets in Tyrode's-HEPES buffer were stimulated with thrombin 0.5 U/mL for 1 minute at RT and spread on poly-L-lysine (Sigma-Aldrich) or fibrinogen (Sigma-Aldrich)-coated coverslips for different times at 37°C. For the adhesion assay, washed platelets were coated on collagen (StemCell Technologies, Canada) or fibrinogen coverslips.

In all cases, coverslips were incubated with Oregon Green 514 Phalloidin (Thermo Fisher) for 20 minutes at RT in the dark.[21] Samples were visualized using a Leica TCS-SP8 confocal microscope, and images were analyzed using ImageJ software (National Institutes of Health, Maryland, United States).

Platelet adhesion was estimated as the percentage of platelet-covered area in 15 fields (100x) for each combination of genotype and condition. Spreading was evaluated as the platelet area (12,000x) (15 platelets/genotype per condition).

### Clot Retraction

Platelet-rich plasma (PRP) ($1 \times 10^8$ platelets), supplemented with 400 µL of Tyrode's-HEPES buffer and 10 µL of red blood cells, from four mice/genotype, were stimulated with thrombin 1 U/mL. Platelet-poor plasma was used as a negative control. Clot retraction was evaluated over 2 hours, and determined by its weight, as previously described.[26]

### Immunofluorescence Assays

Washed platelets, obtained from the combined blood of four mice/genotype, were stimulated with thrombin 1 U/mL or PMA 3 µM (1 minute at 37°C, and shaken at 900 rpm). Samples were incubated on coverslips with monoclonal antiphospho-PKCα/β (Thr638/641) antibody (Cell Signaling Technology, Inc., Massachusetts, United States), and anti-rabbit Cy3 antibody (Jackson Immunoresearch, United Kingdom) as the secondary antibody. The actin platelet structure was distinguished by incubation with Oregon Green 514 Phalloidin (Thermo Fisher).[21]

PKC phosphorylation was assessed by ImageJ, measuring the mean fluorescence intensity of Cy3 in ten 12,000 × -fields per condition and genotype.

### RNA Isolation and Quantitative PCR

PRP samples from three mice/genotype were obtained by cardiac puncture. Platelet pellets were resuspended in RLT-plus lysis buffer from an RNeasy kit (Qiagen, Germany), following the manufacturer's specifications for total RNA extraction.

To measure the levels of expression of *Prkca* and *Prkcb*, 50 ng of total mRNA was in vitro retrotranscribed using a SuperScript III First-Strand Synthesis Super Mix kit (Thermo Fisher). *Prkca* and *Prkcb* mRNAs were quantified by quantitative PCR (Applied Biosystems, California, United States) using gene-specific oligonucleotides (►**Supplementary Table S3**, available in the online version) and SYBR Green PCR Master Mix (Applied Biosystems). *Gapdh* mRNA expression was used as an internal control (►**Supplementary Table S3**, available in the online version). The experiments were performed in triplicate for each data point. The relative levels of gene expression were quantified using the $2^{-\Delta Ct}$ method.[27]

### Megakaryopoiesis

Bone marrow cells (BMCs) from six mice per genotype were used. The megakaryocytes (MKs) were enriched by culturing BMCs in the presence of thrombopoietin (TPO, Innovative Research, Michigan, United States) for 5 days to promote megakaryopoiesis. Assessment of MK counts, differentiation and maturation, and the DNA content of MKs was analyzed by flow cytometry, as previously described.[28]

### Ethics Statement

All experimental procedures were conducted in accordance with the guidelines of the National Institutes of Health Guide for the Care and Use of Laboratory Animals, and were approved by the Bioethics Committee of the University of Salamanca and the Junta de Castilla y León, Spain (0000107).

### Statistical Analysis

Data were summarized as the mean ± standard error of the mean (SEM). Differences between experimental groups were analyzed by means of an unpaired Student's *t*-test (for normally distributed data) or the Mann–Whitney U-test (for nonnormally distributed data). Differences were considered significant for values of $p < 0.05$.

## Results

### Developing the RUNX1 p.Leu56Ser Murine Model Using the CRISPR/Cas9 System

The *knock-in* murine model was developed by integrating the point alteration c.127–128CT > TC by homologous recombination. Two founder mice were generated, giving rise to the RUNX1 p.Leu43Ser mouse variant in heterozygosis and mimicking the p.Leu56Ser human variant (►**Fig. 1A, B**).

A total number of 75 mice; 25 per genotype ($RUNX1^{WT/WT}$, $RUNX1^{WT/L43S}$, and $RUNX1^{L43S/L43S}$), were generated by cross-breeding. The generated allele was transmitted at frequencies consistent with the principles of Mendelian inheritance.

To ensure that the potential effects observed in edited mice were attributable to the RUNX1 variant, and despite using Cas9 nickase, which produces single-strand breaks and thereby minimizes off-targets,[29] we analyzed the sequences of the top-10 sgRNA-predicted off-targets. PCR and Sanger sequencing identified no off-targets in mice of F3 and subsequent generations when analyzing sgRNA targets together or individually (data not shown).

### Effect of the RUNX1 p.Leu43Ser Variant on Hemostasis and Platelet Count and Function

To study the effect of the RUNX1 p.Leu43Ser variant on hemostasis, we performed tail-bleeding assays in mice at weaning. As shown in ►**Fig. 2A**, $RUNX1^{L43S/L43S}$ and $RUNX1^{WT/L43S}$ mice had longer bleeding times than $RUNX1^{WT/WT}$ (170.1 ± 26.8 and 154.4 ± 26.0 vs. 94.2 ± 14.2 seconds; $p = 0.016$ and 0.048, respectively), and increased bleeding volume (data not shown). No significant differences in bleeding times were observed between $RUNX1^{L43S/L43S}$ and $RUNX1^{WT/L43S}$ ($p = 0.68$).

We also found that the platelet count in $RUNX1^{L43S/L43S}$ was slightly, but significantly, lower than in $RUNX1^{WT/L43S}$ and $RUNX1^{WT/WT}$ mice (480.9 ± 28.1 vs. 563.3 ± 28.2 and 587.2 ± 29.2 [$\times 10^3$] platelets/ μL; $p = 0.044$ and 0.012, respectively) (►**Fig. 2B**). No differences in the platelet size or their expression of GPVI, GPIb-IX, and integrin $\alpha_{IIb}\beta_3$ was found between the genotypes (►**Supplementary Fig. S1**, available in the online version).

To investigate mild thrombocytopenia in $RUNX1^{L43S/L43S}$ mice further, we evaluated the megakaryopoiesis process in vitro. First, we found no differences in MK production between the genotypes (►**Supplementary Fig. S2A**, available in the online version). Moreover, MKs cultured in the presence of TPO for 5 days revealed no differences in MK polyploidy over that period (►**Supplementary Fig. S2B**, available in the online version). MK maturation on days 0 and 2 of TPO stimulation was similar in all genotypes (►**Supplementary Fig. S2C**, available in the online version). In contrast, we observed a slight reduction in CD41+ CD61+ MKs after 5 days of TPO culture in the $RUNX1^{L43S/L43S}$ mice when compared with $RUNX1^{WT/WT}$ (66.8 ± 1.6 vs. 77.0 ± 2.0%, $p = 0.018$), while all mice had similar levels of CD42b+ CD61+ MKs (►**Supplementary Fig. S2C**, available in the online version). These results suggest that maturation and differentiation of megakaryoblast (CD41+ CD61+ CD42 − ) and/or promegakaryocyte (CD41+ CD61+ CD42 +/− ) in the $RUNX1^{L43S/L43S}$ mice may have been delayed, which would account for their slightly lower platelet count.

As regards the effect of the p.Leu43Ser variant on the platelet function phenotype, $RUNX1^{L43S/L43S}$ and $RUNX1^{WT/L43S}$ displayed significantly lower levels of binding of JON/A antibody (►**Fig. 3A**) than $RUNX1^{WT/WT}$, in response to platelet activation with thrombin and PMA (10.6 ± 0.6 and 12.0 ± 1.2% vs. 16.8 ± 0.9%; $p < 0.001$ and $p = 0.003$, respectively). These results suggest that the variant has a deleterious effect on the agonist-induced conformational change of integrin $\alpha_{IIb}\beta_3$ (the inside-out signaling pathway). This hypothesis was supported by a reduction in fibrinogen binding in $RUNX1^{L43S/L43S}$ and $RUNX1^{WT/L43S}$ compared with $RUNX1^{WT/WT}$ after thrombin and PMA treatment, or following treatment with ADP (►**Fig. 3B**). No differences were found in fibrinogen binding after treatment with CRP between mice of all three genotypes (►**Fig. 3B**).

In addition, similar platelet hyporesponsiveness of $RUNX1^{L43S/L43S}$ and $RUNX1^{WT/L43S}$ mice was observed when evaluating P-selectin secretion from α-granules after stimulation with thrombin and PMA (►**Fig. 3C**). In contrast, platelet CD63 secretion from δ-granules was similar in both genotypes (►**Fig. 3D**). No significant differences were either detected in ATP release after stimulation with thrombin and PMA (►**Fig. 3E**), ruling out a functional defect in δ-granule secretion in RUNX1 p.Leu43Ser mutant mice.

Platelet aggregation was also investigated by flow cytometry assay using PMA, high and low doses of thrombin, and ADP (►**Fig. 4**), and by LTA (►**Supplementary Fig. S3**, available in the online version). $RUNX1^{L43S/L43S}$ and $RUNX1^{WT/L43S}$ mutant mice displayed significantly less aggregation in response to PMA than did wild-type (WT) animals at different times (►**Fig. 4A**) (platelet aggregates: 22.1 ± 2.8 and 19.4 ± 2.5% vs. 36.6 ± 3.1%; $p = 0.001$ and $p < 0.001$, respectively, with PMA 5 minutes; 42.5 ± 5.4 and 48.6 ± 4.4% vs. 69.2 ± 3.3%, $p < 0.001$ and $p = 0.001$, with PMA 10 minutes; 54.7 ± 5.2 and 64.0 ± 4.0% vs. 80.7 ± 2.6%, $p < 0.001$ and $p = 0.001$, with PMA 15 minutes). The aggregation responses to high doses of thrombin (0.5 U/mL) and ADP were significantly lower in $RUNX1^{L43S/L43S}$ than in $RUNX1^{WT/WT}$ mice (►**Fig. 4B, C**). Otherwise, $RUNX1^{WT/L43S}$ mice showed significantly less aggregation in the short term after agonist stimulation, and a trend toward less aggregation over longer periods (►**Fig. 4B, C**). LTA results validated the hypoaggregation ability of the mutant murine platelets after high doses

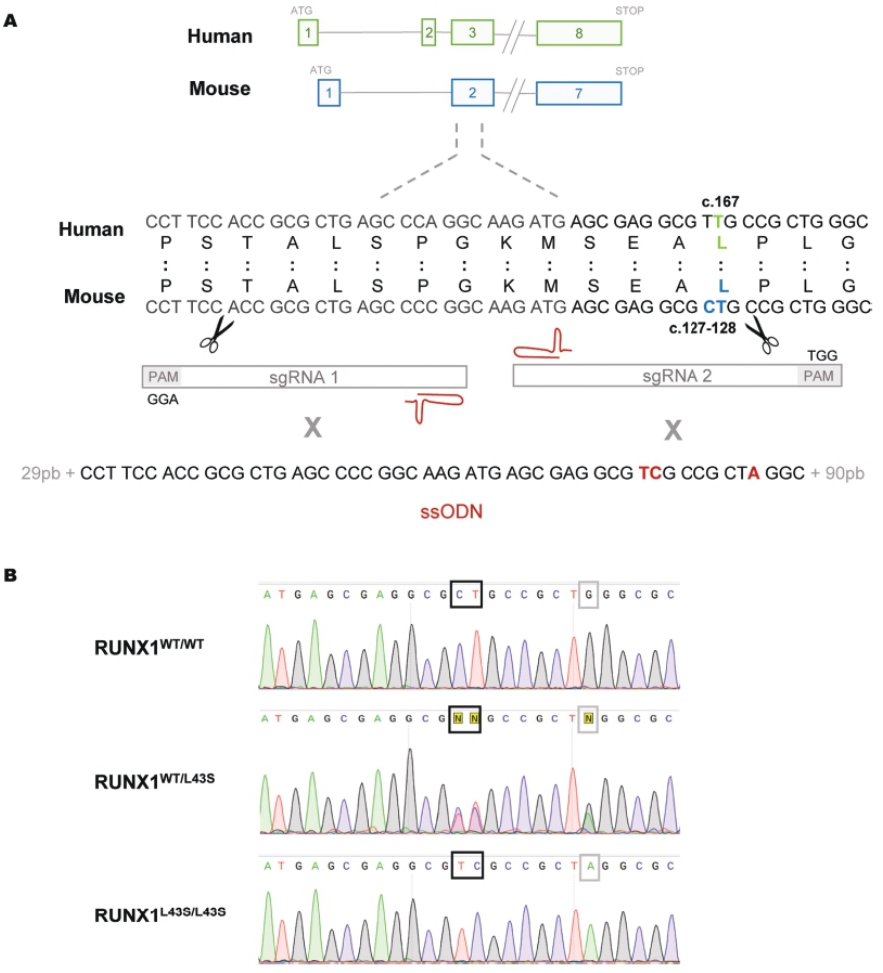


**Fig. 1** Generation of the RUNX1 p.Leu56Ser murine model by the CRISPR/Cas9 genome editing system. (**A**) Schematic representation of the targeting strategy used to generate the murine model reproducing the human alteration. The alignment of sequences (*RUNX1*: ENST00000300305.7; *Runx1*: ENSMUST00000023673.13) showed homology between human and mouse: the human c.167T (amino acid Leu56) is correlated with the murine c.127–128CT (amino acid Leu43). Two sgRNAs were designed close to the site to be edited and spaced closer than 100 bp, driving Cas9 nickase to produce single-strand cuts in both strands of DNA (sgRNA1 antisense; sgRNA2 sense), but mimicking double-strand cuts, which will lead to homologous reparation using an ssODN template. ssODN carries the point alteration c.127–128CT > TC, leading to the p.Leu43Ser amino acid change in the RUNX1 protein, and a silent mutation that destroys the PAM sequence of sgRNA2. (**B**) DNA sequence of WT ($RUNX1^{WT/WT}$), heterozygous ($RUNX1^{WT/L43S}$) and homozygous ($RUNX1^{L43S/L43S}$) carriers of the alteration. *Black squares* indicate the region of interest c.127–128CT > TC, while *gray squares* represent the mutated base that destroys the PAM sequence, working as a homologous recombination control. sgRNA, single-guide RNA; ssODN, single-strand DNA oligonucleotide.

of thrombin treatment (►**Supplementary Fig. S3**, available in the online version).

No differences in platelet aggregation were observed between genotypes upon short-duration stimulation with low doses of thrombin (0.1 U/mL) and 2 mM $CaCl_2$ (►**Fig. 4D**). These results suggest that early platelet activation, which is highly dependent on calcium-mediated pathways, is unaffected in mutant mice, while a second sustained peak of activation with high doses and long periods of thrombin or PMA stimulation, mediated by the PKC pathway,[30] is impaired by the presence of the p.Leu43Ser variant.

In this context, we evaluated the platelet level of phospho-PKCα/β by immunofluorescence. Thus, PMA and thrombin-stimulated platelets produced a higher level of PKC phosphorylation than noted in resting platelets (►**Fig. 5A**). We found a significantly lower level of PKC phosphorylation after stimulation with PMA 3 µM in $RUNX1^{L43S/L43S}$ and $RUNX1^{WT/L43S}$ mice compared with $RUNX1^{WT/WT}$ ($7.2 \pm 0.9$ and $7.1 \pm 0.7$ vs. $12.3 \pm 0.5$; $p < 0.001$ and $p < 0.001$, respectively) (►**Fig. 5B, D**). Moreover, $RUNX1^{L43S/L43S}$ had lower levels of p-PKC than $RUNX1^{WT/WT}$ upon stimulation with thrombin 1 U/mL ($7.0 \pm 0.7$ vs. $10.0 \pm 0.8$; $p = 0.027$) (►**Fig. 5C, D**). We next

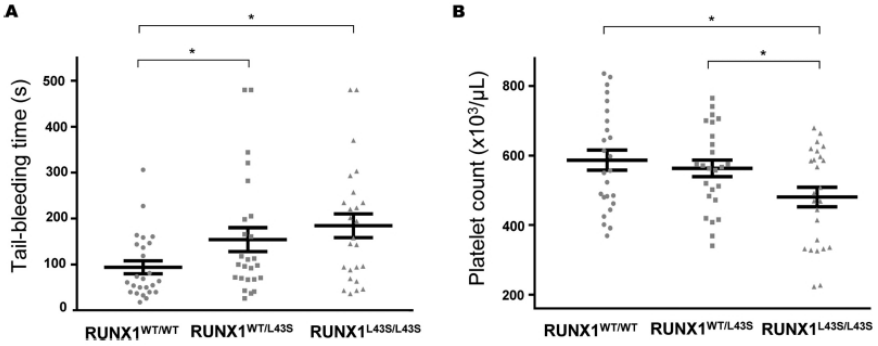


**Fig. 2** The RUNX1 p.Leu43Ser variant alters platelet hemostasis in mice. (**A**) Tail-bleeding assay in RUNX1$^{WT/WT}$, RUNX1$^{WT/L43S}$, and RUNX1$^{L43S/L43S}$ mice at weaning. The scatter plots indicate the bleeding time of 25 animals per genotype. The mean ± SEM are shown. (**B**) Platelet count of RUNX1$^{WT/WT}$, RUNX1$^{WT/L43S}$, and RUNX1$^{L43S/L43S}$ mice. The scatter plots indicate the APC-labeled anti-CD41+ platelets. The mean ± SEM are shown. $^{*}p < 0.05$. SEM, standard error of the mean.

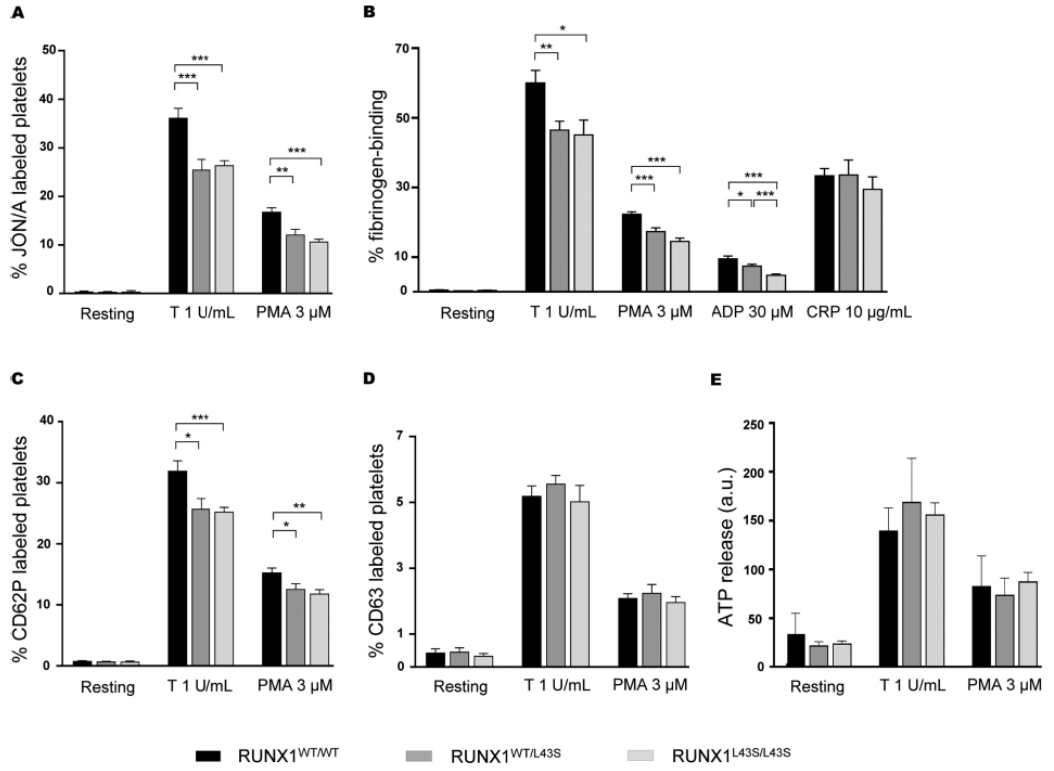


**Fig. 3** RUNX1 p.Leu43Ser variant impairs platelet activation of integrin $\alpha_{IIb}\beta_3$ and α-granule secretion. (**A**)–(**D**) Whole blood from RUNX1$^{WT/WT}$, RUNX1$^{WT/L43S}$, and RUNX1$^{L43S/L43S}$ mice were (A) nonstimulated, stimulated with thrombin 1 U/mL and PMA 3 µM, and incubated with JON/A–PE antibody to detect the conformational change of the activated integrin $\alpha_{IIb}\beta_3$; (B) nonstimulated and stimulated with thrombin 1 U/mL, PMA 3 µM, ADP 30 µM, and CRP 10µg/mL in combination with Alexa Fluor 488-labeled fibrinogen, to detect the percentage of platelets with activated integrin $\alpha_{IIb}\beta_3$; (C) nonstimulated, stimulated with thrombin 1 U/mL and PMA 3 µM, and incubated with anti-CD62P–FITC to determine the percentage of platelets presenting P-selectin on the surface, as a measure of α-degranulation; (D) nonstimulated, stimulated with thrombin 1 U/mL and PMA 3 µM, both supplemented with $CaCl_2$ 2 mM, and labeled with CD63–APC to detect δ-granule secretion. The histograms represent mean ± SEM of the percentage of labeled platelets. (**E**) ATP release from δ-granules in RUNX1$^{WT/WT}$, RUNX1$^{WT/L43S}$, and RUNX1$^{L43S/L43S}$ washed platelets, after 10 minutes of nonstimulation, and thrombin 1 U/mL and PMA 3 µM stimulation. The histograms show the mean ± SEM of the luminescence (arbitrary units). $^{*}p < 0.05$; $^{**}p < 0.01$; $^{***}p < 0.001$. SEM, standard error of the mean.

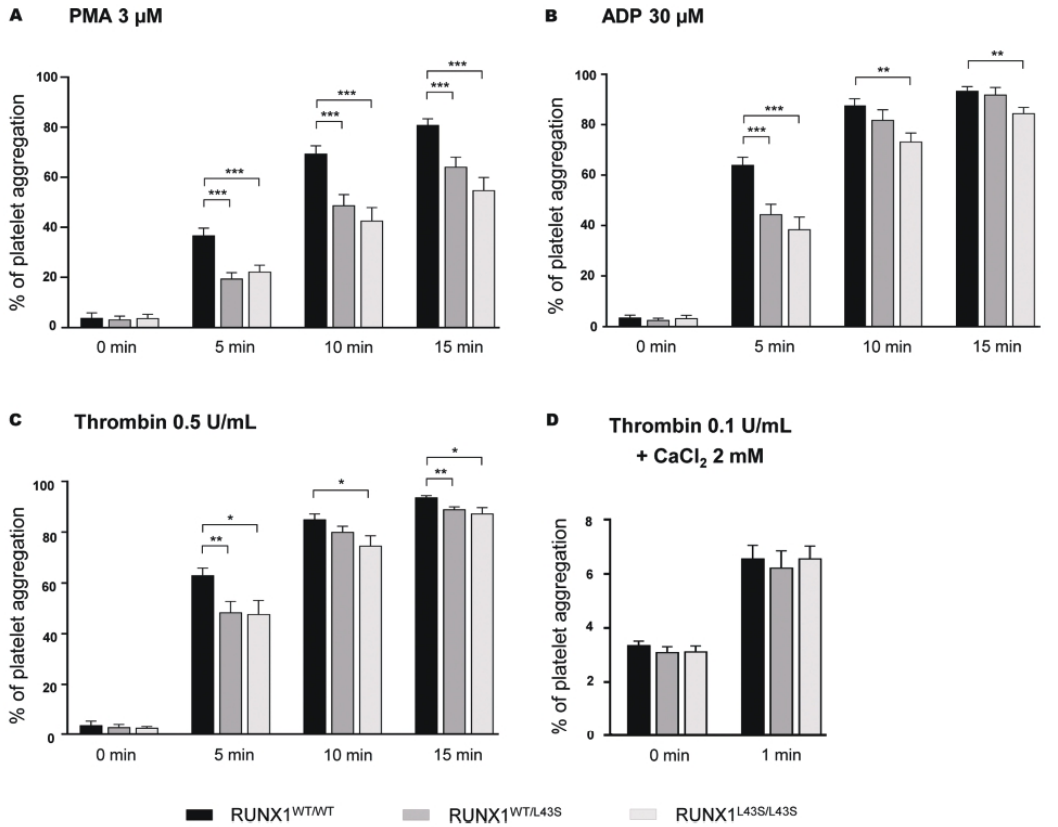


**Fig. 4** RUNX1 p.Leu43Ser variant mice display impaired platelet aggregation with several agonists. Histograms show the mean ± SEM of the percentage of platelet aggregation in RUNX1$^{WT/WT}$, RUNX1$^{WT/L43S}$, and RUNX1$^{L43S/L43S}$ at different times after stimulation of diluted whole blood with (**A**) PMA 3 µM, (**B**) ADP 30 µM, (**C**) thrombin 0.5 U/mL, and (**D**) thrombin 0.1 U/mL, supplemented with $CaCl_2$ 2 mM. $^{*}p < 0.05$; $^{**}p < 0.01$; $^{***}p < 0.001$. SEM, standard error of the mean.

explored whether this alteration in PKCα/β phosphorylation could be explained by lower levels of expression of *Prkca* and *Prkcb*, which code for PKCα and PKCβ. As shown in ►**Fig. 5E**, no differences in mRNA expression were found in PKCα or PKCβ, suggesting that the impaired PKC-mediated platelet response associated with p.Leu43Ser RUNX1 variant is not due to PKCα/β deficiency at the transcriptional level.

We also examined whether the hypoactivation of the integrin $\alpha_{IIb}\beta_3$ affects the signaling cascades that trigger cytoskeletal reorganization and platelet spreading through outside-in signaling pathways. As illustrated in ►**Fig. 6**, the poly-L-lysine coverslips revealed a reduced platelet area in RUNX1$^{L43S/L43S}$ and RUNX1$^{WT/L43S}$ versus RUNX1$^{WT/WT}$ after 30 minutes of thrombin 0.5 U/mL stimulation ($7.3 \pm 0.4$ and $7.9 \pm 0.3\,\mu m^2$ vs. $12.1 \pm 2.1\,\mu m^2$, $p = 0.037$ and $p = 0.06$) (►**Fig. 6A, B**). This result suggested that there was a defect in the cytoskeleton remodeling required for platelet spreading after thrombin stimulation. Analysis of fibrinogen-coated coverslips at different times revealed remarkable differences in both RUNX1$^{L43S/L43S}$ and RUNX1$^{WT/L43S}$ mice compared with WT, such as alterations in platelet shape and incomplete spreading (►**Fig. 6A, C**). There were no apparent alterations in filopodium formation, as these structures appear quickly after platelet stimulation, when no differences in platelet area were found (poly-L-lysine: 5 minutes). However, after long periods of stimulation and/or in the presence of fibrinogen, the absence of full spreading could be explained by an alteration in lamellipodium formation. This alteration in the outside-in signaling through platelet integrin $\alpha_{IIb}\beta_3$ in RUNX1$^{L43S/L43S}$ and RUNX1$^{WT/L43S}$ mice was supported by the observation of a lower capacity of clot retraction in these animals compared with RUNX1$^{WT/WT}$ mice (►**Supplementary Fig. S4**, available in the online version).

Finally, we found no differences between the genotypes in the platelet-covered area in collagen-coated coverslips, suggesting normal platelet adhesion mediated by the GPIa/IIa and GPVI-signaling pathways (►**Fig. 7**). Adhesion to fibrinogen coverslips was less extensive in RUNX1$^{L43S/L43S}$ and RUNX1$^{WT/L43S}$ than in RUNX1$^{WT/WT}$ ($1.5 \pm 0.2$ and $1.4 \pm 0.2\%$ vs. $3.1 \pm 0.2\%$, $p < 0.001$ and $p < 0.001$, respectively) (►**Fig. 7**), according to the previous alteration detected by flow cytometry in the integrin $\alpha_{IIb}\beta_3$

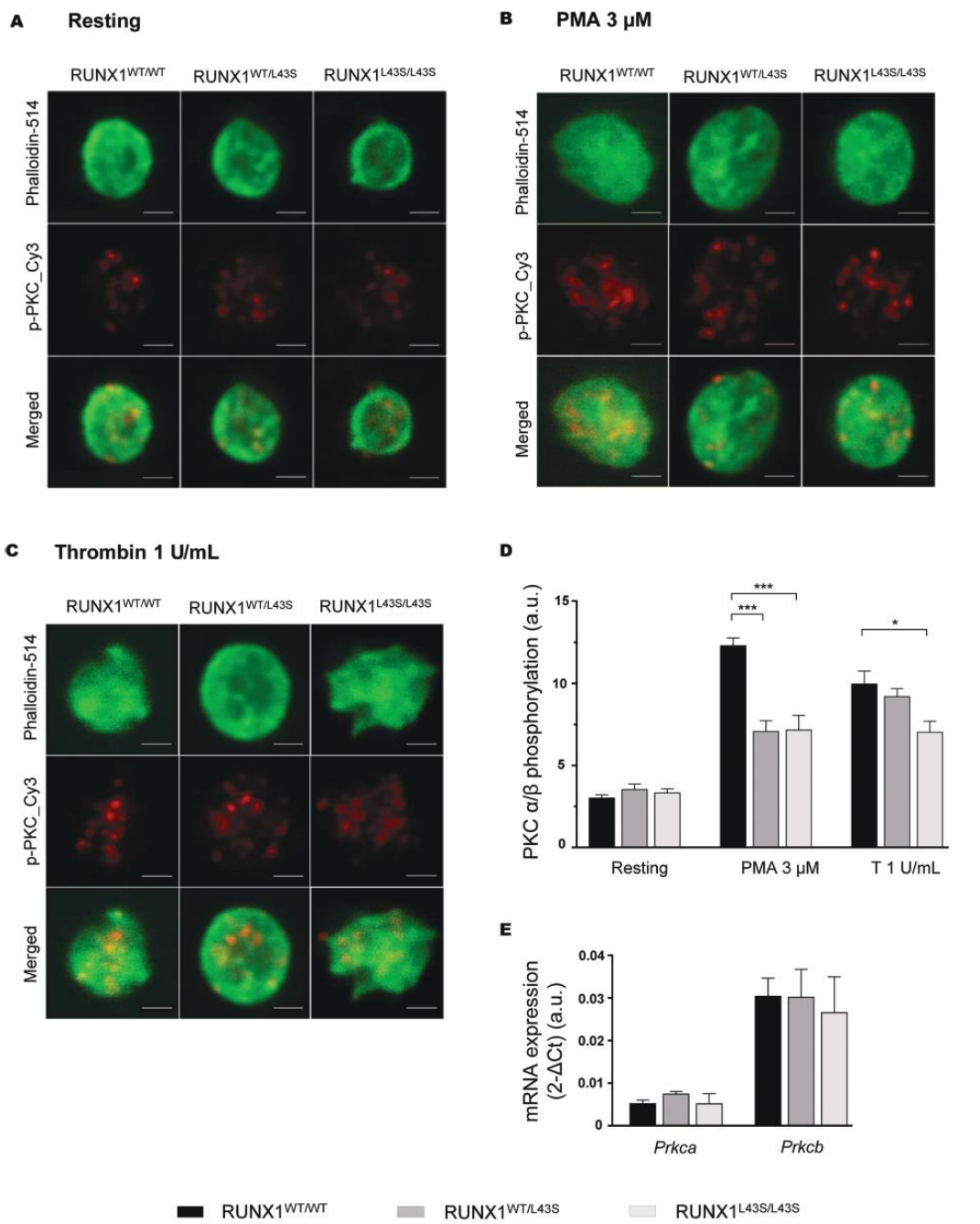


**Fig. 5** The deleterious effect of the RUNX1 p.Leu43Ser variant on platelet function is related to impaired PKC phosphorylation. (**A**)–(**C**) Representative immunofluorescence confocal microscopy images of platelets of each genotype. RUNX1$^{WT/WT}$, RUNX1$^{WT/L43S}$, and RUNX1$^{L43S/L43S}$ platelets were labeled with anti-pPKC_Cy3 (*red*) and phalloidin (actin, *green*) after treatment with (A) vehicle, (B) PMA (3 µM), and (C) thrombin (1 U/mL). (**D**) Histogram showing p-PKC levels of resting platelets and cells activated with PMA or thrombin 1 U/mL. The fluorescence intensity (arbitrary units) was quantified by ImageJ. (**E**) *Prkca* and *Prkcb* mRNA expression (arbitrary units) in RUNX1$^{WT/WT}$, RUNX1$^{WT/L43S}$, and RUNX1$^{L43S/L43S}$ platelets. Histogram represents the mean ± SEM of values using the $2^{-\Delta Ct}$ method. Bar: 1 µm. $^{*}p < 0.05$; $^{***}p < 0.001$. SEM, standard error of the mean.

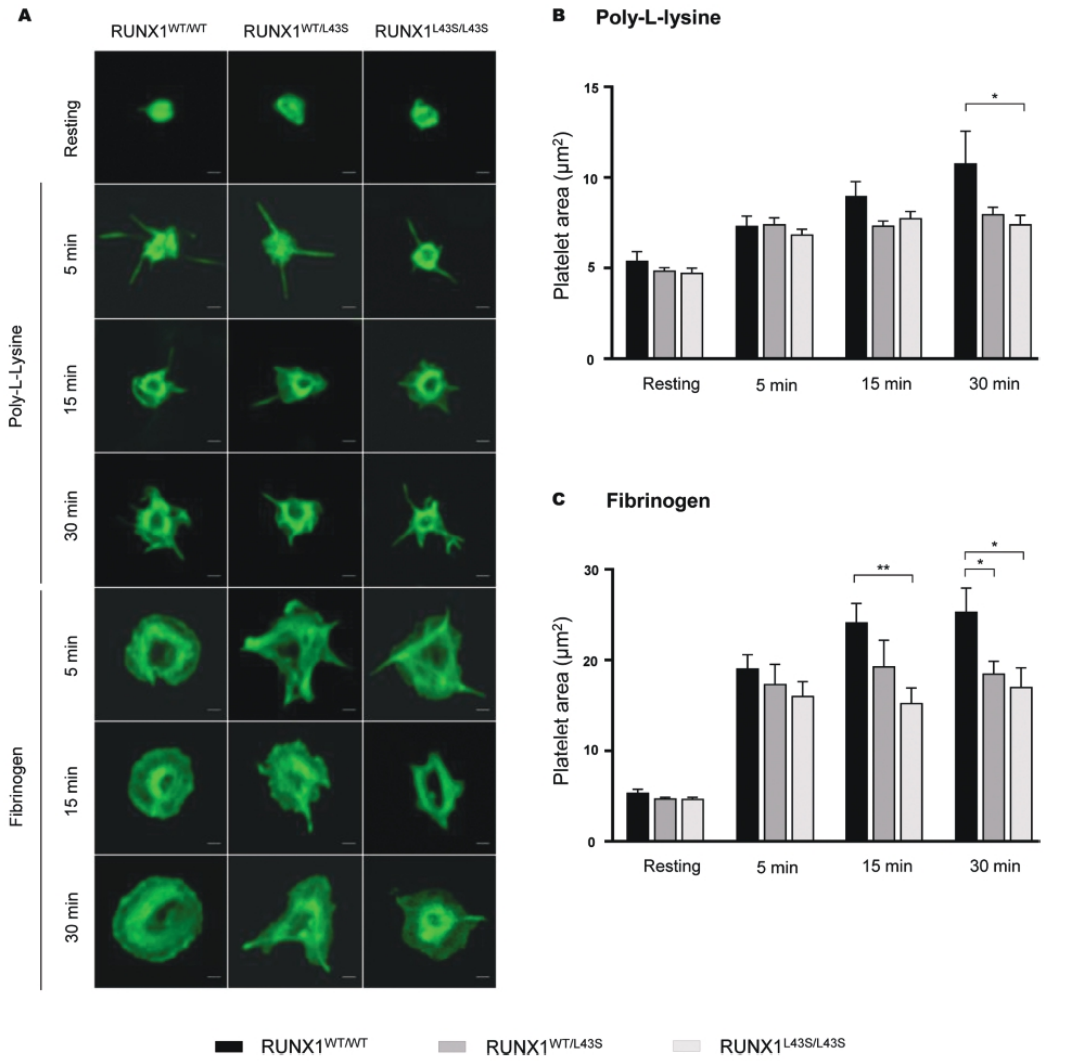


**Fig. 6** Platelets of RUNX1 p.Leu43Ser variant mice show impaired spreading. (**A**) Representative immunofluorescence confocal microscopy images of RUNX1$^{WT/WT}$, RUNX1$^{WT/L43S}$, and RUNX1$^{L43S/L43S}$ platelets after nonstimulation and stimulation with thrombin 0.5 U/mL for 5, 15, and 30 minutes, spread in poly-L-lysine and fibrinogen coverslips. (**B** and **C**) Histogram showing the platelet area in (B) poly-L-lysine coverslips and (C) fibrinogen coverslips. Values are the mean ± SEM of the platelet area, analyzed using ImageJ. Bar: 1 µm. $^{*}p < 0.05$; $^{**}p < 0.01$. SEM, standard error of the mean.

activation and by fibrinogen binding in RUNX1$^{L43S/L43S}$ and RUNX1$^{WT/L43S}$ versus RUNX1$^{WT/WT}$.

## Discussion

The clinical presentation of FPD/AML is remarkably heterogeneous. The severity of the bleeding disorder differs among affected individuals as a consequence of abnormal MK differentiation and polyploidization, impaired platelet formation, and/or the severity of the functional platelet defect.[31] About 40% of patients who are carriers of RUNX1 variants may develop AML or mixed myeloproliferative (myeloproliferative neoplasm)/MDS syndromes, while, in other carriers, no malignancy is developed over the life course.[32] The implementation of HTS platforms in routine clinical practice has enabled the identification of *RUNX1* variants in some patients with suspected IPD who lack a specific phenotype.[7,10] However, the definitive diagnosis of FPD/AML in these patients requires an accurate assessment of the pathogenicity of their *RUNX1* variants.[16,17]

In this context, the p.Leu56Ser alteration in RUNX1 has been found in some patients with clinical and laboratory suspicion of FPD/AML, but is also a relatively frequent variant in the general population (up to 0.017 in the European non-Finnish population, according to GnomAD). Although p.Leu56Ser is usually considered to be a benign or likely benign variant,[16] its pathogenic potential is yet to be clearly established.[14,15] In this study we used the novel CRISPR/Cas9 system technology to create a

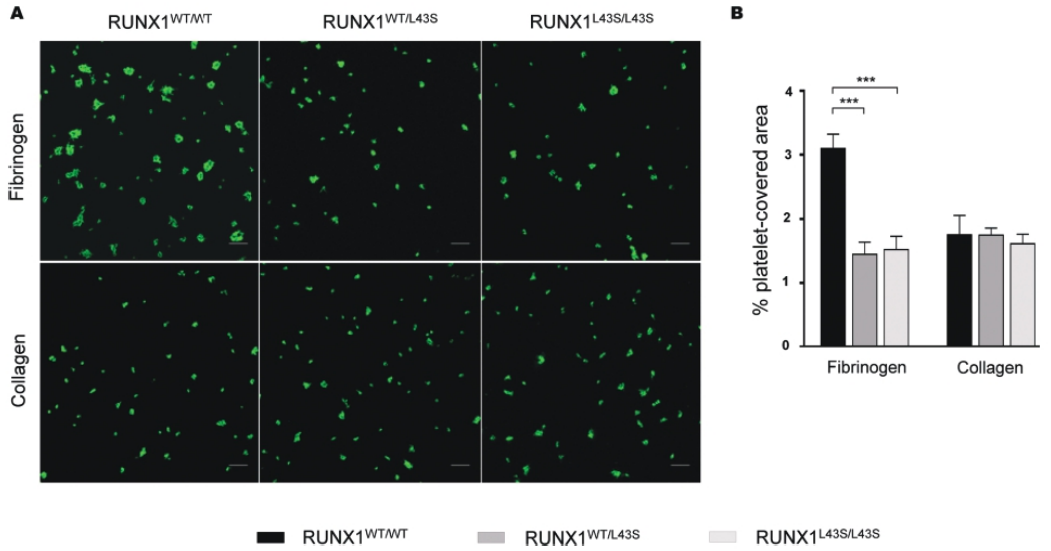


**Fig. 7** The RUNX1 p.Leu43Ser variant displays normal collagen–platelet adhesion, but impaired fibrinogen binding. (**A**) Representative immunofluorescence confocal microscopy images of adhesion to fibrinogen and collagen coverslips of RUNX1$^{WT/WT}$, RUNX1$^{WT/L43S}$, and RUNX1$^{L43S/L43S}$ platelets after treatment with thrombin 0.5 U/mL for 1 minute. (**B**) Histogram showing platelet adhesion, measured as the percentage of area covered by platelets on a fibrinogen and collagen surface. The mean ± SEM are shown. Bar: 10 µm. $^{***}p < 0.001$. SEM, standard error of the mean.

*knock-in* murine model carrying RUNX1 p.Leu43Ser (equivalent to human p.Leu56Ser), with the aim of specifically assessing the effect of this variant on the bleeding and platelet phenotype.

Thrombocytopenia with normal platelet volume occurs in many, but not all, FPD/AML patients,[14,16,31,33] while a varying degree of platelet dysfunction is present in most affected patients.[34,35] Consistent with this, we found RUNX1$^{L43S/L43S}$ mice to have mild thrombocytopenia, with unaffected platelet size, compared with RUNX1$^{WT/L43S}$ and RUNX1$^{WT/WT}$ animals. Our in vitro megakaryopoiesis experiments suggested that the reduced platelet count is related to a slightly delayed MK maturation during the middle stages of megakaryopoiesis in RUNX1$^{L43S/L43S}$ mice. Otherwise, RUNX1$^{WT/L43S}$ mice showed a normal platelet count, indicating a dose-allele effect of the variant in platelet production, thereby highlighting the relevance of allele burden in the clinical presentation of *RUNX1*-RD.[36] The finding of mildly, but significantly longer tail-bleeding time and increased bleeding volume in RUNX1$^{L43S/L43S}$ and RUNX1$^{WT/L43S}$ mice strongly suggests that the p.Leu43Ser variant impairs normal hemostasis. This is unlikely to be due to the small reduction in platelet count, since only severe thrombocytopenia ($<200 \times 10^3$ platelets/µL) compromised hemostasis and increased tail-bleeding times in mice.[37] Thus, the abnormal hemostasis reflected in the prolonged bleeding time and volume may be explained by impaired platelet function, similar to that observed in FPD/AML patients.[14,16,31,33] The evident platelet dysfunction found in the heterozygous mice is consistent with the autosomal dominant effect described in FPD/AML patients.

RUNX1$^{L43S/L43S}$ and RUNX1$^{WT/L43S}$ mice displayed no changes in GP expression levels, but they did experience impaired agonist-induced platelet activation, granule secretion, aggregation, and spreading.

The fact that the RUNX1 p.Leu43Ser variant impaired agonist-induced α-granule secretion, but not δ-granule release, is not surprising, since they do not share the same secretory mechanisms.[38] However, these findings are different from the reduced secretion of the α- and δ-granules observed in many FPD/AML patients.[34] Defective fibrinogen/JONA binding and spreading in fibrinogen in mutant mice indicated that the deleterious effect of p.Leu43Ser affects $\alpha_{IIb}\beta_3$ integrin inside-out and outside-in signaling, respectively. It is worth mentioning that abnormal integrin $\alpha_{IIb}\beta_3$ activation has been previously reported in FPD/AML patients.[35,39,40] In one patient, the granule content was normal and this platelet dysfunction was considered to have arisen solely from a lower level of integrin $\alpha_{IIb}\beta_3$ function.[39] In contrast, in another pedigree, storage pool disease and impaired integrin $\alpha_{IIb}\beta_3$ activation both seemed to contribute to the phenotype,[35,40] highlighting the heterogeneity of platelet dysfunction in *RUNX1* carriers.

We found no differences between mutant and control mice in the analyses of platelet aggregation with low-dose thrombin when assays were performed in the presence of $CaCl_2$. After stimulation with thrombin, platelets are rapidly activated in a calcium-dependent pathway. However, thrombin induces a second wave of activation that is mediated by PKC, and mostly $Ca^{2+}$-independent.[30,41] Thus, our finding of impaired activation and aggregation with PMA could be explained by an alteration in the signaling pathways downstream of PKC.[30] This hypothesis is supported by the twin observations that platelet reactivity is

reduced in RUNX1$^{L43S/L43S}$ and RUNX1$^{WT/L43S}$ mice when exposed to high doses and long exposures of thrombin, while there is a normal aggregation response with low doses and short exposures to thrombin and $CaCl_2$.

Several PKC isoforms have been described in platelets that seem to have no redundant roles in platelet function. PKC-α is critically involved in granule secretion; PKC-β and PKC-θ have important roles in integrin $\alpha_{IIb}\beta_3$ outside-in signaling and platelet spreading on fibrinogen.[42] The phenotype observed in our murine model suggests a possible underlying PKC-α/β dysfunction. We observed significantly lower levels in thrombin-induced and especially in PMA-induced phosphorylation of PKC-α/β in RUNX1$^{L43S/L43S}$ and RUNX1$^{WT/L43S}$ compared with in RUNX1$^{WT/WT}$ mice, as assessed by immunofluorescence. This supports the hypothesis that the PKC-signaling pathway becomes altered. It is worth noting that *RUNX1* haplodeficiency downregulates transcription of *PRKCQ*, which codes for PKC-θ.[43] Studies in U937 cells have shown PKC-β to be a direct RUNX1 target,[44] although patients with *RUNX1* haplodeficiency had normal PKC-β.[45] In our murine model, we found no differences in the mRNA levels of *Prkca* and *Prkcb*, indicating that impaired PKC-mediated platelet response associated with the p.Leu43Ser RUNX1 variant is not due to PKC-α/β deficiency at the transcriptional level.

We found no differences between genotypes in vitro in platelet adhesion on collagen. This fact, in addition to the normal levels of GPVI detected on the platelet surface, suggests that RUNX1 p.Leu43Ser does not affect platelet adhesion under physiological conditions, although studies under flow conditions would be necessary to confirm this. Indeed, no differences in fibrinogen binding were found after platelet stimulation with CRP in mice of all three genotypes, suggesting normal collagen-mediated function. This result is in accordance with previous reports,[46] which have demonstrated that Par4 and GPVI receptor function in mice are independent, and therefore, thrombin- and collagen-induced platelet activation can play partially redundant roles. In contrast, we detected reduced levels of fibrinogen-platelet adhesion in RUNX1$^{L43S/L43S}$ and RUNX1$^{WT/L43S}$ compared with RUNX1$^{WT/WT}$ mice, which may be explained by the impaired activation of the integrin $\alpha_{IIb}\beta_3$. This defect was reinforced by the less extensive fibrinogen binding and defective spreading function in RUNX1$^{L43S/L43S}$ and RUNX1$^{WT/L43S}$ than in RUNX1$^{WT/WT}$, due to a delay in lamellipodium formation. All the results confirmed a mechanism of platelet dysfunction based on the outside-in activation signaling pathway, reinforced by the delay in the clot retraction detected in mice harboring the variant, especially in homozygosis.

Overall, the findings from our RUNX1 p.Leu56Ser murine model are highly consistent with the heterogeneity of platelet functional defects reported in FPD/AML patients.[33,47] The best animal model for reproducing human platelet diseases has yet to be developed.[48] While the murine model presented here is potentially useful, other groups have developed models of IPDs in zebrafish, or iPSC models.[19,49,50]

In conclusion, we have successfully used the CRISPR/Cas9 technology to generate an in vivo *knock-in* RUNX1 model of the p.Leu56Ser variant. This model has allowed us to demonstrate that this variant tends to exhibit bleeding due to moderate platelet dysfunction caused by several mechanisms. For this reason, the pathogenicity score of this variant may have to be revised.

## What is known about this topic?

- *RUNX1*-related disorder (*RUNX1*-RD) features heterogeneous clinical symptoms, such as thrombocytopenia and/or platelet function defects, which lead to bleeding. It has no specific clinical or laboratory phenotype, making genetic diagnosis necessary.
- Although international recommendations have been established to classify the pathogenicity of genetic variants, it is still a challenge to identify the alteration causing the disorder in *RUNX1*-RD, especially for variants of uncertain significance (VUS).

## What does this paper add?

- The generation of a *knock-in* murine model by the CRISPR/Cas9 technology has allowed us to evaluate the pathogenicity of a VUS in *RUNX1* identified in humans.
- This variant, p.Leu56Ser, in RUNX1 is related to the hypoactivation of the integrin $\alpha_{IIb}\beta_3$, and a functional alteration in the PKC-mediated signaling pathway. They are reflected in an aggregated, α-granule secretion, platelet-spreading defect, leading to prolonged bleeding times.

Funding
This work was partially supported by grants from Instituto de Salud Carlos III (ISCIII) and Feder (PI17/01311, PI17/01966, and CB15/00055), Fundación Séneca (19873/GERM/15), Gerencia Regional de Salud (GRS 2061A/19 and 1647/A/17), Fundación Mutua Madrileña (FMM, AP172142019), and Sociedad Española de Trombosis y Hemostasia (SETH-FETH; Premio López Borrasca 2019 and Ayuda a Grupos de Trabajo en Patología Hemorrágica 2019). The authors' research on IPDs is conducted in accordance with the aims of the Functional and Molecular Characterization of Patients with Inherited Platelet Disorders Project, which is supported by the Hemorrhagic Diathesis Working Group of the Spanish Society of Thrombosis and Haemostasis. A.M.-Q., C.F.-I., and L.H.-C. were supported by predoctoral grants from the Junta de Castilla y León, Spain. E.V. was supported by the predoctoral grant from the University of Salamanca, Spain. IG-T and RB were supported by "Contratos postdoctorales Programa II) from the University of Salamanca, Spain.

Conflict of Interest
None declared.

**Acknowledgments**

We thank the Transgenic Facility for generating and managing the murine model; Lucía Méndez Sánchez for her help with mouse handling; Sara González Briones and Irene Rodríguez Iglesias for technical support with experiments; the CIC-IBMCC Microscopy and Cytometry Service for technical assistance with the confocal immunofluorescence studies; the CIC-IBMCC Genomics Service for mice genotyping; Dr. María de la Luz Sánchez García, from Separation/Cytometry Service of Nucleus, University of Salamanca, for her support with flow-cytometry assays; The Molecular Pathology Unit; and Dr. Phil Mason for his help with technical aspects.

## References

1 Kurokawa M. AML1/Runx1 as a versatile regulator of hematopoiesis: regulation of its function and a role in adult hematopoiesis. Int J Hematol 2006;84(02):136–142
2 Ichikawa M, Asai T, Saito T, et al. AML-1 is required for megakaryocytic maturation and lymphocytic differentiation, but not for maintenance of hematopoietic stem cells in adult hematopoiesis. Nat Med 2004;10(03):299–304
3 Growney JD, Shigematsu H, Li Z, et al. Loss of Runx1 perturbs adult hematopoiesis and is associated with a myeloproliferative phenotype. Blood 2005;106(02):494–504
4 Wang Q, Stacy T, Binder M, Marin-Padilla M, Sharpe AH, Speck NA. Disruption of the Cbfa2 gene causes necrosis and hemorrhaging in the central nervous system and blocks definitive hematopoiesis. Proc Natl Acad Sci U S A 1996;93(08):3444–3449
5 Arber DA, Orazi A, Hasserjian R, et al. The 2016 revision to the World Health Organization classification of myeloid neoplasms and acute leukemia. Blood 2016;127(20):2391–2405
6 Song WJ, Sullivan MG, Legare RD, et al. Haploinsufficiency of CBFA2 causes familial thrombocytopenia with propensity to develop acute myelogenous leukaemia. Nat Genet 1999;23(02):166–175
7 Bastida JM, Benito R, Lozano ML, et al. Molecular diagnosis of inherited coagulation and bleeding disorders. Semin Thromb Hemost 2019;45(07):695–707
8 Stockley J, Morgan NV, Bem D, et al; UK Genotyping and Phenotyping of Platelets Study Group. Enrichment of FLI1 and RUNX1 mutations in families with excessive bleeding and platelet dense granule secretion defects. Blood 2013;122(25):4090–4093
9 Lentaigne C, Freson K, Laffan MA, Turro E, Ouwehand WHBRIDGE-BPD Consortium and the ThromboGenomics Consortium. Inherited platelet disorders: toward DNA-based diagnosis. Blood 2016;127(23):2814–2823
10 Bastida JM, Lozano ML, Benito R, et al. Introducing high-throughput sequencing into mainstream genetic diagnosis practice in inherited platelet disorders. Haematologica 2018;103(01):148–162
11 Brown AL, Arts P, Carmichael CL, et al. RUNX1-mutated families show phenotype heterogeneity and a somatic mutation profile unique to germline predisposed AML. Blood Adv 2020;4(06):1131–1144
12 Richards S, Aziz N, Bale S, et al; ACMG Laboratory Quality Assurance Committee. Standards and guidelines for the interpretation of sequence variants: a joint consensus recommendation of the American College of Medical Genetics and Genomics and the Association for Molecular Pathology. Genet Med 2015;17(05):405–424
13 Garcia JS, Madzo J, Cooper D, et al. Pre-Donor evaluation of an HLA matched sibling identifies a novel inherited RUNX1 mutation encoding a missense mutation found outside of the RUNT domain in familial platelet disorder. Blood 2010;116(21):2709
14 Koh CP, Wang CQ, Ng CEL, et al. RUNX1 meets MLL: epigenetic regulation of hematopoiesis by two leukemia genes. Leukemia 2013;27(09):1793–1802
15 Prieto-Conde MI, Labrador J, Hermida G, et al. Genomic analysis of a familial myelodysplasia/acute myeloid leukemia and inherited *RUNX1* mutations without a pre-existing platelet disorder. Leuk Lymphoma 2020;61(01):181–184
16 Brown AL, Hahn C, Hiwase D, Godley LA, Scott HS. Correct application of variant classification guidelines in germline *RUNX1* mutated disorders to assist clinical diagnosis. Leuk Lymphoma 2020;61(01):246–247
17 Duployez N, Fenwarth L. Controversies about germline *RUNX1* missense variants. Leuk Lymphoma 2020;61(02):497–499
18 Sakurai M, Kunimoto H, Watanabe N, et al. Impaired hematopoietic differentiation of RUNX1-mutated induced pluripotent stem cells derived from FPD/AML patients. Leukemia 2014;28(12):2344–2354
19 Lamolda M, Montes R, Simón I, et al. GENYOi005-A: an induced pluripotent stem cells (iPSCs) line generated from a patient with familial platelet disorder with associated myeloid malignancy (FPDMM) carrying a p.Thr196Ala variant. Stem Cell Res (Amst) 2019;41:101603
20 Liu Y, Jennings NL, Dart AM, Du XJ. Standardizing a simpler, more sensitive and accurate tail bleeding assay in mice. World J Exp Med 2012;2(02):30–36
21 Gutiérrez-Herrero S, Fernández-Infante C, Hernández-Cano L, et al. C3G contributes to platelet activation and aggregation by regulating major signaling pathways. Signal Transduct Target Ther 2020;5(01):29
22 Lood C, Tydén H, Gullstrand B, et al. Decreased platelet size is associated with platelet activation and anti-phospholipid syndrome in systemic lupus erythematosus. Rheumatology (Oxford) 2017;56(03):408–416
23 Hardy AT, Palma-Barqueros V, Watson SK, et al. Significant hyporesponsiveness to GPVI and CLEC-2 agonists in pre-term and full-term neonatal platelets and following immune thrombocytopenia. Thromb Haemost 2018;118(06):1009–1020
24 Gutiérrez-Herrero S, Maia V, Gutiérrez-Berzal J, et al. C3G transgenic mouse models with specific expression in platelets reveal a new role for C3G in platelet clotting through its GEF activity. Biochim Biophys Acta 2012;1823(08):1366–1377
25 De Cuyper IM, Meinders M, van de Vijver E, et al. A novel flow cytometry-based platelet aggregation assay. Blood 2013;121(10):e70–e80
26 Tucker KL, Sage T, Gibbins JM. Clot retraction. Methods Mol Biol 2012;788:101–107
27 Livak KJ, Schmittgen TD. Analysis of relative gene expression data using real-time quantitative PCR and the 2(-Δ Δ C(T)) method. Methods 2001;25(04):402–408
28 Ortiz-Rivero S, Baquero C, Hernández-Cano L, et al. C3G, through its GEF activity, induces megakaryocytic differentiation and proplatelet formation. Cell Commun Signal 2018;16(01):101
29 Trevino AE, Zhang F. Genome editing using Cas9 nickases. Methods Enzymol 2014;546:161–174
30 Cifuni SM, Wagner DD, Bergmeier W. CalDAG-GEFI and protein kinase C represent alternative pathways leading to activation of integrin alphaIIbbeta3 in platelets. Blood 2008;112(05):1696–1703
31 Hayashi Y, Harada Y, Huang G, Harada H. Myeloid neoplasms with germ line RUNX1 mutation. Int J Hematol 2017;106(02):183–188
32 Duarte BKL, Yamaguti-Hayakawa GG, Medina SS, et al. Longitudinal sequencing of RUNX1 familial platelet disorder: new insights into genetic mechanisms of transformation to myeloid malignancies. Br J Haematol 2019;186(05):724–734
33 Owen CJ, Toze CL, Koochin A, et al. Five new pedigrees with inherited RUNX1 mutations causing familial platelet disorder with propensity to myeloid malignancy. Blood 2008;112(12):4639–4645

34 Rao AK, Poncz M. Defective acid hydrolase secretion in RUNX1 haplodeficiency: evidence for a global platelet secretory defect. Haemophilia 2017;23(05):784–792
35 Glembotsky AC, Bluteau D, Espasandin YR, et al. Mechanisms underlying platelet function defect in a pedigree with familial platelet disorder with a predisposition to acute myelogenous leukemia: potential role for candidate RUNX1 targets. J Thromb Haemost 2014;12(05):761–772
36 Antony-Debré I, Manchev VT, Balayn N, et al. Level of RUNX1 activity is critical for leukemic predisposition but not for thrombocytopenia. Blood 2015;125(06):930–940
37 Morowski M, Vögtle T, Kraft P, Kleinschnitz C, Stoll G, Nieswandt B. Only severe thrombocytopenia results in bleeding and defective thrombus formation in mice. Blood 2013;121(24):4938–4947
38 Heijnen H, van der Sluijs P. Platelet secretory behaviour: as diverse as the granules … or not? J Thromb Haemost 2015;13(12):2141–2151
39 Gabbeta J, Yang X, Sun L, McLane MA, Niewiarowski S, Rao AK. Abnormal inside-out signal transduction-dependent activation of glycoprotein IIb-IIIa in a patient with impaired pleckstrin phosphorylation. Blood 1996;87(04):1368–1376
40 Sood R, Kamikubo Y, Liu P. Role of RUNX1 in hematological malignancies. Blood 2017;129(15):2070–2082
41 Franke B, van Triest M, de Bruijn KMT, et al. Sequential regulation of the small GTPase Rap1 in human platelets. Mol Cell Biol 2000;20(03):779–785
42 Harper MT, Poole AW. Diverse functions of protein kinase C isoforms in platelet activation and thrombus formation. J Thromb Haemost 2010;8(03):454–462
43 Jalagadugula G, Mao G, Kaur G, Dhanasekaran DN, Rao AK. Platelet protein kinase C-θ deficiency with human RUNX1 mutation: PRKCQ is a transcriptional target of RUNX1. Arterioscler Thromb Vasc Biol 2011;31(04):921–927
44 Hug BA, Ahmed N, Robbins JA, Lazar MA. A chromatin immunoprecipitation screen reveals protein kinase Cbeta as a direct RUNX1 target gene. J Biol Chem 2004;279(02):825–830
45 Sun L, Mao G, Rao AK. Association of CBFA2 mutation with decreased platelet PKC-θ and impaired receptor-mediated activation of GPIIb-IIIa and pleckstrin phosphorylation: proteins regulated by CBFA2 play a role in GPIIb-IIIa activation. Blood 2004;103(03):948–954
46 Bynagari-Settipalli YS, Cornelissen I, Palmer D, et al. Redundancy and interaction of thrombin- and collagen-mediated platelet activation in tail bleeding and carotid thrombosis in mice. Arterioscler Thromb Vasc Biol 2014;34(12):2563–2569
47 Schlegelberger B, Heller PG. RUNX1 deficiency (familial platelet disorder with predisposition to myeloid leukemia, FPDMM). Semin Hematol 2017;54(02):75–80
48 Jagadeeswaran P, Cooley BC, Gross PL, Mackman N. Animal models of thrombosis from zebrafish to nonhuman primates. Circ Res 2016;118(09):1363–1379
49 Lin Q, Zhang Y, Zhou R, et al. Establishment of a congenital amegakaryocytic thrombocytopenia model and a thrombocyte-specific reporter line in zebrafish. Leukemia 2017;31(05):1206–1216
50 Marconi C, Di Buduo CA, LeVine K, et al. Loss-of-function mutations in *PTPRJ* cause a new form of inherited thrombocytopenia. Blood 2019;133(12):1346–1357

## Supplementary Material

### Generation of RUNX1 p.Leu56Ser Murine Model

#### CRISPR/Cas9 System Design

Two complementary RNA guides (single-guide RNAs, sgRNAs) were designed with the CRISPR design tool (http://crispr.mit.edu/), closer than 100 bp, targeting *Runx1* exon 2, and including two 4-bp overhang sequences corresponding to Bbsi nuclease (*Runx1* UP and LO oligos, ►**Supplementary Table S1**). Both *Runx1* pairs of sgRNAs were denatured at 95°C for 5 minutes, ramp-cooled to 25°C for 45 minutes to allow annealing. These annealed oligonucleotides were ligated into pSpCas9n(BB)-2A-GFP (PX461), a gift from Feng Zhang (Addgene plasmid #48140), previously linearized by Bbsi nuclease, and containing Cas9 nickase.[1]

Sanger sequencing confirmed the correct insertion of the sgRNA sequences. SgRNA sequences were polymerase chain reaction (PCR)-amplified from PX461-based vector with oligonucleotides carrying the T7 RNA polymerase promoter at the 5′ ends (*Runx1* T7 S and *Runx1* T7 AS oligos, ►**Supplementary Table S1**). PCR products were purified (NZYGelpure, NZYTech, Portugal) and used as a template for T7 RNA polymerase transcription in vitro (MEGAshortscript T7 Transcription Kit, Thermo Fisher, California, United States).

The Cas9 nuclease ORF, including NLS, was also PCR-amplified from PX461 vector with oligonucleotides carrying the T7 RNA polymerase promoter at the 5′ ends (T7-Cas9n S and T7-Cas9n AS oligos, ►**Supplementary Table S1**). The Cas9 PCR product was purified and used as a template for in vitro transcription, 5′ capping (mMESSAGE mMACHINE T7 Transcription Kit, Thermo Fisher), and 3′ poly(A) tailing (Poly(A) Tailing Kit, Thermo Fisher). Transcription products were purified with an RNeasy Mini Kit (Qiagen, Germany) and eluted in nuclease-free EmbryoMax microinjection buffer (Millipore, Massachusetts, United States).

Concurrently, a single-strand DNA oligonucleotide (ssODN) (Integrated DNA Technologies, IDT, Iowa, United States) was designed as a template for homologous recombination repair,[2] carrying the c.127–128CT > TC alteration, which gives rise to the protein variant p.Leu43Ser, which corresponds to the human p.Leu56Ser, and carries a silent mutation that destroys PAM sequences. The ssODN has a total length of 149 bp (ssODN, ►**Supplementary Table S1**).

#### Mouse Embryo Microinjections

One-cell-stage embryos from superovulated C57BL/6J females were harvested and microinjected with 20 ng/µL of the CRISPR/Cas9 system and 20 ng/µL of ssODN template solution into the pronucleus. Microinjected embryos were grown overnight on KSOM with nonessential amino acids (Millipore), at 37°C in a 5% $CO_2$ atmosphere. Two-cell-stage embryos were recovered and transferred to foster CD1 females.[3]

#### Analysis of Cas9-system Target Sites

Edited founders were identified by PCR amplification (Taq polymerase, Roche, Switzerland) with oligonucleotides flanking exon 2 (*Runx1* F and R oligos, ►**Supplementary Table S2**). PCR products were purified using a PCR Product Purification Kit (NZYtech) and sequenced by the standard Sanger method. The selected founder was crossed with wild-type C57BL/6J to eliminate possible unwanted off-targets and to generate pure heterozygotes. F3 generations of *RUNX1* heterozygous carriers of the p.Leu43Ser variant mice were crossed to produce homozygous RUNX1 p.Leu43Ser. Mice were genotyped by Sanger sequencing of PCR products produced from tail-biopsy DNA.

#### Off-Target Genotyping

Potential off-targets of the selected *Runx1* sgRNAs were analyzed using the online target predictor CRISPR design tool (http://crispr.mit.edu/). The top 10 off-target sites were evaluated using specific PCR oligos and Sanger by sequencing (►**Supplementary Table S2**).

### Platelet Phenotyping of the RUNX1 p.Leu56Ser Mouse Model

#### Analysis of Platelet Structure and Receptor Levels

Platelet size was evaluated by flow cytometry as logarithmic forward scattering (FSC) in whole-blood samples. Platelets were gated based on their FSC/SSC properties, as well as expression of CD61+ platelets, before comparing the mean FSC values of mice of all three genotypes.[4]

Levels of platelet glycoproteins VI (GPVI), GPIb-IX, and integrin $\alpha_{IIb}\beta_3$ were evaluated as the mean fluorescence intensity for rat anti-mouse GPVI–FITC (Emfret Analytics), rat anti-mouse CD42b–FITC (Emfret Analytics), and rat anti-mouse CD61–PE (Thermo Fisher), respectively, upon acquisition of 10,000 CD41+ platelets on BD Accuri C6.[5]

#### Light Transmission Aggregometry Assay

Blood was obtained by cardiac puncture into trisodium citrate microtubes. Samples from six mice/genotype were pooled. Washed platelets were prepared and diluted in Tyrode's-HEPES buffer ($135 \times 10^3$ platelets/µL). Aggregation was induced with thrombin 1 U/mL and recorded for 6 minutes using a TA-8V aggregometer (Stago, France).

#### ATP Release

Combined blood from eight mice/genotype were used ($1 \times 10^8$ platelets). Washed platelets in 600 µL of Tyrode's-HEPES were stimulated with thrombin 1 U/mL or PMA 3 µM for 10 minutes at 37°C with slow shaking. Both agonists were analyzed in triplicate for each genotype. Samples were centrifuged for 30 seconds at 10,000 *g* postaggregation and the supernatants were collected. ATP release was evaluated with Cell Titer-Glo reagents (Promega, Wisconsin, United States), added to fresh samples for 30 minutes at

room temperature (RT). The luminescence was determined in a Synergy 4 Microplate Reader (BioTek, Vermont, United States).[6]

### Megakaryopoiesis

Megakaryopoiesis was analyzed as previously described.[7] Briefly, femora from two mice/genotype were stained with hematoxylin-eosin, and visualized using a Leica optical microscope to count megakaryocytes (MKs) in 20 40× yields.

Bone marrow cells (BMCs) from six mice/genotype were obtained from femora and tibiae by flushing with PBS. The MKs were enriched by culturing BMCs in RPMI supplemented with 20% horse serum, streptomycin/penicillin, and 50 ng/mL thrombopoietin (TPO, Innovative Research, Michigan, United States) for 5 days to promote megakaryopoiesis. Flow cytometry analysis of MK differentiation and maturation, and analysis of DNA content were performed on 0, 2, and 5 days of TPO culture.

For MK differentiation and maturation, BMCs were stained with CD41-APC, CD61-PE, and CD42b-FITC, and incubated for 20 minutes at RT. To determine the ploidy status, BMCs were fixed with ethanol by adding 0.5 mL of cold 70% ethanol dropwise. After incubation (1 hour to 7 days) at 4°C, cells were washed with PBS, stained with anti-CD61-PE antibody, and incubated with a mixture of 100 µg/mL RNase (Promega) and 50 µg/mL propidium iodide (Sigma) in PBS for 20 minutes at RT in the dark.

Fluorescence of both experiments was measured using a BD Accuri cytometer and analyzed using FlowJo V10 software.

**Supplementary Table S1** Oligo design for sgRNA guides, in vitro transcription of sgRNA and Cas9 mRNA, PCR genotyping and ssODN carrying the point mutation c.127–128CT > TC

| Oligos | Sequence |
|---|---|
| *Runx1*_1UP | caccGGATGAGCGAGGCGCTGCCGC |
| *Runx1*_1LO | aaacGCGGCAGCGCCTCGCTCATCc |
| *Runx1*_2UP | caccGCCGGGGCTCAGCGCGGTGGA |
| *Runx1*_2LO | aaacTCCACCGCGCTGAGCCCCGGc |
| *Runx1*_1 T7 S | TAATACGACTCACTATAGGGATGAGC GAGGCGCTGCCGC |
| *Runx1*_2 T7 S | TAATACGACTCACTATAGGGCCGGG GCTCAGCGCGGTGGA |
| *Runx1* T7 AS | GCACCGACTCGGTGCCACT |
| T7-Cas9n S | TAATACGACTCACTATAGGGATGGCC CCAAAGAAGAAGCGGA |
| T7-Cas9n AS | CTTTTTCTTTTTTGCCTGGCC |
| *Runx1*_F | AGTTGCTAACCCTGCTTGGG |
| *Runx1*_R | CTAGGCTCACTCTGGCCATC |
| ssODN Runx1 mut c.127–128CT > TC | AGTGCTTCATGAGAGATGCCAGCACG AGCCGCCGCTTCACGCCGCCTTCCAC CGCGCTGAGCCCCGGCAAGATGAGC GAGGCG**TC**GCCGCT**A**GGCGCCCCG-GATGGCGGCGCCGCCCTGGCCAGC AAGCTGAGGAGCGGCGACCGCAGC ATGGTGGAGGTACTA |

Abbreviations: S: sense; AS: antisense; F: forward; R: reverse; ssODN: single-strand DNA oligonucleotide.
Note: Small letters indicate the sequence corresponding to Bbsi nuclease; underlining indicates shared sequences; bold face indicates the point mutation of interest.

**Supplementary Table S2** PCR oligos used to evaluate sgRNA off-targets (F: forward; R: reverse)

| Oligos | Sequence |
|---|---|
| Myo3a F | CTCGATTTTGCAAAACTGCGAAGCT |
| Myo3a R | TCATTAGGGGGATAGGAGTGACAGGC |
| Whsc1l1 F | CAGCACCCATGTTTTTCATGTAAAGTGTC |
| Whsc1l1 R | TCTTCTTGGTCCCTAGATGGAGACTAATAGT |
| Anks3 F | GTCCCCGTGCTGAGTACGG |
| Anks3 R | GCAGGCTCCCGTGTGG |
| Six5 F | GGAGGAAGCGCGCCAG |
| Six5 R | GAACTTCTTGCGCAGCCGG |
| Trpc7 F | AACGAGAAGGGCACGAGCCT |
| Trpc7 R | TCCGTGCACTCATTGCACTTG |
| Ntmt1 F | TGGCTTTGCTGTTTTGCTCC |
| Ntmt1 R | ACCCAATCACCGCTTAGCTC |
| Gm26578 F | CCCGTAAGCAATGGGGTTCA |
| Gm26578 R | CCGATTGCGGGATCTCTACC |
| Uvrag F | CCGGTTTCTAGGCTGTAGGG |
| Uvrag R | AAAGGAAACCCCAACGTCCC |
| Exoc3l4 F | AGGCCGAGGGTGATTTCTTG |
| Exoc3l4 R | ACCCGTTTTCCGTGATCTCC |
| Celsr2 F | GGCTCATATCCCTCTTCCGC |
| Celsr2 R | TACCGTGATCCTGTGCAGTG |

Abbreviations: PCR, polymerase chain reaction; sgRNA, single-guide RNA.

**Supplementary Table S3** qPCR oligonucleotides (F: forward; R: reverse)

| Oligos | Sequence |
|---|---|
| qPCR-*Prkca* F | CGTTACGTTCTCTTGTCCGG |
| qPCR-*Prkca* R | CATTCATGTCGCAGGTGTCAC |
| qPCR-*Prkcb* F | GCAGAAGAACGTGCACGAGG |
| qPCR-*Prkcb* R | GGAGAACGTGACGAACTCATGG |
| qPCR-*Gapdh* F | TGCACCACCAACTGCTTAGC |
| qPCR-*Gapdh* R | CACCACCTTCTTGATGTCATCA |

Abbreviation: qPCR, quantitative polymerase chain reaction.

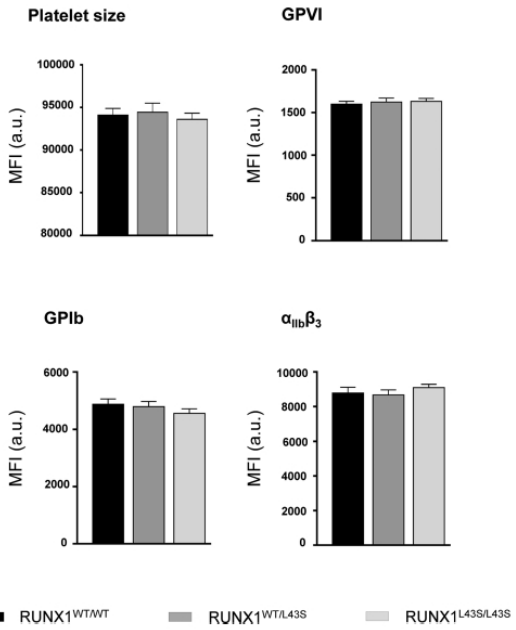


**Supplementary Fig. S1** Flow cytometric assessment of platelet size and expression of glycoproteins on the platelet surface of p.Leu43Ser variant mice. Platelet size evaluated as FSC value (arbitrary units), while levels of GPVI, GP1b, and integrin $\alpha_{IIb}\beta_3$ on the platelet surface evaluated as the mean fluorescence intensity (arbitrary units). Histograms show mean ± SEM of the results. SEM, standard error of the mean.

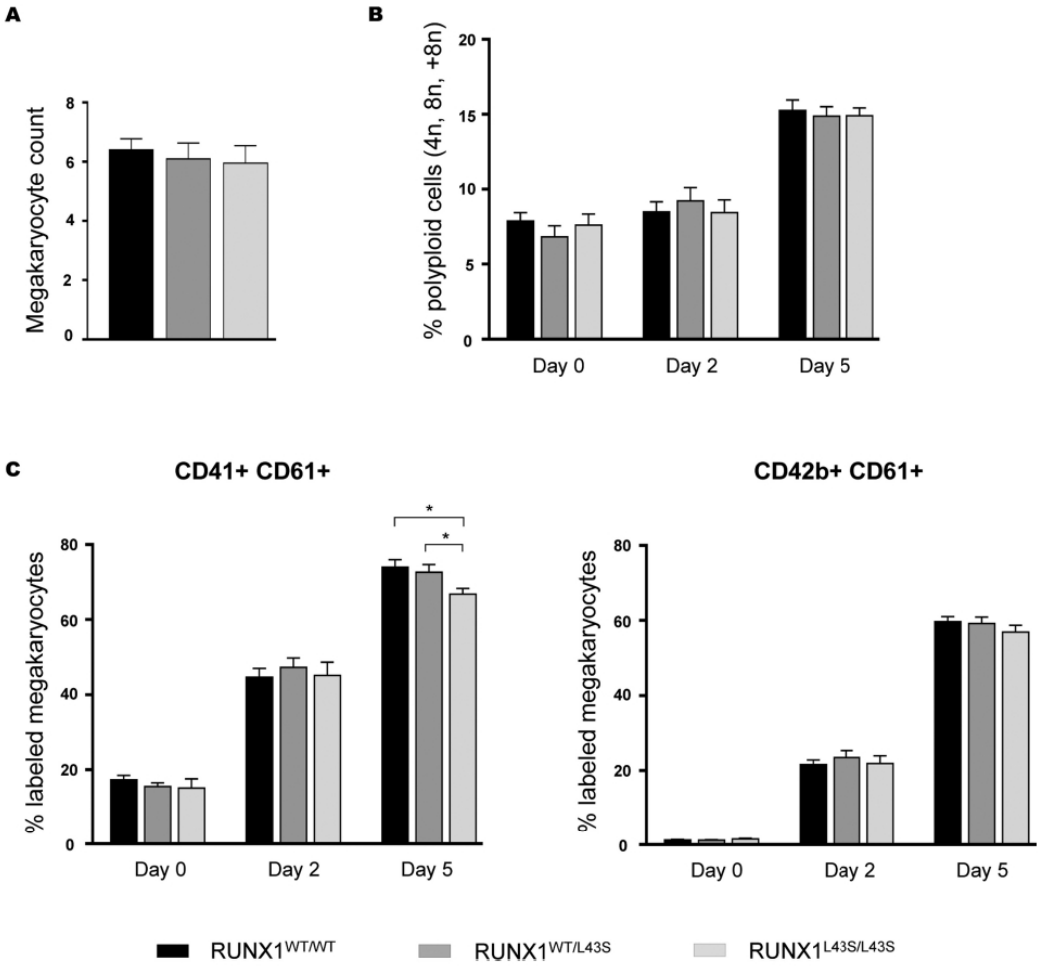


**Supplementary Fig. S2** Megakaryopoiesis of p.Leu43Ser variant mice. (**A**) Megakaryocytes (MKs) count in 40× yields along the femur. (**B**) Flow cytometry analysis of the MK polyploidy and DNA content in RUNX1$^{WT/WT}$, RUNX1$^{WT/L43S}$, and RUNX1$^{L43S/L43S}$ after 0, 2, and 5 days of treatment with thrombopoietin, and evaluated with propidium iodide. (**C**) Flow cytometry analysis of the MK differentiation and maturation after 0, 2, and 5 days of treatment with thrombopoietin. CD41+ CD61+ CD42− correspond to megakaryoblasts/promegakaryocytes; and CD41+ CD61+ CD42+ correspond to mature MKs. Histograms show the mean ± SEM of values. $^{*}p < 0.05$. SEM, standard error of the mean.

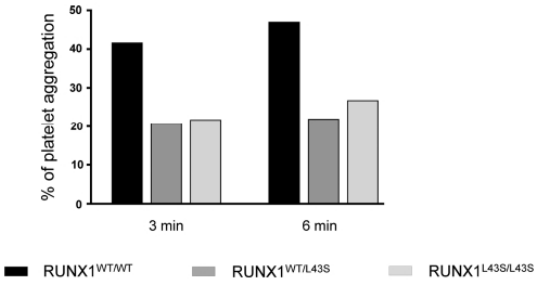


**Supplementary Fig. S3** RUNX1 p.Leu43Ser variant mice display impaired platelet aggregation. Representative example of platelet aggregation by light-transmission aggregometry (LTA) assay, after 3 and 6 minutes of thrombin 1 U/mL stimulation. The histogram shows the value at each time.

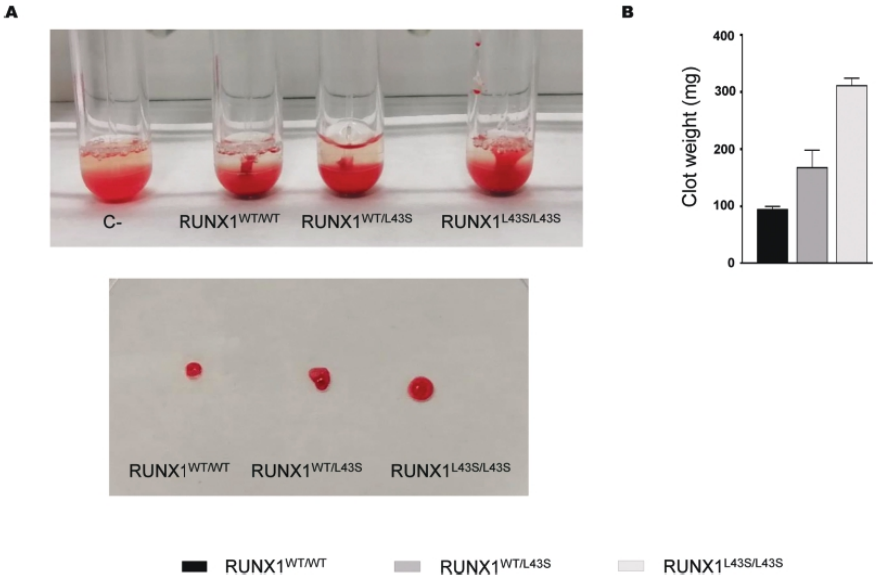


**Supplementary Fig. S4** RUNX1 p.Leu43Ser variant mice display impaired clot retraction. (**A**) Representative images of the clot retraction in RUNX1$^{WT/WT}$, RUNX1$^{WT/L43S}$, and RUNX1$^{L43S/L43S}$. Platelet-poor plasma (PPP) was used as a negative control. All samples were stimulated with thrombin 1 U/mL. (**B**) Histogram represents the mean ± SEM of the clot weights. SEM, standard error of the mean.

## Supplementary References

1 Ran FA, Hsu PD, Wright J, Agarwala V, Scott DA, Zhang F. Genome engineering using the CRISPR-Cas9 system. Nat Protoc 2013;8 (11):2281–2308
2 Quadros RM, Miura H, Harms DW, et al. Easi-CRISPR: a robust method for one-step generation of mice carrying conditional and insertion alleles using long ssDNA donors and CRISPR ribonucleoproteins. Genome Biol 2017;18(01):92
3 García-Tuñón I, Vuelta E, Lozano L, et al. Establishment of a conditional Nomo1 mouse model by CRISPR/Cas9 technology. Mol Biol Rep 2020;47(02):1381–1391
4 Lood C, Tydén H, Gullstrand B, et al. Decreased platelet size is associated with platelet activation and anti-phospholipid syndrome in systemic lupus erythematosus. Rheumatology (Oxford) 2017;56(03):408–416
5 Hardy AT, Palma-Barqueros V, Watson SK, et al. Significant hyporesponsiveness to GPVI and CLEC-2 agonists in pre-term and full-term neonatal platelets and following immune thrombocytopenia. Thromb Haemost 2018;118(06):1009–1020
6 Pleines I, Lebois M, Gangatirkar P, et al. Intrinsic apoptosis circumvents the functional decline of circulating platelets but does not cause the storage lesion. Blood 2018;132(02):197–209
7 Ortiz-Rivero S, Baquero C, Hernández-Cano L, et al. C3G, through its GEF activity, induces megakaryocytic differentiation and proplatelet formation. Cell Commun Signal 2018;16(01):101

# CHAPTER 2

## Expanding the role of germline *RUNX1* variants in leukemogenesis in a murine model generated by CRISPR/Cas9

Marin-Quilez A[1], Sanz D[1], del Rey M[1], Ordoñez JL[1,2], Diaz-Ajenjo L[1], González-Porras JR[3], Guerrero C[1], Pérez-Losada J[1], Rivera J[4,#], Hernández-Rivas JM[1,3], Benito R[1], García-Tuñón I[1], Bastida JM[3,#].

[1] Cancer Research Center - CSIC, University of Salamanca, Instituto de Investigación Biomédica de Salamanca (IBSAL), Spain; [2] Laboratory of Pharmacology, Department of Physiology and Pharmacology, Faculty of Pharmacy, University of Salamanca, Salamanca, Spain; [3] Department of Hematology - University Hospital of Salamanca - IBSAL, Spain; [4] Servicio de Hematología y Oncología Médica, Hospital Universitario Morales Meseguer, Centro Regional de Hemodonación, University of Murcia, IMIB - Arrixaca, CIBERER-U765, Murcia, Spain; [#] On behalf of the "Grupo Español de Alteraciones Plaquetarias Congénitas, (GEAPC)".

*Manuscript in preparation.*

# Expanding the role of germline *RUNX1* variants in leukemogenesis in a murine model generated by CRISPR/Cas9

Marin-Quilez A[1], Sanz D[1], del Rey M[1], Ordoñez JL[1,2], Diaz-Ajenjo L[1], González-Porras JR[3], Guerrero C[1], Pérez-Losada J[1], Rivera J[4,#], Hernández-Rivas JM[1,3], Benito R[1], García-Tuñón I[1], Bastida JM[3,#].

[1] Cancer Research Center - CSIC, University of Salamanca, Instituto de Investigación Biomédica de Salamanca (IBSAL), Spain

[2] Laboratory of Pharmacology, Department of Physiology and Pharmacology, Faculty of Pharmacy, University of Salamanca, Salamanca, Spain

[3] Department of Hematology - University Hospital of Salamanca - IBSAL, Spain

[4] Servicio de Hematología y Oncología Médica, Hospital Universitario Morales Meseguer, Centro Regional de Hemodonación, University of Murcia, IMIB - Arrixaca, CIBERER-U765, Murcia, Spain

[#] On behalf of the "Grupo Español de Alteraciones Plaquetarias Congénitas, (GEAPC)"

Germline monoallelic variants in *RUNX1* cause the Congenital Platelet Disorder with Myeloid Leukemia Predisposition (FPD/AML). It is estimated that 40% of patients develop a hematological neoplasm by acquiring a second somatic event. Although large pedigrees have been studied to characterize the preleukemia and the second hit, the mechanisms of leukemogenesis are not well understood. Cellular and/or animal models provide a useful tool to determine the pathogenicity of *RUNX1* variants and to uncover their potential role in the disease development and progression. We used a *knock-in* murine model previously generated by the CRISPR/Cas9 system, carrying the RUNX1 p.Leu43Ser variant (mimicking human p.Leu56Ser) to settle definitively its role in leukemogenesis and to determine the second-hit mechanisms involved. 75 mice were studied: 25 of each genotype ($RUNX1^{WT/WT}$, $RUNX1^{WT/L43S}$, $RUNX1^{L43S/L43S}$). Peripheral blood (PB), bone marrow (BM), and spleen were analyzed by flow cytometry and histopathology. To detect second events, all exons of *Runx1*

were sequenced, and deregulated genes of 3 mice/genotype were analyzed by RNA-seq in BM. We detected the presence of aberrant myeloid Mac1$^+$ Sca1$^+$ ckit$^-$ cells in PB of two homozygous mice: 15.3% in Hom#1 at 15 months, and 7.3% in Hom#2 at 20 months, while 2.4% aberrant cells were detected in only one heterozygous mouse (Het#1) at 21 months of age. Mac1$^+$ Sca1$^+$ ckit$^-$ cells were present in both BM and spleen in all three affected mice. In addition, the BM showed atypical and hypercellular morphology, while the spleen of Hom#1 and Hom#2 mice showed a destructured white/red pulp, with the presence of apoptotic cells, and splenomegaly. No Mac1$^+$ Sca1$^+$ ckit$^-$ cells were detected in any RUNX1$^{WT/WT}$ mice. DNA-seq analyses showed no additional somatic mutations in *Runx1* in the three affected mice. However, RNA-seq studies showed 698 genes significantly downregulated in the 3 Mac1$^+$ Sca1$^+$ mice vs. 6 healthy RUNX1$^{WT/WT}$, RUNX1$^{WT/L43S}$ and RUNX1$^{L43S/L43S}$ mice, highlighting the overexpression of *Rapgef1*, whose alteration has been previously linked to chronic myeloid leukemia and solid tumors. These results suggest that the variant p.Leu43Ser in heterozygosis is associated with a weak predisposition and late progression to myeloid neoplasm, correlating with the phenotype associated with RUNX1 p.Leu56Ser variant in the clinical setting, but a more aggressive phenotype in homozygous mice, associated with higher overexpression of *Rapgef1,* and remarkably bone marrow and spleen affectation.

**Keywords:** *RUNX1*, myeloid leukemia, FPD/AML, RNA-seq, *Rapgef1*

## INTRODUCTION

The runt-related transcription factor 1 (*RUNX1*) gene encodes a transcriptional factor crucial in hematopoiesis, which is found mutated in ~10% of adult acute myeloid leukemia (AML).[1,2] Although it is frequently diagnosed as an acquired alteration, the frequent use of high-throughput sequencing (HTS) techniques in genetic diagnostic practice has unveiled that inherited *RUNX1* mutations are more frequent than thought.[3,4] In fact, in the World Health Organization classification 2016, germline monoallelic alterations in *RUNX1* have been incorporated as a new subgroup: Familial Platelet Disorders with a predisposition to Acute Myeloid Leukemia (FPD/AML).[5,6] It is estimated that only ~40% of individuals with FPD/AML will develop a myeloid neoplasm, since germline *RUNX1* mutations alone are insufficient to induce AML, and second-hit mutational events are necessary.[7] Most frequent somatic mutations associated with leukemic progression has been described in the second allele of *RUNX1*, but also in genes such as the cell cycle regulator *CDC25C*, the transcriptional factor *GATA2*, or genes associated with CHIP (Clonal Hematopoiesis of Indeterminate Potential), like *ASXL1* or *TET2*.[8,9]

The recent appearance of the Variant Curation Expert Panels has been of relevant guidance to categorize the *RUNX1* variants found and to carefully monitor patients for genetic counseling.[10,11] However, the application of these recommendations is still challenging, and there may be alternative interpretations or high controversies for many genetic variants.[12] The appearance of murine models genetically modified, the use of induced pluripotent stem cells (iPSCs), or *in vitro* models have proven to be a suitable model system to study genetic disorders, getting new insight into FPD/AML disorder.[13,14]

Our group previously published the generation of the RUNX1 p.Leu43Ser murine model generated by CRISPR/Cas9, reproducing the human RUNX1 p.Leu56Ser variant, to characterize the related-platelet disorder.[15] Here, we explore its role in leukemogenesis, and we uncovered the overexpression of *Rapgef1* in leukemic mice as a potential novel second-hit event associated with the disease.

## MATERIALS & METHODS

### Murine model and experimental design

We used a murine model mimicking the human RUNX1 p.Leu56Ser variant, previously generated by the CRISPR/Cas9 technology.[15] Mice were housed at the *Servicio de Experimentación Animal* (SEA), University of Salamanca (Spain), a temperature-controlled specific-pathogen-free animal house facility. 75 mice were investigated, 25 of each genotype ($RUNX1^{WT/WT}$, $RUNX1^{WT/L43S}$, and $RUNX1^{L43S/L43S}$). Mice were followed daily, and blood cell populations were screened routinely

by flow cytometry every 3 months or upon suspicion of myeloid disease. Mice were sacrificed at the end of the experiment (22 months) or when presenting symptoms of leukemia. Peripheral blood, bone marrow, and spleen samples were collected at sacrifice.

Characterization of hematopoietic cells by flow cytometry

Blood (100-200 μL) was collected from the submandibular vein of adult mice and anticoagulated with EDTA for routine screening. At sacrifice, blood was collected by cardiac puncture in anesthetized mice (tribromoethanol), bone marrow cells were obtained by flushing from the long bones, and spleen cells by mechanical procedures. In all cases, contaminating red blood cells were lysed with red cells lysis buffer (RCLB: $NH_4Cl$, $KHCO_3$, EDTA), and the remaining cells were washed in PBS for flow cytometry. Cells were stained with a customized panel: Gr1*FITC (1:100); Mac1*PE (1:200); CD45*PerCP-Cy5.5 (1:100); ckit*PECy7 (1:50); CD3*APC (1:100); B220*APCH7 (1:100); Sca1*PacificBlue (1:50) (Biolegend, California, USA). Samples were incubated for 30 minutes, at room temperature (RT), in the dark, and acquired in a BD FACSAria Cytometer (BD Biosciences, California, USA). Data were analyzed using FlowJo V10 (Tree Star, Inc., Oregon, USA).

Histopathology

Paraformaldehyde-fixed femur and spleen tissue samples were immersed in paraffin and cut into 2 μm-thick slices. Blood films were fixed with ethanol. All samples were stained with hematoxylin-eosin. Representative samples were photographed under an Olympus BX51 microscope connected to an Olympus DP70 camera (Olympus, Japan). The histopathological diagnosis was carried out by experts from The Molecular Pathology Unit (Salamanca, Spain).

Amplicon based-DNAseq and RNA-seq from bone marrow samples

Leukocytes from mice bone marrow were resuspended into RLTplus lysis buffer from a RNeasy kit (Qiagen, Germany). Total DNA and RNA extraction were obtained following the manufacturer's specifications.

Somatic mutations of *Runx1* were analyzed by amplicon-based DNA seq, using specific primers (Table S1), and run in a MiSeq sequencer (Illumina, California, USA).

RNA-seq and bioinformatic analysis were performed at the Sequencing Service of NUCLEUS, University of Salamanca. Raw fastq files were first quality filtered using fastp (v0.23.2), and processed fastq files were aligned to the mouse genome (mm10) using the STAR aligner (v2.7.8a). FeatureCounts (v1.50) was used to summarize the reads across the genes, using the vM25 version of the comprehensive

GENCODE mouse gene annotation. Differential expression analysis between experimental groups was performed using DESeq2 (v2.11.40.6); lastly, goseq (v1.44.0) enrichment analysis package was used to conduct gene ontology analysis of differentially expressed genes.[16,17]

Ethics Statement

All experimental procedures were conducted according to the National Institutes of Health Guide guidelines for the Care and Use of Laboratory Animals and were approved by the Bioethics Committee of the University of Salamanca and the Junta de Castilla y León, Spain (0000107).

Statistical analysis

Data were summarized as the mean ± standard error of the mean (SEM). Statistical analyses were performed using GraphPad Prism 8 Software (GraphPad Software). Differences among groups were tested with t-student, one- and two-way ANOVA, and Tukey's multiple comparisons test. Differences were considered significant (*) for values of $p<0.05$.

## RESULTS

**Phenotyping of leukemic cells in peripheral blood, bone marrow and spleen.**

To study the effect of the RUNX1 p.Leu43Ser variant on leukemia predisposition and progression, we followed the mature and immature hematopoietic populations in peripheral blood throughout life. We observed normal counts of red blood cells, but an allele-dependent reduction of platelets, previously described as congenital thrombocytopenia,[15] and leukocyte counts in peripheral blood (Figure 1A) without changes in the expected proportion of mature cells (B and T lymphocytes, granulocytes, and monocytes) at sacrifice (Figure 1B). Regarding immature cells, no $Lin^-$ $ckit^+$ $sca1^+$ (LSK) cells were detected in peripheral blood. However, we detected the presence of an aberrant population, previously described and characterized as myeloid leukemic cells,[18] double-positive for the markers Mac1 and Sca1, and negative for ckit, in three mice (two $RUNX1^{L43S/L43S}$, referred as Hom#1 and Hom#2; and one $RUNX1^{WT/L43S}$, referred as Het#1) (Figure 1C). Mouse Hom#1 displayed 13.4% of $Mac1^+$ $Sca1^+$ cells at 14 months and 15.3% of cells at sacrifice (15 months). Conversely, mouse Hom#2 displayed a milder and later appearance of the aberrant population (7.3% at 20 months). Finally, only one heterozygous mouse, Het#1, presented the $Mac1^+$ $Sca1^+$ population at an advanced age (21 months: 2.4% of cells) (Figure 1C). The aberrant population show a morphology similar to mature monocytes, with similar levels of CD45 marker, but cells were smaller and less complex. (Figures 1D and 1E).

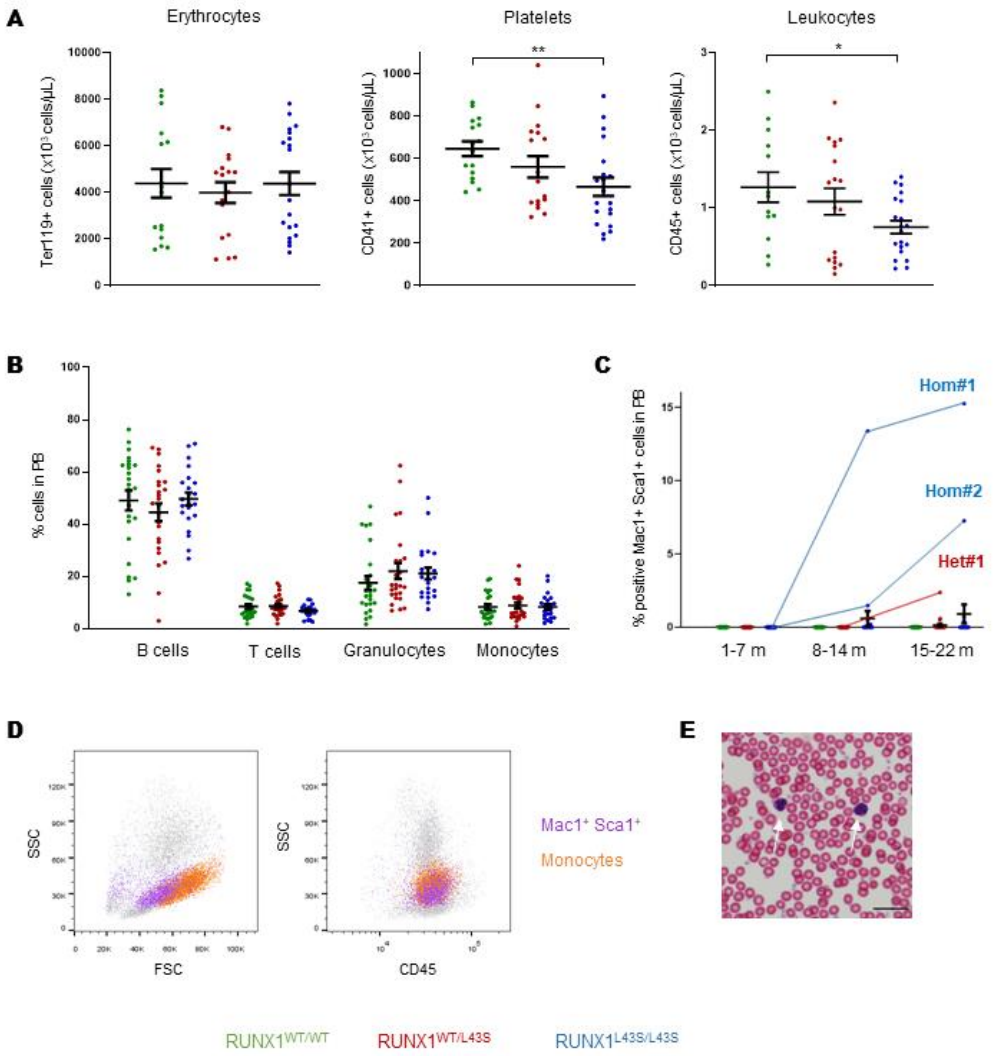


**Figure 1. Characterization of hematopoietic cells in peripheral blood from RUNX1$^{WT/WT}$, RUNX1$^{WT/L43S}$, and RUNX1$^{L43S/L43S}$ mice. A)** Number of erythrocytes, platelets, and leukocytes, measured by flow cytometry, using the monoclonal antibodies anti-Ter119, anti-CD41, and anti-CD45, respectively. Plots show the total number of cells/µL. **B)** Leukocytes were stained with specific monoclonal antibodies to measure the percentage of B cells (anti-B220), T cells (anti-CD3), granulocytes (double positives for anti-Gr1 and anti-Mac1), and monocytes (negative for anti-Gr1 and positive for anti-Mac1) in peripheral blood at sacrifice. **C)** Leukocytes were stained with the monoclonal antibodies anti-Mac1 and anti-Sca1 to detect the aberrant population. The percentage of double positive population is shown at different periods of life for RUNX1$^{WT/WT}$, RUNX1$^{WT/L43S}$, and RUNX1$^{L43S/L43S}$ mice, including the three affected mice Hom#1, Hom#2 and Het#1). **D)** FCS/SSC and CD45+/SSC plots gating the Mac1$^+$ Sca1$^+$ aberrant population (purple) and the mature monocytes (orange) in the affected mice Hom#1. **E)** Morphological appearance of the Mac1$^+$ Sca1$^+$ aberrant population in blood film, stained with hematoxylin-eosin, in the affected mice Hom#1. Dot plots represent the mean ± SEM. * p<0.05, ** p<0.01. m: months.

Regarding hematopoietic organs, we did not observe significant differences in stem cell levels ($Lin^- Sca1^+ ckit^+$) or in progenitors ($Lin^- Sca1^- ckit^+$) between $RUNX1^{WT/L43S}$ and $RUNX1^{L43S/L43S}$ and $RUNX1^{WT/WT}$ mice (Figure 2A). Indeed, normal proportion of mature cells was found, in accordance with finding of peripheral blood (data not shown). However, the three affected mice with the aberrant population in peripheral blood presented high levels, above average, of both stem cells and progenitor populations in bone marrow (Figure 2A). In fact, aberrant $Mac1^+ Sca1^+$ cells were found in these mice (Figure 2A). This population apparently has a differentiation stage that is intermediate between HSCs and mature monocytes (Figure 2B). The anatomopathological study revealed a bone marrow hyperplasia with anomalous distributions of the different series in mice Hom#1, Hom#2, and Het#1 compared with $RUNX1^{WT/WT}$, but also with unaffected $RUNX1^{WT/L43S}$ and $RUNX1^{L43S/L43S}$ mice (Figure 2C).

A similar phenotype was found in the spleen of the affected mice Hom#1, Hom#2, and Het#1, characterized by a substantial increase in both stem cells and progenitor populations, and the appearance of the $Mac1^+ Sca1^+$ population (Figure 3A). Indeed, the $RUNX1^{L43S/L43S}$ genotype exhibited a tendency (non-significant, p=0.08) of splenomegaly (Figure 3B). As shown in Figures 3B-E, the $RUNX1^{WT/L43S}$ mice do not associate with spleen affectation, including the Het#1 mouse, while $RUNX1^{L43S/L43S}$ displayed variability in spleen size and weight (Figures 3B and 3C). Splenomegaly was only notable for the mouse Hom#2 (Figures 3C), although Hom#1 also presented with a remarkable tissue destructuration characterized by necrotic and apoptotic cells (Figures 3D and 3E).

**RNA-seq revealed an increased expression of *Rapgef1* in Hom#1 and Hom#2 mice.**

To investigate the second hit promoting the myeloid neoplasm, we first performed an amplicon-based sequencing of all *Runx1* exons since the somatic mutation of the gene is the most frequent event.[8] However, no pathogenic somatic mutations of *Runx1*, following the expected allele frequency (5-20%), were found in the bone marrow of mice Hom#1, Hom#2, and Het#1.

Conversely, an RNA-seq was performed to investigate possible pathways and genes dysregulated in the affected mice that could explain the phenotype. We first compared three unaffected mice carrying the variant (one $RUNX1^{WT/L43S}$ and two $RUNX1^{L43S/L43S}$) vs. three $RUNX1^{WT/WT}$, and we observed only 5 dysregulated genes (*Gm16698, Vκ21G, Rbm44, Gzma,* and the LncRNA 5830416I19Rik), confirming that the variant p.Leu43Ser *per se* it is not causative of the disease. Therefore, these six mice were grouped into the RNA-seq analysis as healthy mice and compared with the affected

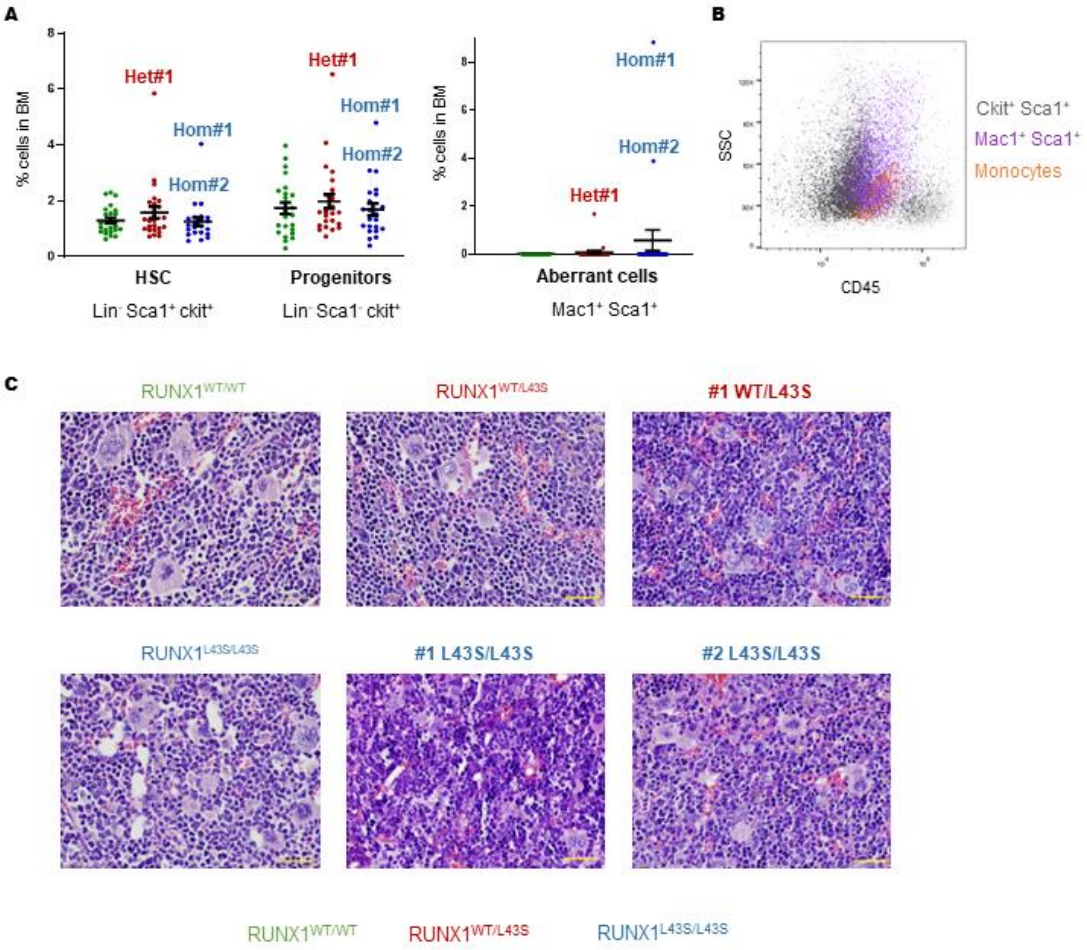


**Figure 2. Characterization of the aberrant cell population in bone marrow from Het#1, Hom#1, and Hom#2 mice. A)** Leukocytes from bone marrow were stained with lineage specific monoclonal antibodies (Lin: anti-B220, anti-CD3, anti-Gr1, and anti-Mac1), and specific monoclonal antibodies to analyze immature cells (Sca1 and ckit). The aberrant population was detected with the double positive population Mac1 and Sca1. Dot plots represent the mean ± SEM of the % of the cell population. **B)** CD45+/SSC plots gating the Mac1⁺ Sca1⁺ aberrant population (purple), the mature monocytes (orange), and the HSCs (sca1⁺ ckit⁺; black) in the affected mice Hom#1. **C)** Histopathological assessment of the bone marrow anatomy after staining with hematoxylin-eosin.

mice group with the aberrant population Mac1⁺ Sca1⁺ (Hom#1, Hom#2, and Het#1 mice).

Using the Wallenius method, the top over-represented categories revealed that the most disrupted pathways are related to changes in protein binding and immune system regulation (Figure 4A). Besides, 698 genes were dysregulated in the affected Mac1⁺ Sca1⁺ mice vs. the healthy mice group. The top 50 dysregulated genes are shown in Figure 4B and Table S2. Twelve target genes were deeply investigated

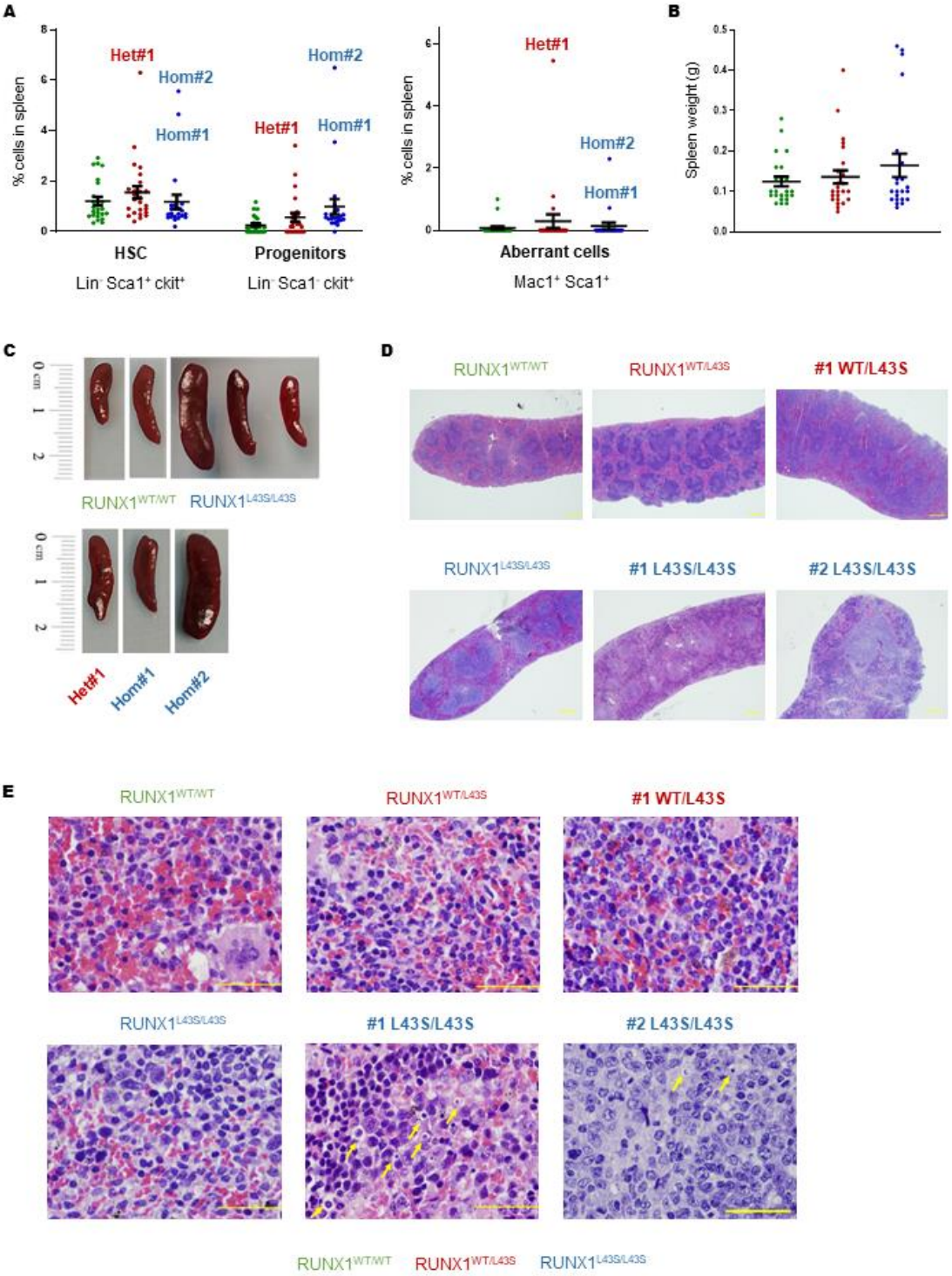
A
% cells in spleen
Het#1
Hom#2
Hom#1
Het#1
Hom#2
Hom#1
HSC
Lin⁻ Sca1⁺ ckit⁺
Progenitors
Lin⁻ Sca1⁻ ckit⁺
% cells in spleen
Het#1
Hom#2
Hom#1
Aberrant cells
Mac1⁺ Sca1⁺
B
Spleen weight (g)
C
RUNX1WT/WT
RUNX1L43S/L43S
Het#1
Hom#1
Hom#2
D
RUNX1WT/WT
RUNX1WT/L43S
#1 WT/L43S
RUNX1L43S/L43S
#1 L43S/L43S
#2 L43S/L43S
E
RUNX1WT/WT
RUNX1WT/L43S
#1 WT/L43S
RUNX1L43S/L43S
#1 L43S/L43S
#2 L43S/L43S
RUNX1WT/WT
RUNX1WT/L43S
RUNX1L43S/L43S

**Figure 3. Characterization of the aberrant cell population in spleen from Het#1, Hom#1, and Hom#2 mice. A)** Leukocytes from spleen were stained with monoclonal antibodies for lineage specific (anti-B220, anti-CD3, anti-Gr1, and anti-Mac1) and immature population (Sca1 and ckit). The aberrant population was detected with the double positive population Mac1 and Sca1. Dot plots represent the mean ± SEM of the % of the cell population. **B)** Splenomegaly was determined by the spleen weight (g). Dot plots represent the mean ± SEM of values per each genotype. **C)** Representative figure of the splenomegaly associated to $RUNX1^{L435/L435}$ vs. $RUNX1^{WT/WT}$ mice, and the spleen of the three affected mice. **D-E)** Histopathological assessment of the spleen anatomy after staining with hematoxylin-eosin. The yellow arrows indicate apoptotic cells.

according to the profile of expression of the three affected mice vs. the six control mice.

Among the downregulated genes in the affected mice with $Mac1^{+}$ $Sca1^{+}$ aberrant cells, we observed *Klra1*, a membrane receptor expressed mainly on the surface of NK cells and other cells of the immune system; *Fcer2a*, involved in the humoral immune response; *Ppp1r42*, a regulator of centrosome separation; *Rhoc*, a member of the Rac subfamily of the Rho GTPases; *Bnip3*, a gene that interacts with anti-apoptotic proteins, including BCL2; *Tmem38a*, a cation channel required for the maintenance of rapid intracellular calcium release; and *Cr2*, which codifies for the receptor 2 of the complement C3d protein. Otherwise, overexpressed genes in affected mice included *Parm1*, a mucin-like androgen-regulated gene; *Rapgef1* (also known as C3G), a guanine nucleotide exchange factor that activates Rap1 GTPases, with a relevant function in platelet hemostasis,[19–21] *Dnajb13*, involved in sperm terminal differentiation; *Gpr55*, a G-protein-coupled receptor superfamily that regulates proliferation; and *Slco2a1*, a prostaglandin transporter.

Overexpression of *Rapgef1* has been previously associated with several hematopoietic malignancies.[22,23] In fact, we found in our affected mice that the more aggressive phenotype of the disease is associated with an increased expression of *Rapgef1,* since Hom#1 and Hom#2 mice presented a higher overexpression of the gene than Het#1 mice (Figure 3B).

These results suggest that the PKC signaling pathway could be involved in FPD/AML. Normal levels with reduced function of PKC-$\alpha/\beta$ are implicated in the platelet dysfunction.[15,24] Meanwhile, during the leukemic progression, overexpression of *Rapgef1* could increase the cell proliferation and myeloid neoplasm progression in our affected mice through hyperactivation of the Rap1 signaling pathway, as previously described.[22,25,26]

## DISCUSSION

The landscape evolving FPD/AML is complex and heterogenous. The molecular evolution in clonal hematopoietic cells of germline *RUNX1*-

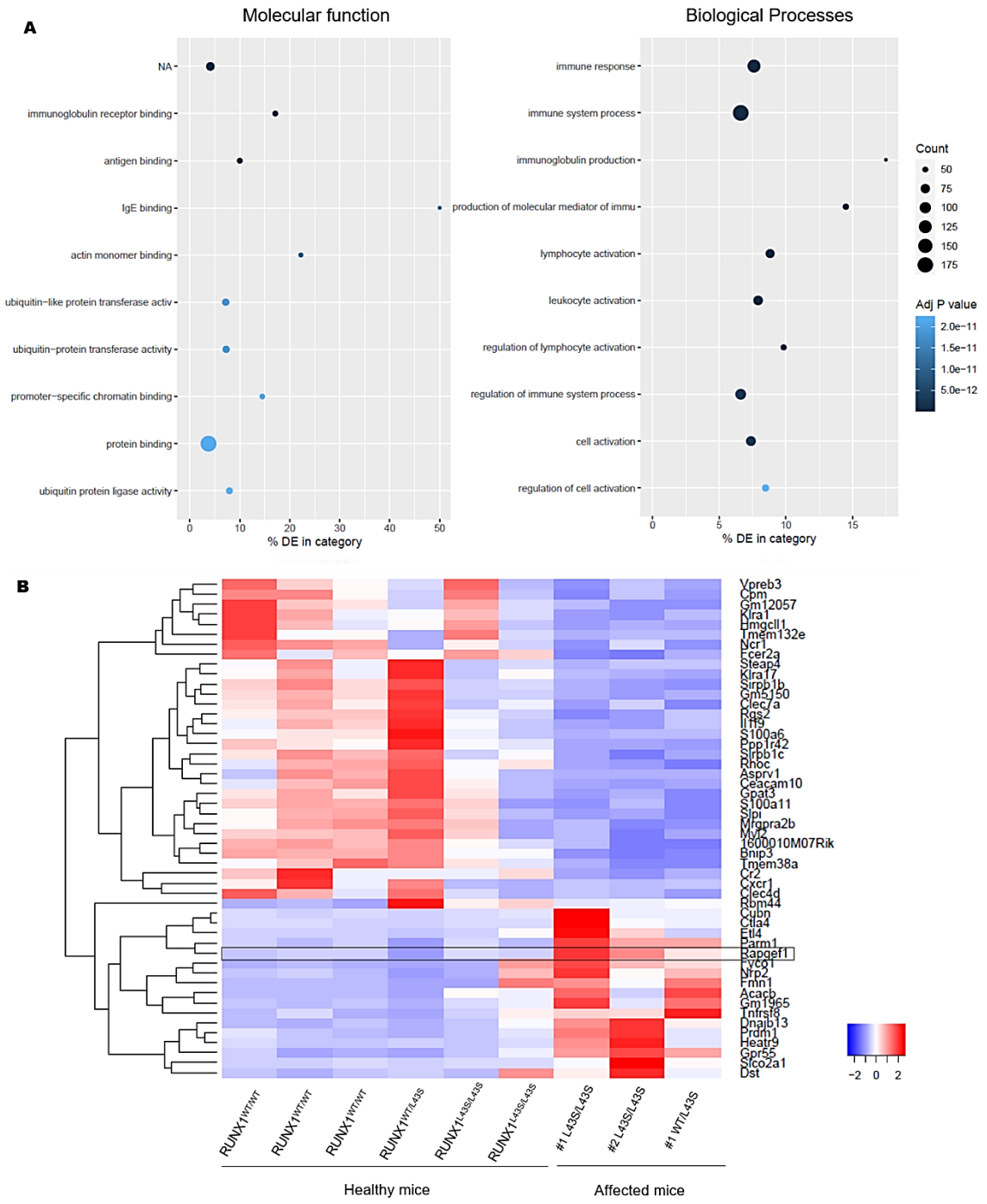


**Figure 4. RNA-seq revealed disrupted pathways related to changes in protein binding and immune system regulation, and the overexpression of *Rapgef1* in the three affected mice with Mac1$^+$ Sca1$^+$ aberrant cells. A)** Top 10 over−represented categories in Molecular Function (left) and Biological Processes (right) Gene Ontology terms identified using the GOseq package. **B)** Heatmap of the top 50 differentially expressed genes in affected mice vs. healthy mice. The heatmap was built using DESeq2 and Heatmap2 on normalized gene counts.

mutated patients leading to myeloid malignancy development remains poorly understood.[27] It is well stablished that less than half percent of patients with germline *RUNX1* variants develop myelodysplastic syndrome (MDS) or acute myeloid leukemia (AML), while inherited thrombocytopenia is found in patients with higher penetrance. This evidence suggests that *RUNX1* variants *per se* are enough to cause a platelet disorder but requires second-hit mutational events for leukemogenesis.[28] Throughout the years, multiple family pedigrees with patients affected with FPD/AML have been studied in order to uncovered somatic mutations in different genes that could justify the appearance of the neoplasm.[29,30] The most frequent second event in FPD/AML patients is the somatic mutation of the unaffected allele of *RUNX1*,[8] however, mutations in other genes such as *CDC25C, CBL, FLT3, TP53* or *ASXL1*, among others, have also been described.[31,32]

The penetrance of the disease is mainly related with the pathogenicity of the germline *RUNX1* variant found. To date, more than 30 pathogenic or likely pathogenic variants have been described in *RUNX1*, and up to 80 variants of uncertain significance (VUS).[11] Recently, the appearance of Variant Curation Expert Panels allowed the reclassification of the pathogenicity of several variants described in patients. In fact, among the 80 variants, 30 are now reclassified as benign or pathogenic variants.[10,11] This improvement in the classification of the variants is essential since it can provide targets for early detection of the myeloid neoplasm or for future therapies. Moreover, the increasing use of genome editing tools has allowed the development of cellular or animal models reproducing the *RUNX1* variants to characterize the mechanisms of pathogenicity associated.[33–35] In 2021, Decker et al. published the functional characterization of nine previously reported VUS *RUNX1* variants by addressing the heterodimerization capacity with CBFβ, the phosphorylation of RUNX1, and the ability of RUNX1 to activate the transcription, using 6 known pathogenic variants and wild-type *RUNX1* as controls. Among the 9 variants of study, we found RUNX1 p.Leu56Ser, which was described to have normal dimerization with CBFβ and RUNX1 phosphorylation, but reduced transcriptional activation of genes such as r*ETV1* and r*CSF1R*.[13] Furthermore, Koh et. al described the inability of RUNX1 p.Leu56Ser to bind MLL, suggesting a novel model of leukemogenesis related with the variant.[36] All these results, together with the variability of the *in silico* prediction tools classifying the variant as benign but also pathogenic, focus the functional classification of the variant as uncertain significance. However, given the high penetrance of the variant in heterozygosis in the population (0.0152 – GnomAD exomes / 0.0127 – GnomAD genomes) and following the rules of

the ACMG MM-VCEP, this variant should be classified as benign.[11]

Recently, our group described the optimal generation of a murine model carrying the RUNX1 p.Leu43Ser variant, generated by the CRISPR/Cas9 tool, and mimicking the human p.Leu56Ser. Heterozygous, but especially homozygous mice displayed an impaired platelet function characterized by decreased $\alpha_{IIb}\beta_3$ integrin activation, aggregation, and PKC $\alpha/\beta$ phosphorylation, demonstrating the role of the variant in the platelet disorder.[15] Therefore, to settle definitively the role of the variant in the leukemic progression and the pathogenicity associated, we followed the mature and immature hematopoietic populations thought life. We reported the appearance of an aberrant population in blood, previously described as myeloid leukemic cells,[18] double positive for the markers Mac1 and Sca1, and negative for ckit, in two homozygous mice (Hom# and Hom#2). The presence of the aberrant population is somehow different in both mice, since Hom#1 displayed earlier disease presentation and higher percentage of leukemic cells than Hom#2. In contrast, only one heterozygous mouse presented the aberrant $Mac1^+Sca1^+$ population, at a remarkably advanced age (21 months, equivalent to 60-70 years in humans) and with relatively lower levels than homozygotes. Moreover, bone marrow analysis of the three mice showed increased levels of hematopoietic stem cells, progenitors, and aberrant cells, as well as anatomical hyperplasia and anomalous distributions of the different series. No alterations in spleen had been found in the $RUNX1^{WT/L43S}$ genotype, while $RUNX1^{L43S/L43S}$ is associated with splenomegaly, especially in both Hom#1 and Hom#2 mice. It has been previously described that the levels of *RUNX1* activity are critical for leukemic predisposition,[37] justifying the pathological phenotype found in our $RUNX1^{L43S/L43S}$ but much less significant in $RUNX1^{WT/L43S}$. Nevertheless, the overall penetrance of myeloid neoplasm related to this variant is remarkable lower than the described for *RUNX1* mutated patients,[38] since only 4% of heterozygous mice (1/25) and 8% of homozygous mice (2/25) developed the disease, compared to 44% of leukemic progression in FPD/AML patients described in the literature.[1] Thus, these results suggest that RUNX1 p.Leu43Ser in heterozygosis is associated with very low penetrance of leukemogenesis, as previously suggested in patients with RUNX1 p.Leu56Ser,[1] but also with an advanced age, similar to spontaneous AML (70 years old),[39] than the described for FPD/AML (33 years old).[2] Somehow different, RUNX1 p.Leu43Ser in homozygosis is related with an increased penetrance and earlier age of presentation, but high variability in the phenotype.

To further characterize the mechanism underlying the appearance of the aberrant

population in the three mice (Hom#1, Hom#2, and Het#1) we first analyzed the acquisition of secondary mutations in *RUNX1,* since it is the most frequent second-hit.[8] However, no pathogenic somatic mutations were found. Therefore, we performed an RNAseq, to investigated unregulated genes, and we uncovered the overexpression of *Rapgef1.* This guanine nucleotide exchange factor activates several members of the Ras superfamily of GTPases, mainly Rap1, the main GTPase that regulates platelet function, and its alteration has been described in several neoplasms, including hematological malignances such as chronic myeloid leukemia.[22,23] In fact, it has been described the regulation of this gene by PKCα/β functional activity.[20,40]

Moreover, we found a correlation between the overexpression of *Rapgef1* and the genotype and phenotype, since the higher expression of this gene is more remarkable in RUNX1$^{L43S/L43S}$ mice, which displayed a more aggressive phenotype. These results are in agreement with previous studies demonstrating the importance of allelic burden in RUNX1 and its relevance to FPD/AML progression,[37] suggested that *RUNX1* alterations could impaired the PKCα/β signaling pathway, promoting the disease appearance. However, these results should be expanded and confirmed by studying patients and more mutations in the *RUNX1* gene.

In summary, we have characterized the RUNX1 p.Leu56Ser variant in a murine model generated by the CRISPR/Cas9 genome editing tool to set out its implication in FPD/AML. We observed that the variant in heterozygosis is associated with a weak predisposition to myeloid neoplasm. This fact, together with the high allelic frequency in the population, and the autosomal dominant inheritance of the disease, drive the classification of the variant as benign, as described by the ClinGen Myeloid Malignancy Variant Curation Expert Panel.[10] However, we observed a more aggressive phenotype in homozygous mice, associated with high levels of aberrant cells in blood (7-15%), the affectation of the bone marrow and the spleen, and the overexpression of *Rapgef1* as a potential and novel second-hit. The variant in homozygosis has been described in 47 of 231814 patients included in GnomAD exomes (MAF: 0.0002), therefore, the monitoring of these patients should be of major consideration for genetic counselling and future therapeutic strategies.

**ACKNOWLEDGMENTS**

We thank the Transgenic Facility and Lucía Méndez Sánchez for the help with mouse handling and managing; Eva Lumbreras, Sara González Briones, and Irene Rodríguez Iglesias for technical support with experiments; Sandra Santos-Mínguez and Cristina Miguel-García for preparing DNA and RNA samples for sequencing; the CIC–IBMCC Microscopy and Cytometry Service and the Separation/Cytometry Service of Nucleus

for technical assistance with flow-cytometry assays; The Molecular Pathology Unit for helping with the histopathological diagnosis; and Sequencing Service of NUCLEUS for carrying out the RNA-seq.

This work was supported by grants from Instituto de Salud Carlos III (ISCIII) & Feder (PI17/01966, PI20/00926) and co-funded by European Union (ERDF/ESF, "Investing in your future"), Gerencia Regional de Salud (GRS2061/A/2019, GRS2135/A/2020, GRS2314/A/2021), Fundación Mutua Madrileña (FMM, AP172142019), Sociedad Española de Trombosis y Hemostasia (SETH-FETH; Premio López Borrasca 2019 and Ayuda a Grupos de Trabajo en Patología Hemorrágica 2020 and 2021), Fundación Castellano Leonesa de Hematología y Hemoterapia (FUCALHH 2020), Red Temática de Investigación Cooperativa en Cáncer (RTICC) (RD12/0036/0069), Centro de Investigación Biomédica en Red de Cáncer (CIBERONC CB16/12/00233). A.M.Q. is fully supported by an "Ayuda predoctoral de la Junta de Castilla y León" by the Fondo Social Europeo (JCYL-EDU/556/2019 PhD scholarship).

## AUTHORSHIP CONTRIBUTIONS

JMHR, CG, JPL, RB and JMB designed the study. AMQ undertook the phenotypic characterization assays in the mice model. MdR, JLO, LDA and IGT contributed to experimental design and assays. JMB, JR, JPL, CG, and RB conducted experiments. DS, RB and IGT conducted RNA-seq analysis. AMQ, JMB, IGT, and RB analyzed data. AMQ, RB and JMB wrote the manuscript. All authors critically revised the manuscript for important intellectual content and gave final approval for the version to be published. The corresponding author, JMB and AMQ had full access to all the data in the study and had final responsibility for the decision to submit for publication.

## CONFLICT OF INTERESTS

The authors state that they have no conflict of interest.

## REFERENCES

1. Simon L, Spinella JF, Yao CY, et al. High frequency of germline RUNX1 mutations in patients with RUNX1-mutated AML. *Blood*. 2020;135(21):1882–1886.
2. Bellissimo DC, Speck NA. RUNX1 Mutations in Inherited and Sporadic Leukemia. *Front. Cell Dev. Biol.* 2017;5:111.
3. Ernst MPT, Kavelaars FG, Löwenberg B, Valk PJM, Raaijmakers MHGP. RUNX1 germline variants in RUNX1-mutant AML: how frequent? *Blood*. 2021;137(10):1428–1431.
4. Brown AL, Arts P, Carmichael CL, et al. RUNX1-mutated families show phenotype heterogeneity and a somatic mutation profile unique to germline predisposed AML. *Blood Adv*. 2020;4(6):1131–1144.
5. Arber DA, Orazi A, Hasserjian R, et al. The 2016 revision to the World Health Organization classification of myeloid neoplasms and acute leukemia. *Blood*. 2016;127(20):2391–2405.
6. Jung J, Cho BS, Kim HJ, et al. Reclassification of acute myeloid leukemia according to the 2016 who classification. *Ann. Lab. Med.* 2019;39(3):311–316.
7. Koeffler HP, Leong G. Preleukemia: One name, many meanings. *Leukemia*. 2017;31(3):534–542.
8. Preudhomme C, Renneville A, Bourdon V, et al. High frequency of RUNX1 biallelic alteration in acute myeloid leukemia secondary to familial platelet disorder. *Blood*. 2009;113(22):5583–5587.
9. Antony-Debré I, Duployez N, Bucci M, et al. Somatic mutations associated with leukemic progression of familial platelet disorder with

predisposition to acute myeloid leukemia. *Leukemia*. 2016;30(4):999–1002.

10. Luo X, Feurstein S, Mohan S, et al. ClinGen Myeloid Malignancy Variant Curation Expert Panel recommendations for germline RUNX1 variants. *Blood Adv*. 2019;3(20):2962–2979.
11. Wu D, Luo X, Feurstein S, et al. How I curate: Applying American Society of Hematology-Clinical Genome Resource Myeloid Malignancy Variant Curation Expert Panel rules for RUNX1 variant curation for germline predisposition to myeloid malignancies. *Haematologica*. 2020;105(4):870–887.
12. Duployez N, Fenwarth L. Controversies about germline RUNX1 missense variants. *Leuk. Lymphoma*. 2020;61(2):497–499.
13. Decker M, Lammens T, Ferster A, et al. Functional classification of RUNX1 variants in familial platelet disorder with associated myeloid malignancies. *Leukemia*. 2021;35(11):3304–3308.
14. Borst S, Nations CC, Klein JG, et al. Study of inherited thrombocytopenia resulting from mutations in ETV6 or RUNX1 using a human pluripotent stem cell model. *Stem Cell Reports*. 2021;16(6):1458–1467.
15. Marín-Quílez A, García-Tuñón I, Fernández-Infante C, et al. Characterization of the Platelet Phenotype Caused by a Germline RUNX1 Variant in a CRISPR/Cas9-Generated Murine Model. *Thromb. Haemost.* 2021;121(9):1193–1205.
16. Love MI, Huber W, Anders S. Moderated estimation of fold change and dispersion for RNA-seq data with DESeq2. *Genome Biol.* 2014;15(12):550.
17. Young MD, Wakefield MJ, Smyth GK, Oshlack A. Gene ontology analysis for RNA-seq: accounting for selection bias. *Genome Biol.* 2010;11(2):R14.
18. Campbell KJ, Bath ML, Turner ML, et al. Elevated Mcl-1 perturbs lymphopoiesis, promotes transformation of hematopoietic stem/progenitor cells, and enhances drug resistance. *Blood*. 2010;116(17):3197–3207.
19. Gutiérrez-Herrero S, Maia V, Gutiérrez-Berzal J, et al. C3G transgenic mouse models with specific expression in platelets reveal a new role for C3G in platelet clotting through its GEF activity. *Biochim. Biophys. Acta*. 2012;1823(8):1366–1377.
20. Gutiérrez-Herrero S, Fernández-Infante C, Hernández-Cano L, et al. C3G contributes to platelet activation and aggregation by regulating major signaling pathways. *Signal Transduct. Target Ther.* 2020;5(1):29.
21. Martín-Granado V, Ortiz-Rivero S, Carmona R, et al. C3G promotes a selective release of angiogenic factors from activated mouse platelets to regulate angiogenesis and tumor metastasis. *Oncotarget*. 2017;8(67):110994–111011.
22. Carabias A, Guerrero C, de Pereda JM. C3G self-regulatory mechanism revealed: implications for hematopoietic malignancies. *Mol. Cell. Oncol.* 2021;8(1):1837581.
23. Gutiérrez-Berzal J, Castellano E, Martín-Encabo S, et al. Characterization of p87C3G, a novel, truncated C3G isoform that is overexpressed in chronic myeloid leukemia and interacts with Bcr-Abl. *Exp. Cell Res.* 2006;312(6):938–948.
24. Harper MT, Poole AW. Diverse functions of protein kinase C isoforms in platelet activation and thrombus formation. *J. Thromb. Haemost.* 2010;8(3):454–462.
25. Kometani K, Ishida D, Hattori M, Minato N. Rap1 and SPA-1 in hematologic malignancy. *Trends Mol. Med.* 2004;10(8):401–408.
26. Minato N, Kometani K, Hattori M. Regulation of Immune Responses and Hematopoiesis by the

Rap1 Signal. *Adv. Immunol.* 2007;93:229–264.

27. Sood R, Kamikubo Y, Liu P. Role of RUNX1 in hematological malignancies. *Blood.* 2017;129(15):2070–2082.
28. Hayashi Y, Harada Y, Huang G, Harada H. Myeloid neoplasms with germ line RUNX1 mutation. *Int. J. Hematol.* 2017;106(2):183–188.
29. Duarte BKL, Yamaguti-Hayakawa GG, Medina SS, Siqueira LH, Snetsinger B, Costa FF, Rauh MJ & Ozelo M. Longitudinal sequencing of RUNX1 familial platelet disorder: new insights into genetic mechanisms of transformation to myeloid malignancies. *Br. J. Haematol.* 2019;186(5):724–734.
30. Ng IK, Lee J, Ng C, et al. Preleukemic and second-hit mutational events in an acute myeloid leukemia patient with a novel germline RUNX1 mutation. *Biomark. Res.* 2018;11(6):16.
31. Yoshimi A, Toya T, Kawazu M, et al. Recurrent CDC25C mutations drive malignant transformation in FPD/AML. *Nat. Commun.* 2014;5:4770.
32. Sakurai M, Kasahara H, Yoshida K, et al. Genetic basis of myeloid transformation in familial platelet disorder/acute myeloid leukemia patients with haploinsufficient RUNX1 allele. *Blood Cancer J.* 2016;6(2):e392.
33. Growney JD, Shigematsu H, Li Z, et al. Loss of Runx1 perturbs adult hematopoiesis and is associated with a myeloproliferative phenotype. *Blood.* 2005;106(2):494–504.
34. Lam K, Muselman A, Du R, et al. Hmga2 is a direct target gene of RUNX1 and regulates expansion of myeloid progenitors in mice. *Blood.* 2014;124(14):2203–2212.
35. Sakurai M, Kunimoto H, Watanabe N, et al. Impaired hematopoietic differentiation of RUNX1-mutated induced pluripotent stem cells derived from FPD/AML patients. *Leukemia.* 2014;28(12):2344–2354.
36. Koh CP, Wang CQ, Ng CE, Ito Y, Araki M, Tergaonkar V, Huang G OM. RUNX1 meets MLL: epigenetic regulation of hematopoiesis by two leukemia genes. *Leukemia.* 2013;27(9):1793–1802.
37. Antony-Debré I, Manchev VT, Balayn N, et al. Level of RUNX1 activity is critical for leukemic predisposition but not for thrombocytopenia. *Blood.* 2015;125(6):930–940.
38. Churpek JE, Pyrtel K, Kanchi KL, et al. Genomic analysis of germ line and somatic variants in familial myelodysplasia/acute myeloid leukemia. *Blood.* 2015;126(22):2484–2490.
39. Récher C, Röllig C, Bérard E, et al. Long-term survival after intensive chemotherapy or hypomethylating agents in AML patients aged 70 years and older: a large patient data set study from European registries. *Leukemia.* 2022;36(4):913–922.
40. Gutiérrez-Herrero S, Fernández-Infante C, Hernández-Cano L, et al. C3G contributes to platelet activation and aggregation by regulating major signaling pathways. *Signal Transduct. Target. Ther.* 2020;5(1):29.

## SUPPLEMENTAL MATERIAL

---

# Expanding the role of germline *RUNX1* variants in leukemogenesis in a murine model generated by CRISPR/Cas9

Marín-Quílez A, et al.

**Supplemental Tables**

| Oligos | Sequence |
|---|---|
| Runx1ex1F | ATAATTCTTTCCCCCACCCCC |
| Runx1ex1R | CATTCAGAGCAAGGCACAGCC |
| Runx1ex2F | ACCCTCCGGTAGTAATAAAGGC |
| Runx1ex2R | GGATACCTCTGAGGCTGACCC |
| Runx1ex3F | CCACACCTGTCTCTGCATCG |
| Runx1ex3R | ATTCACGCATCACACACTGTGC |
| Runx1ex4F | ATGCACTATGCCCCACCTGG |
| Runx1ex4R | TCTTAACTCATCTGAGTTGGCC |
| Runx1ex5F | AAAAGTCCCCTCCACAACACG |
| Runx1ex5R | TCCTGTGGAGTTTGATACCTG |
| Runx1ex6F | CAGAGTCATCAAATACTTGGGC |
| Runx1ex6R | TCCCAAAGGGATGGACTAAGG |
| Runx1ex7F | ACTCTGGCAGTCTAGGAAGC |
| Runx1ex7R | GATTCTTCCTGGTGGCCTCC |

**Table S1. Oligonucleotides used for amplicon-based DNA seq.** F: forward; R: reverse.

| Gene | RUNX1$^{WT/WT}$ | RUNX1$^{WT/WT}$ | RUNX1$^{WT/WT}$ | RUNX1$^{WT/L43S}$ | RUNX1$^{L43S/L43S}$ | RUNX1$^{L43S/L43S}$ | Het#1 | Hom#1 | Hom#2 |
|---|---|---|---|---|---|---|---|---|---|
| Ppp1r42 | 0.558906 | 0.289661 | 0.077168 | -0.252448 | 2.205.372 | -0.056555 | -1.013.067 | -0.95226 | -0.856777 |
| Dst | -0.583506 | -0.78697 | -0.636148 | 1.084.784 | -0.515731 | -0.73115 | -0.123486 | 2.150.056 | 0.14215 |
| Ctla4 | -0.371183 | -0.409479 | -0.479272 | -0.351053 | -0.44979 | -0.364074 | -0.13732 | -0.080078 | 2.642.249 |
| Nrp2 | -0.573635 | -0.506295 | -0.681789 | 0.712352 | -1.013.037 | -0.747846 | 0.660269 | 0.047947 | 2.102.035 |
| Cxcr1 | 0.201482 | 2.050.578 | -0.149377 | -0.838894 | 1.216.819 | -0.687824 | -0.599104 | -0.637878 | -0.555802 |
| Gpr55 | -0.485263 | -0.886883 | -0.763874 | -0.109389 | -0.932528 | -0.549356 | 0.88392 | 1.861.796 | 0.981576 |
| Rbm44 | -0.820427 | -0.735174 | -0.897398 | 0.426836 | 2.386.037 | 0.122353 | -0.099055 | -0.130178 | -0.252995 |
| Rgs2 | 0.185304 | 0.632017 | 0.54915 | -0.440512 | 2.050.178 | -0.154953 | -0.599786 | -1.020.378 | -1.201.019 |
| Cr2 | 0.632148 | 2.181.269 | -0.161538 | 0.398463 | -0.147095 | -0.113613 | -0.838243 | -1.066.337 | -0.885053 |
| Cubn | -0.404638 | -0.432632 | -0.364417 | -0.264588 | -0.458001 | -0.338003 | -0.207862 | -0.184132 | 2.654.274 |
| Etl4 | -0.501469 | -0.500305 | -0.469805 | 0.080866 | -0.591281 | -0.486943 | -0.507882 | 0.489518 | 2.487.301 |
| Il1f9 | -0.162715 | 0.745365 | 0.45509 | -0.598517 | 2.154.401 | -0.065421 | -0.623128 | -0.99703 | -0.908045 |
| Rapgef1 | -0.590348 | -0.50162 | -0.512481 | -0.490053 | -1.005.928 | -0.409493 | 0.272892 | 1.169.154 | 2.067.876 |
| Fmn1 | -0.679122 | -0.660874 | -0.677919 | 1.380.197 | -0.896373 | -0.88091 | 1.364.395 | -0.084851 | 1.135.456 |
| Slpi | 0.05754 | 0.82818 | 0.875017 | -0.733171 | 1.655.685 | 0.357956 | -1.191.963 | -0.863144 | -0.9861 |
| Sirpb1b | 0.440795 | 1.185.963 | 0.407285 | -0.413213 | 1.739.417 | -0.480386 | -1.075.222 | -1.006.629 | -0.798009 |
| Sirpb1c | 0.218195 | 1.154.188 | 0.736047 | -0.021334 | 1.540.075 | -0.448419 | -0.890645 | -1.361.018 | -0.927088 |
| Gm5150 | 0.327173 | 0.844059 | 0.365137 | -0.46834 | 2.062.869 | -0.514319 | -0.785272 | -1.000.536 | -0.83077 |
| S100a6 | -0.102228 | 0.264322 | 0.287327 | -0.583242 | 2.426.874 | -0.118292 | -0.699084 | -0.649196 | -0.826481 |
| S100a11 | 0.439489 | 0.937197 | 0.745634 | -1.023.923 | 1.436.282 | 0.430818 | -1.200.231 | -0.686449 | -1.078.817 |
| Rhoc | -0.279139 | 0.846896 | 0.902028 | 0.253875 | 1.637.207 | -0.09767 | -1.327.467 | -0.99092 | -0.94481 |
| Tnfrsf8 | -0.689166 | -0.328437 | -0.837714 | 0.153972 | -0.952293 | -0.434948 | 2.297.369 | 0.346865 | 0.44435 |
| Steap4 | -0.091836 | 1.062.987 | -0.167527 | -0.404712 | 2.221.023 | -0.607337 | -0.622976 | -0.610116 | -0.779505 |
| Parm1 | -0.469106 | -0.723601 | -0.491563 | -0.672556 | -0.99111 | -0.392903 | 0.913843 | 0.868228 | 1.958.769 |
| Gpat3 | 0.250134 | 0.9378 | 0.308419 | -0.72927 | 1.850.943 | 0.293821 | -1.175.278 | -0.746677 | -0.989891 |
| Acacb | -0.639302 | -0.686634 | -0.638757 | -0.115029 | -0.89515 | 0.036334 | 1.846.076 | -0.426199 | 1.518.661 |
| Myl2 | 0.49745 | 0.545195 | 0.719258 | -0.882953 | 1.671.849 | 0.436333 | -0.923 | -1.340.814 | -0.723319 |
| Asprv1 | -0.539831 | 1.064.246 | 0.771125 | -0.678382 | 1.876.715 | -0.046691 | -0.798497 | -0.814164 | -0.834521 |
| Gm1965 | -0.568492 | -0.704696 | -0.589107 | -0.11333 | -0.810972 | -0.396216 | 138.458 | -0.21259 | 2.010.823 |
| Clec4d | 1.614.632 | 0.759651 | -0.318417 | -0.825021 | 1.430.165 | -0.346878 | -0.991108 | -0.734501 | -0.588524 |
| Clec7a | 0.29636 | 0.910805 | 0.187983 | -0.209559 | 2.014.219 | -0.555306 | -1.214.199 | -0.449875 | -0.980429 |
| Klra17 | 0.068612 | 0.908421 | -0.181225 | 0.0222 | 2.192.296 | -0.594916 | -0.918219 | -0.828456 | -0.668712 |
| Klra1 | 1.931.474 | 0.907966 | -0.163794 | -0.401343 | -0.061993 | 0.645428 | -0.690527 | -1.159.272 | -1.007.938 |
| Ncr1 | 1.595.008 | 1.098.288 | 0.907605 | -0.425993 | -0.751007 | 0.184277 | -1.130.822 | -0.36687 | -1.110.485 |
| Ceacam10 | -0.267766 | 0.700753 | 0.983818 | -0.670362 | 1.874.816 | 0.109807 | -0.877483 | -0.97733 | -0.876254 |
| Mrgpra2b | 0.028811 | 0.856532 | 1.090.924 | -0.886261 | 1.324.563 | 0.591708 | -1.156.845 | -1.186.322 | -0.66311 |
| Dnajb13 | -0.643361 | -0.776472 | -0.553134 | -0.065198 | -0.801178 | -0.567556 | 0.181314 | 2.099.562 | 1.126.023 |
| 1600010M07Rik | 0.82756 | 1.047.546 | 0.656525 | -0.35917 | 1.232.192 | 0.012445 | -1.361.713 | -1.321.586 | -0.733798 |
| Bnip3 | 0.932248 | 0.77917 | 0.801365 | -0.083074 | 1.204.163 | -0.000802 | -1.198.942 | -1.328.328 | -1.105.801 |
| Fcer2a | 1.458.201 | -0.241552 | 0.723287 | 0.463469 | -0.010437 | 1.016.579 | -0.813037 | -1.375.252 | -1.221.256 |
| Tmem38a | -0.105109 | 0.595138 | 1.487.806 | -0.271705 | 1.273.925 | 0.268631 | -1.267.617 | -1.194.437 | -0.786633 |
| Hmgcll1 | 1.914.651 | 0.662582 | -0.258402 | -0.580037 | 0.001482 | 0.987723 | -0.909908 | -0.775588 | -1.042.504 |
| Slco2a1 | -0.459979 | -0.448145 | -0.410022 | -0.364777 | -0.471128 | -0.392415 | 0.02382 | 262.661 | -0.103964 |
| Fyco1 | -0.80163 | -0.696537 | -0.765406 | 1.006.844 | -0.864533 | -0.772183 | 0.400404 | 0.671626 | 1.821.416 |
| Prdm1 | -0.296337 | -0.559196 | -0.665289 | -0.283206 | -0.758095 | -0.600061 | -0.259345 | 2.043.329 | 13.782 |
| Vpreb3 | 1.556.189 | 0.492794 | 0.015502 | -0.650973 | -0.400275 | 1.554.576 | -0.886471 | -0.580657 | -1.100.684 |
| Cpm | 1.212.029 | 1.203.126 | 0.023148 | -0.532268 | -0.449596 | 133.834 | -1.018.871 | -0.578668 | -119.724 |
| Gm12057 | 1.932.122 | 0.561999 | 0.23489 | -0.34299 | -0.443741 | 0.898229 | -1.064.918 | -1.066.842 | -0.708748 |
| Tmem132e | 1.975.742 | -0.040734 | 0.080088 | -0.412917 | -0.831655 | 1.324.645 | -0.66919 | -0.653777 | -0.772202 |
| Heatr9 | -0.382836 | -0.633734 | -0.599 | -0.357446 | -0.526891 | -0.559485 | -0.304556 | 2.240.446 | 1.123.502 |

**Table S2. Top 50 dysregulated genes.**

# CHAPTER 3

## A novel nonsense variant in *TPM4* caused dominant macrothrombocytopenia, mild bleeding tendency and disrupted cytoskeleton remodeling.

Ana Marín-Quílez[1], Elena Vuelta[1,2], Lorena Díaz-Ajenjo[1], Cristina Fernández-Infante[1], Ignacio García-Tuñón[1], Rocío Benito[1], Verónica Palma-Barqueros[3], Jesús María Hernández-Rivas[1,4], José Ramón González-Porras[4], José Rivera[2,5*], and José María Bastida[4,5*].

[1] IBSAL, CIC, IBMCC, Universidad de Salamanca-CSIC, Salamanca, Spain; [2] Transgenic Facility, Nucleus, University of Salamanca, Salamanca, Spain; [3] Department of Hematology and Oncology, Hospital Universitario Morales Meseguer, Centro Regional de Hemodonación, Universidad de Murcia, IMIB-Arrixaca, CIBERER-U765, Spain; [4] Department of Hematology, Complejo Asistencial Universitario de Salamanca (CAUSA), Instituto de Investigación Biomédica de Salamanca (IBSAL), Universidad de Salamanca (USAL), Spain; [5] On behalf of "Grupo Español de Alteraciones Plaquetarias Congénitas (GEAPC)", SETH. *These authors share senior authorship.

*Journal of Thrombosis and Haemostasis*. 2022;20(5):1248-1255. doi: 10.1111/jth.15672. PMID: 35170221

Received: 21 November 2021 | Accepted: 14 February 2022
DOI: 10.1111/jth.15672

BRIEF REPORT

# A novel nonsense variant in *TPM4* caused dominant macrothrombocytopenia, mild bleeding tendency and disrupted cytoskeleton remodeling

## Abstract

**Background:** Rare inherited thrombocytopenias are caused by alterations in genes involved in megakaryopoiesis, thrombopoiesis and/or platelet release. Diagnosis is challenging due to poor specificity of platelet laboratory assays, large numbers of culprit genes, and difficult assessment of the pathogenicity of novel variants.

**Objectives:** To characterize the clinical and laboratory phenotype, and identifying the underlying molecular alteration, in a pedigree with thrombocytopenia of uncertain etiology.

**Patients/Methods:** Index case was enrolled in our Spanish multicentric project of inherited platelet disorders due to lifelong thrombocytopenia and bleeding. Bleeding score was recorded by ISTH-BAT. Laboratory phenotyping consisted of blood cells count, blood film, platelet aggregation and flow cytometric analysis. Genotyping was made by whole-exome sequencing (WES). Cytoskeleton proteins were analyzed in resting/spreading platelets by immunofluorescence and immunoblotting.

**Results:** Five family members displayed lifelong mild thrombocytopenia with a high number of enlarged platelets in blood film, and mild bleeding tendency. Patient's platelets showed normal aggregation and granule secretion response to several agonists. WES revealed a novel nonsense variant (c.322C>T; p.Gln108*) in *TPM4* (NM_003290.3), the gene encoding for tropomyosin-4 (TPM4). This variant led to impairment of platelet spreading capacity after stimulation with TRAP-6 and CRP, delocalization of TPM4 in activated platelets, and significantly reduced TPM4 levels in platelet lysates. Moreover, the index case displayed up-regulation of *TPM2* and *TPM3* mRNA levels.

**Conclusions:** This study identifies a novel *TPM4* nonsense variant segregating with macrothrombocytopenia and impaired platelet cytoskeletal remodeling and spreading. These findings support the relevant role of *TPM4* in thrombopoiesis and further expand our knowledge of *TPM4*-related thrombocytopenia.

## 1 | INTRODUCTION

Inherited thrombocytopenias (ITs) are a large heterogeneous group of rare platelet disorders characterized by low platelet counts which mainly lead to an increased bleeding tendency.[1,2] ITs are caused by defects in genes involved in megakaryocyte (Mk) differentiation, maturation and migration, but also in proplatelet formation and/or platelet release into blood.[2,3] Their prevalence has been estimated to be around 2.7 of 100 000 individuals but it is likely that this is an underestimate.[1] Diagnostic algorithms for ITs consist of a stepwise process based on clinical data and several laboratory tests, including the use of whole blood electronic counters to evaluate platelet count and size, blood film analysis with or without immunofluorescence staining, and platelet function assays.[4,5] Nowadays, the appropriateness of using next generation sequencing (NGS) procedures in the mainstream of diagnosis of inherited platelet disorders is well established.[6] Since

José Rivera and José María Bastida authors share senior authorship
Manuscript Handled by: Wolfgang Bergmeier
Final decision: Wolfgang Bergmeier, 14 February 2022

2010, both whole-exome and whole-genome sequencing (WES/WGS) approaches have allowed the identification of up to 15 new genes involved in ITs.[5,7] According to the International Society on Thrombosis and Haemostasis (ISTH) Scientific and Standardization Committee (SSC) for Genetics in Thrombosis and Haemostasis (GinTH), there are 71 Tier1 genes related to inherited platelet disorders[8,9] (https://www.isth.org/page/GinTh_GeneLists accessed 20th November 2021).

The most common ITs are macrothrombocytopenia (MCT), characterized by reduced platelet count and increased platelet size or mean platelet volume (MPV). These MCTs are mainly caused by genetic defects affecting early megakaryopoiesis and proplatelet formation.[7,10] In particular, proplatelet formation is highly dependent on cytoskeletal proteins, including myosin IIA, actin filaments and tubulins.[2,7,10,11] Thus, genetic changes affecting genes of the actomyosin cytoskeleton, such as *MYH9*, *ACTN1*, or in recent years, *FLNA*, *DIAPH1 or TUBB1* associate with MCT.[6,12] In 2017, the first five patients from two unrelated pedigrees with mild bleeding and *TPM4*-related thrombocytopenia (*TPM4*-RT) due to the nonsense variant p.Arg69* (NM_003290.3) were identified.[13] Recently, Stapley, et al. have just reported two new *TPM4*-RT cases carrying novel missense variants; p.Arg182Cys and p.Ala183Val (NM_001145160.2) related to relevant bleeding, platelet dysfunction, and mild or absent thrombocytopenia.[14] At the 2021 ISTH Meeting, we advanced the identification of a Spanish pedigree with *TPM4*-RT,[15] which clinical, laboratory and molecular characterization is formally reported here. Acknowledging our new family with *TPM4*-RT prompted the ISTH SSC-GinTH to include *TPM4* in the Tier1 genes for Inherited bleeding, thrombotic, and platelet disorders (BTPD).[16]

**Essentials**

- A novel nonsense variant in *TPM4* was identified in a family with mild bleeding and mild macrothrombocytopenia.
- The *TPM4* p.Gln108* variant displayed a deleterious effect on platelet cytoskeleton remodeling.
- This alteration leads to the delocalization of tropomyosin-4 in the spreading structures.
- This new pedigree with *TPM4*-RT expands the genetic and clinical spectrum and supports *TPM4* as a Tier 1 gene.

## 2 | METHODS

### 2.1 | Patients and blood sampling

This study involved patients with suspected ITs recruited in the Spanish multicenter project "Functional and Molecular Characterization of Patients with Inherited Platelet Disorders" coordinated by Grupo Español de Alteraciones Plaquetarias Congénitas (GEAPC). Investigations abided by the Helsinki Declaration and were approved by the Ethics Committee of the Instituto de Investigación Biomédica de Salamanca. All patients gave written informed consent. Bleeding symptoms were scored using ISTH-BAT questionnaire.[17] Venous blood samples were drawn into 7.5% K3 EDTA (blood cells count, blood film, nucleic acid purification and protein lysates) and buffered 0.105 M sodium citrate for platelet functional studies.[18] Platelet (P) count and mean platelet volume (MPV) were performed using a Advia 2120i hematological counter (Siemens). To measure platelet dimensions on May–Grünwald–Giemsa-stained blood smears, 100 platelets were evaluated and classified as normal (diameter <3 μm), large (3–4 μm) or giant (>4 μm).[4]

### 2.2 | Platelet functional tests

Platelet functional characterization was performed in the index case [II.2] in parallel with a healthy control. Detailed platelet phenotyping was made as described.[12,19] Briefly, platelet-rich-plasma (PRP) was obtained by centrifugation at low speed (100×*g*, 10 min). Light transmission aggregometry (LTA) was performed using an TA-8V Aggregometer (Stago) and was recorded during 5 min upon PRP stimulation with agonists.

Platelet expression of major glycoproteins (GPs) was assessed in diluted whole blood (1:10 in PBS) by flow cytometry (FC) with specific antibodies (anti-CD42a*PE, anti-CD42b*PE, anti-GPVI*FITC, anti-CD61*PE and anti-CD41*APC) (BD Biosciences). Platelets were stained at room temperature (RT) for 30 min under static conditions. For platelet function analysis, PRP was stimulated for 30 min with ADP, CRP and TRAP6, and fibrinogen-binding (fibrinogen*AF488, Invitrogen), α-granule (anti-CD62*PE antibody), and δ-granule secretion (anti-CD63*PE antibody) (BD Biosciences) were evaluated by FC using an Accuri C6™ cytometer (BD). Mean Fluorescence Intensity (MFI) or the percentage of positive platelets were analyzed using FlowJo software (vX.0.7. TreeStar).

Platelets were washed in modified Tyrode's buffer and platelet lysates were prepared as previously described.[12] Tropomyosin-4 (TPM4) (Invitrogen), β-tubulin, actinin-1, filamin A, Nonmuscle Myosin Heavy Chain II-A (NMHC-IIA) and β-actin (Cell Signaling), were detected by immunoblotting in platelet lysates, and by immunofluorescence (IF) under resting and spreading conditions using washed platelets in fibrinogen-coated coverslips (Sigma-Aldrich). Samples were visualized using a Leica TCS-SP8 confocal microscope, and images were analyzed using ImageJ software (National Institutes of Health). Platelet spreading assays in the proband and in a healthy control were performed essentially as reported.[12] We evaluated the increase in the mean platelet surface between resting and agonist (TRAP6 and CPR) stimulated conditions, upon evaluation of 50 platelets per condition.

Platelet RNA was extracted using RLT-plus lysis buffer (RNeasy kit, Qiagen), and tropomyosin mRNA levels in the patients were quantified by qPCR (Applied Biosystems) and compared to those in

a healthy control using the $2^{-\Delta\Delta CT}$ method. *GAPDH* was used as the housekeeping gene. Three different qPCR experiments, each one in triplicate, to obtain a mean average Ct value, were performed in patients and in the control for each gen.

### 2.3 | Molecular analysis by exome sequencing based on candidate gene panel

Genomic DNA was extracted from peripheral blood samples using a DNeasy blood and tissue kit, following the manufacturer's protocol (Qiagen). The propositus (II.2), and both siblings (II.3, II.4) (Figure 1A) were analyzed by WES after capture and library preparation using an academic protocol that included enrichment with the xGEN® Exome Research Panel v2 (Integrated Technologies).[20,21] Sequencing was performed with an S1 Flow Cell on the NovaSeq 6000 system with a mean target coverage of 50× at the sequencing service MLL Münchner Leukämielabor GmbH. Variant was confirmed and segregated in the rest of family members (I.1, I.2 and II.1, Figure 1A) by Sanger sequencing.

We followed the guidelines of the American College of Medical Genetics and Genomics and Association for Molecular Pathology (ACMG) to qualify variant pathogenicity.[22] General information about variants was obtained using the Varsome web tool.[23]

## 3 | RESULTS AND DISCUSSION

A 40 year-old female (propositus, II.2) (Figure 1A) was referred due to lifelong mild macrothrombocytopenia ($p = 111 \times 10^9$/L [Normal range: $p = 150–400 \times 10^9$/L] and MPV 14.7fL [7.2–11.1 fL]). She has a lifelong mild bleeding tendency (ISTH-BAT = 6) characterized by hematomas, gum bleeding, and menorrhagia which needed iron and hormonal therapy. Several family members (I.1, I.2, II.1, II.4), which were either asymptomatic or have a mild bleeding tendency, also displayed mild thrombocytopenia (Figure 1A). Peripheral blood film revealed giant (31%) and enlarged platelets (39%) in the propositus (II.2) (Figure 1B).

DNA analysis by WES identified a novel nonsense variant (c.322C>T; p.Gln108*) in *TPM4* (NM_003290.3) in all affected family members (Figure 1A). This variant was located in exon 3, affecting the coiled coil domain (Figure 1C). Following the ACMG/AMP guidelines, it was classified as likely pathogenic variant (PVS1, PM2).[22]

Carrier of the variant displayed normal platelet aggregation with several agonists, including low doses of TRAP-6 and collagen. A mild impairment and delay in the platelet aggregation response to low dose of ADP and epinephrine was observed (Figure 2A). Indeed, we observed slightly increased levels of major GPs, in accordance with the increased platelet size (Figure 2B), and normal fibrinogen-binding and α and δ-granule secretion upon platelet activation with

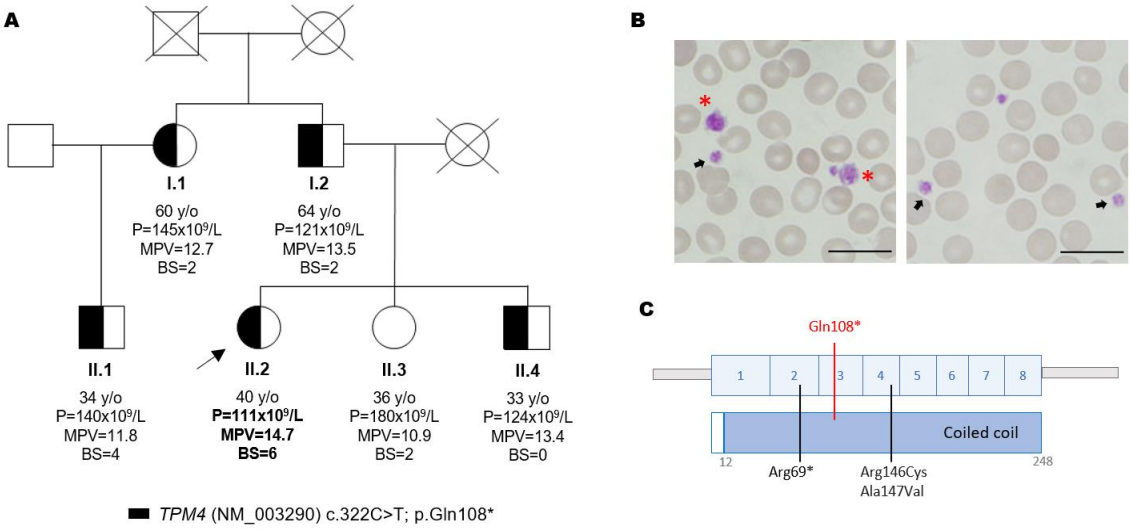


**FIGURE 1** Molecular alteration and clinical and laboratory parameters of a family with tropomyosin-4 related macrothrombocytopenia (TPM4-RT). (A) Pedigree of a family with lifelong dominant inherited macrothrombocytopenia and bleeding tendency. The index case is indicated with a black arrow. Partially filled black symbols indicate heterozygosis for the indicated *TPM4* variant. (B) Representative peripheral blood film from II.2 patient (propositus) after May-Grunwald Giemsa staining (×100). Variable platelet size was observed with large (black arrows) and giant (red asterisk) platelets. Bar: 20 μm (C) Schematic representation of the TPM4 protein, which contains 248 amino acids and a unique coiled-coil domain. Figure shows the previously reported variants (in black), p.Arg69*,[13] p.Arg146Cys and p.Ala147Val,[14] and the novel genetic change p.Gln108* (in red) found in the pedigree reported here. All genetic alterations are numbered according to positions in the NM_003290.3 transcript for *TPM4*. Variants p.Arg146Cys and p.Ala147Val correspond to described p.Arg182Cys and p.Ala183Val (NM_001145160.2)[14]

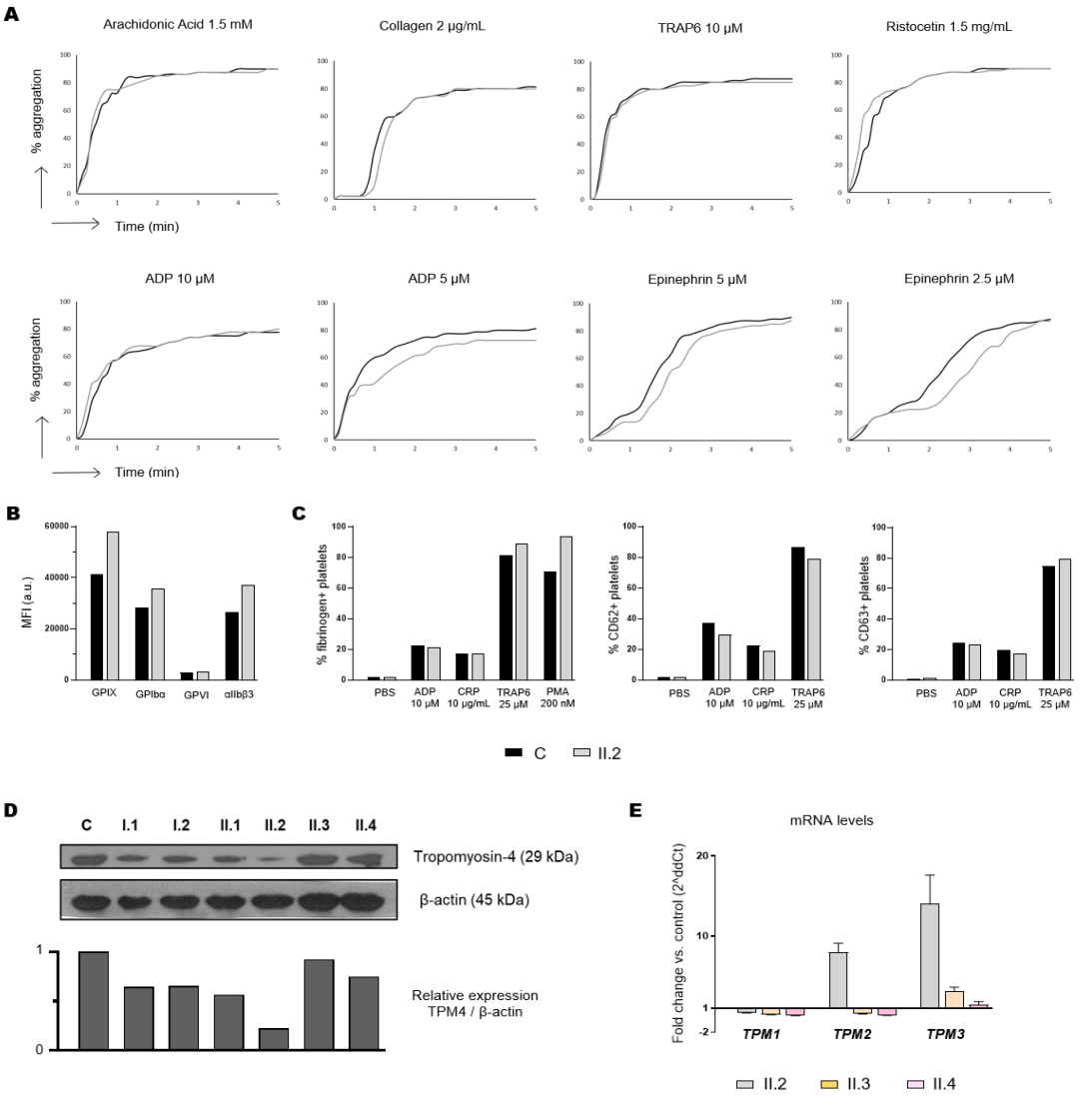


**FIGURE 2** Platelet functional phenotyping performed by light transmission aggregometry and flow cytometry (propositus) and immunoblotting (all family members). (A) Platelet aggregation, with several agonists, was evaluated in control and in the propositus. (B) Glycoproteins (GPs) expression profiles were assessed by flow cytometry with indicated fluorescently labeled antibodies. The mean fluorescence intensity (MFI) is represented. (C) Fibrinogen binding and alpha and dense granules secretion were evaluated by FC in the propositus and healthy control. (D) Western blot of tropomyosin-4 levels in platelet lysates from family members and a healthy control. β-actin was used as internal control. (E) *TPM1*, *TPM2* and *TPM3* mRNA levels in platelets from cases II.2, II.3 and II.4, relative to those in a healthy control, were assessed by qRT-PCR using the $2^{ddCt}$ method and using *GAPDH* as housekeeping gen. For each gene, three different qPCR experiments, each one in triplicate, to obtain a mean average Ct value were performed in patients and in the control. Histogram represents the mean ±standard error of the $2^{ddCt}$ values in the three qPCR experiments

by TRAP-6, ADP, and CRP (Figure 2C). A mild bleeding tendency and an almost unaffected platelet phenotype was previously observed in carriers of the *TPM4* p.Arg69* (NM_003290.3) variant.[13] In contrast, carriers of the missense variants p.Arg182Cys and p.Ala183Val (NM_001145160.2) have been recently described to have relevant bleeding, significantly impaired platelet secretion and aggregation, and normal or slightly reduced platelet count and TPM4 levels.[14] The reasons for such differences in bleeding and platelet phenotype in these *TPM4*-RT patients are still unknown. We speculate that heterozygous *TPM4* nonsense variants, such as p.Arg69*[13] and

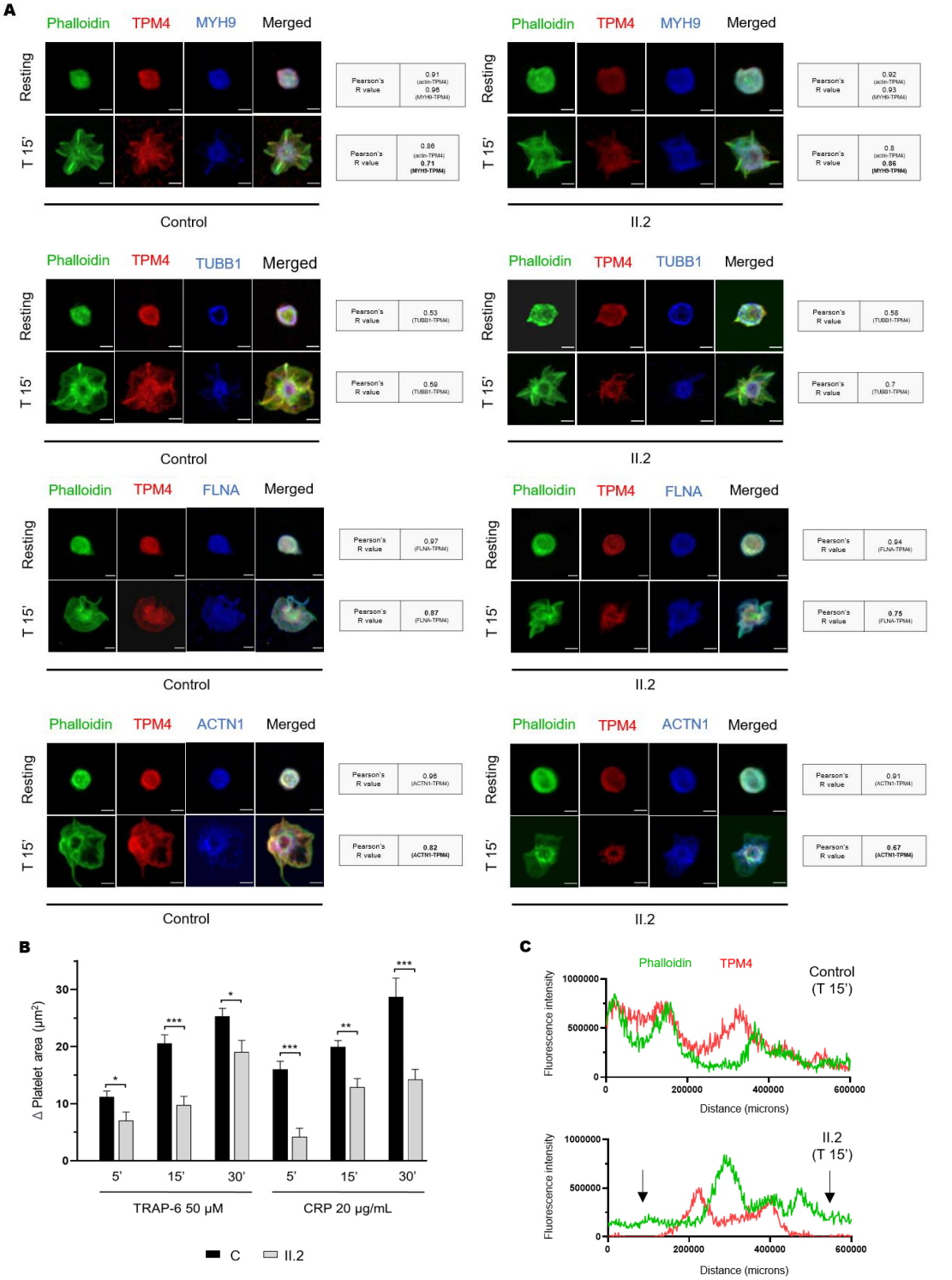


FIGURE 3 Legend on next page

**FIGURE 3** Deleterious effect of p.Gln108* TPM4 variant in cytoskeleton remodeling. Platelet spreading on fibrinogen coverslips was analyzed in washed platelets from control and II.2 patient. (A) Representative immunofluorescence image of platelet spreading under no treatment (resting), and at 15 min from activation with 50 μM TRAP-6 (T 15´). Platelets were labeled Oregon Green 514 Phalloidin (actin, green), anti-TPM4_568 (red), and anti-MYH9_647 (blue) or TUBB1_647 (blue) or FLNA_647 (blue) or ACTN1_647 (blue). Co-localization of TPM4 with other proteins of the cytoskeleton was determined with Pearson's R value (Coster *p* value =1). Images were acquired in a Leica TCS-SP8 confocal microscope, with a 100× objective lens, and images were analyzed using ImageJ software. Scale bars are 2 μm. (B) Platelet spreading assays were performed in the proband and in a healthy control. Histogram bars correspond to the increase (mean ±standard error, $n = 50$) in the area ($\mu m^2$) of agonist (TRAP6 and CPR) stimulated platelets vs. the area of resting platelets (50 platelets evaluated for each condition). *$p<.05$, **$p<.01$ and ***$p<.001$ for patient platelets vs. control platelets. (C) The line profile plots represent the fluorescence intensity distribution of channels: actin (green) and TPM4 (red) at 15 min from TRAP-6 50 μM treatment in control and II.2 platelets. Black arrows indicate the protein distribution in the spreading structures

p.Gln108*, reported here, mainly cause haploinsufficiency, which is suggested by a reduction in tropomyosin-4 levels (Figure 2D), while missense variants could present a genetic negative dominant effect exacerbating *TPM4* dysfunction and leading to major platelet disorder. Variably mild thrombocytopenia with minor, if any, associated bleeding tendency also happens in other inherited thrombocytopenias caused by mutations in structural platelet proteins.[12] Indeed, as previously described,[13] proplatelet formation is TPM4 dose-dependent, which could justify that both nonsense variants (p.Arg69* and p.Gln108*) are associated with thrombocytopenia, while the missense variants are not. Alternatively, additional platelet or hemostatic abnormalities yet undiscovered, and beyond *TPM4*, may be present in the patients reported by Stapley, et al.[14]

Interestingly, we observed that *TPM2* and *TPM3* mRNA levels in the propositus platelets were 8 and 14 times higher, respectively, than those in control platelets (Figure 2E). The fact that mutant *TPM4* associates with macrothrombocytopenia despite an increased level of other tropomyosins, further supports a highly specific and key effect of *TPM4* in megakaryopoiesis and platelet biogenesis. This finding is in agreement with previous reports suggesting that other tropomyosin isoforms have non-redundant functions with *TPM4*,[13] since *TPM1* and *TPM2* are mainly expressed in skeletal muscle, and *TPM3* in both muscle and non-muscle cells.[24] Although *TPM3* has an important role in cytoskeleton, overexpression of the isoform does not restore *TPM4* function in Mks. Besides the important involvement of *TPM4* in the cytoskeleton, it is also expressed in the striated and smooth muscle,[25] however, no associated myopathies have been reported in any *TPM4*-RT patient.

Finally, platelet spreading studies, revealed a significance reduction in the formation of filipodia and lamellipodia, as well as severe reduction of full-spreading structures (Figure 3A) in the propositus vs. control platelets, leading to an impaired spreading function, evaluated as the increased platelet area, upon stimulation with TRAP-6 and CRP for different times (Figure 3B). These results are consistent with the previously reported finding in other *TPM4*-RT cases.[13,14] In addition, we first show that while TPM4 in control platelets is homogeneously distributed throughout the cytoplasm along with actin filaments, Gln108* mutant TPM4 is accumulated mainly in the center of the patient platelets, and the protein is reduced in filopodia/lamellipodia in spread platelets, as shown in the fluorescence diagram of distribution (Figure 3C). Thus, this genetic alteration leads to a mild reduction in the localization of TPM4 with other proteins of the cytoskeleton (10%–20%) (Figure 3A). The moderate reduction of TPM4 in the spreading structures could account for the defect in cytoskeleton remodeling. However, no alterations in the level (data not shown) and localization of other cytoskeleton proteins (β-actin, actinin-1, β1-tubulin, filamin A, and NMHC-IIA) were found (Figure 3A). These data were unexpected, since previous studies in $Tpm4^{plt53}$ mutant mice demonstrated increased levels of degraded filamin A and actinin-1.[13] Finally, immunoblotting of platelet lysates showed a reduction of TPM4 levels in all p.Gln108* carriers, which was more pronounced in the index case (II.2, 80% reduction vs. level of TPM4 in control platelets) (Figure 2D). Thus, patients with *TPM4*-RT showed variable phenotypic expression, indicating differences in genetic penetrance of the different *TPM4* variants, and/or the contribution of other unrecognized factors in some affected patients.

Although no patients with *TPM4*-RT receiving thrombopoietin receptor agonists have been reported to date, the effectiveness of agents have been shown in other inherited thrombocytopenias with defects of the platelet cytoskeleton, such as *MYH9* or *DIAPH1*.[10,26] In summary, we have identified and characterized a novel nonsense variant in *TPM4*, c.322C>T [p.Gln108*], which is associated with mild macrothrombocytopenia and a deleterious effect on platelet cytoskeleton remodeling. Our findings reinforce the key role of *TPM4* in thrombopoiesis and expand the phenotype and genotype spectrum of *TPM4*-RT. This new *TPM4*-RT pedigree guarantees the inclusion of *TPM4* as a Tier1 list of gene involved in ITs.

**KEYWORDS**

inherited platelet disorders, macrothrombocytopenia, *TPM4*, tropomyosin-4, whole-exome sequencing

**ACKNOWLEDGEMENTS**

We thank Sandra Santos-Mínguez and Cristina Miguel-García for preparing DNA samples for sequencing; Sara González Briones and Irene Rodríguez Iglesias for technical support with experiments; the CIC-IBMCC Microscopy and Cytometry Service for technical assistance with the confocal immunofluorescence studies; María Díez-Campelo, Félix López-Cadenas, María de los Ángeles Manrique Gonzalo, Nuria Vicente Holgado, Mercedes Rodríguez Martín, Isabel Ramos Sevillano, María del Mar Cambronero Estévez and Beatriz Oreja Martín for blood samples collection, hemograms and blood smears.

## CONFLICT OF INTEREST

The authors state that they have no conflict of interest.

## AUTHOR CONTRIBUTION

JMB, JMHR and JRGP designed the research; AMQ, CFI, VPB, JR and EV performed the functional experiments. RB and JMB conducted the whole exome sequencing analysis. AMQ, IGT, JRGP and JMB analyzed and interpretated the results; AMQ, JR and JMB wrote the paper. All authors reviewed the results and approved the final version of the manuscript.

## FUNDING INFORMATION

This work was partially supported by grants from Instituto de Salud Carlos III (ISCIII) and Feder (PI17/01966, PI20/00926), Gerencia Regional de Salud (GRS2061A/19, GRS2135/A/2020, GRS2314/A/2021), Fundación Mutua Madrileña (FMM, AP172142019) and Sociedad Española de Trombosis y Hemostasia (SETH-FETH; Premio López Borrasca 2019 and Ayuda a Grupos de Trabajo en Patología Hemorrágica 2020 and 2021). The author's research on Inherited Platelet Disorders is conducted in accordance with the aims of the Functional and Molecular Characterization of Patients with Inherited Platelet Disorders Project, which is supported by "Grupo Español de Alteraciones Plaquetarias Congénitas (GEAPC)". AMQ and CFI hold a predoctoral grant from the Junta de Castilla y León.

Ana Marín-Quílez[1]
Elena Vuelta[1,2]
Lorena Díaz-Ajenjo[1]
Cristina Fernández-Infante[1]
Ignacio García-Tuñón[1]
Rocío Benito[1]
Verónica Palma-Barqueros[3]
Jesús María Hernández-Rivas[1,4]
José Ramón González-Porras[4]
José Rivera[3,5]
José María Bastida[4,5]

[1]*IBSAL, CIC, IBMCC, Universidad de Salamanca-CSIC, Salamanca, Spain*
[2]*Transgenic Facility, Nucleus, University of Salamanca, Salamanca, Spain*
[3]*Department of Hematology and Oncology, Hospital Universitario Morales Meseguer, Centro Regional de Hemodonación, Universidad de Murcia, IMIB-Arrixaca, Murcia, Spain*
[4]*Department of Hematology, Complejo Asistencial Universitario de Salamanca (CAUSA), Instituto de Investigación Biomédica de Salamanca (IBSAL), Universidad de Salamanca (USAL), Salamanca, Spain*
[5]*On behalf of "Grupo Español de Alteraciones Plaquetarias Congénitas (GEAPC)", SETH, Madrid, Spain*

**Correspondence**
José María Bastida, Unidad de Trombosis y Hemostasia, Hospital Universidad de Salamanca, Paseo de San Vicente, 182, 37007 Salamanca, Spain.
Email: jmbastida@saludcastillayleon.es

## ORCID

*Ana Marín-Quílez* https://orcid.org/0000-0002-2005-1919
*José María Bastida* https://orcid.org/0000-0002-8007-3909

## REFERENCES

1. Balduini CL, Melazzini F, Pecci A. Inherited thrombocytopenias—recent advances in clinical and molecular aspects. *Platelets*. 2017;28(1):3-13.
2. Nurden AT, Nurden P. Inherited thrombocytopenias: history, advances and perspectives. *Haematologica*. 2020;105(8):2004-2019.
3. Rodeghiero F, Pecci A, Balduini CL. Thrombopoietin receptor agonists in hereditary thrombocytopenias. *J Thromb Haemost*. 2018;16(9):1700-1710.
4. Zaninetti C, Greinacher A. Diagnosis of inherited platelet disorders on a blood smear. *J Clin Med*. 2020;9(2):539.
5. Bastida JM, Benito R, Lozano ML, et al. Molecular diagnosis of inherited coagulation and bleeding disorders. *Semin Thromb Hemost*. 2019;45(7):695-707.
6. Bastida JM, Lozano ML, Benito R, et al. Introducing high-throughput sequencing into mainstream genetic diagnosis practice in inherited platelet disorders. *Haematologica*. 2018;103(1):148-162.
7. Bury L, Falcinelli E, Gresele P. Learning the ropes of platelet count regulation: inherited thrombocytopenias. *J Clin Med*. 2021;10(3):533.
8. Megy K, Downes K, Simeoni I, et al. Curated disease-causing genes for bleeding, thrombotic, and platelet disorders: communication from the SSC of the ISTH. *J Thromb Haemost*. 2019;17(8):1253-1260.
9. Megy K, Downes K, Morel-Kopp MC, et al. GoldVariants, a resource for sharing rare genetic variants detected in bleeding, thrombotic, and platelet disorders: communication from the ISTH SSC subcommittee on genomics in thrombosis and hemostasis. *J Thromb Haemost*. 2021;19(10):2612-2617.
10. Bastida JM, Gonzalez-Porras JR, Rivera J, Lozano ML. Role of thrombopoietin receptor agonists in inherited thrombocytopenia. *Int J Mol Sci*. 2021;22(9):4330.
11. Collins J, Astle WJ, Megy K, Mumford AD, Vuckovic D. Advances in understanding the pathogenesis of hereditary macrothrombocytopenia. *Br J Haematol*. 2021;195(1):25-45.
12. Palma-Barqueros V, Bury L, Kunissima S, et al. Expanding the genetic spectrum of TUBB1- related thrombocytopenia. *Blood Adv*. 2021;5(24):5453-5467.
13. Pleines I, Woods J, Chappaz S, et al. Mutations in tropomyosin 4 underlie a rare form of human macrothrombocytopenia. *J Clin Invest*. 2017;127(3):814-829.
14. Stapley RJ, Poulter NS, Khan AO, et al. Rare missense variants in Tropomyosin-4 (TPM4) are associated with platelet dysfunction, cytoskeletal defects and excessive bleeding. *J Thromb Haemost*. 2021;20(2):478-485.
15. Marín-Quílez A, Fernández-Infante C, Manrique Gonzalo MÁ, et al. Characterization of a new family with lifelong macrothrombocytopenia caused by a novel nonsense variant in TPM4. *Res Pr Thromb Haemost*. 2021;5(suppl 2):1.
16. Freson K. Hemostatic phenotypes and genetic disorders. *Res Pr Thromb Haemost*. 2021;5(5):e12532.
17. Rodeghiero F, Tosetto A, Abshire T, et al. ISTH/SSC bleeding assessment tool: a standardized questionnaire and a proposal for

a new bleeding score for inherited bleeding disorders. *J Thromb Haemost*. 2010;8(9):2063-2065.
18. Frelinger AL, Rivera J, Connor DE, et al. Consensus recommendations on flow cytometry for the assessment of inherited and acquired disorders of platelet number and function: communication from the ISTH SSC subcommittee on platelet physiology. *J Thromb Haemost*. 2021;19(12):3193-3202.
19. Marín-Quílez A, García-Tuñón I, Fernández-Infante C, et al. Characterization of the platelet phenotype caused by a germline RUNX1 variant in a CRISPR/Cas9-generated murine model. *Thromb Haemost*. 2021;121(9):1193-1205.
20. xGen Exome Research Panel v2 targets. 2020. Accessed November 20, 2021. https://sfvideo.blob.core.windows.net/sitefinity/docs/default-source/flyer/idt_xgen-exome-research-panel-v2.pdf?sfvrsn=fda61707_10.
21. Tilleman L, Heindryckx B, Deforce D, Van Nieuwerburgh F. Pan-cancer pharmacogenetics: targeted sequencing panels or exome sequencing? *Pharmacogenomics*. 2020;21(15):1073-1084.
22. Richards S, Aziz N, Bale S, et al. Standards and guidelines for the interpretation of sequence variants: a joint consensus recommendation of the American college of medical genetics and genomics and the association for molecular pathology. *Genet Med*. 2015;17(5):405-424.
23. Kopanos C, Tsiolkas V, Kouris A, et al. VarSome: the human genomic variant search engine. *Bioinformatics*. 2019;35(11):1978-1980.
24. Lin JJC, Eppinga RD, Warren KS, McCrae KR. Human tropomyosin isoforms in the regulation of cytoskeleton functions. *Adv Exp Med Biol*. 2008;644:201-222.
25. Abouhamed M, Reichenberg S, Robenek H, Plenz G. Tropomyosin 4 expression is enhanced in dedifferentiating smooth muscle cells in vitro and during atherogenesis. *Eur J Cell Biol*. 2003;82(9):473-482.
26. Pecci A, Gresele P, Klersy C, et al. Eltrombopag for the treatment of the inherited thrombocytopenia deriving from MYH9 mutations. *Blood*. 2010;116(26):5832-5837.

**How to cite this article:** Marín-Quílez A, Vuelta E, Díaz-Ajenjo L, et al. A novel nonsense variant in *TPM4* caused dominant macrothrombocytopenia, mild bleeding tendency and disrupted cytoskeleton remodeling. *J Thromb Haemost*. 2022;00:1–8. doi:10.1111/jth.15672

# CHAPTER 4

## Novel variants in *GALE* cause syndromic macrothrombocytopenia by disrupting glycosylation and thrombopoiesis.

Ana Marín-Quílez[1#], Christian Andrea Di Buduo[2#], Lorena Díaz-Ajenjo[1], Vittorio Abbonante[2], Elena Vuelta[1], Paolo María Soprano[2], Cristina Miguel-García[1], Sandra Santos-Mínguez[1], Inmaculada Serramito-Gómez[1], Pedro Ruiz-Sala[3], María Jesús Peñarrubia[4], Emilia Pardal[5], Jesús María Hernández-Rivas[1,6], José Ramón González-Porras[6], Ignacio García-Tuñón[1], Rocío Benito[1], José Rivera[7*#], Alessandra Balduini[2,8#], José María Bastida[6*#].

[1] IBSAL, CIC, IBMCC, Universidad de Salamanca-CSIC, Salamanca, Spain; [2] Department of Molecular Medicine, University of Pavia, Pavia, Italy; [3] Centro de Diagnóstico de Enfermedades Moleculares, Universidad Autónoma de Madrid, CIBERER, IdIPAZ, Madrid, Spain; [4] Department of Hematology, Hospital Clínico Universitario de Valladolid, Spain; [5] Department of Hematology, Hospital Virgen del Puerto, Plasencia, Spain; [6] Department of Hematology, Complejo Asistencial Universitario de Salamanca (CAUSA), Instituto de Investigación Biomédica de Salamanca (IBSAL), Universidad de Salamanca (USAL), Spain; [7] Department of Hematology and Oncology, Hospital Universitario Morales Meseguer, Centro Regional de Hemodonación, Universidad de Murcia, IMIB-Arrixaca, CIBERER-U765, Spain; [8] Department of Biomedical Engineering, Tufts University, Medford, MA, USA. *On behalf of “Grupo Español de Alteraciones Plaquetarias Congénitas (GEAPC)”, Sociedad Española de Trombosis y Hemostasia (SETH). # Equal authors´ contributions

*Blood. Second Revision.*

# Novel variants in *GALE* cause syndromic macrothrombocytopenia by disrupting glycosylation and thrombopoiesis

Ana Marín-Quílez, MSc[1#], Christian Andrea Di Buduo, PhD[2#], Lorena Díaz-Ajenjo, MSc[1], Vittorio Abbonante, PhD[2], Elena Vuelta, MSc[1], Paolo Maria Soprano, MSc[2], Cristina Miguel-García, BSc[1], Sandra Santos-Mínguez, MSc[1], Inmaculada Serramito-Gómez, PhD[1], Pedro Ruiz-Sala, PhD[3], María Jesús Peñarrubia, MD, PhD[4], Emilia Pardal, MD, PhD[5], Jesús María Hernández-Rivas, MD, PhD[1,6], José Ramón González-Porras, MD, PhD[6], Ignacio García-Tuñón, PhD[1], Rocío Benito, PhD[1], José Rivera, PhD[7*#], Alessandra Balduini, MD, PhD[2,8#], José María Bastida, MD, PhD[6*#].

1. IBSAL, CIC, IBMCC, Universidad de Salamanca-CSIC, Salamanca, Spain.
2. Department of Molecular Medicine, University of Pavia, Pavia, Italy.
3. Centro de Diagnóstico de Enfermedades Moleculares, Universidad Autónoma de Madrid, CIBERER, IdIPAZ, Madrid, Spain.
4. Department of Hematology, Hospital Clínico Universitario de Valladolid, Spain.
5. Department of Hematology, Hospital Virgen del Puerto, Plasencia, Spain.
6. Department of Hematology, Complejo Asistencial Universitario de Salamanca (CAUSA), Instituto de Investigación Biomédica de Salamanca (IBSAL), Universidad de Salamanca (USAL), Spain.
7. Department of Hematology and Oncology, Hospital Universitario Morales Meseguer, Centro Regional de Hemodonación, Universidad de Murcia, IMIB-Arrixaca, CIBERER-U765, Spain
8. Department of Biomedical Engineering, Tufts University, Medford, MA, USA.

* On behalf of "Grupo Español de Alteraciones Plaquetarias Congénitas (GEAPC)", Sociedad Española de Trombosis y Hemostasia (SETH).

# Equal authors´ contributions
AMQ and CADB contributed equally
JMB, AB and JR share senior authorship.

Glycosylation is recognized as a key process for proper megakaryopoiesis and platelet formation. The enzyme UDP-galactose-4-epimerase, encoded by *GALE*, is involved in galactose metabolism and protein glycosylation. Here, we studied three patients from two unrelated families who showed lifelong severe thrombocytopenia, bleeding diathesis, mental retardation, mitral valve prolapse, and jaundice. Whole-exome sequencing revealed four variants affecting *GALE*, three of them previously unreported (Pedigree A: p.Lys78ValfsX32 and p.Thr150Met; Pedigree B: p.Val128Met and p.Leu223Pro). Platelet phenotype analysis showed giant and/or grey platelets, impaired platelet aggregation, severely reduced alpha and dense granule secretion, and increased apoptosis. Enzymatic activity of the UDP-galactose-4-epimerase enzyme was severely decreased in all patients. Immunoblotting of platelet lysates revealed reduced GALE protein levels, a significant decrease of N-acetyl-lactosamine (LacNAc), demonstrating a hypoglycosylation pattern, and reduced surface expression of GPIbα-IX-V complex and mature β1 integrin. In vitro studies performed in the K652 cell line overexpressing the identified *GALE* missense variants and in patient's CD34+ cell derived megakaryocytes (Mks), demonstrated normal Mks ploidy and maturation. These novel *GALE* variants were associated with impaired glycosylation of the GPIbα and β1 integrin, their reduced externalization to the Mks and platelet surface, being retained in the endoplasmic reticulum, and leading to impaired proplatelet formation. Overall, this study expands our knowledge of *GALE*-related thrombocytopenic disorder and emphasized the critical role of *GALE* in the physiological glycosylation of key proteins in platelet production and function.

- *GALE* is expressed during late-stage megakaryopoiesis, regulating the glycosylation and surface exposure of GPIbα and β1 integrin.
- Novel *GALE* variants cause syndromic macrothrombocytopenia associated with impaired platelet formation and function.

**Keywords:** Thrombocytopenia, blood platelet disorders, thrombopoiesis, UDP-Galactose 4-epimerase, glycosylation, *GALE*.

## INTRODUCTION

Inherited thrombocytopenias (ITs) are a group of rare and heterogeneous platelet disorders characterized by low platelet counts, which lead to variable increased risk of bleeding depending on the degree of thrombocytopenia and the concomitant association of significant platelet dysfunction.[1] It is currently well established that many ITs evolve with the development of other serious congenital defects affecting different organs or additional diseases including hematological malignancies, bone marrow failure, and/or non-hematological defects.[2,3] ITs are caused by genetic alterations in megakaryopoiesis-related genes. Early stages of megakaryopoiesis leading to megakaryocyte (Mk) differentiation can be disrupted by alterations in genes that have major roles in the fine-tuning of hematopoietic stem cell homeostasis or regulating the thrombopoietin (TPO) signaling axis. The late stages of the megakaryopoiesis, which include Mk maturation and migration, proplatelet formation, and platelet release into the bloodstream, can be impaired by rare molecular changes in genes encoding for critical transcriptional factors, vesicle trafficking or biochemical signals, but also for cytoskeletal proteins, platelet surface glycoproteins (GP), ion channels, metabolic genes, and genes affecting platelet survival.[4–10] Protein glycosylation, and the linked sialylation, are common and complex post-translational modifications, with a critical role in different biological processes such as protein clearance and degradation, immunity, thrombosis and hemostasis.[11] These post-translational modifications are also important in megakaryopoiesis,[12] since mice with genetic deficiencies in glycosylation/sialylation present thrombocytopenia.[11,13,14] The use of whole-exome sequencing (WES) unveiled rare cases of syndromic ITs caused by recessive variants in glycosylation related-genes involved in sialic acid synthesis such as *GNE*;[15,16] the sialic transporter gene *SLC35A1*,[17,18] or *GALE*, which encodes the UDP-galactose-4-epimerase.[19–21] Here, we report three patients from two unrelated families presenting lifelong syndromic thrombocytopenia and platelet dysfunction caused by compound heterozygosity of four rare *GALE* variants, three of them previously unreported. Our data further support the key role of *GALE* in protein glycosylation. We unveil *GALE* variants driving novel mechanisms of pathological thrombopoiesis, consisting in impaired externalization of GPIbα and β1 integrin during late-stage megakaryopoiesis, which lead to altered proplatelet formation and the production of platelets with impaired morphology, function, and viability.

## PATIENTS, MATERIALS & METHODS

*Additional methodological details can be found in the Supplemental Material.*

Patients

Three patients from two unrelated and non-consanguineous families presenting with syndromic thrombocytopenia of unknown origin (Figure 1A) were recruited for the Spanish multicenter project "Functional and Molecular Characterization of Patients with Inherited Platelet Disorders" coordinated by the "Grupo Español de Alteraciones Plaquetarias Congénitas (GEAPC)". Patients' general features characteristics are summarized in Table 1. Venous blood samples were drawn into EDTA or sodium citrate according to the different studies.

Platelet tests

Assessment of platelet phenotype was performed as previously described.[22,23]

Whole exome sequencing and variant interpretation

Whole exome sequencing (WES) was performed in four members of pedigree A and in three members of pedigree B (Figure 1A), as recently published.[23] The identified candidate variants were classified according to the guidelines of the American College of Medical Genetics and Genomics and Association for Molecular Pathology (ACMG).[24] *GALE* variants were confirmed and segregated in the rest of the family members by Sanger sequencing.

UDP-galactose-4-epimerase activity and immunoblotting

UDP-galactose-4-epimerase activity was measured in dried blood spots (DBS) by high-performance liquid chromatography with tandem mass spectrometry (HPLC/MS/MS), adapted from previous publications.[25] Protein levels were assessed in platelet lysates by standard immunoblotting and probed with selected antibodies. Protein levels in Mk were evaluated by automated capillary-based Western-Blotting.

Cellular model of mutant *GALE* and differentiation assays

Human K562 (hK562) cells overexpressing *GALE*-WT or mutant *GALE*-150Met, *GALE*-128Met, or *GALE*-223Pro were treated with 20 nM phorbol 12-myristate 13-acetate (PMA) for 7 days, as previously reported.[26,27] Mks differentiation, based on polyploidization and maturation assessment was monitored by flow cytometry on days 3, 5, and 7.

Human megakaryocyte differentiation

$CD45^+$ or $CD34^+$ cells were separated by immunomagnetic bead selection (Miltenyi Biotec, Bologna, Italy) and cultured in the presence of TPO, as previously described.[28,29] At the end of the culture ($14^{th}$ day), polyploidization, maturation, apoptosis, and total and surface (permeabilized and non-permeabilized cells, respectively) protein expression were analyzed by flow cytometry. Mature Mks were characterized by microscopy

using a Leica TCS-SP5 or TCS-SP8 confocal microscope. Images were analyzed using ImageJ software.

Adhesion to extracellular matrices (ECM)

Control and patient platelets were set in coverslips ($1x10^6$ per coverslip) coated with laminin, fibronectin, collagen, or Haemate-P®, as described,[30] and stained with selective antibodies.

Statistical analysis

Statistical analyses were performed using GraphPad Prism 8 Software (GraphPad Software). Differences among groups were tested with t-student, one- and two-way ANOVA, and Tukey's multiple comparisons test. Statistical significance difference was achieved for *p*-values $<0.05$.

Ethics statement

The study was abided by the Helsinki Declaration and approved by the Ethics Committees of the Instituto de Investigación Biomédica de Salamanca (IBSAL), Salamanca, Spain (reference PI5505/2017). All patients, family members, and healthy controls gave written informed consent. Umbilical cord blood units were collected after obtaining the parents' written informed consent at enrolment in accordance with the ethical committee of the I.R.C.C.S. Policlinico San Matteo Foundation of Pavia and the principles of the Declaration of Helsinki.

Data Sharing Statement

Reagents and detail experimental procedures can be found in the supplemental material available with the online version of this article. High-throughput sequencing data are available at SRA under accession number PRJNA839436.

## RESULTS

### Clinical presentation of two unrelated families

The three probands [siblings II.1 & II.4 in pedigree A; II.2 in pedigree B] presented lifelong severe macrothrombocytopenia associated with moderate to severe bleeding tendency, and other clinical features such as mental retardation, mitral valve prolapse, and increased bilirubin levels (Figure 1A, Table 1). Proband A.II.1 and B.II.2 displayed 76% and 43% of reticulated platelets, respectively (Table 1). Noteworthy, siblings II.1 & II.4 in pedigree A had been previously misdiagnosed with immune thrombocytopenia and were treated with corticosteroids and immunoglobulins, and lastly underwent splenectomy (A.II.1). In contrast, an IT was suspected in proband II.2 from pedigree B, and he was only treated with platelet transfusions prior to invasive procedures (Table 1).

| Patient | Pedigree A. II.1 | Pedigree A. II.4 | Pedigree B. II.2 |
|---|---|---|---|
| Age, years | 45 | 37 | 38 |
| Sex | Male | Female | Male |
| Bleeding score, ISTH-BAT | 8 | 10 | 6 |
| Bleeding symptoms | Mucocutaneus (1), epistaxis (2), minor wounds (2) conjunctival and vitrectomy (3) | Mucocutaneus (1), epistaxis (2), dental extraction (2), menorrhagia (2), surgical hemostasis after ovarian cyst (3) | Mucocutaneus (2) and gastrointestinal (4) |
| Hemoglobin level, g/dL (N 12 - 16 g/dL) | 12.1 | 11.5 | 13 |
| White blood cells (N 3.8 - 11 x $10^9$/L) | 9.9 x $10^9$/L | 3.5 x $10^9$/L | 8.8 x $10^9$/L |
| Neutrophils (N 1.4 - 6.5 x $10^9$/L); | 5.1 x $10^9$/L | 1.6 x $10^9$/L | 5.6 x $10^9$/L |
| Platelet count (N 150 - 450 x $10^9$/L) | 12.7 x $10^9$/L | 5.3 x $10^9$/L | 17 x $10^9$/L |
| MPV (fL) (N 7.2 - 11.1 fL) | 17.4 | 19.2 | 20 |
| IPF, % (N 1.1 - 6.1%) | 76 | NA | 43 |
| Blood film (MPD) | Large: 14%<br>Giant: 30%<br>Grey: 54% | Large: 24%<br>Giant: 48%<br>Grey: 24% | Large: 16%<br>Giant: 72%<br>Grey: 8% |
| Bone marrow aspirate | Erythroid hyperplasia and increased Mks | Erythroid hyperplasia and increased Mks | Not done |
| Previous diagnosis | Immune thrombocytopenia | Immune thrombocytopenia | Di George syndrome<br>Grey platelet syndrome |
| Treatments | Corticosteroids<br>Immunoglobulins<br>Splenectomy | Corticosteroids<br>Immunoglobulins | No |
| Red blood cells transfusions | Yes | Yes | Yes |
| Platelet transfusions | Yes | Yes | Yes |
| Additional symptoms: | Yes | Yes | Yes |
| Neurological | Mental retardation | Mental retardation | Mental retardation |
| Cardiovascular | Mitral valve prolapse and mitral insufficiency | Mitral valve prolapse and mitral insufficiency | Mitral valve prolapse and mitral insufficiency |
| Ophthalmological | Retinal disease<br>Cataracts | Retinal disease<br>Cataracts | No |
| Orthopedic | No | Hip dysplasia | Equine foot |
| Hepatic | Jaundice<br>Hepatomegaly | Jaundice<br>Hepatomegaly | Jaundice<br>Hepatomegaly |
| The parents and other relatives in both families were asymptomatic and had normal platelet count and volume. | | | |

**Table 1. Clinical and laboratory characteristics of 3 patients from the 2 unrelated families.** Bleeding symptoms were scored (n) by ISTH-BAT questionnaire. IPF, immature platelet fraction; Mks, megakaryocytes; MPD, mean platelet diameter; MPV, mean platelet volume; N, normal; NA. not available.

**Assessment of patients' platelet phenotype**

Blood film revealed a significant proportion of enlarged, giant, and/or grey platelets in all probands (Figure 1B) (Table 1). Moreover, typical morphological findings of splenectomized patients, such as erythroblast, were observed in the blood film from proband A.II.1. No other relevant morphological abnormalities appeared.

All probands displayed significantly reduced platelet aggregation upon stimulation with several agonists (Figure S1A). Flow cytometry analysis showed a comparable expression of GPVI and $\alpha_{IIb}\beta_3$ integrin in probands *vs*. non-affected relatives and healthy control, but a significant reduction in the GPIb and GPIX levels (GPIb-IX-V complex) (50-70%) (Figure 1C). Furthermore, agonist-induced P-selectin and CD63 exposure were severely impaired (Figures 1D and 1E). Lastly, patients' platelets also showed a slightly reduced fibrinogen binding and normal TRAP6-induced platelet spreading on fibrinogen, suggesting substantial preservation of the $\alpha_{IIb}\beta_3$ function (Figures S1B-S1D).

**WES analysis in patients and relatives identified *GALE* candidate variants**

WES unveiled the presence of compound heterozygous variants in *GALE* (NM_001127621.2) in all the probands (Figure

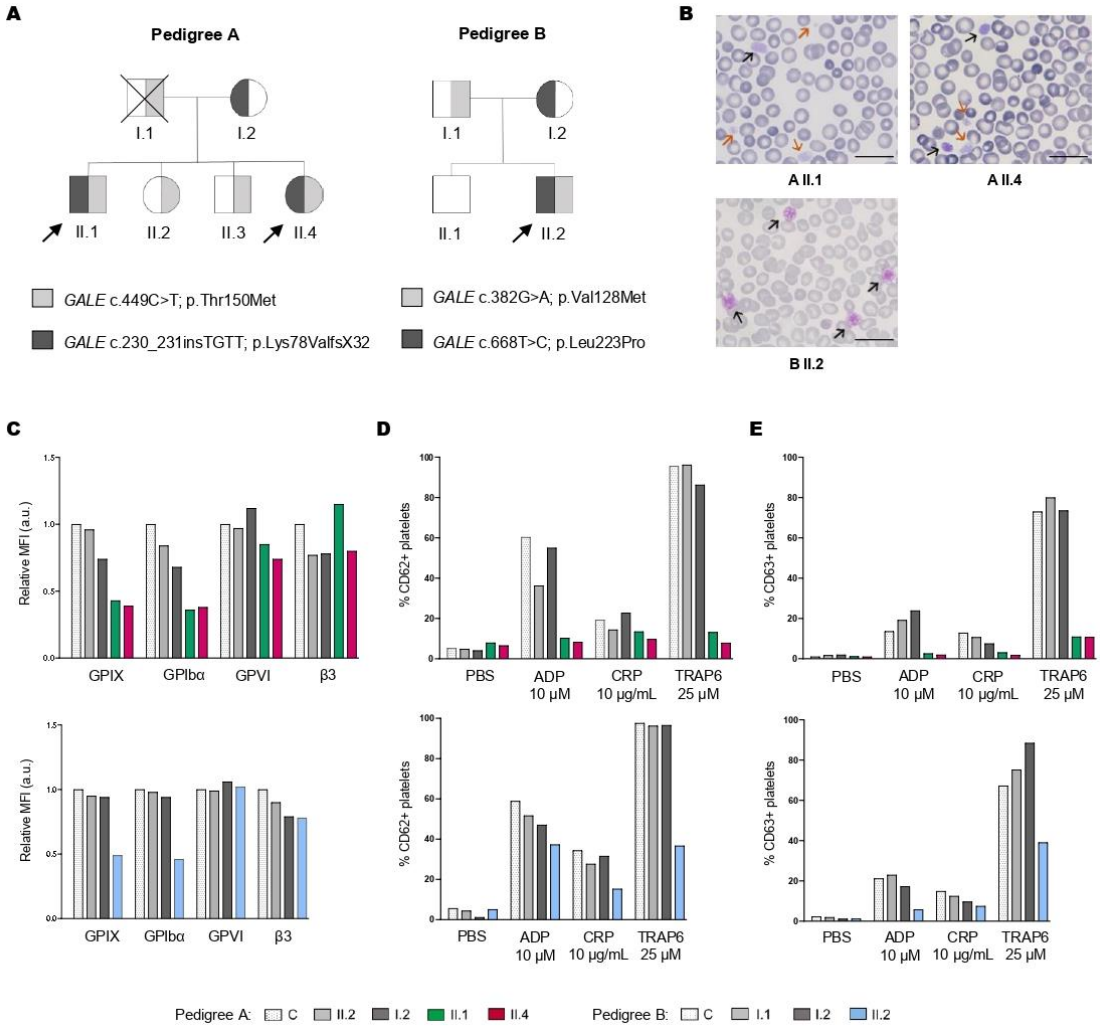


**Figure 1. Patients carrying *GALE* variants showed giant and/or grey platelets in blood films and impaired granules secretion. A)** Family segregation of the variants affecting *GALE* identified by whole-exome sequencing. Probands are indicated with black arrows. Partially filled symbols in light and/or dark grey represent heterozygous status for the indicated *GALE* variant. **B)** Representative peripheral blood films from probands of the two pedigrees after May-Grunwald Giemsa staining (x100). Red and black arrows indicate grey and giant platelets, respectively. **C)** Platelet glycoproteins (GPs) expression in control and patients, as assessed by flow cytometry with fluorescent-labeled antibodies anti-CD42a, CD42b, GPVI, and CD61. The mean fluorescence intensity (MFI) of each antibody, standardized by size [FSC] and relative to the control sample, is represented. **D-E)** Platelets from a healthy control and family members were stimulated with agonists in the presence of appropriate monoclonal antibodies to assess **D)** alpha granules secretion (anti-CD62P), **E)** dense granules secretion (anti-CD63), and evaluated by flow cytometry. Plots shows the percentage of positive platelets.

1A), according to the recessive inheritance of their disease. Patients from pedigree A (II.1 and II.4) carried the previously reported missense variant c.449C>T [p.Thr150Met],[21] affecting exon

5, and the novel insertion c.230_231insTGTT [p.Lys78ValfsX32], affecting exon 3. The proband from pedigree B (II.2) carried the two novel missense variants c.382G>A [p.Val128Met] and c.668T>C [p.Leu223Pro] at exons 5 and 7, respectively. Noteworthy, all these mutations are located nearby the NADH protein binding site or the substrate-binding site of the *GALE*-encoded protein UDP-galactose-4-epimerase (Figure S2). Considering these data, variants were reclassified as pathogenic variants (Table S1).

**_GALE_ variants lead to reduced levels and impaired enzymatic activity of UDP-galactose-4-epimerase, and increased platelet apoptosis**

Immunoblotting assays revealed reduced platelet levels of UDP-galactose-4-epimerase (GALE protein) in patients compared to unaffected family members and the healthy controls. As shown in Figure 2A, platelets from patients A.II.1 and A.II.4 have a 50% overall expression of GALE in comparison with control platelets, due to p.Lys78ValfsX32 variant. In addition, samples from patients A.II.1 and A.II.4 presented a tiny protein band with different electrophoretic mobility corresponding to the mutant form of the enzyme (p.Thr150Met). The total expression of the enzyme in the unaffected A.II.2 was similar to that in the healthy control, but two bands corresponding to native and mutant (p.Thr150Met) proteins were detectable (Figure 2A). In contrast, A.I.2, the patient's mother carrying p.Lys78ValfsX32, displayed a 50% reduced expression of the protein, which is consistent with haploinsufficiency (Figure 2A). In pedigree B, platelet from proband II.2 displayed a 65% reduced level of UDP-galactose-4-epimerase *vs.* control platelets, whereas platelets from the unaffected relatives B.I.1 and B.I.2 showed a milder decrease (49% and 35% reduced expression, respectively), suggesting the existence of a protein instability phenomenon, in agreement with the negative effect reported for other mutations.[31,32] Furthermore, the novel missense GALE variants identified (p.Val128Met and p.Leu223Pro) had a negligible effect on the electrophoretic mobility of UDP-galactose-4-epimerase (Figure 2A).

Consequently, all patients exhibited a sharp decrease in the enzymatic activity of UDP-galactose-4-epimerase, in comparison with healthy controls (A.II.1: 15%, A.II.4: 15%, and B.II.2: 7,5%) (Figure 2B).

Since UDP-galactose-4-epimerase catalyzes the interconversion of UDP-glucose to UDP-galactose, and UDP-N-acetyl-glucosamine to UDP-N-acetyl-galactosamine, thus acting on four molecules involved in the N-linked and O-linked glycosylation (Figure S3), we decided to assess the glycosylation pattern in platelet lysates. Immunoblotting assays with lectin ECL, which specifically binds to N-acetyl-lactosamine (LacNAc) (a dimer of N-acetyl-glucosamine and galactose molecules), showed decreased LacNAc

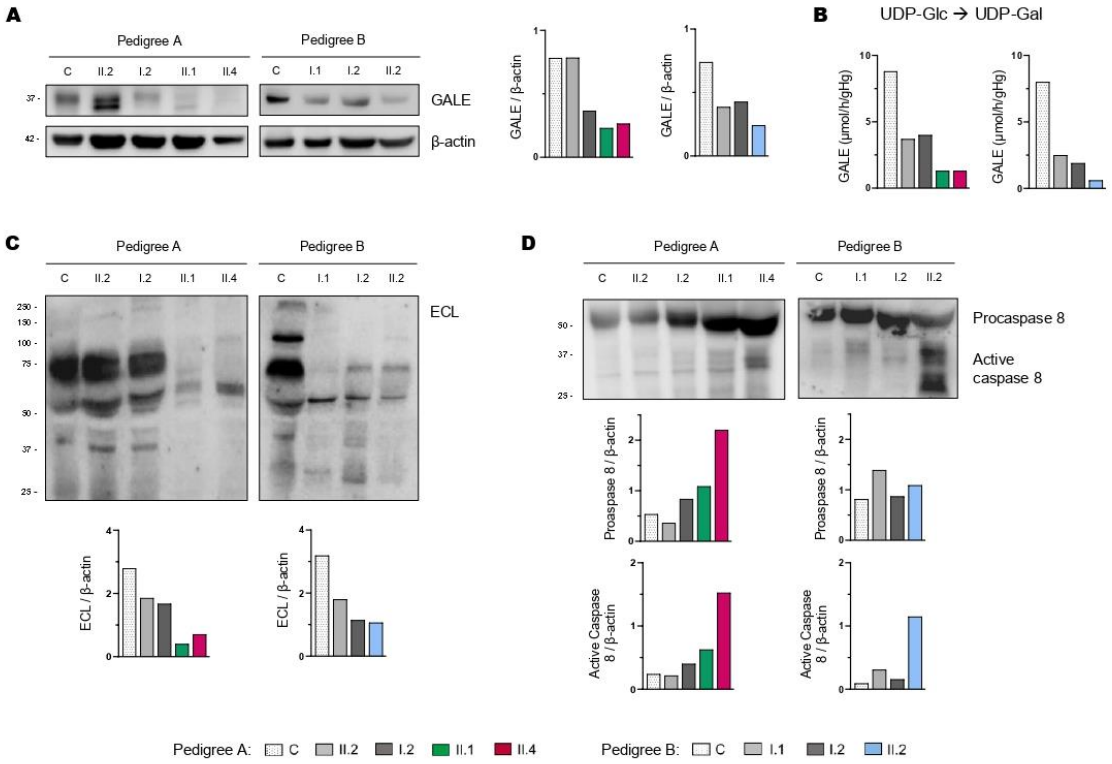


**Figure 2. *GALE* variants associated with reduced GALE protein levels, impaired enzymatic activity, platelet hypoglycosylation, and increased apoptosis.**

**A)** Western blotting from platelet lysates of patients from both pedigrees, unaffected relatives, and controls. Membranes were blotted with anti-GALE and anti-β actin as an internal control. A.II.2 presented total levels of GALE protein similar to controls, but two GALE bands with different electrophoretic mobility were observed (top: GALE-WT; bottom: GALE p.Thr150Met), while A.I.2 displayed a 50% reduction of total GALE protein. Probands from pedigree A (II.1 and II.4) showed reduced protein levels (50%) and a tiny band corresponding to GALE p.Thr150Met. Individuals from pedigree B I.1, I.2 and II.2 showed reduced total GALE protein levels (51%,65% and 35%, respectively vs. control). **B)** Enzymatic activity of UDP-galactose-4-epimerase assessed in members of pedigrees A and B. The activity of a healthy control was evaluated in parallel. Probands of both families showed a sharp reduction in the GALE enzymatic activity (A.II.1: 15%, A.II.4: 15% and B.II.2: 7,5%), while heterozygous carriers in both families displayed a moderate reduction (A.II.2, 42%; A.I.1, 45%; B.I.1, 31% and B.I.2, 24%). **C)** To assess the glycosylation profile, platelet lysates were probed with lectin ECL, which specifically binds to N-acetyl-lactosamine (LacNAc), a dimer of N-acetyl-glucosamine and galactose molecules. β actin staining, as shown in panel A, was used as an internal control. A sharp decrease in ECL binding was found in all probands, less pronounced in heterozygous carriers of a single GALE variant. **D)** Platelet lysates were probed with antibodies again procaspase 8 (56 kDa) (top band) or the active–cleaved form of caspase 8 (bottom bands). -β actin (shown in panel A) was the internal protein control. Proband from pedigree A displayed increased procaspase 8 and active caspase 8 level, while only the second was increased in the pedigree B proband. Band intensities in either blot were quantified by densitometric analysis using the 'Image J' software.

levels in platelets from the patients (A.II.1 & II.4; B.II.2) in comparison with control platelets, thus reflecting the deleterious effect of these *GALE* variants on the enzyme activity (Figure 2C). It is known that proteins involved in apoptotic pathways carry glycosylation sites, and *GALE*-deficient HEK293 cells are hyper sensitive to FasL-induced apoptosis.[33] To assess the potential effect of the hypoglycosylation on platelet lifespan, we evaluated apoptosis-linked caspase activity in patient´s platelet lysates. As shown in Figure 2D, probands from Pedigree A displayed an increased level of both procaspase 8 and cleaved caspase 8, in comparison with control and healthy relatives. Conversely, proband B.II.2 displayed normal level of procaspase 8, but an increase amount of active caspase 8 (Figure 2D).

**Platelets from patients carrying *GALE* variants show a sharp reduction of GPIbα and glycosylated β1 integrin**

Given the hypoglycosylated profile in patient´ platelets, we assessed in platelet lysates the level of several relevant platelet proteins known to undergo glycosylation. Interestingly, we found a sharp reduction in GPIbα and mature/glycosylated β1 integrin in all probands, while the levels of the hypoglycosylated isoform were similar compared to control and healthy members (Figure 3). In contrast, normal levels of β3 integrin and thrombopoietin receptor (TPO-R) were detected in probands, suggesting that physiological glycosylation and/or maturation of these receptors is preserved in these *GALE* patients. Assessment of von Willebrand Factor (vWF) reduced in the platelet lysates from the probands from Pedigree A (Figure 3), in accordance with the high percentage of grey platelets observed in A.II.1 and A.II.4 blood films (54% and 24%, respectively) (Table 1). In contrast, B.II.2 proband, who presented less than 10% grey platelets in blood film, displayed normal vWF storage (Figure 3 and Table 1).

**hK562 cells overexpressing patient's *GALE* variants show normal ploidy and reduced CD42b megakaryocyte marker**

To elucidate the effects of the identified GALE missense variants (p.Thr150Met, p.Val128Met, and p.Leu223Pro), we established a hK562 cell model that can be differentiated into a Mk-like phenotype with PMA (Figures S4A-S4C). We found a normal or higher proportion of polyploid cells overexpressing *GALE*-128Met, *GALE*-150Met, and *GALE*-223Pro, than *GALE*-WT in PMA-induced Mk differentiation (Figure S4D). To study the impact of these variants in Mk maturation, we followed the expression of the Mk markers CD61 (β3) and CD42b (GPIbα). Cells overexpressing *GALE*-150Met and *GALE*-128Met showed significantly lower percentage of $CD42b^+$ cells on days 5 and 7 than those overexpressing *GALE*-WT (Figure S4E). Cells overexpressing *GALE*-223Pro *vs*. *GALE*-WT also showed a significantly lower number of $CD42b^+$ cells after 5 days of culture, while this significant difference

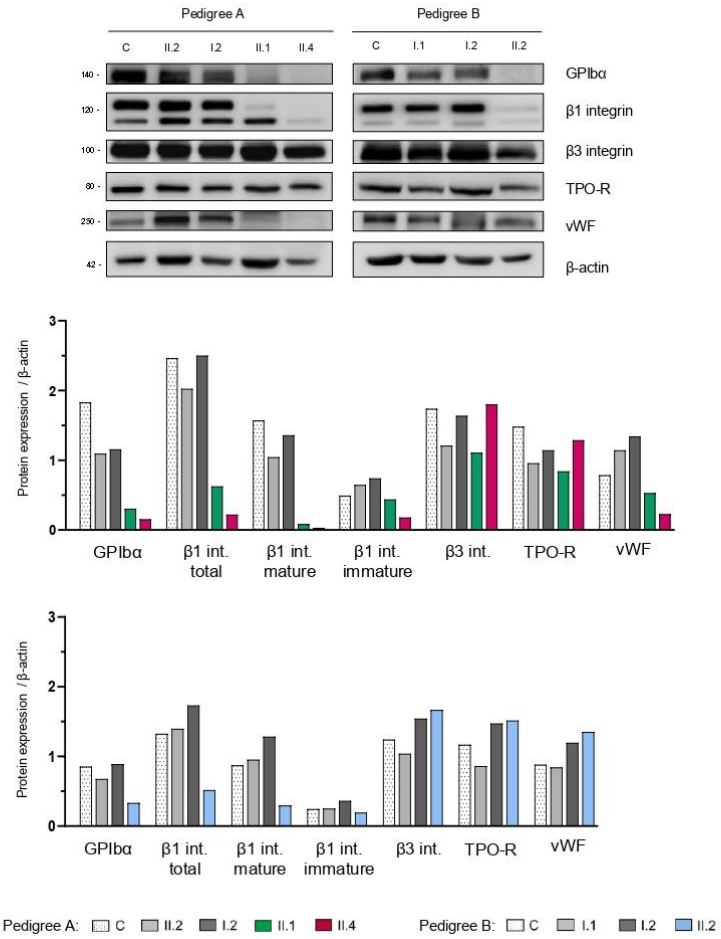


**Figure 3. Immunoblotting of platelet lysates revealed severely reduced levels of GPIbα and glycosylated β1 integrin.** Platelet lysates of controls, healthy realtives, and patients from both pedigrees were immunoblotted with anti-GPIbα, anti-β1 integrin, anti-β3 integrin, anti-TPO receptor, anti-vWF, and anti-β-actin as an internal control. Band intensities in blots were quantified by densitometric analysis using the 'Image J' software. Bar graphs represents each protein expression relative to β-actin. Impaired GPIbα and β1 integrin levels was observed in proband from both pedigrees. vWF level was also reduced in Pedigree A patients. Platelet β3 integrin and TPO levels were unaffected in these patients.

disappeared on day 7 (Figure S4E).

**GALE protein expression increases with megakaryocyte maturation and is localized in the endoplasmic reticulum**

To get insight into the role of GALE in megakaryopoiesis, we used cord blood-derived $CD34^+$ cells, a well-characterized source of *in vitro* differentiated human Mks.[34] We observed that GALE is poorly expressed in $CD34^+$ hematopoietic stem and progenitor cells (Figure S5A). During the TPO-induced differentiation, the expression of GALE was increasing being higher in mature Mks ($CD61^+CD42b^{high}$) than in

immature Mks ($CD61^+CD42b^{low}$) (Figure 4A, Figures S5B and S5C). In released platelet-like particles, the expression of GALE was reduced (Figure S5D). These results suggest that GALE is mainly expressed during the late-stage of megakaryopoiesis.

To assess the cellular distribution of GALE in Mks, we performed a colocalization assay of GALE with GPIbα (plasma membrane) and the endoplasmic reticulum (ER) protein calreticulin (Figure 4B). GALE showed a higher level of colocalization with calreticulin (Pearson's value: 0.86), than with GPIbα (Pearson's value: 0.48).

**Normal megakaryocyte maturation but impaired proplatelet formation in carrier of GALE p.Val128Met and p.Leu223Pro variant**

To further investigate the mechanisms of thrombocytopenia, we differentiated Mks *in vitro* from peripheral blood progenitors from the proband B.II.2 and four healthy controls, according to our standard protocols.[28,29] We observed a 50% reduced expression of GALE in mature Mks from proband *vs*. healthy controls (Figures 5A and 5B).

Patient Mks displayed a similar percentage of polyploid cells with respect to the healthy controls (Figure 5C). Mks size and differentiation, evaluated as $CD61^+$ Mks at the end of the culture, were comparable between the patient and the healthy controls (Figures 5D-F). Indeed, no differences in Mk viability were found between controls and the proband B.II.2 (Figure 5G). However, the patient had a significantly reduced proportion of Mks extending proplatelets *vs*. controls both in suspension (data not shown) and in adhesion on fibrinogen (6% vs. 12.3%) (Figures 5H-5J). The patient's proplatelets exhibited an impaired morphology that was characterized by reduced length and bifurcation of the shafts, resulting in a smaller number of proplatelet-free ends and tips with increased size (Figures 5H and 5I) but normal microtubules assembly (Figure 5J).

The analysis of vWF expression in the patient's Mks revealed normal levels of the alpha granules (Figures 6A and 6B), in accordance with the analysis of peripheral blood platelets (Figure 3). However, proplatelet-forming Mks from the healthy controls showed the distribution of granules both near the cell membrane and within the cytoplasm, while the patient's Mks displayed a preferential location within the cell cytoplasm (Figures 6A and 6C).

**GALE p.Val128Met and p.Leu223Pro affect GPIbα and β1 integrin glycosylation, externalization, and delivery to platelets**

Proband B.II.2 and healthy controls had a comparable surface expression of β3 integrin, but reduced GPIbα (38% *vs*. the healthy control) and β1 integrin (33%), leading to the overall reduction of $CD61^+CD42b^+$ and $CD61^+CD29^+$ populations of Mks at the end of the culture (Figures 7A and 7B). Of note, the total levels of GPIbα and β1 integrin were similar to control

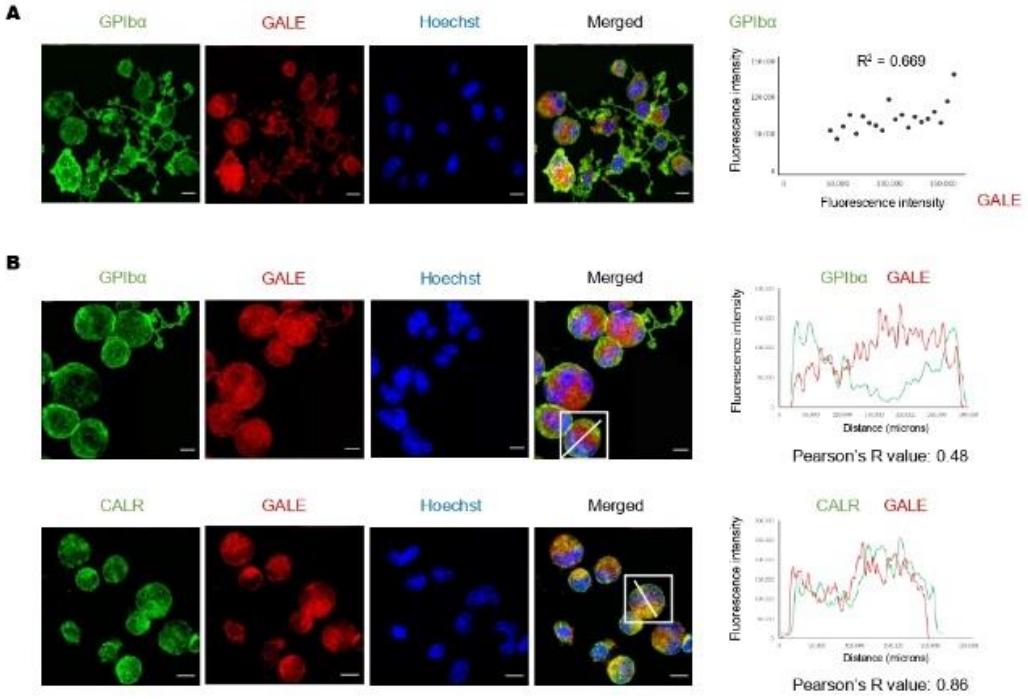


**Figure 4. Characterization of *GALE* expression among the megakaryopoiesis.**

Human CD34⁺ from cord blood were cultured for 13 days in the presence of TPO and IL-11. Megakaryocytes (Mk) were seeded on fibrinogen-coated coverslips overnight and stained with anti-GALE (red) and anti-GPIbα (green) or anti-calreticulin (green). Hoechst (blue) was used for counterstaining nuclei. **A)** Representative image of Mk at different stages of maturation ($CD42b^{low}$, $CD42b^{high}$, forming proplatelets). Diagram represents the fluorescence intensity (arbitrary units), quantified by ImageJ, of GPIbα (y-axis) vs. GALE (x-axis) in individual Mks. Twenty Mks in different fields were evaluated. $R^2$ represents the correlation coefficient of GPIbα and GALE fluorescence intensity. **B)** Representative image of Mk stained with GALE (red) and membrane (GPIbα, green) or endoplasmic reticulum proteins (calreticulin, green). The line profile plots represent the fluorescence intensity distribution of channels. Pearson's R values indicate the colocalization between GALE and GPIbα or calreticulin.

Mks (Figure 7A), thus suggesting that the observed reduction at the Mk and platelet surfaces could be due to their impaired externalization. Immunoblotting analysis of Mk lysates revealed the presence of GPIbα and β1 integrin bands of a slightly lower molecular weight in the proband *vs.* the healthy control, which can be expected according to the hypoglycosylation of these proteins (Figure 7C). To further confirm their reduced exposure at the membrane and a preferential accumulation within the ER, we assessed their colocalization with the ER protein calreticulin. We found that GPIbα and β1 integrin were increasingly associated with calreticulin in proband B.II.2 *vs.* the healthy control (GPIbα: 66% *vs.* 28%, β1

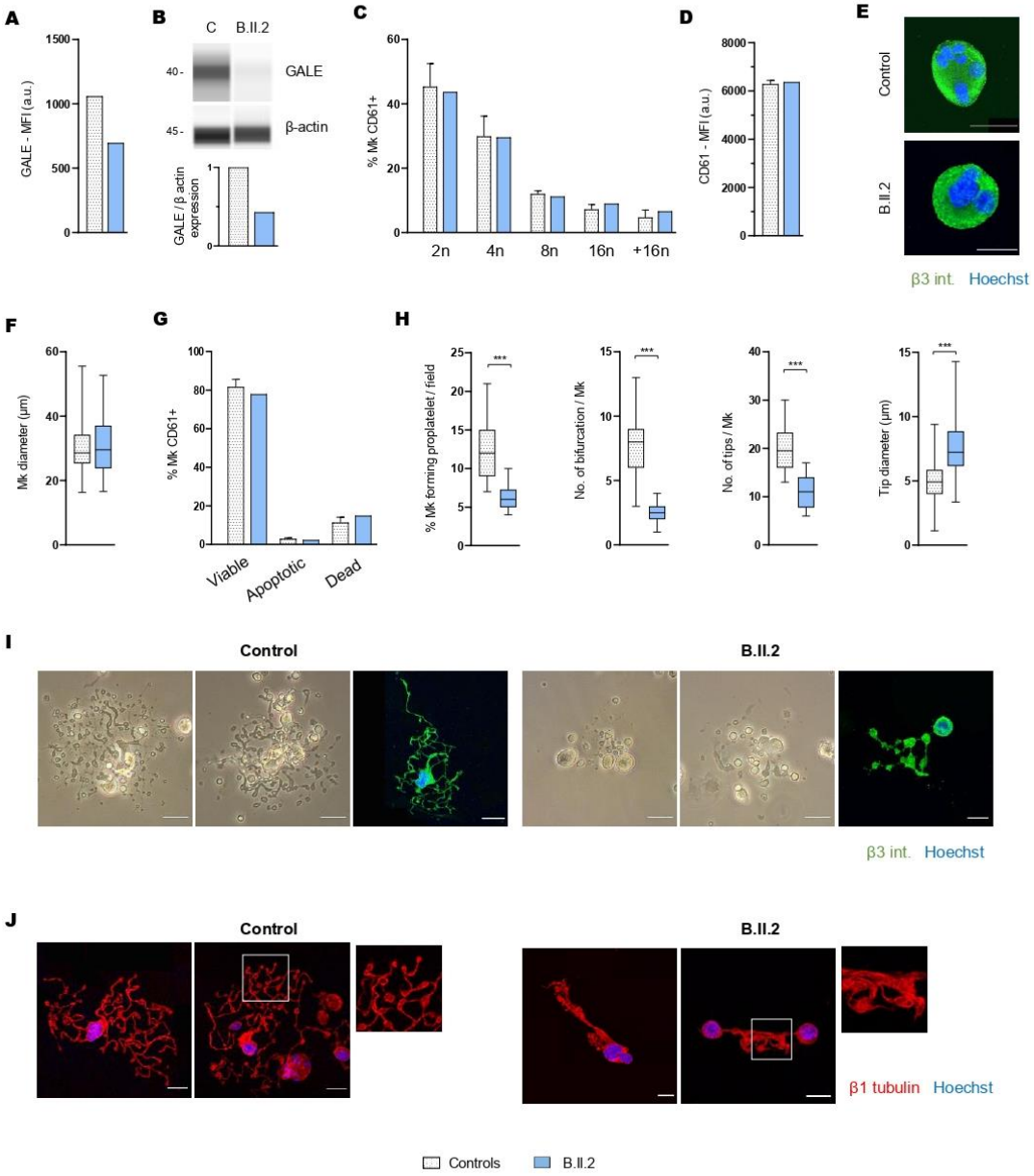


**Figure 5. Megakaryocyte culture from proband carrying GALE p.Val128Met and p.Leu223Pro variants showed normal polyploidization and maturation but impaired proplatelet formation.**

Mks were differentiated from peripheral blood progenitor cells (proband B.II.2) through a 14-days culture, in parallel with healthy controls. **A)** MFI evaluated by flow cytometry of GALE in permeabilized Mks from control and B.II.2. Data was relativized with the control value. **B)** Immunoblotting of Mk lysates. Control and B.II.2 samples were probed with anti-GALE and anti-β actin, as an internal control. **C)** Percentage of polyploid Mks after propidium iodide labeling. **D)** Mk differentiation assessed as $CD61^+$ cells was measured by MFI by flow cytometry. **E)** Representative images of mature and polynuclear Mks labeled with an anti–β3 integrin antibody (green fluorescence). Hoechst (blue) was used for counterstaining nuclei. Scale bars, 20 μm. **F)** Diameter measurement of Mk from B.II.2 and healthy control, in fibrinogen-

coated coverslips (n=100). **G)** Assessment of Mk viability and apoptosis rates at the end of the culture (14th day), using Annexin V - propidium iodide labeling. The % of CD61+ megakaryocytes that are negative for both markers (viable cells), Annexin $V^+$ $PI^-$ (apoptotic cells), and double-positive (dead cells) is represented. **H)** Characterization of impaired platelet formation in fibrinogen-coated coverslips in proband B.II.2 vs. control. Left to right plots: i) Rate of proplatelet formation measured as the proportion of Mks displaying ≥1 proplatelet with respect to the total number of Mks; ii) Number of bifurcations of proplatelet shafts per Mk. ≥10 Mks fields were investigated for each individual (patient or control); iii) Number of proplatelet free ends (tips) measured in ≥10 Mks from different fields; iv) Diameter measurement of proplatelet free ends (tips) from B.II.2 and healthy control (n=100). Box and whiskers graphs are shown. The central line represents the median value, while percentiles 25 to 75 are included in the box. Whiskers represent the min and max values. **I-J)** Representative image of proplatelet formation in optical and immunofluorescence microscope. Mks were plated on fibrinogen-coated coverslips and incubated for 16 hours at 37°C and 5% $CO_2$. **I)** Cells were stained with an anti–CD61 antibody (green). **J)** Cells were stained with an anti–β1 tubulin to investigate microtubule assembly in megakaryocytes forming proplatelets. Hoechst (blue) was used for counterstaining nuclei. Scale bars, 20 μm. *** $p < 0.001$, 2-tailed Student *t*-test.

integrin: 89% *vs*. 62%) (Figure 7D). Moreover, GPIbα and β1 integrin fluorescence was distributed at the plasma membrane of control Mks (Figure 7E), while the signal was mainly localized within the cytoplasm of patient's Mks. Of mention, B.II.2 patient platelets displayed severely reduced adhesion onto vWF, moderate decrease onto laminin and fibronectin, and slight impaired adhesion onto collagen, compared to controls platelets (Figure S6). Lack of GPIbα and β1 integrin in the Mk surface, makes it conceivable that these receptors cannot be delivered to mature platelets, thus affecting their adhesion to physiologically-relevant extracellular matrices.

## DISCUSSION

In the last decade, high throughput sequencing technology, and particularly WES, has revolutionized the genetic landscape of ITs with the identification of novel causative genes.[35–37] One of these is the *GALE* gene,[38] encoding an enzyme, the UDP-galactose-4-epimerase, which is involved in a wide range of biological processes like N-linked and O-linked glycosylation (Figure S3).[33] Genetic variants in *GALE* cause an autosomal recessive disorder (OMIM 230350) categorized as generalized, intermediate and peripheral forms. Compound heterozygous variants in *GALE* usually provoke partial impairment of GALE activity, being associated with non-generalized forms or even asymptomatic presentations, while homozygous variants are related to generalized forms of this condition, which usually present classical galactosemia.[39–42] In addition, the long–term complications may include learning difficulties, developmental delay, and poor growth,[43] while cardiac failure and dysmorphic features are less

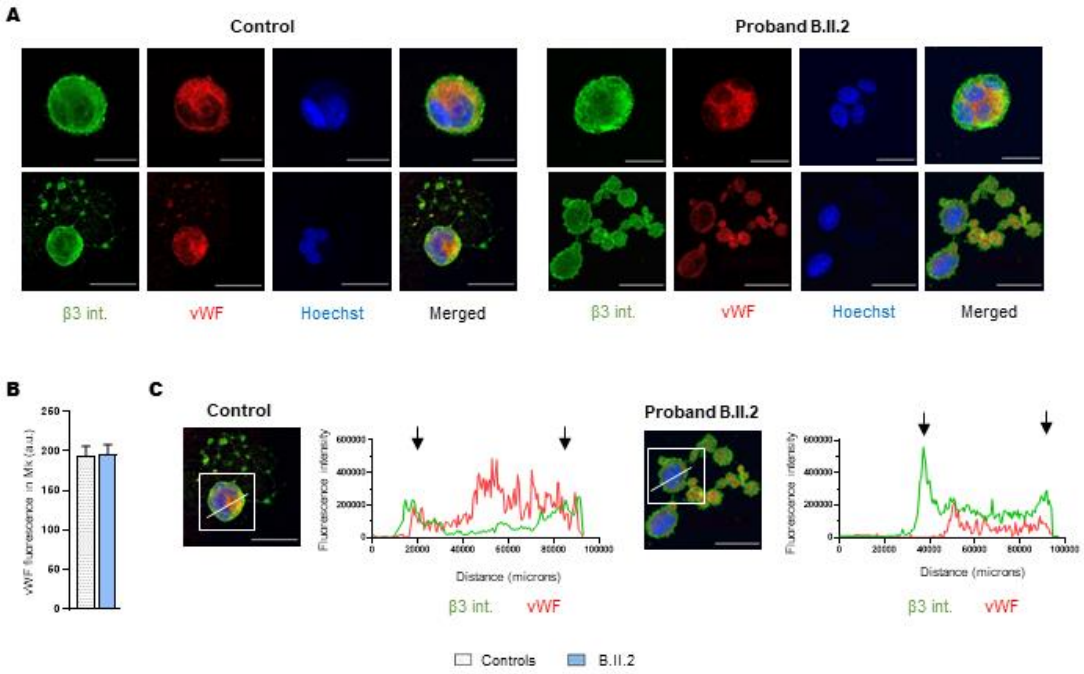


**Figure 6. Carrier of GALE p.Val128Met and p.Leu223Pro variant displayed vWF delocalization within the megakaryocyte membrane.**

**A)** Representative image of alpha granules in mature-polyploid Mks (top) and Mk forming proplatelets (bottom) in control and B.II.2. Cells were stained with an anti–CD61 antibody (green). Alpha granules were stained with anti-vWF (red). Hoechst (blue) was used for counterstaining nuclei. **B)** Anti-vWF levels in Mks. The fluorescence intensity (arbitrary units) was quantified by ImageJ. **C)** The line profile plots represent the fluorescence intensity distribution of channels: anti–CD61 (green) and anti–vWF (red). Arrows show the distribution in the membrane of Mk.

common manifestations.[44] The phenotypes and outcomes of generalized forms of *GALE* deficiency remain poorly understood.[45] Until recently, there was no evidence linking *GALE* defects and hematological alterations. In 2019, Seo et al. reported for the first time six patients from one pedigree affected by severe thrombocytopenia, febrile neutropenia, and mild anemia, who were homozygous for the GALE p.Arg51Trp variant.[19] Febres-Aldana et al. have recently described a child with bone marrow dysfunction and complex congenital heart disease associated with compound heterozygosity in GALE (p.Arg51Trp and p.Gly237Asp).[20] In 2021, Markovitz et al. have reported a patient with pancytopenia and immune dysregulation due to a previously reported homozygous GALE variant (p.Thr150Met).[21] In these previous reports, the authors agreed that the identification of new patients and/or further *in vitro* studies are necessary to consolidate the correlation between

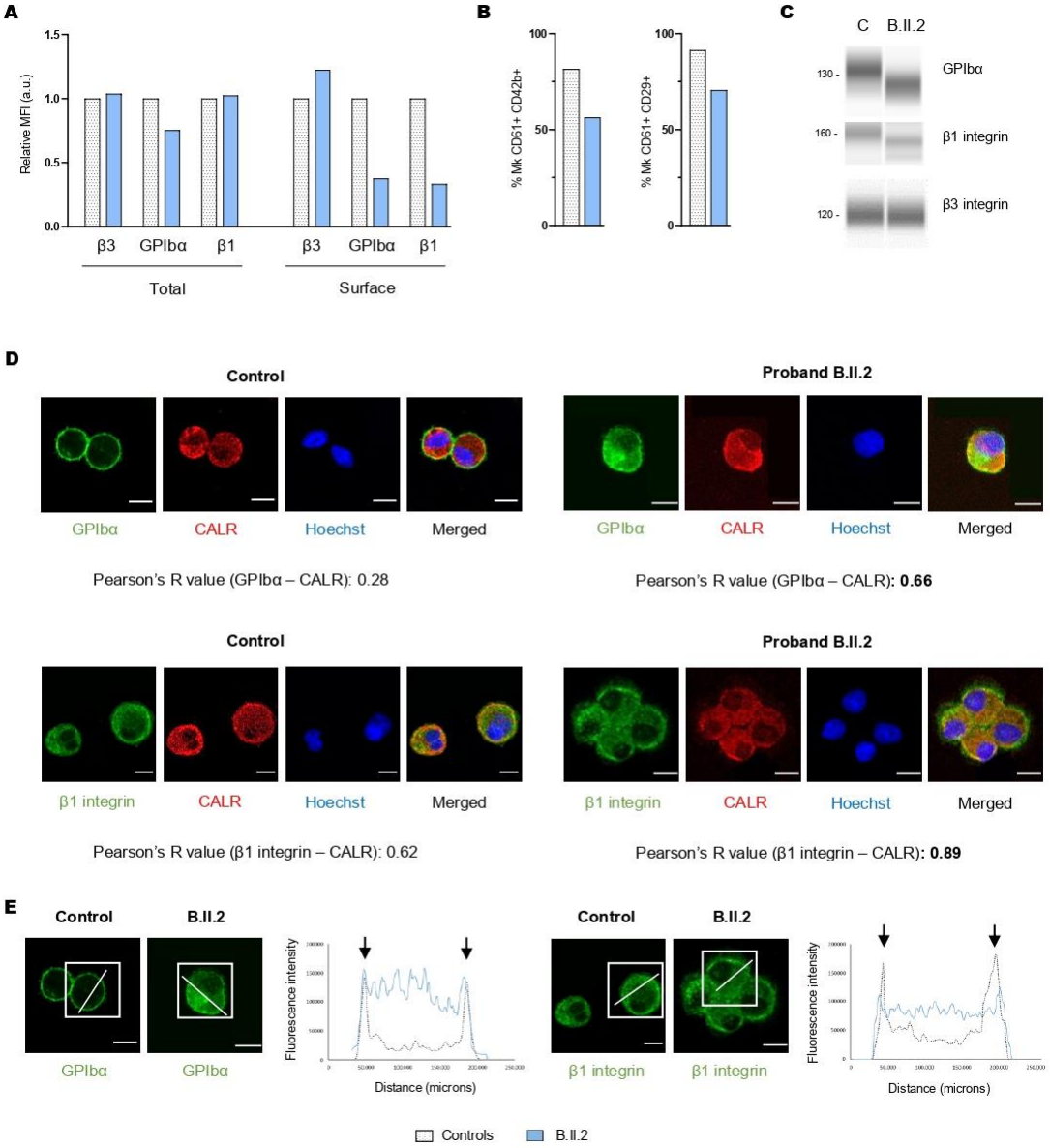


**Figure 7. Megakaryocytes from proband carrying p.Val128Met and p.Leu223Pro variant show impaired GPIbα and β1 glycosylation and externalization.**

Mks were differentiated from peripheral blood progenitor cells (proband B.II.2) through a 14-days culture, in parallel with healthy control. **A)** MFI of β3 integrin (anti-CD61), GPIbα (anti-CD42b), and β1 integrin (anti-CD29) in permeabilized Mks (total levels) and non-permeabilized Mks (surface levels) from control and B.II.2 are represented. Data were normalized against control values. **B)** Mk surface markers measurement assessed as the percentage of $CD61^+$ cells co-expressing the CD42b antigen or CD29, measured by flow cytometry. **C)** Automized immunoblotting of GPIbα and β1 integrin revealed a band with lower molecular weight in Mk from proband B.II.2 compared to control Mk. β3 integrin (internal control) was used as an internal control. **D)** Representative image of control and B.II.2 megakaryocytes. Cells were cytospin and stained with anti-GPIbα or anti-β1 integrin antibodies (green). The endoplasmic reticulum was stained with anti-calreticulin (red

fluorescence). Hoechst (blue) was used for counterstaining nuclei. Pearson's R values indicate the colocalization rate between GPIbα or β1 integrin with calreticulin in control and proband B.II.2 Mks. **E)** The line profile plots represent the fluorescence intensity distribution of GPIbα and β1 integrin in control vs. patient. Arrows indicate the distribution in the membrane of Mk. Control Mks presented a high peak of fluorescence and major distribution of GPIbα and β1 integrin in the membrane, with reduced intracellular levels, while patient fluorescence distribution is uniform, mainly central and without a fluorescence peak in the membrane.

*GALE* molecular alterations and abnormal organ morphogenesis or hematologic disorders. In this context, we described the clinical and laboratory features of three new adult patients with syndromic macrothrombocytopenia due to compound heterozygosity of four variants affecting *GALE*. In contrast with previously reported cases, our patients displayed a syndromic type of IT, characterized by mental retardation, cardiovascular abnormalities, and jaundice. Moreover, their platelet phenotype revealed giant and/or grey platelets with remarkable reduction of granule secretion.

From a mechanistic point of view, these variants caused a severe reduction in the protein levels and the enzymatic activity of UDP-galactose-4-epimerase, which is reflected in a strongly impaired N-linked and O-linked protein glycosylation in platelets[11,14,46] In addition, the fact that all the phases of the heart valve morphogenesis are mediated by N-glycosylated proteins may explain that our 3 probands had mitral valve prolapse that had to be corrected at birth.[20,43,44] Taken together, these data pointed out the essential role of *GALE* in the glycosylation process. Proper performance of glycosylation is thought to be critical for physiological hematopoiesis, since it would favor proliferation and clearance of the hematopoietic precursors[11,46] which are especially relevant in platelet development.[46,47] The hypoglycosylation profile found in platelets from our patients associated with reduced surface expression of the GPIb-IX-V complex and almost absence of glycosylated β1 integrin. Also, hypoglycosylated platelets were prone to an increased apoptosis in accordance with previous studies.[48,49]

Recently, thrombocytopenia has been described in other congenital disorders of glycosylation, including the *GNE*-related disorders, but the mechanisms remain unclear.[15,16,50,51] To our knowledge, there is scarce information about the performance of megakaryopoiesis in patients with thrombocytopenia associated with *GALE* variants. Here, we demonstrate that *GALE* variants disrupt thrombopoiesis. It is well established that Mk differentiation leads to proplatelet formation.[7,52] After polyploidization, Mks increase the cytoplasm volume, and develop the demarcation membrane system (DMS), suffering a remodeling into pseudopodia by a process based on microtubules.[53] However, polyploidization is dispensable for terminal Mk maturation.[52] Using a cell line, we observed

similar polyploidization when comparing *GALE*-WT and our *GALE*-mutants, but a significant reduction in the expression of the CD42b Mk surface marker. Accordingly, normal ploidy was observed in Mks cultured from the proband B.II.2 carrier of the GALE p.Val128Met and p.Leu223Pro variants. Interestingly, we observed a normal microtubule assembly in the patient's Mks despite their impaired ability to extend proplatelets, reinforcing that proplatelet formation is contributed by multiple elements.

There is great controversy about the events that give rise to DMS and the subsequent formation of platelets during thrombopoiesis, but also about the role of GPIbα during the DMS and proplatelet formation. It is well known that the dynamic reorganization of tubulin (specially β1-tubulin) is essential for proplatelet formation.[22,54] In addition, the absence of GPIbα at the Mk surface is associated with impaired proplatelet formation, as described in Bernard Soulier Syndrome.[55,56] DMS formation is critically dependent on GPIbα and the lack of this GP was shown to inhibit microtubule assembly and proplatelet formation in mice.[56,57] However, it has been described that GPIbα expression could appear only during the pre-DMS stage in Mks and at later steps of DMS formation.[58]

We show that impaired proplatelet formation in carriers of *GALE* variants is not related to a defect in the Mks maturation and/or cytoskeleton remodeling, but rather to a defect in the glycosylation of key Mk receptors and a subsequent defect in their externalization to the cell membrane. Reduced levels of GALE in Mks are associated with hypoglycosylation of both GPIbα and β1 integrin, and their retention at the ER, not being delivered to the surface of mature platelets. In contrast, the surface expression of other Mk receptors, such as β3 integrin and c-Mpl, was preserved indicating that different pathways of glycosylation apply to specific target.

vWF relocation on the Mk plasma membrane and binding to GPIbα is crucial for proplatelet formation.[30] β1 integrin signaling is required for regulating Mk function and proplatelet formation.[58,59] β1 integrin function was shown to be dependent on LacNac, which is highly expressed in Mks. LacNac synthesis is regulated by β4GALT1 (beta1,4-galactosyltransferase), which deficiency has been associated with thrombocytopenia.[14,46] Therefore, impaired proplatelet formation in the presence of *GALE* variants could be due to an alteration of both GPIbα and β1 integrin maturation and function, and vWF delocalization. *In vivo*, a further reduction of platelet count in *GALE*-patients may be contributed by an increasing susceptibility to platelet apoptosis (Figure S7). Extending the analysis to additional receptors and proteins may open new paths toward the understanding of the impact of the glycosylation pathways in megakaryopoiesis. In summary, we have identified four variants in *GALE* causing syndromic thrombocytopenia and moderate

platelet dysfunction. These variants severely reduced the enzymatic activity of UDP-galactose-4-epimerase resulting in impaired platelet glycosylation. *In vitro* differentiated Mks from one of the patients carrying these *GALE* variants, showed reduced externalization of GPIbα and β1 integrin into the cell membrane, likely leading to the impaired proplatelet formation. Our new data strongly reinforce the role of *GALE* in the glycosylation and unveil novel mechanisms underlying the *GALE*–related thrombocytopenias mediated by defective glycosylation of β1 integrin and the GPIb-IX-V complex.

**ACKNOWLEDGEMENTS**

We thank Eva Lumbreras, Silvia Tocino Antonio, Sara González Briones, Irene Rodríguez Iglesias and Daisy Castiñeiras-Ramos for technical support with experiments; the CIC-IBMCC Microscopy and Cytometry Service for technical assistance with the confocal immunofluorescence studies; María de los Ángeles Manrique Gonzalo, Nuria Vicente Holgado, Mercedes Rodríguez Martín, Isabel Ramos Sevillano, María del Mar Cambronero Estévez and Beatriz Oreja Martín for blood samples collection, hemograms and blood films; 'Centro Grandi Strumenti' of the University of Pavia, Italy, for technical assistance with flow cytometry and confocal microscopy; Dr. Cesare Perotti and Dr. Claudia Del Fante of the I.R.C.C.S. Policlinico San Matteo of Pavia, Italy, for providing cord blood samples; the group of Prof. Carlo Gaetano of the I.R.C.C.S. Fondazione Maugeri of Pavia, Italy, for helping with Wes, ProteinSimple analysis.

This work was supported by grants from Instituto de Salud Carlos III (ISCIII) & Feder (PI17/01966, PI20/00926) and co-funded by European Union (ERDF/ESF, "Investing in your future"), Gerencia Regional de Salud (GRS2061/A/2019, GRS2135/A/2020, GRS2314/A/2021), Fundación Mutua Madrileña (FMM, AP172142019), Sociedad Española de Trombosis y Hemostasia (SETH-FETH; Premio López Borrasca 2019 and Ayuda a Grupos de Trabajo en Patología Hemorrágica 2020 and 2021), Fundación Castellano Leonesa de Hematología y Hemoterapia (FUCALHH 2020), Red Temática de Investigación Cooperativa en Cáncer (RTICC) (RD12/0036/0069), Centro de Investigación Biomédica en Red de Cáncer (CIBERONC CB16/12/00233),Progetti di ricerca di rilevante interesse Nazionale (PRIN 2017Z5LR5Z), and the European Commission (H2020-FETOPEN-1-2016-2017-SilkFusion ID 767309). The author´s research on Inherited Platelet Disorders is conducted in accordance with the aims of the multicentric project "Functional and Molecular Characterization of Patients with Inherited Platelet Disorders" of Grupo Español de Alteraciones Plaquetarias Congénitas (GEAPC).

A.M.Q. is fully supported by an "Ayuda predoctoral de la Junta de Castilla y León" by the Fondo Social Europeo (JCYL- EDU/556/2019 PhD scholarship) and received an "Ayuda para breves estancias formativas" from the Sociedad Española de Hematología y Hemoterapia (SEHH-FEHH); E.V. is fully supported by an "Ayuda para contratos predoctorales de la Universidad de Salamanca cofinanciadas por el banco Santander", programa propio III convocatoria 2018; I.S.G. is supported by a contract from the University of Salamanca co-financed by the Junta de Castilla y León (Council of Education) and FEDER-European Union [ref. SA0118P20 (2)]; S.S.M. and C.M.G. received funding from the European Research Council (ERC) under the ERA-Per-Med programme (ERAPERMED2018-275) SYNtherapy and ISCIII (AC18/00093) co-funded by ERDF/ESF, "Investing in your future"; I.G.T. and R.B. are supported by a grant from the Universidad de Salamanca

("Contrato postdoctoral Universidad de Salamanca programa propio II, 2019").

## AUTHOR CONTRIBUTIONS

J.M.B., I.G.T. and A.B. designed the research; A.M.Q., C.A.D.B., E.V., L.D.A., J.R. and I.S.G. performed the functional experiments. C.A.D.B., V.A. and A.M.Q. performed glycosylation assays. A.M.Q., C.A.D.B. and P.M.S. performed human megakaryocyte cultures. S.S.M. and C.M.G. prepared samples for whole exome sequencing. A.M.Q., S.S.M., C.M.G., R.B., J.M.H.R. and J.M.B. conducted whole exome sequencing analysis and interpretation. P.R.S. performed enzymatic analysis and interpretation. M.J.P., E.P. and J.R.G.P. provide clinical information and managing the patients. A.M.Q., R.B., C.A.D.B., I.G.T., A.B. and J.M.B. analyzed and interpreted the results; A.M.Q., C.A.D.B., J.R., A.B. and J.M.B. wrote the paper. All authors reviewed the results and approved the final version of the manuscript.

## CONFLICT OF INTEREST

M.J.P. reports honoraria from Abbvie, Celgene, Janssen, Roche, Servier, Takeda., Astra-Zeneca and Gilead, and participation on Advisory Board from Amgen, Janssen, Roche, Takeda and Abbvie outside of the submitted work; J.M.H.R. reports research support from Novartis and Celgene/BMS, consulting fees from GSK, honoraria from Amgen, Novartis, Celgene/BMS, Pfizer, GSK, and participation on Advisory Board from Novartis, Pfizer, Amgen and Celgene/BMS outside of the submitted work; J.R.G.P. reports honoraria from Novo Nordisk, Shire, SOBI, Roche, Daiichi Sankyo, Pfizer, Rovi, Amgen, and Novartis and participation on Advisory Board from Amgen, Novartis, SOBI, Grifols and CSL Behring outside of the submitted work; J.R. reports honoraria from NovoNordisk and participation on Advisory Board from Terumo BCT outside of the submitted work; J.M.B. reports honoraria from NovoNordisk, Roche, Takeda, CSL Behring, Sobi, Novartis, Janssen, and Rovi and participation on Advisory Board from Sobi, Novartis outside of the submitted work. The remaining authors declare no competing financial interests.

## REFERENCES

1. Balduini CL, Melazzini F, Pecci A. Inherited thrombocytopenias—recent advances in clinical and molecular aspects. *Platelets*. 2017;28(1):3–13.
2. Pecci A, Balduini CL. Inherited thrombocytopenias: an updated guide for clinicians. *Blood Rev*. 2021;48:100784.
3. Palma-Barqueros V, Revilla N, Sánchez A, et al. Inherited platelet disorders: An updated overview. *Int. J. Mol. Sci.* 2021;22(9):1–31.
4. Bastida JM, Benito R, Janusz K, et al. Two novel variants of the ABCG5 gene cause xanthelasmas and macrothrombocytopenia: a brief review of hematologic abnormalities of sitosterolemia. *J. Thromb. Haemost.* 2017;15(9):1859–1866.
5. Bury L, Falcinelli E, Gresele P. Learning the Ropes of Platelet Count Regulation: Inherited Thrombocytopenias. *J. Clin. Med.* 2021;10(3):533.
6. Collins J, Astle WJ, Megy K, Mumford AD, Vuckovic D. Advances in understanding the pathogenesis of hereditary macrothrombocytopenia. *Br. J. Haematol.* 2021;1–21.
7. Mbiandjeu S, Balduini A, Malara A. Megakaryocyte Cytoskeletal Proteins in Platelet Biogenesis and Diseases. *Thromb. Haemost.* 2021.
8. Nurden AT, Nurden P. Inherited thrombocytopenias: history, advances and perspectives. *Haematologica*. 2020;105(8):2004–2019.
9. Freson K. Hemostatic Phenotypes and Genetic Disorders. *Res Pr. Thromb Haemost.* 2021;5(5):e12532.

10. Bastida JM, Gonzalez-Porras JR, Rivera J, Lozano ML. Role of thrombopoietin receptor agonists in inherited thrombocytopenia. *Int. J. Mol. Sci.* 2021;22(9):4330.
11. Lee-Sundlov MM, Stowell SR, Hoffmeister KM. Multifaceted role of glycosylation in transfusion medicine, platelets, and red blood cells. *J. Thromb. Haemost.* 2020;18(7):1535–1547.
12. Grozovsky R, Giannini S, Falet H, Hoffmeister KM. Regulating billions of blood platelets: Glycans and beyond. *Blood.* 2015;126(16):1877–1884.
13. Ma X, Li Y, Kondo Y, et al. Slc35a1 deficiency causes thrombocytopenia due to impaired megakaryocytopoiesis and excessive platelet clearance in the liver. *Haematologica.* 2021;106(3):759–769.
14. Giannini S, Lee-Sundlov MM, Rivadeneyra L, et al. β4GALT1 controls β1 integrin function to govern thrombopoiesis and hematopoietic stem cell homeostasis. *Nat. Commun.* 2020;11(1):356–371.
15. Revel-Vilk S, Shai E, Turro E, et al. GNE variants causing autosomal recessive macrothrombocytopenia without associated muscle wasting. *Blood.* 2018;132(17):1851–1854.
16. Futterer J, Dalby A, Lowe GC, et al. Mutation in GNE is associated with severe congenital thrombocytopenia. *Blood.* 2018;132(17):1855–1858.
17. Jones C, Denecke J, Strter R, et al. A novel type of macrothrombocytopenia associated with a defect in α2,3-sialylation. *Am. J. Pathol.* 2011;179(4):1969–1977.
18. Kauskot A, Pascreau T, Adam F, et al. A mutation in the gene coding for the sialic acid transporter SLC35A1 is required for platelet life span but not proplatelet formation. *Haematologica.* 2018;103(12):e613–e617.
19. Seo A, Gulsuner S, Pierce S, et al. Inherited thrombocytopenia associated with mutation of UDP-galactose-4-epimerase (GALE). *Hum. Mol. Genet.* 2019;28(1):133–142.
20. Febres-Aldana CA, Pelaez L, Wright MS, et al. A Case of udp-galactose 4'-epimerase deficiency associated with dyshematopoiesis and atrioventricular valve malformations: An exceptional clinical phenotype explained by altered n-glycosylation with relative preservation of the leloir pathway. *Mol. Syndromol.* 2020;11(5–6):320–330.
21. Markovitz R, Owen N, Satter LF, et al. Expansion of the clinical phenotype of GALE deficiency. *Am. J. Med. Genet. Part A.* 2021;185(10):3118–3121.
22. Palma-Barqueros V, Bury L, Kunissima S, et al. Expanding the genetic spectrum of TUBB1-related thrombocytopenia. *Blood Adv.* 2021;5(24):5453–5467.
23. Marín-Quílez A, Vuelta E, Díaz-Ajenjo L, et al. A novel nonsense variant in TPM4 caused dominant macrothrombocytopenia, mild bleeding tendency and disrupted cytoskeleton remodeling. *J Thromb Haemost.* 2022;20(5):1248–1255.
24. Richards S, Aziz N, Bale S, et al. Standards and guidelines for the interpretation of sequence variants: A joint consensus recommendation of the American College of Medical Genetics and Genomics and the Association for Molecular Pathology. *Genet. Med.* 2015;17(5):405–424.
25. Ko DH, Jun SH, Park KU, et al. Newborn screening for galactosemia by a second-tier multiplex enzyme assay using UPLC-MS/MS in dried blood spots. *J. Inherit. Metab. Dis.* 2011;34(2):409–414.
26. Jacquel A, Herrant M, Defamie V, et al. A survey

of the signaling pathways involved in megakaryocytic differentiation of the human K562 leukemia cell line by molecular and c-DNA array analysis. *Oncogene*. 2006;25(5):781–794.

27. Long MW, Heffner CH, Williams JL, Peters C, Prochownik E V. Regulation of megakaryocyte phenotype in human erythroleukemia cells. *J. Clin. Invest.* 1990;85(4):1072–1084.
28. Di Buduo CA, Laurent PA, Zaninetti C, et al. Miniaturized 3d bone marrow tissue model to assess response to thrombopoietin-receptor agonists in patients. *Elife*. 2021;10:1–30.
29. Di Buduo CA, Alberelli MA, Glembostky AC, et al. Abnormal proplatelet formation and emperipolesis in cultured human megakaryocytes from gray platelet syndrome patients. *Sci. Rep*. 2016;6:23213.
30. Balduini A, Pallotta I, Malara A, et al. Adhesive receptors, extracellular proteins and myosin IIA orchestrate proplatelet formation by human megakaryocytes. *J. Thromb. Haemost.* 2008;6(11):1900–1907.
31. Bang YL, Nguyen TTT, Trinh TTB, et al. Functional analysis of mutations in UDP-galactose-4-epimerase (GALE) associated with galactosemia in Korean patients using mammalian GALE-null cells. *FEBS J.* 2009;276(7):1952–1961.
32. Timson DJ. Functional analysis of disease-causing mutations in human UDP-galactose 4-epimerase. *FEBS J.* 2005;272(23):6170–6177.
33. Broussard A, Florwick A, Desbiens C, et al. Human UDP-galactose 4′-epimerase (GALE) is required for cell-surface glycome structure and function. *J. Biol. Chem.* 2020;295(5):1225–1239.
34. Di Buduo CA, Soprano PM, Miguel CP, et al. A Gold Standard Protocol for Human Megakaryocyte Culture Based on the Analysis of 1,500 Umbilical Cord Blood Samples. *Thromb. Haemost.* 2021;121(4):538–542.
35. Bastida JM, Lozano ML, Benito R, et al. Introducing high-throughput sequencing into mainstream genetic diagnosis practice in inherited platelet disorders. *Haematologica.* 2018;103(1):148–162.
36. Bastida JM, Benito R, Lozano ML, et al. Molecular Diagnosis of Inherited Coagulation and Bleeding Disorders. *Semin. Thromb. Hemost.* 2019;45(7):695–707.
37. Ver Donck F, Downes K, Freson K. Strengths and limitations of high-throughput sequencing for the diagnosis of inherited bleeding and platelet disorders. *J. Thromb. Haemost.* 2020;18(8):1839–1845.
38. Kumar SU, Sankar S, Kumar DT, et al. Molecular dynamics, residue network analysis, and cross-correlation matrix to characterize the deleterious missense mutations in GALE causing galactosemia III. *Cell Biochem. Biophys.* 2021;79(2):201–219.
39. Wasilenko J, Lucas ME, Thoden JB, Holden HM, Fridovich-Keil JL. Functional characterization of the K257R and G319E-hGALE alleles found in patients with ostensibly peripheral epimerase deficiency galactosemia. *Mol. Genet. Metab.* 2005;84(1):32–38.
40. McCorvie TJ, Timson DJ. In silico prediction of the effects of mutations in the human UDP-galactose 4′-epimerase gene: Towards a predictive framework for type III galactosemia. *Gene*. 2013;524(2):95–104.
41. Openo KK, Schulz JM, Vargas CA, et al. Epimerase-deficiency galactosemia is not a binary condition. *Am. J. Hum. Genet.* 2006;78(1):89–102.
42. Wohlers TM, Christacos NC, Harreman MT,

Fridovich-Keil JL. Identification and characterization of a mutation, in the human UDP-galactose-4-epimerase gene, associated with generalized epimerase-deficiency galactosemia. *Am. J. Hum. Genet.* 1999;64(2):462–470.

43. Fischer A, Steidl C, Wagner TU, et al. Combined loss of Hey1 and HeyL causes congenital heart defects because of impaired epithelial to mesenchymal transition. *Circ. Res.* 2007;100(6):856–863.
44. Frieden LA, Townsend TA, Vaught DB, et al. Regulation of heart valve morphogenesis by Eph receptor ligand, ephrin-A1. *Dev. Dyn.* 2010;239(12):3226–3234.
45. Fridovich-Keil J, Bean L, He M, Schroer R. Eimerase Deficiency Galactosemia. 2011.
46. Di Buduo CA, Giannini S, Abbonante V, et al. Increased B4GALT1 expression is associated with platelet surface galactosylation and thrombopoietin plasma levels in MPNs. *Blood.* 2021;137(15):2085–2089.
47. Li R, Hoffmeister KM, Falet H. Glycans and the platelet life cycle. *Platelets.* 2016;27(6):505–511.
48. McArthur K, Chappaz S, Kile BT. Apoptosis in megakaryocytes and platelets: the life and death of a lineage. *Blood.* 2018;131(6):605–610.
49. Edward Quach M, Chen W, Li R. Mechanisms of platelet clearance and translation to improve platelet storage. *Blood.* 2018;131(14):1512–1521.
50. Bottega R, Marzollo A, Marinoni M, et al. GNE-related thrombocytopenia: evidence for a mutational hotspot in the ADP/substrate domain of the GNE bifunctional enzyme. *Haematologica.* 2021;1–19.
51. Chang IJ, He M, Lam C. Congenital disorders of glycosylation. *Ann Transl Med.* 2018;6(24):477.
52. Vainchenker W, Raslova H. Megakaryocyte polyploidization: role in platelet production. *Platelets.* 2020;31(6):707–716.
53. Schulze H, Korpal M, Hurov J, et al. Characterization of the megakaryocyte demarcation membrane system and its role in thrombopoiesis. *Blood.* 2006;107(10):3868–3875.
54. Italiano JE, Lecine P, Shivdasani RA, Hartwig JH. Blood platelets are assembled principally at the ends of proplatelet processes produced by differentiated megakaryocytes. *J. Cell Biol.* 1999;147(6):1299–1312.
55. Clementson KJ. A short history of platelet glycoprotein Ib complex. *Thromb. Haemost.* 2007;98(1):63–68.
56. Strassel C, Eckly A, Léon C, et al. Intrinsic impaired proplatelet formation and microtubule coil assembly of megakaryocytes in a mouse model of Bernard-Soulier syndrome. *Haematologica.* 2009;94(6):800–810.
57. Dütting S, Gaits-Iacovoni F, Stegner D, et al. A Cdc42/RhoA regulatory circuit downstream of glycoprotein Ib guides transendothelial platelet biogenesis. *Nat. Commun.* 2017;8:15838.
58. Kawaguchi T, Hatano R, Yamaguchi K, et al. Fibronectin promotes proplatelet formation in the human megakaryocytic cell line UT-7/TPO. *Cell Biol. Int.* 2012;36(1):39–45.
59. Abbonante V, di Buduo CA, Gruppi C, et al. A new path to platelet production through matrix sensing. *Haematologica.* 2017;102(7):1150–1160.

## SUPPLEMENTAL MATERIAL

# Novel variants in *GALE* cause syndromic macrothrombocytopenia by disrupting glycosylation and thrombopoiesis

Marín-Quílez A, et al.

**Supplemental Methods**

Blood samples and peripheral blood film

In this study, we investigated two unrelated Spanish families with suspicion of inherited macrothrombocytopenia, recruited in the multicenter project "Functional and Molecular Characterization of Patients with Inherited Platelet Disorders" conducted by the "Grupo Español de Trastornos Plaquetarios Congénitos (GEAPC).[1,2] From the first family (Pedigree A), four family members were included (index case [II.1], and affected sister [II.4], and healthy father [I.1] and healthy mother [I.2]). The heterozygous carrier I.1 died during the period; therefore, the platelet characterization was performed in the healthy sister [II.2] with the same genotype. From the second family (Pedigree B), three family members (index case [II.2], and healthy parents [I.1 & I.2]) were included (Figure 1A).

Venous blood from patients, relatives, and healthy volunteers, were drawn into 7.5% K3 EDTA (for blood cells count, blood film, nucleic acid purification, and protein extraction), buffered 0.105 M sodium citrate for platelet functional studies (aggregometry, flow cytometry, and immunofluorescence assays) and ACD Vacutainer B for megakaryocyte (Mk) culture from peripheral blood. Complete blood counts, including platelet count and mean platelet volume (MPV) assessment, were performed using an Advia 2120i hematological counter (Siemens, Berlin, Germany). To measure platelet dimensions on May–Grünwald–Giemsa-stained blood smears, 50 platelets were evaluated and classified as normal (diameter <3 μm), large (3-4 μm) or giant (>4 μm).[3,4]

Platelet functional assays

Detailed platelet phenotyping was conducted as previously described.[5,6] For platelet aggregation assays, platelet-rich plasma (PRP), from patients with significant macrothrombocytopenia, was obtained by centrifugation at low speed (100 x g, 10 min), with a platelet count of 25-50 $x10^9$/L. The PRP in subjects with normal platelet counts was obtained by standard centrifugation (200 x g, 10 min) and the platelet count was adjusted as to that in patients with platelet-poor plasma (PPP; 1000 x g, 20 min). Light transmission aggregometry (LTA) in these PRP samples was performed using a TA-8V Aggregometer (Stago, Asnieres Sur Seine, France) and was recorded for 5 minutes upon PRP stimulation with agonists: 1.5 mM Arachidonic Acid, 10 μM ADP, 10 μg/mL Collagen, 50 μM TRAP-6, 5 μM Epinephrin and 1.5 mg/mL Ristocetin.

Platelet expression of major glycoproteins (GPs) was assessed in diluted whole blood (1:10 in PBS) by flow cytometry (FC) with specific antibodies (anti-CD42a*PE, anti-CD42b*PE, anti-GPVI*FITC, anti-CD61*PE, and anti-CD41*APC) (1:100) (BD Biosciences, San Jose, CA, USA), and anti-CD42d*PE (1:20) (R&D Systems, Minneapolis, MN, USA). Cells were stained at room temperature (RT) for 30 minutes under

static conditions. 10.000 CD41+ platelets were recorded in an Accuri C6™ cytometer (BD), and MFI from CD42a, CD42b, CD42d, GPVI, and CD61 was analyzed using FlowJo software (vX.0.7. TreeStar, Woodburn, OR, USA). Data were standardized using FCS MFI, due to the macrothrombocytopenia relative to patients, as described[7], and relative to the control sample.

To evaluate platelet function by FC,[6,8] PRPs (20 x $10^9$ platelets/L) from patients, healthy relatives, and healthy controls were stimulated for 30 minutes at RT under static conditions with 10 μM ADP, 10 μg/mL CRP and 25 μM TRAP6, in the presence of fibrinogen-labeled antibody (*AF488, ThermoFisher Scientific, Waltham, MA, USA) and alpha-granule (anti-CD62*PE antibody) or dense-granule secretion (anti-CD63*PE antibody) (BD Biosciences). Platelet staining was evaluated in 10.000 CD41+ platelets using an Accuri C6™ cytometer and data were analyzed using FlowJo software.

Washed platelets in modified Tyrode's HEPES buffer[6] were used to analyze the spreading function under resting conditions and after 20 minutes of stimulation with 25 μM TRAP6 stimulation, using fibrinogen-coated coverslips ($1x10^6$ platelets/coverslip). Platelets were stained with Phalloidin-Oregon Green-514 (ThermoFisher) and visualized using a Leica SP8 confocal microscope with 100X objective lens.

Whole Exome Sequencing approach, filtering workflow, and variant interpretation

Genomic DNA was extracted from peripheral blood samples using a DNeasy Blood and Tissue Kit, following the manufacturer's protocol (Qiagen, Hilden, Germany). DNA quantity was assessed by Qubit 4.0 using a double-strand kit (High/Broad Sensitivity) (Invitrogen Life Technologies, Carlsbad, CA, USA).

Four family members from Pedigree A, including both probands (II.1, II.4) and 3 family members from Pedigree B, including the index case (II.2) (Figure 1A, Table 1), were analyzed by WES after capture and library preparation using an established protocol that included enrichment with the xGEN® Exome Research Panel v2 (Integrated DNA Technologies).[6,9]

Library preparation was performed with the Illumina Nextera Flex with Enrichment Kit using Unique Dual Indexes (UDI). DNA was enzymatically tagmented generating 180bp fragments. A minimum of 600ng of DNA with sufficient fragment length was required as starting material (quality check required for FFPE DNA). The minimum quality of DNA was established at 1,8-2,0 for A260/280 ratio and a concentration of at least 20 ng/μl was required.

Then, the DNA target regions were enriched using the IDT Hybridization Capture Protocol and the corresponding xGen™ Exome Research Panel V2 (Integrated DNA Technologies). The exome design was downloaded from the

supplier's website [xGen Exome Research Panel v2 targets". (2020)].

Sequencing was performed on a NovaSeq 6000 system at the Sequencing service of MLL (Münchner Leukämielabor GmbH, Munich, Germany) using a S1 Flow Cell (200 cycles). Based on the generated fastq files, reads were aligned to the human reference genome hg19 (Star Aligner) and variants were annotated using the ACMG Annotator software (v8.4.5) (Biostars, New Taipei, Taiwan). Each pedigree was analyzed independently (Table S2). To identify single-nucleotide and indel variants shared among the family members of each family, Burrows-Wheeler Aligner, and SAMtools softwares were used. Polymorphisms were removed by screening the dbSNP build (154) on the human assembly hg19/GRCh38, the GenomAD and the ExAC databases. Novel variants with Minor Allele Frequency (MAF<0.01) were analyzed based on the amino acid sequence, the assignation of the coverage-dependent Phred-scaled mutation probability (call status), and the predicted effect on the protein using SIFT and PolyPhen. Further validation was performed by manual review using the Integrative Genomics Viewer (IGV) (Broad Institute, Cambridge, MA, USA).

The annotated variants were filtered based on their location on the genome and type of variation, functions (5'flank, 5'utr, exonic and splicing regions), coding impact (frameshift, missense, nonsense, stop loss, exon deletion, in frame, start loss, splice junction loss), allele frequencies (gnomAD, exome and genome frequencies), status (heterozygous and homozygous) and inheritance pattern. Then, we selected variants with MAF<0,01 excluding those classified as Likely Benign Variants (LBV), and Benign Variants (BV). Furthermore, for parents in each evaluated trio, we retained nucleotide positions that were found in common with the probands. As the thrombocytopenic phenotype in the pedigrees displayed autosomal recessive inheritance, causative homozygous or compound heterozygous variants in the alleles of homologous chromosomes were suspected.

Finally, aiming at identifying those variants which were associated with the platelet phenotype and clinical features in the patients, we employed the comprehensive online tool VARSOME (https://varsome.com/). Variants were confirmed by Sanger sequencing using specific oligonucleotides (Table S3). Pathogenicity of variants was assessed according to the ACMG rules[10] (Table S1).

UDP-galactose-4-epimerase activity measurement

UDP-galactose-4-epimerase (GALE) activity was measured in dried blood spots (DBS) by high-performance liquid chromatography with tandem mass spectrometry (HPLC/MS/MS) adapted from previous publications.[11] Two rehydrated-punched 5-mm DBSs were used to determine the hemoglobin concentration and

two other DBSs were incubated with the reaction mixture using UDP-glucose as substrate. After a 2-hour incubation, the final product from the reaction, UDP-galactose, was measured in a Sciex 4500QTrap HPLC/MS/MS (Framingham, MA, USA), using UDP-N-acetylglucosamine as the internal standard. UDP-galactose and UDP-glucose were separated by an ACQUITY (HSS)-T3 column (2.1x100 mm, 1.8 μm) and registered by multiple reaction monitoring (m/z 565/323) joined to the internal standard (m/z 606/385). A calibration curve of UDP-galactose was prepared for the quantification.

Standard and automized Immunoblotting

Platelet protein lysates (30 ng) were resolved by gel electrophoresis (SDS-PAGE) and transferred to polyvinylidene fluoride (PVDF) membrane (BioRad, Berkeley, CA, USA). Membranes were probed with biotinylated Erythrina cristagalli (ECL) (1:1000, Vector laboratories, Burlingame, CA, USA); anti-GALE (1:5000, Abcam, Cambridge, UK), anti-Caspase 8 (1:1000, Cell Signaling, Danvers, MA, USA), anti-GPIbα (1:1000, ThermoFisher), anti-β1 integrin (1:1000, Abcam), anti-β3 integrin (1:300, Cell Signaling), anti-TPO-R (1:1000, Merck, Darmstadt, Germany), anti-vWF (1:1000, Dako, Agilent, Santa Clara, CA, USA), and anti-β-actin (1:3000, Abcam) as an internal control. Immunoreactive bands were detected by horseradish peroxidase-labeled streptavidin, or the appropriate horseradish peroxidase-labeled secondary antibodies (anti-rabbit, anti-mouse, 1:3000, BioRad), using enhanced chemiluminescence reagent (Millipore, Darmstadt, Germany). Band intensities from individual western blots were quantified by densitometric analysis using the 'Image J' software (NIH).

Mks lysates from patients and healthy subjects were analyzed with an automated capillary-based immunoassay platform (Wes, ProteinSimple), according to the manufacturer's instructions. Briefly, Mk lysates were diluted to the required concentration with sample buffer, then prepared by adding a master mix containing 200 mM dithiothreitol (DTT), sample buffer, and fluorescent standards (Standard Pack 1, PS-ST01-8) and boiled for 5 min at 95°C. Wes 12–230 kDa prefilled microplates were used (SM-W004). Compass Software for Simple Western was used to analyze results (version 3.1.7, ProteinSimple). Separation time was set to 25 min, stacking loading time to 15 s and sample loading time to 9 s. Primary antibodies were incubated for 30 min and the High Dynamic Range (HDR) profile was used for detection. For each antibody, a lysate dilution experiment was performed first to confirm the optimal dynamic range of the corresponding protein on Wes. This was followed by an antibody optimization experiment to compare a range of dilutions and to select an antibody concentration that was close to saturation level to allow a quantitative comparison of signals between samples.[12]

Overexpression plasmid construction

Total mRNA was isolated from peripheral blood and 100ng were retrotranscribed to cDNA using First-Strand SuperScript III kit (ThermoFisher), following the manufacturer's instructions. *GALE* cDNA was PCR-amplified using *GALE* SalI forward (F) and *GALE* SalI reverse (R) oligonucleotides, containing SalI restriction site (Table S4). PCR product was purified and incubated with SalI endonuclease for 1 hour at 37ºC and cloned into pShuttle CMV-F2A-T2A-Venus plasmid (pShuttle-CMV-F2A-T2A-Venus was a gift from Zheng-Xu Wang, Addgene plasmid #62621; http://n2t.net/addgene:62621; RRID: Addgene_62621).

*GALE* c.449C>T [p.Thr150Met], c.382G>A [p.Val128Met]) and c.668T>C [p.Leu223Pro] variants were obtained by directed mutagenesis. We amplified pShuttle-*GALE*-WT plasmid by PCR using *GALE*-150Met F and R, *GALE*-128Met F and R, and *GALE*-223Pro F and R oligonucleotides, respectively (Table S4), followed by DPNI restriction endonuclease treatment, phosphorylation, and re-ligation reaction. Products were transformed into DH5alpha competent bacteria to plasmid amplify and extraction was performed through QIAprep spin Maxiprep Kit (Qiagen). The sequence of all generated constructions was confirmed by Sanger sequencing method.

Cell culture and electroporation

The human CML-derived cell line K562 was obtained from the DMSZ collection (Leibniz-Institut DSMZ-Deutsche Sammlung von Mikroorganismen und Zellkulturen GmbH, Germany). K562 cells were cultured in RPMI 1640 medium (Gibco, ThermoFisher) supplemented with 10% heat-inactivated FBS, and 1% penicillin/streptomycin (ThermoFisher). Cell lines were cultured at 37°C in a 5% $CO_2$ atmosphere.

$1x10^6$ K562 cells were electroporated with 10 μg of plasmid using Neon Transfection System 100 μL Kit (ThermoFisher) following the manufacturer's instructions (Figure S4A). The electroporation parameters were 1450v, 10ms and 3 pulses.

RT-PCR, quantitative PCR and Immunobloting of *GALE* overexpression cell model

Total mRNA from cells was extracted by RNeasy mini kit (Qiagen) and 150 ng were in vitro-retrotranscribed (SuperScript III First-Strand Synthesis Super Mix kit, ThermoFisher). cDNA was used as a template for PCR-amplification and Sanger-sequencing (Table S4).

*GALE* and *GAPDH* expression were quantified by qPCR (Applied Biosystems, CA, USA) using specific human *GALE* qPCR and *GAPDH* qPCR oligonucleotides, respectively (Table S4) (Figure S4B). Full-length *GALE* cDNA showed a peak at 1047 bp in all samples. As negative control we used WT RNA without retrotranscription (-RT).

Finally, immunoblotting of anti-GALE (1:6000, Abcam) and anti-β-actin (1:3000, Cell Signaling) in Mock and *GALE* variants (WT, 150Met, 128Met and 223Pro) were analyzed to confirm the overexpression (Figure S4C).

hK562 differentiation assay

The human CML cell K562 line was electroporated with overexpression plasmids harboring the wild-type (WT) and different versions of the human coding sequence of the *GALE* gene (150Met, 128Met and 223Pro). An empty vector was used (Mock) as control. Green Fluorescence protein (GFP) expression was used to evaluate the electroporation efficiency of the different *GALE* plasmids (Figure S4A). All conditions showed around 60% of positive cells 24 hour after electroporation. A total of 1,5 x $10^5$ electroporated cells were seeded per condition and treated with phorbol 12-myristate 13-acetate (PMA) 20 nM for 7 days to promote their differentiation to a megakaryocyte-like phenotype, as previously described.[13,14] Mk differentiation was monitored by FC at days 3, 5 and 7 of culture by measuring polyploidization and maturation. Polyploidy was determined by measuring the DNA content in the cell cycle phase (PI labeling after cell permeabilization) (FACScalibur, BD Applications). Mk maturation was measured by analyzing the expression of surface markers with anti-CD61 (*APC) and anti-CD42b (*PE) (BD Bioscience) antibodies, using a BD Accuri C6 Cytometer.

Differentiation of human megakaryocytes from peripheral blood

Venous blood samples were drawn into ACD tubes (BD Vacutainer, solution B). The study was performed in four healthy control and the patient from Pedigree B. $CD45^+$ from peripheral blood were separated by immunomagnetic bead selection (Miltenyi Biotec, Bergisch Gladbach, Germany) and cultured in Stem Span medium supplemented with 1% penicillin-streptomycin, 1% L-glutamine, 10 ng/mL TPO, and 10 ng/mL IL-11 at 37 °C in a 5% $CO_2$ fully humidified atmosphere, as previously described.[15–17]

To investigate Mk differentiation and maturation by FC, aliquots of 20x$10^3$ cells were collected at the end of the culture (14th day). Polyploidy was determined in permeabilized Mk (70% ethanol, 24 hours). Mks were stained with Propidium Iodide (PI) and anti-CD61 (*APC) (BD Biosciences). Mk viability in culture was evaluated with an Apoptosis Detection Kit (Beckman Coulter, Brea, CA, USA), containing Annexin V*FITC and Propidium Iodide (PI), and following the manufacturer instructions. To measure Mk markers, cells were double-stained with anti-CD61 (*FITC) and anti-CD42b (*PE) or anti-CD29 (*PE) antibodies (eBioscience) at room temperature, in the dark, for 30 minutes. Cells were analyzed using a BD FACS Lyric (Becton Dickinson).

Total β3 integrin, GPIbα, β1 integrin, and *GALE* were measured in permeabilized Mk. Aliquots of 50 x$10^3$ cells were permeabilized using the

Fixation/Permeabilization Kit (BD Biosciences) and stained with anti-CD61 (*FITC), anti-CD42b (*PE), or anti-CD29 (*PE), and rabbit anti-GALE (Abcam). Anti-rabbit*AF633 (ThermoFisher) was used as a secondary antibody to detect *GALE* in FC. A minimum of 10,000 events were acquired in a BD FACS Lyric (Becton Dickinson).

Proplatelet formation was investigated at the end of the culture in suspension and in adhesion on fibrinogen.[18] Cells on fibrinogen or cytospin were fixed in 4% paraformaldehyde, permeabilized with 0.1% Triton X-100, and stained with mouse anti-CD61, mouse anti-CD42b, rabbit anti-β1 tubulin, rabbit anti-calreticulin (1:100, 1:50, 1:500, 1:100 respectively, Abcam), mouse anti- β1 integrin (1:50, Milipore) and rabbit anti-von Willebran Factor (vWF) primary antibody (1:100, Dako), and Alexa Fluor-conjugated antibodies (anti mouse 488, anti rabbit 594, 1:400, Life Technologies). Nuclei were stained with Hoechst 33258 (1:10000) (Merck). For all experiments, the coverslips were mounted onto glass slides with ProLong Gold antifade reagent (Invitrogen).

Mks forming proplatelets were identified as $CD61^+$ cells displaying at least one filamentous structure ending with platelet-sized tips. At least 10 fields per sample were analyzed using a Leica SP5 or SP8 confocal microscope with 63X objective lens. The number of proplatelet free ends (tips) per Mk and the number of bifurcations of proplatelet shafts per Mk were measured by image analysis (Image J software).

Differentiation of megakaryocytes from cord blood.

Mks were differentiated from human $CD34^+$ cells using previously described methods.[19] $CD34^+$ were separated by immunomagnetic bead selection (Miltenyi Biotec, Bologna, Italy) and cultured for 13 days and cultured in Stem Span medium supplemented with 1% penicillin-streptomycin, 1% L-glutamine, 10 ng/mL TPO, and 10 ng/mL IL-11 at 37 °C in a 5% $CO_2$ fully humidified atmosphere. The culture medium was renewed every 3 days. GALE was measured in permeabilized Mk at days 0, 7, 13, and 15 (platelets) of culture.

Aliquots of 50 $x10^3$ cells were permeabilized using the Fixation/Permeabilization Kit (BD Biosciences) and stained anti-CD34*FITC (day 0) or anti-CD61 (*FITC) and anti-CD42b (*PE) (day 7, 13 and 15). Rabbit anti-GALE (1:30, Abcam) and Anti rabbit*AF633 (ThermoFisher) were used to detect *GALE* in FC. A minimum of 10,000 events were acquired in a BD FACS Lyric (Becton Dickinson) .

For immunofluorescence assay, Mks forming proplatelets were seed in fibrinogen coverslips fixed in 4% paraformaldehyde, permeabilized with 0.1% Triton X-100, and stained with rabbit anti-CD42b (1:100, ThermoFisher), mouse anti-GALE (1:50, Novus Biologicals, Englewood, CO, USA) and rabbit anti-calreticulin (1:100, Abcam). Alexa Fluor-conjugated antibodies (anti mouse 488, anti rabbit 594, 1:400, Life Technologies) were used, and nuclei were stained with Hoechst

33258 (1:10000) (Merck). The coverslips were mounted onto glass slides with ProLong Gold antifade reagent (Invitrogen) and visualized using a Leica SP5 or SP8 confocal microscope with 63X objective lens. Diagrams of fluorescence were analyzed by ImageJ.

Platelet adhesion assay

Coverslips were coated overnight with 10 µg/mL Haemate P (1200 IU von Willebrand Factor, 500 IU FVIII) (Aventis-Behring, King of Prussia, PA, USA), 50 µg/mL fibronectin, 50 µg/mL laminin, 10 µg/mL collagen (Sigma).

Washed-platelets in modified Tyrode's HEPES buffer were adjusted to $1x10^6$ platelets/coverslips in control and patient samples. Platelets were fixed and incubated on the different substrates per 2 hours at RT, permeabilized with 0.1% Triton X-100, stained with Phalloidin-Oregon Green-514 (ThermoFisher) and visualized using a Leica SP8 confocal microscope with 100X objective lens. The adhesion was quantified as the number of platelets per field.

**Supplemental Bibliography**

1. Sánchez-Guiu I, Antón AI, Padilla J, et al. Functional and molecular characterization of inherited platelet disorders in the Iberian Peninsula: Results from a collaborative study. *Orphanet J. Rare Dis.* 2014;24(9):213.
2. Bastida JM, Lozano ML, Benito R, et al. Introducing high-throughput sequencing into mainstream genetic diagnosis practice in inherited platelet disorders. *Haematologica.* 2018;103(1):148–162.
3. Noris P, Klersy C, Gresele P, et al. Platelet size for distinguishing between inherited thrombocytopenias and immune thrombocytopenia: A multicentric, real life study. *Br. J. Haematol.* 2013;162(1):112–119.
4. Greinacher A, Pecci A, Kunishima S, et al. Diagnosis of inherited platelet disorders on a blood smear: a tool to facilitate worldwide diagnosis of platelet disorders. *J. Thromb. Haemost.* 2017;15(7):1511–1521.
5. Marín-Quílez A, García-Tuñón I, Fernández-Infante C, et al. Characterization of the Platelet Phenotype Caused by a Germline RUNX1 Variant in a CRISPR/Cas9-Generated Murine Model. *Thromb. Haemost.* 2021;121(9):1193–1205.
6. Marín-Quílez A, Vuelta E, Díaz-Ajenjo L, et al. A novel nonsense variant in TPM4 caused dominant macrothrombocytopenia, mild bleeding tendency and disrupted cytoskeleton remodeling. *J Thromb Haemost.* 2022;20(5):1248–1255.
7. Javela K, Kekomäki R. Mean platelet size related to glycoprotein-specific autoantibodies and platelet-associated IgG. *Int. J. Lab. Hematol.* 2007;29(6):433–441.

8. Palma-Barqueros V, Bury L, Kunissima S, et al. Expanding the genetic spectrum of TUBB1- related thrombocytopenia. *Blood Adv.* 2021;5(24):5453–5467.
9. Tilleman L, Heindryckx B, Deforce D, Van Nieuwerburgh F. Pan-cancer pharmacogenetics: Targeted sequencing panels or exome sequencing? *Pharmacogenomics*. 2020;21(15):1073–1084.
10. Richards S, Aziz N, Bale S, et al. Standards and guidelines for the interpretation of sequence variants: A joint consensus recommendation of the American College of Medical Genetics and Genomics and the Association for Molecular Pathology. *Genet. Med.* 2015;17(5):405–424.
11. Ko DH, Jun SH, Park KU, et al. Newborn screening for galactosemia by a second-tier multiplex enzyme assay using UPLC-MS/MS in dried blood spots. *J. Inherit. Metab. Dis.* 2011;34(2):409–414.
12. Vögtle T, Sharma S, Mori J, et al. Heparan sulfates are critical regulators of the inhibitory megakaryocyte-platelet receptor G6B-B. *Elife*. 2019;8:e46840.
13. Long MW, Heffner CH, Williams JL, Peters C, Prochownik EV. Regulation of megakaryocyte phenotype in human erythroleukemia cells. *J. Clin. Invest.* 1990;85(4):1072–1084.
14. Jacquel A, Herrant M, Defamie V, et al. A survey of the signaling pathways involved in megakaryocytic differentiation of the human K562 leukemia cell line by molecular and c-DNA array analysis. *Oncogene*. 2006;25(5):781–794.
15. Balduini A, Di Buduo CA, Kaplan DL. Translational approaches to functional platelet production ex vivo. *Thromb. Haemost*. 2016;115(2):250–256.
16. Di Buduo CA, Laurent PA, Zaninetti C, et al. Miniaturized 3d bone marrow tissue model to assess response to thrombopoietin-receptor agonists in patients. *Elife*. 2021;10:1–30.
17. Di Buduo CA, Alberelli MA, Glembostky AC, et al. Abnormal proplatelet formation and emperipolesis in cultured human megakaryocytes from gray platelet syndrome patients. *Sci. Rep.* 2016;6:23213.
18. Marconi C, DI Buduo CA, LeVine K, et al. Loss-of-function mutations in PTPRJ cause a new form of inherited thrombocytopenia. *Blood*. 2019;133(12):1346–1357.
19. Di Buduo CA, Soprano PM, Miguel CP, et al. A Gold Standard Protocol for Human Megakaryocyte Culture Based on the Analysis of 1,500 Umbilical Cord Blood Samples. *Thromb. Haemost.* 2021;121(4):538–542.

## Supplemental Tables

| Variant | p.Thr150Met | p.Lys78Valfs*32 | p.Val128Met | p.Leu223Pro |
|---|---|---|---|---|
| **Current** | Likely Pathogenic<br>PS3:strong<br>PP5:moderate<br>PM2:supporting<br>PP2:supporting<br>PP3:supporting | Pathogenic<br>PVS1:very strong<br>PM2:moderate<br>PP3:supporting | VUS<br>PM2:moderate<br>PP2:supporting<br>PP3:supporting | Likely Pathogenic<br>PM2:strong<br>PP2:supporting<br>PP3:supporting |
| **New Classification** | **Pathogenic**<br>PM3:moderate | **Pathogenic** | **Pathogenic**<br>PS3:strong<br>PM3:moderate | **Pathogenic**<br>PS3:strong |

**Table S1. Pathogenicity assessment of identified GALE variants according to the ACMG rules.** General information about these variants is available on Varsome web tool (https://varsome.com/) (Accessed 30th December 2021). ACMG: American College of Medical Genetics; VUS: Variant of uncertain significance.

| Pedigree A | ID | Number of variants | % 10X reads | % 20X reads |
|---|---|---|---|---|
| Father (I.1) | 102496 | 129 735 | 98.4 | 97.4 |
| Mother (I.2) | 102495 | 122 095 | 98.4 | 97.6 |
| Proband 1 (II.1) | 102497 | 113 589 | 98.3 | 97.1 |
| Proband 2 (II.4) | 102494 | 113 122 | 98.2 | 97.1 |
| **Pedigree B** | | | | |
| Father (I.1) | 104470 | 106 697 | 96.4 | 87.7 |
| Mother (I,2) | 104469 | 105 328 | 95.9 | 85.3 |
| Proband (II.2) | 103686 | 104 849 | 96.8 | 90.7 |

**Table S2. Number of variants identified by WES in all family members.**

| Oligos | Sequence |
|---|---|
| *GALE* Lys78Valfs*32 F | GATGGCAGAAGCAAAACCCT |
| *GALE* Lys78Valfs*32 R | AGTGGTGCCATCTCAGCTCA |
| *GALE* Thr150Met F | TCACTGATGCCATCTCTCCA |
| *GALE* Thr150Met R | TTACAGGTATGAGCCACTGC |
| *GALE* Val128Met F | CACAGAGCCCAAGCTGTATC |
| *GALE* Val128Met R | TGCCTGAGCCTTAGCTTCCT |
| *GALE* Leu223Pro F | TTGGAACGCAGTGCTGCTGC |
| *GALE* Leu223Pro R | GGCAGCCACACTGTTCTTTC |

**Table S3. Oligonucleotides for Sanger Sequencing validation.** F: forward; R: reverse

| Oligos | Sequence |
|---|---|
| *GALE* sall F | aaaGTCGACaccATGGCAGAGAAGGTGCTGG |
| *GALE* sall R | aaaGTCGACAGGCTTGCGTGCCAAAGC |
| *GALE*-150Met F | CCACCCCA**t**GGGTGGTTGTA |
| *GALE*-150Met R | GCCTCATCAAGGGGCAGGTA |
| *GALE*-128Met F | GAAGAACCTG**a**TGTTCAGCAGC |
| *GALE*-128Met R | ACCCCGTGGGCCTTCATGAT |
| *GALE*-223Pro F | GGGAGGCCC**c**GAATGTCTTTG |
| *GALE*-223Pro R | GTCGCCCGATCGCCACCTG |
| *GALE* qPCR F | AGGCAGACAAGACTTGGAACG |
| *GALE* qPCR R | GCCATCCTCTGTGTCATAGTC |
| *GAPDH* qPCR F | TGCACCACCAACTGCTTAGC |
| *GAPDH* qPCR R | CACCACCTTCTTGATGTCATCA |

**Table S4. PCR and qPCR oligonucleotides.** Small letters indicate the sequence corresponding to SalI nuclease; bold face indicates the point mutation of interest. F: forward; R: reverse

## Supplemental Figures

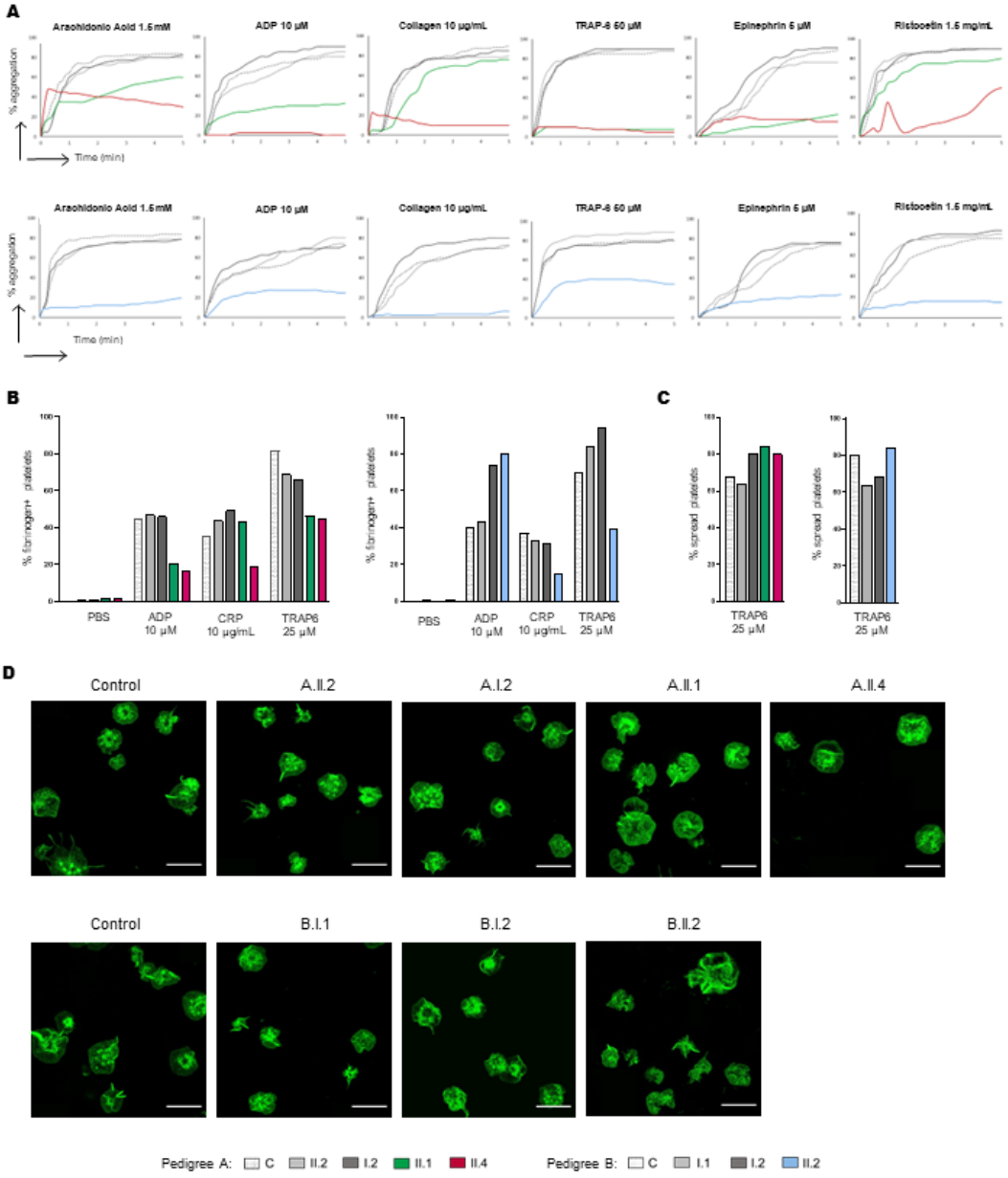


**Figure S1. Normal fibrinogen-binding and platelet spreading was observed in both pedigrees. A)** Platelet aggregation in response to several agonists in Pedigree A: heterozygous carriers of GALE variants (II.2, I.2) and probands (II.1, II.4) and in Pedigree B: heterozygous carriers of GALE variants (I.1, I.2) and proband (II.2). In both A) and B) panels, healthy controls were included. **B)** Platelets from patients, healthy relatives and controls were stimulated with agonists in the presence of fibrinogen*AF488 and evaluated by FC. The percentage of positive platelets was shown. **C-D)** Platelet spreading on fibrinogen was analyzed in washed platelets stained with Phalloidin-OregonGreen514 (green) after 20 minutes of TRAP6 25µM stimulation. **C)** Quantification of the percentage of totally spread platelets (n=50, different fields). **D)** Representative image from members from Pedigree A and from Pedigree B. Scale bar: 10µm

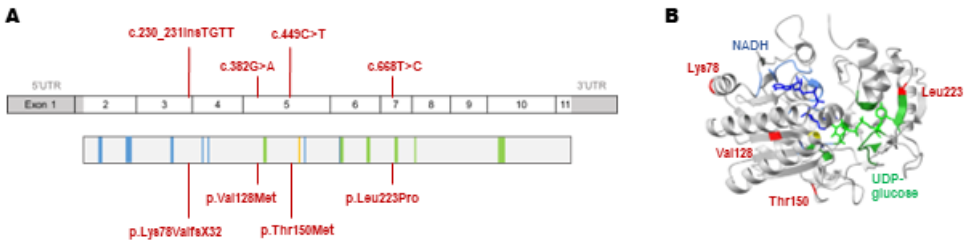


**Figure S2. Schematic representation and structural 3D representation of GALE protein**. **A)** Schematic representations of *GALE* mRNA and UDP-galactose 4-epimerase (GALE protein), indicating the position of the variants found in our patients. GALE encodes a 348 amino acids protein containing multiples sites for NADH binding (blue), substrate UDP-glucose binding (green) and a proton acceptor site (yellow). **B)** Structural analysis of the reported missense variants by using a GALE 3D model (1ek6). The protein is coloured grey, with NADH-binding sites in light blue, UDP-glucose-binding sites in green, and the mutant residues coloured in red. NADH molecule and UDP-glucose are represented in dark blue and light green, respectively.

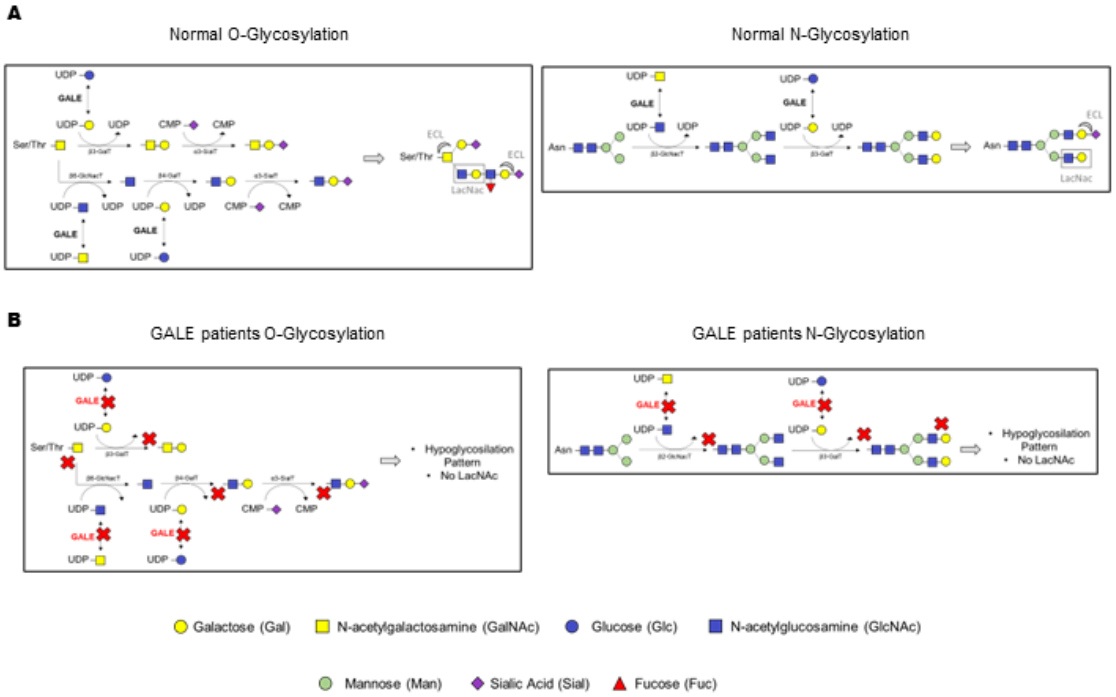


**Figure S3. O-linked and N-linked glycosylation in Wild-Type and mutant *GALE*.** The normal O-linked and N-linked glycosylation of *GALE* is shown in panel A. The proposed model of changes in glycosylation in *GALE* as a result of the genetic variant in our patients is drawn in panel B.

GALE protein allows interconversion of UDP-glucose and UDP-galactose, and that of UDP-N-acetyl-galactosamine and UDP-N-acetyl-glucosamine. These four molecules are essential in the glycosylation process, by serving as substrates for other enzymes incorporating the carbohydrates of interest and releasing UDP. Branches of carbohydrates are produced during glycosylation. LacNac, which is formed by several combinations of N-acetyl-glucosamine and galactose (both molecules incorporated into the branch by GALE protein) is essential in both N-glycosylation and O-glycosylation processes. A final sialic acid cleavage prevents platelet for clearance. In this representation, patients carrying *GALE* variants are unable to incorporate LacNAc molecules, accounting for the hypoglycosylation pattern found in platelet proteins.

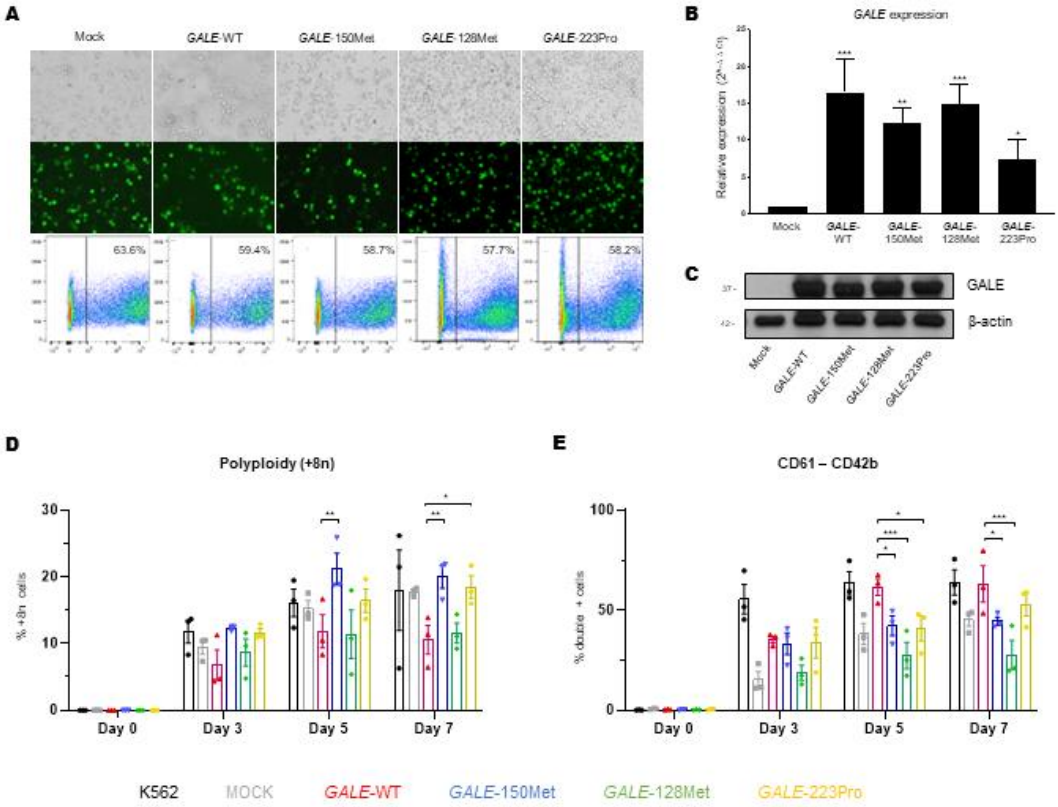


**Figure S4. Overexpression of *GALE* variants in the human K562 cell line. A)** Fluorescence microscopy and flow cytometry was used in hK562 cells electroporated with plasmids containing the different versions of *GALE* (Mock, WT, p.Thr150Met, p.Val128Met and p.Leu223Pro, obtained by directed mutagenesis in a pShuttle CMV-F2A-T2A-Venus vector) to screen the expression of the variants. The percentage of Venus positive cells in each condition is also indicated. **B)** Quantitative PCR of *GALE* expression in K562 cells electroporated with *GALE* variants vs. Mock (Bars represent mean ± SEM; *p<0.05, **p<0.01, ***p<0.001, n=3). Data were normalized with *GAPDH*. **C)** Immunoblotting of GALE levels in Mock and *GALE* variants (WT, Thr150Met, Val128Met, and Leu223Pro). β-actin was used as an internal control. **D-E)** The parental cell line (K562), negative control (mock), and cells overexpressing *GALE* WT and *GALE* variants Thr150Met, Val128Met and Leu223Pro, were evaluated at 3-, 5- and 7-days post PMA 20nM treatment by FC: **D)** Percentage of polyploid cells (8n, +8n) after propidium iodide labeling. **E)** Cells were subjected to FC with specific anti-CD61 and -CD42b antibodies. The percentage of double-positive cells is represented. Three independent replicates were carried out (points represented mean±SEM; * p<0.05, ** p<0.01, ***p<0.001).

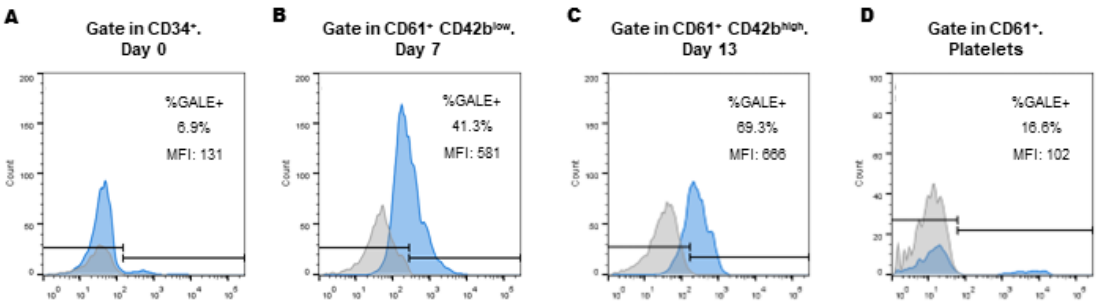


**Figure S5.** ***GALE*** **is mainly expressed in late-megakaryopoiesis.** Human CD34+ were cultured for 13 days in the presence of TPO and IL-11. Aliquots of permeabilized cells were used to evaluate *GALE* on day 0, 7, 13, and 15 of culture. **A)** Analysis of *GALE* in $CD34^+$ cells at day 0 of culture. **B)** Analysis of *GALE* in $CD61^+CD42b^{low}$ cells at day 7 of culture. **C)** Analysis of *GALE* in $CD61^+CD42b^{high}$ cells at day 13 of culture. **D)** Analysis of *GALE* in platelets $CD61^+$ at day 15 of culture. The % of positive cells and the Mean Fluorescence Intensity (MFI) is represented.

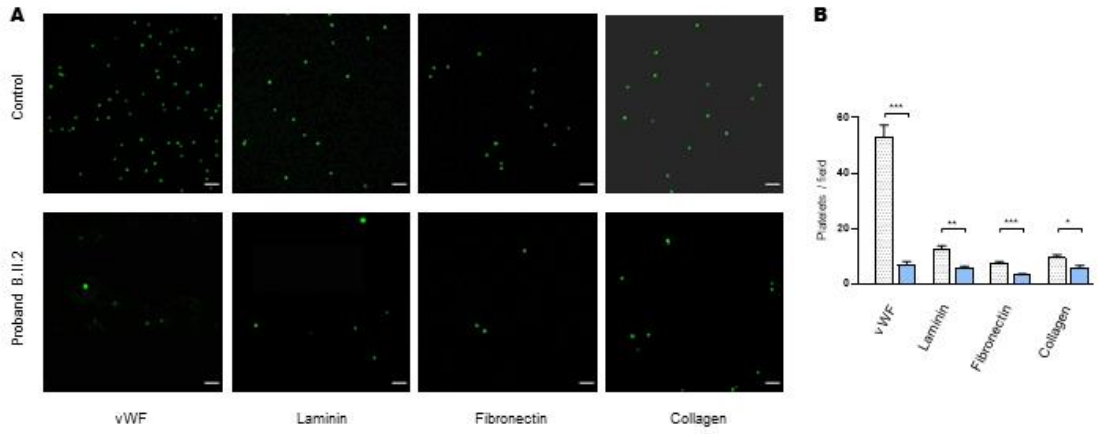


**Figure S6. Platelets from proband carrying *GALE* p.Val128Met and p.Leu223Pro variants displayed impaired adhesion to several extracellular matrices (ECM).** Control and patient platelets were equally adjusted and seeded in coverslips coated with extracellular matrices that bind to GPIbα and β1 integrin; von Willebrand Factor, and laminin, fibronectin, and collagen, respectively. **A)** Representative image of control and proband platelet adhesion. Platelets were incubated for 2h in each ECM and stained with Phalloidin-OregonGreen514 (green fluorescence). **B)** Quantification of the number of platelets adhering in each field (n=10 different fields). Scale bar: 20μm. Mean±SEM is represented; * $p<0.05$, ** $p<0.01$, *** $p<0.001$.

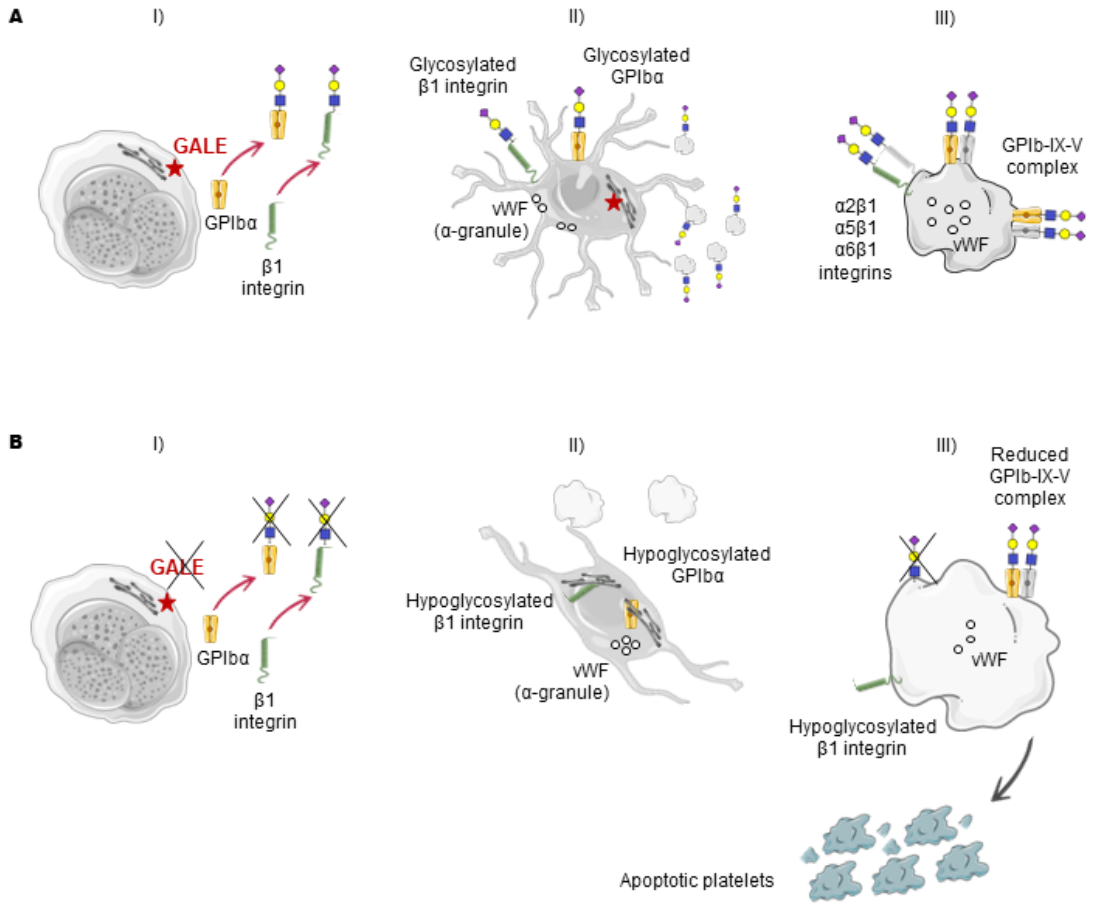


**Figure S7. Schematic representation of the mechanism leading to macrothrombocytopenia in patients with biallelic variants in GALE. In panel A**, I) Physiological glycosylation of GPIbα and β1 integrin by GALE in the endoplasmic reticulum (ER). II) Glycosylated GPIbα and β1 integrin in the megakaryocyte membrane led to physiological proplatelet formation. III) Glycosylated platelets with GPIb-IX-V complex and mature β1 integrin on the surface and normal storage of vWF. **In panel B**, the proposed model of macrothombocytopenia in our patients with GALE variants. I) Reduced levels and function of GALE impairs the glycosylation of GPIbα and β1 integrin. II) Immature and hypoglycosylated GPIbα and β1 integrin are retained in the ER. Their reduced externalization and exposure on the Mk membrane, together with vWF delocalization, impairs thrombopoiesis. III) Giant and/or grey platelets are produced, without mature β1 integrin and reduced levels of GPIb-IX-V complex. These hypoglycosylated platelets are prone to apoptosis.

# GENERAL DISCUSSION

Congenital Platelet Disorders [CPDs] are a wide group of rare disorders commonly associated with thrombocytopenia and/or bleeding symptoms, but also predisposing to severe complications, such as hematological malignancies or multisystemic manifestations. Patients with CPDs represent a diagnostic challenge due to the high heterogeneity of the disorders, with multiple genes involved in the development of the disease that can give rise to diverse, but overlapping, clinical and laboratory phenotypes.[79,85,89] However, we are currently undergoing a revolution in the genetic and molecular diagnosis due to the development of the high-throughput sequencing [HTS] methods. This technology provides in a rapid and economical manner a large amount of genetic information, facilitating the identification of genetic variants underlying diseases with molecular basis, and it is potentially replacing conventional sequencing tools.[158,194,204,207]

In this context, our group in Salamanca has been pioneer in the use of HTS, to study patients with CPDs involved in the project "Functional and Molecular characterization of patients with Inherited Platelet Disorders", on behalf of Grupo Español de Alteraciones Plaquetarias Congénitas (GEAPC) (https://www.seth.es/index.php/investigacion.html) by using a designed and validated panel of 72 genes,[158] and later, an update version of 85 genes.[283] This approach has provided a direct benefit in the diagnostic efficacy, which has increased from the 38% obtained with conventional diagnostic techniques to the 70% derived from the use of HTS tools targeting known genes.[158,194,204,207] Because of that, this approach has been incorporated into the routine clinical practice.[97,158]

However, the broad use of HTS in research and clinical laboratories has led to an increasing detection of germline variants of unknown significance in genes involved in hematopoiesis and lineage differentiation that contribute to myeloid neoplasms.[163,164] Although recommendations from the ACMG / AMP have been established to classify the variants,[162] there is an interlaboratory variability or alternative interpretations for many genetic variants, especially for novel variants. Thus, they are classified as uncertain significance or discordantly classified among different laboratories.[208]

The curation of gene variants associated with diseases is relevant and is currently underway by the Clinical Genome Resource (ClinGen) with the Variant Curation Expert Panels. The approach supports the classification of a genomic variant on a spectrum from pathogenic to benign with respect to a particular disease and inheritance pattern.[81,83] To date, specifically adapted ACMG / AMP rules have been reported only for *RUNX1,*[164,165] and *ITGA2B* / *ITGB3* in autosomal recessive Glanzmann Thrombasthenia.[166] Regarding this approach, the pathogenicity of several *RUNX1* variants described in patients was reclassified: among the 80 variants of uncertain significance [VUS] previously described, 30 are now reclassified as benign or pathogenic variants.[164,165] This improvement in the classification of the variants is essential since it can provide targets for early detection of the myeloid neoplasm or for future therapies.[164,284]

However, controversies surrounding germline *RUNX1* missense variants, especially outside of the runt homology domain (RHD), still persist.[285] Of these variants, the previously described missense variant c.167T>C [p. Leu56Ser], located in the N-terminal region of RUNX1,[286] has controversies whether it is a leukemia-predisposing allele or a benign polymorphism.[287] This variant has been found in some patients with clinical and laboratory suspicion of FPD/AML, as reported by several groups.[286,288,289] But it is also a relatively frequent variant in the general population (MAF: 0.0127 in GnomAD), which focus its classification as benign.[164,165,290] Discrepant pathogenicity classification can be also found in several databases (COSMIC: Pathogenic; dbSNP: Likely Benign; ClinVar: Benign), and according to its *in-silico* prediction (MutationTaster: Causing disease; PROVEAN: Neutral; SIFT: Tolerated).

Recently, Decker et al. published the functional characterization of nine previously reported VUS *RUNX1* variants, using 6 known pathogenic variants and wild-type *RUNX1* as controls. Thus, p.Leu56Ser was described to have normal dimerization with CBFβ and RUNX1 phosphorylation, but reduced transcriptional activation of genes such as r*ETV1* and r*CSF1R.*[291] Furthermore, Koh et. al described the inability of RUNX1 p.Leu56Ser to bind MLL, suggesting a novel model of leukemogenesis related with the variant.[288]

To settle definitively the controversy about the pathogenicity of the RUNX1 p.Leu56Ser variant, but also for elucidating the mechanisms of molecular pathogenesis, we develop by the CRISPR/Cas9 genome editing tool a *knock-in* murine model carrying p.Leu43Ser, mimicking the human alteration [253] **(Results Section – Chapter 1: Figure 1).**

In general, platelet counts in FPD/AML patients are most often mild to moderately low (70-145 × $10^9$/L), but they can be lower or within the low-normal range in patients.[292,293] In this context, we observed that RUNX1$^{L43S/L43S}$ mice had a slightly, but significantly, lower platelet counts than RUNX1$^{WT/L43S}$ and RUNX1$^{WT/WT}$ mice. No thrombocytopenia was found in RUNX1$^{WT/L43S}$. Nevertheless, both RUNX1$^{L43S/L43S}$ and RUNX1$^{WT/L43S}$ mice had longer bleeding times than RUNX1$^{WT/WT}$, pointing out that RUNX1 p.Leu43Ser variant has an effect on hemostasis **(Results Section – Chapter 1: Figure 2)**. Platelet functional studies showed a reduction in fibrinogen binding and platelet aggregation in RUNX1$^{L43S/L43S}$ and RUNX1$^{WT/L43S}$ compared with RUNX1$^{WT/WT}$ after thrombin, PMA, and ADP treatment, without differences after CRP stimulation. A similar platelet hyporesponsiveness of RUNX1$^{L43S/L43S}$ and RUNX1$^{WT/L43S}$ mice was observed when evaluating α-granules, without changes in δ-granules secretion **(Results Section – Chapter 1: Figures 3 and 4)**. These findings are rather different from the observed in many FPD/AML patients, where both granules secretion dysfunction has been previously reported, as well as abnormal integrin αIIbβ3 activation.[294–296] However, it highlights the heterogeneity of platelet dysfunction in *RUNX1* variant carriers.

Moreover, we observed a correlation between genotype and phenotype, since RUNX1$^{L43S/L43S}$ mice displayed a remarkable decreased function than RUNX1$^{WT/L43S}$ genotype, in accordance with previously results demonstrating the importance of the allele burden and *RUNX1* levels in the disease presentation.[297]

The phenotypic heterogeneity in families with *RUNX1* germline variants implies that additional genomic or epigenetic alterations may be important modifiers to both penetrance and phenotype regarding the development of a hematological malignancy.[298] RUNX1 could act as a late trigger event for inherited preleukemic states, forcing the acquisition of different cooperating

molecular alterations.[299,300] Carriers can exhibit evidences of premalignant bone marrow abnormalities, most commonly dysmegakaryopoiesis;[40,301] or, in some cases, they have aberrant expression of cell surface markers, such as CD123, which is a well-characterized marker of leukemic stem cells.[302]

To uncover the role of the variant p.Leu56Ser in the leukemic progression and the second hit promoting the disorder, we followed the mature and immature hematopoietic populations in our mice model thought life. We detected the presence of an aberrant myeloid $Mac1^{+}$ $Sca1^{+}$ $ckit^{-}$ population, previously described as leukemic cells,[303] in peripheral blood from two homozygous mice: 15.3% in Hom#1 at 15 months, and 7.3% in Hom#2 at 20 months, while only one heterozygous mouse (Het#1) displayed 2.4% aberrant cells at 21 months of age. In fact, $Mac1^{+}$ $Sca1^{+}$ $ckit^{-}$ cells were present in both bone marrow and spleen in all three affected mice, while no $Mac1^{+}$ $Sca1^{+}$ $ckit^{-}$ cells were detected in any $RUNX1^{WT/WT}$ mice **(Results Section – Chapter 2: Figures 1 and 2)**.

The most frequent second event is the somatic *RUNX1* alteration rather to other different chromatin remodelers and transcriptional regulators, such as *GATA2, BCOR, PHF6,* and *WT1*.[117,293,304] Somatic variants in *RUNX1* has not been observed in carriers prior to the development of malignancy, whereas premalignant somatic variants have been reported in *TET2, DNMT3A, KRAS,* and *SRSF2*.[117,293] Alterations in these genes indicate the potential of the evolution of somatic gene–mutated preleukemic to leukemic states. Mechanistically, acquisition of secondary pathogenic somatic alterations may be the result of increased mutagenic processes in germline *RUNX1* carriers characterized as early-onset clonal hematopoiesis, and potentially a result of dysregulated DNA repair pathways associated with *RUNX1* alterations.[298,299,305]

Our DNA-seq analyses in the three affected mice showed no additional somatic variants in *Runx1*. However, RNA-seq studies showed 698 genes significantly downregulated in the 3 $Mac1^{+}$ $Sca1^{+}$ $ckit^{-}$ mice vs. 6 healthy $RUNX1^{WT/WT}$, $RUNX1^{WT/L43S}$ and $RUNX1^{L43S/L43S}$ mice, highlighting the overexpression of *Rapgef1* (also known as C3G),which is a guanine nucleotide exchange factor that activates Rap1 GTPases with a relevant function in platelet hemostasis,[306–308] and whose alteration has been previously linked to chronic

myeloid leukemia and solid tumors.[308–310] **(Results Section – Chapter 2: Figure 3)**. In fact, we found in our affected mice that the more aggressive phenotype of the disease is associated with an increased expression of *Rapgef1,* since Hom#1 and Hom#2 mice presented a higher overexpression of the gene than Het#1 mice, which presented similar levels than unaffected mice.

We previously described in the murine model the dysfunction of the PKC-α/β signaling pathway, with unaffected transcriptional levels, as the mechanism involved in the platelet disorder **(Results Section – Chapter 1: Figure 5)**. Interestingly, our RNA-seq revealed the overexpression of *Rapgef1* in leukemic mice, which function has been described to be regulated by PKC.[306,307] **(Results Section – Chapter 2: Figure 4)**.

These results suggest that the murine variant p.Leu43Ser associates with increased bleeding due to moderate platelet dysfunction caused by reduced integrin αIIbβ3 activation, α-granule secretion, impaired spreading with normal adhesion, and decreased clot retraction, being more significant in the homozygous state. **(Results Section – Chapter 1)**. Indeed, the variant in heterozygosis is associated with a weak predisposition and late appearance of aberrant cells (4%, at 21 months), correlating with the benign phenotype associated with RUNX1 p.Leu56Ser variant in the clinical setting,[287] but a more aggressive phenotype in homozygous mice (8% of affected mice, 15-20 months), associated with higher overexpression of *Rapgef1,* and remarkably bone marrow and spleen affectation **(Results Section – Chapter 2)**. These data suggest a novel mechanism of platelet dysfunction and hematological neoplasm progression. However, these results should be expanded and confirmed by studying patients and more germline variants in the *RUNX1* gene, since murine models do not exactly reproduce the human disorder.[252]

Despite the significant improvement in the diagnosis of Congenital Platelet Disorders based on gene panel sequencing and the functional characterization of variants of unknown significance to establish the genotype-phenotype causal linkage, as we prove in the **Results Section – Chapter 1 and Chapter 2**, many patients still do not achieve a definitive diagnosis (30% in our specific cohort).[158,283] The main problem with target-gene panel sequencing is the limited

number of genes and regions of interest that can be analyzed, as it requires a prior design that comprises prespecified candidates.[97,201,208] In addition, several processes of the megakaryopoiesis and platelet function are not well characterized, will could explain that a substantial number of disorders are caused by genes not described or well-characterized so far.[97,161] Since 2010, both WES and WGS approaches have allowed the identification of up to 15 new genes involved in ITs.[9,25] Among these genes, we found *GNE,* which was associated with IT for the first time in 2014,[52] and it was established as a new platelet disorder in 2018, with the publication and characterization of two unrelated pedigrees.[137,138] To date, it is the only Tier1 gene associated with alterations in glycosylation.[81,82] Similarly, *DIAPH1* was described for the first time in 2016 by WES in two unrelated pedigrees with IT.[197] Nowadays, more than five pedigrees have been described, and it is included also as a Tier1 gene for platelet disorders.[311–313] In contrast, other genes such as *PTPRJ* or *PRKACG* require further functional studies and the demonstration of the link between genotype-phenotype in more pedigrees to consolidate the platelet disorder, therefore, both are classified as Tier2 genes.[254,314]

*TPM4*, which codifies for the tropomyosin 4, was described for the first time in 2017 by WES in five members of two unrelated families carrying the p.Arg69* variant. Those patients displayed mild bleeding tendency and an almost unaffected platelet phenotype.[108] Until 2021, *TPM4* was considered a rare gene involved in ITs and it was classified as a Tier2 for platelet disorders by the ISTH.[81,82] Acknowledging the identification and the clinical, laboratory, and molecular characterization of a Spanish pedigree with *TPM4*-related thrombocytopenia [RT] (**Results Section – Chapter 3)**, prompted the ISTH SSC-GinTH include *TPM4* in the Tier1 genes.[315] In fact, the incorporation of these gene into the routine clinical practice allowed the identification of other variants in different pedigrees worldwide.[316]

We identified by WES a novel nonsense variant (c.322C>T; p.Gln108*) in the coiled coil domain of TPM4 in all affected family members, which phenotype was characterized by mild macrothrombocytopenia and bleeding tendency (**Results Section – Chapter 3: Figure 1).**[109] Carriers of the variant displayed normal platelet aggregation with several agonist, including low doses of TRAP-6 and

collagen, but a mild impairment and delay in the platelet aggregation response to low dose of ADP and epinephrine, with unaffected levels of major glycoproteins, and normal fibrinogen-binding and α and δ-granule secretion **(Results Section – Chapter 3: Figure 2)**, similar to the platelet phenotype previously observed in carriers of the *TPM4* p.Arg69* variant.[108] In contrast, carriers of the missense variants p.Arg182Cys and p.Ala183Val have been recently described to have relevant bleeding, significantly impaired platelet secretion and aggregation, and normal or slightly reduced platelet count and TPM4 levels.[316] The reasons for such differences in bleeding and platelet phenotype in these *TPM4*-RT patients are still unknown, and require further investigations. We may speculate that heterozygous *TPM4* nonsense variants, such as p.Arg69* and p.Gln108*, mainly cause haploinsufficiency, which is suggested by a reduction in tropomyosin-4 levels, while missense variants could present a genetic negative dominant effect exacerbating *TPM4* dysfunction and leading to major platelet disorder. Indeed, proplatelet formation is TPM4 dose-dependent, which could justify that both nonsense variants (p.Arg69* and p.Gln108*) are associated with thrombocytopenia, while the missense variants are not.[108,109,316] These results suggest that it is important not only the identification of *TPM4* as the molecular alteration causing the disorder, but it is also important to detect the type of variant since it may have a link with the phenotype.

Moreover, our study expanded the functional role of TPM4 in platelet cytoskeleton remodeling. We first observed a significant reduction in the formation of filipodia and lamellipodia, as well as severe reduction of full-spreading structures in the propositus vs control platelets, leading to an impaired spreading function, In addition, we show for the first time that TPM4 in control platelets is homogeneously distributed throughout the cytoplasm along with actin filaments, while Gln108* mutant TPM4 is accumulated mainly in the center of the patient platelets, and the protein is reduced in filopodia/lamellipodia in spread platelets **(Results Section – Chapter 3: Figure 3)**. Thus, this genetic alteration leads to a mild reduction in the localization of TPM4 with other proteins of the cytoskeleton. The moderate reduction of TPM4 in the spreading structures could account for the defect in cytoskeleton remodeling, giving novel insights in the physiological mechanism underlying the disorder.

Our findings support the key role of TPM4 in platelets and expand the phenotype and genotype spectrum of *TPM4*-RT, reinforcing the importance of the functional approaches to validate the variants found by sequencing tools. In a similar way, we described the clinical and laboratory features of three new adult patients with syndromic macrothrombocytopenia due to compound heterozygosity of four variants affecting *GALE,* found by WES, and demonstrating the correlation between *GALE* molecular alterations and impaired platelet and megakaryocyte glycosylation and thrombopoiesis **(Results Section – Chapter 4).**

The first evidence linking *GALE* defects and hematological alterations was in 2019, when Seo et al. reported six patients from one pedigree affected by severe thrombocytopenia, febrile neutropenia, and mild anemia, who were homozygous for the GALE p.Arg51Trp variant.[142] In 2020, Febres-Aldana et al. described a child with bone marrow dysfunction and complex congenital heart disease associated with compound heterozygosity in GALE (p.Arg51Trp and p.Gly237Asp).[143] Lastly, in 2021, Markovitz et al. have reported a patient with pancytopenia and immune dysregulation due to a previously reported homozygous GALE variant (p.Thr150Met).[144] Although three pedigrees carrying *GALE* variants associated with hematological abnormalities and different phenotypes have been reported, there is no evidence about the mechanism driving the disease in patients carrying *GALE* variants.

We have studied *GALE* variants from a functional perspective, to characterize the molecular mechanisms underlying the disease. First, we proved that the glycosylation pattern is impaired in patients' platelets carrying the identified *GALE* variants, uncovering the absence of mature-glycosylated β1 integrin, and a severe reduction of the GPIb-IX-V complex. Normal levels of β3 integrin were found, suggesting a substantial preservation of this protein in the platelet surface. Also, patients' platelets were hypoglycosylated and more apoptotic **(Results Section – Chapter 4: Figures 2 and 3)**. Then, we developed an *in vitro* model based on the overexpression of *GALE* variants in human K652 cells, which were differentiated to a megakaryocyte-like phenotype. Furthermore, we conducted additional experiments by using *in vitro* differentiated Mks from the patient's peripheral blood. This functional characterization allowed us to demonstrate, for

the first time, that the missense *GALE* variants do not alter Mk maturation, but disrupt thrombopoiesis, affecting the proplatelet formation process **(Results Section – Chapter 4: Figure 5)**. We noticed in the patient Mks normal levels of the total GPIbα and β1 integrin, but a significant decrease in their surface exposure, suggesting an impaired externalization of the integrins to the plasma membrane compared to healthy controls. Indeed, total and surface levels of β3 integrin were comparable to healthy controls. Finally, immunoblot analyses of total Mk lysates revealed bands of lower molecular weight for β1 integrin and the GPIbα, suggesting their hypoglycosylation **(Results Section – Chapter 4: Figure 7)**. Therefore, *GALE* dysfunction is associated with impaired glycosylation and externalization of the GPIbα and β1 integrin, being retained in the endoplasmic reticulum of the Mks, where GALE has its major role during late-megakaryopoiesis **(Results Section – Chapter 4: Figure 4)**. Abrogation of both proteins, together with the delocalization of vWF, in the membrane of Mks, justify the impaired proplatelet formation, and the production of platelets with impaired morphology, function, and viability.

Our study not only expand the knowledge of the *GALE*-related disorder unraveling the essential role of *GALE* in glycosylation, platelet formation, function, and clearance, but also provides novel clues to understand the biological mechanisms underlying the biology and pathophysiology of the β1 integrin and the GPIb-IX-V complex, which are key proteins in platelet production and function. Besides, we consider that our investigations demonstrate the causality between genotype-phenotype, and therefore, *GALE* should be included in sequencing panels for the routine screening of Congenital Platelet Disorders.

In summary, the present research highlights the usefulness of high throughput sequencing techniques to identify the molecular basis of an ultra-rare and heterogeneous group of disorders, in combination with functional approaches to understand the biological mechanisms underlying the physiopathology. The combination of both approaches is proposed as an optimal strategy for the correct diagnosis of Congenital Platelet Disorders, not only for targeted gene panel sequencing to validate novel or unknown significant variants, or highly controversial alterations, but also for the study of novel genes with unknown function and significance detected by WES / WGS. Indeed, the improvement in

the interpretation of new genes and variants using automated techniques in the last few years, based on comprehensive databases integrating phenotype-genotype of wide populations, in combination with consortiums of experts in the field, will facilitate the correct diagnosis of patients, providing not only an appropriate healthcare but also a personalized therapy. Finally, the application of the CRISPR/Cas9 technology not only allows us to generate experimental models reproducing the selected genetic variants found in patients, but also establishes the technical basis for their possible use as a therapeutic tool in the future.[317]

# CONCLUDING REMARKS

1. The integrative implementation of high-throughput sequencing techniques and functional approaches to characterize variants in ultra-rare or clinically relevant genes are of great usefulness and importance in Congenital Platelet Disorders.

2. The *knock-in* murine model carrying RUNX1 p.Leu43Ser variant (mimicking the human RUNX1 p.Leu56Ser) allowed to assess its deleterious effect on hemostasis, based on the hypoactivation of the integrin αIIbβ3, and a functional alteration in the PKC-mediated signaling pathway. This is reflected in an aggregation, α-granule secretion, and platelet-spreading defect, justifying the prolonged bleeding times. The phenotype was remarkable in homozygosis, reinforcing the importance of the *RUNX1* levels in the disease phenotype.

3. RUNX1 p.Leu43Ser in homozygosis is related with the presence of an aberrant $Mac1^{+}$ $Sca1^{+}$ $ckit^{-}$ population, morphological alterations of bone marrow and spleen, and a noteworthy overexpression of *Rapgef1*, which is proposed as a potential novel second event in the disease progression that requires further studies.

4. The novel nonsense variant in TPM4 p.Gln108* caused mild bleeding, mild macrothrombocytopenia, and slightly reduction of the platelet aggregation response to weak agonists, expanding and consolidating the clinical phenotype of *TPM4*-related thrombocytopenia. The defect on platelet cytoskeleton remodeling led to the delocalization of the tropomyosin-4 in the spreading structures, which could justify the severely impaired spreading function.

5. Four variants in *GALE* were found in in three patients from two unrelated pedigrees with lifelong severe macrothrombocytopenia, moderate bleeding tendency, mental retardation, mitral valve prolapse, and increased bilirubin levels. These *GALE* variants severely reduced the levels and the enzymatic activity of the UDP-galactose-4-epimerase in platelets and megakaryocytes.

6. *GALE* variants triggered a reduction of GPIbα and β1 integrin glycosylation and externalization to the megakaryocyte surface, being retained in the endoplasmic reticulum, where the UDP-galactose-4-epimerase has its major role during late-megakaryopoiesis. This is reflected in an impaired platelet formation, and the production of platelets with impaired morphology, function, and viability. These new data highlight the key role of *GALE* in platelet glycosylation, production, function, and clearance.

# Resumen en Castellano

**TESIS DOCTORAL**

## Caracterización de nuevos genes y variantes implicados en Trastornos Plaquetarios Congénitos: de los datos genómicos a los estudios funcionales


Supervisores

Dr. José María Bastida Bermejo

Dr. José Ramón González Porras

Dr. Ignacio García-Tuñón Llanio

Tutor

Jesús María Hernández Rivas

**Ana Marín Quílez**


**2022**

# INTRODUCCIÓN

## 1. FORMACIÓN Y FUNCIÓN DE LAS PLAQUETAS

### 1.1 Megacariopoyesis y trombopoyesis

La megacariopoyesis es un proceso en el que las células madre humanas [HSCs] se diferencian y proliferan, dando lugar a megacariocitos [Mk] maduros.[1] Según el modelo clásico de hematopoyesis, la maduración secuencial de las HSCs a progenitores multipotentes dará lugar a los Mks o megacarioblastos inmaduros, que experimentarán el proceso de endomitosis para aumentar su tamaño y su contenido de ADN, durante el proceso denominado poliploidización, además de aumentar su reserva de gránulos y proteínas del citoesqueleto para desarrollar el sistema de demarcación de membrana.[2,3] A continuación, los Mks maduros comienzan a perder su citoplasma, un proceso complejo que requiere la formación de estructuras alargadas denominadas proplaquetas, que conducirán a la formación de plaquetas y a su liberación al torrente sanguíneo. Este proceso terminal se conoce como trombopoyesis (Figura 1A).[4]

Los procesos de diferenciación de las HSCs, la maduración de los Mks y la formación de las proplaquetas están regulados a múltiples niveles por muchas citoquinas y factores ambientales diferentes.[5] La trombopoyetina [TPO] es el principal regulador de la megacariopoyesis y la trombopoyesis y, en combinación con otras citocinas, como la IL-3 o la IL-11, regula todas las etapas del desarrollo de los Mk (Figura 1A).[6,7]

Las glicoproteínas de superficie [GP] aparecen en diferentes etapas de la megacariopoyesis, y se utilizan frecuentemente como marcadores específicos de linaje, como la GPIIb/IIIa (marcadores CD41-CD61) o GPIb-IX-V (CD42a-d).[8] El CD34 se expresa sólo en las HSC y en los progenitores multipotenciales, siendo prácticamente negativo en las Mks inmaduras. Los marcadores CD41-CD61 se expresan desde la megacariopoyesis temprana, así como el CD29 (el marcador de integrina β1) mientras que el CD42a-d o el GPVI aparecen durante la megacariopoyesis tardía (Figura 1A).[9,10]

Sin embargo, estudios recientes han redefinido esta jerarquía, tradicionalmente establecida por los marcadores de superficie, destacando rutas alternativas por las que las HSCs se diferencian a Mks (Figura 1B).[1,5] En primer lugar, el progenitor multipotencial se ha caracterizado en detalle para incluir

varios subpoblaciones de progenitores de linaje. También se ha definido que las HSCs tardías son capaces de diferenciarse unilateralmente en Mks. Por último, la existencia de un progenitor común capaz de producir eritroblastos y megacarioblastos es controvertida, y las nuevas tecnologías han demostrado que este progenitor multipotencial es transitorio y difícil de detectar en la hematopoyesis humana.[11–14]

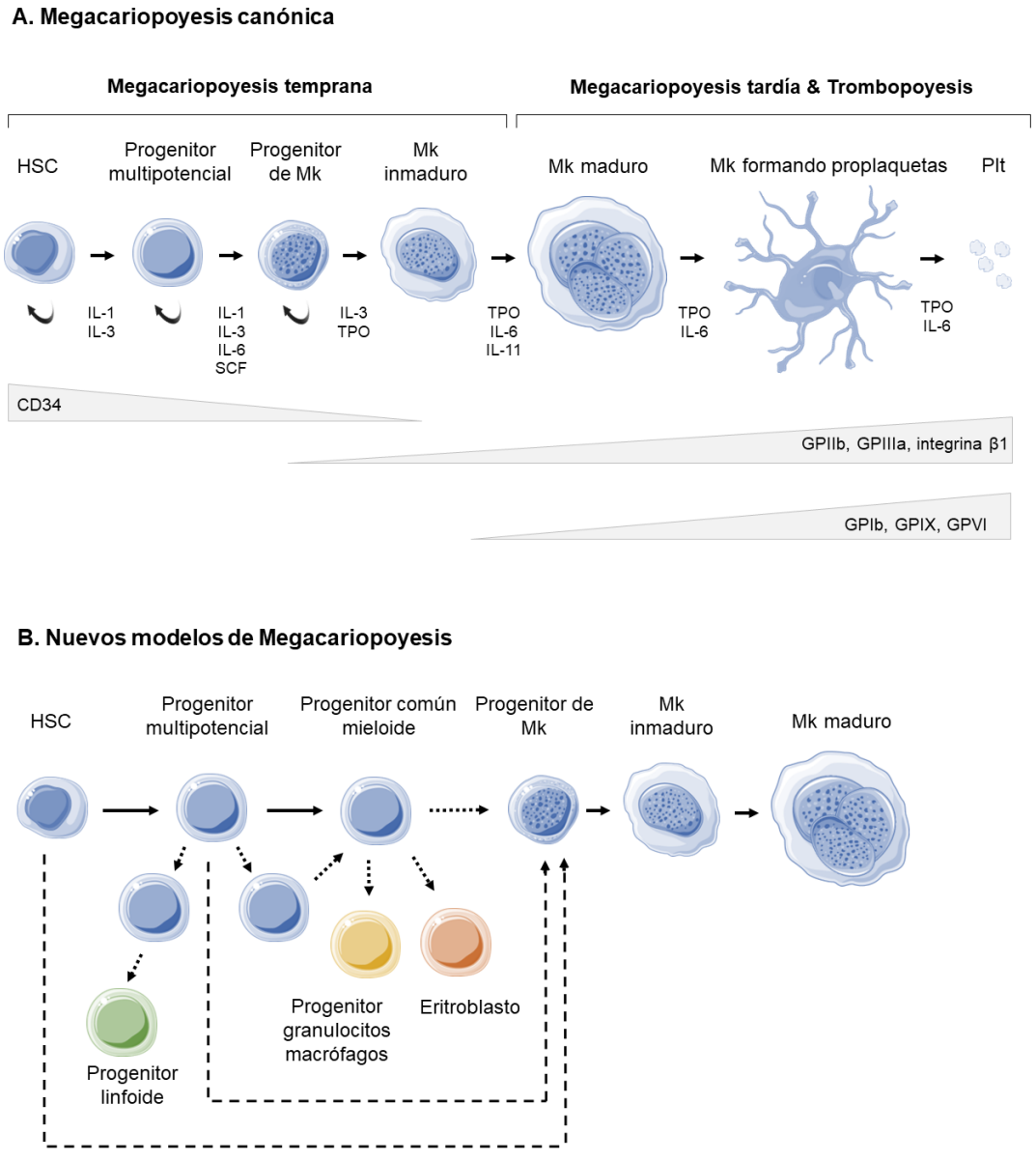


**Figura 1. Diferenciación y maduración de los megacariocitos. A.** Modelo canónico de la megacariopoyesis. Expresión de los marcadores de superficie más relevantes y factores de crecimiento y citoquinas implicados en cada etapa. **B.** Nuevos modelos propuestos para la megacariopoyesis, que señalan rutas alternativas por las que las HSCs se diferencian en Mks.[1,15] Creado con Servier Medical Art (https://smart.servier.com/).

El correcto desarrollo de la hematopoyesis y de la diferenciación y maduración de los Mks están bajo el control de factores transcripcionales esenciales, que se unen a los promotores actuando como represores o activadores dependiendo de su asociación con otros factores transcripcionales. *GATA1* controla la expresión de GPIIb, mientras que *FLI1* regula a GPIbα y GPIX.[1,16–18] Además, *RUNX1* regula la hematopoyesis humana embrionaria y definitiva a través de la dimerización de CBFβ,[19] y desempeña un papel esencial en la maduración y diferenciación de los linajes mieloide, linfoide y megacariocítico.[20,21] De hecho, la pérdida bialélica de función de RUNX1 provoca la letalidad embrionaria debido al fallo en la hematopoyesis.[22]

Las proteínas del citoesqueleto tienen un papel crucial en la megacariopoyesis tardía y en la formación de las proplaquetas.[23,24] Durante las etapas iniciales de la formación de las proplaquetas, las Mks remodelan su citoplasma en pseudópodos mediante un proceso basado en los microtúbulos, especialmente la tubulina β1 (codificada por el gen *TUBB1*),[25,26] y el citoesqueleto de actomiosina.[27,28] El citoesqueleto de actina es fundamental para la formación de sistema de demarcación de membrana, ya que proporciona fuerzas mecánicas que impulsan las invaginaciones en la membrana plasmática, dando lugar a la formación de las proplaquetas,[29] mientras que el citoesqueleto de tubulina guía la iniciación y elongación de dichas proplaquetas.[30]

El citoesqueleto de actomiosina está formado por la unión de múltiples proteínas que actúan frente a diferentes respuestas celulares.[31] La asociación de la β-actina filamentosa con el sistema de demarcación de membrana es crucial para la formación de las proplaquetas.[24,29] La polimerización de la actina es impulsada por la proteína relacionada con la actina 2/3 (Arp2/3). El complejo Arp2/3 muestra una baja actividad intrínseca de nucleación de actina y necesita ser activado por proteínas como la proteína Wiskott-Aldrich Syndrome (WASP) (Figura 2).[32]

Múltiples proteínas de unión a actina son reguladores críticos de la función de los Mks y, en su mayoría, están implicados en la compleja generación de las proplaquetas.[33] La α-actinina es un miembro de la superfamilia de proteínas de enlace de actina que contribuye a este proceso mediante la unión de los filamentos de actina en haces.[34] La tropomiosina-4, codificada por *TPM4*, es una

proteína de dimerización en espiral que se encuentra en el surco de actina de extremo a extremo, y proporciona estabilidad estructural a los filamentos de actina y regula el acceso de otras proteínas que se unen a ésta.[35] Las tropomiosinas están implicadas en la regulación de la morfología celular, la adhesión, la migración, el tráfico de gránulos, la división celular y la apoptosis.[27] Por otro lado, la filamina-A es una proteína multidominio del citoesqueleto que estabiliza las membranas sometidas a tensión de cizallamiento y promueve la adhesión celular mediante la unión de glicoproteínas de membrana, principalmente el receptor GPIb-V-IX, al citoesqueleto de actina (Figura 2).[36]

La migración de los Mks depende de la interacción de la miosina II no muscular con el citoesqueleto de actina. En los Mk se expresan dos tipos: la cadena pesada de miosina no muscular II-A (NMHC-IIA, *MYH9*) y la cadena pesada de miosina no muscular II-B (NMHC-IIB, *MYH10*).[37] La NMHC-IIA es necesaria para mantener la forma de la célula y organizar el citoplasma celular, uniéndose a la actina filamentosa para ayudar al recambio de actina durante la formación de las proplaquetas (Figura 2).[24,38] Por otro lado, la NMHC-IIB se expresa en megacariocitos inmaduros, donde se acumula en el anillo contráctil durante la endomitosis. La expresión de NMHC-IIB está regulada por RUNX1 a través del silenciamiento del gen *MHY10* durante la poliploidización de los Mks. Este proceso es esencial para pasar de la mitosis a la endomitosis para aumentar el nivel de ploidía durante la diferenciación de los megacariocitos.[39,40] De hecho, RUNX1 también se ha descrito como un regulador directo de *MYL9*, que codifica para la cadena ligera de miosina, y desempeña un papel crucial regulando la actividad de la NMHC-IIA mediante la fosforilación reversible de aminoácidos específicos.[41]

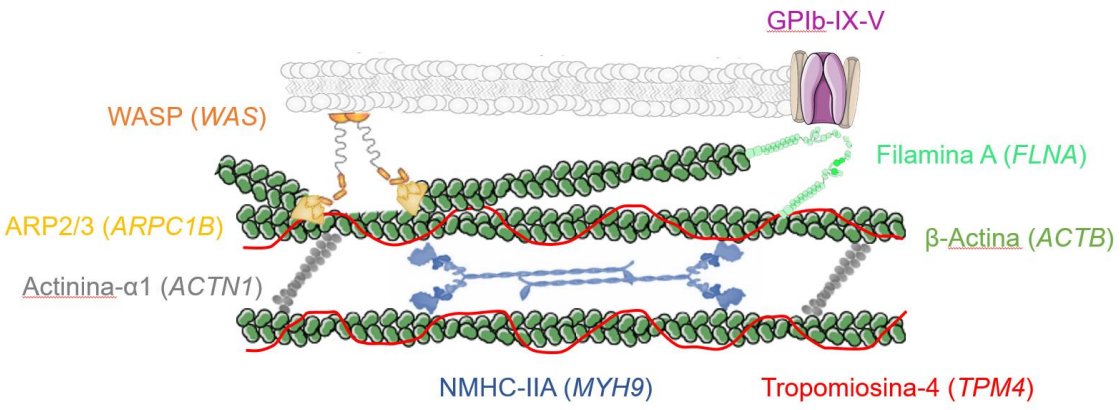

**Figura 2. Proteínas implicadas en el citoesqueleto de actomiosina de los megacariocitos.** La β-actina filamentosa se organiza en una red ramificada. El complejo ARP2/3, controlado por la WASP, entre otras proteínas, inicia la ramificación de los filamentos de actina. Los filamentos de tropomiosina-4, α1-actinina 4 y miosina II se unen a lo largo de la F-actina, controlando la tensión generada por la red de actomiosina y la organización estructural. La filamina-A une las glicoproteínas de membrana al citoesqueleto de actina. Creado con Servier Medical Art (https://smart.servier.com/).

### 1.2 Glicosilación y aclaramiento plaquetario

La glicosilación y la sialilación de las proteínas son modificaciones postraduccionales comunes y complejas, con un papel crítico en diferentes procesos biológicos como el aclaramiento de las proteínas.[42] La conjugación de carbohidratos en las moléculas y receptores específicos es crítica para la hematopoyesis normal, ya que favorece la proliferación y el aclaramiento de los precursores hematopoyéticos. A través de este mecanismo, el recuento de plaquetas circulantes está controlado por el doble equilibrio entre la tasa de producción de plaquetas por parte de los Mks y la cinética de eliminación.[43,44]

Las plaquetas tienen una vida media en la sangre que oscila entre los 8 y los 11 días, tras lo cual pierden el ácido siálico final, y se vuelven apoptóticas y posteriormente fagocitadas por los macrófagos.[45] Aquellas plaquetas sin ácido siálico son reconocidas por receptores en el hígado, actuando así como señal para aumentar los niveles de TPO, que inducen la megacariopoyesis para producir de nuevas plaquetas.[46] De hecho, se ha descrito que los ratones con deficiencias genéticas en la sialilación presentaban recuento plaquetario reducido en sangre,[47,48] lo que demuestra que las plaquetas sin ácido siálico son propensas al aclaramiento.[49]

Varias enzimas son responsables de la adecuada glicosilación y sialilación. *GALE* codifica la uridina difosfato [UDP]-galactosa-4-epimerasa, que cataliza la interconversión bidireccional de UDP-glucosa a UDP-galactosa, y de UDP-N-acetil-glucosamina a UDP-N-acetil-galactosamina (Figura 3). De este modo, GALE equilibra, mediante la epimerización reversible, las reservas de los cuatro azúcares esenciales en la biosíntesis de las glicoproteínas y los glicolípidos.[50,51]

Por otro lado, *GNE* codifica la UDP-N-acetilglucosamina 2-epimerasa, implicada en la biosíntesis del ácido siálico. Esta enzima bifuncional regula los niveles totales de ácido N-acetilneuramínico, un precursor de los ácidos siálicos, mientras que *SLC35A1* codifica el transportador de la citidina-5'-monofosfato [CMP]-ácido siálico, que transporta el CMP- ácido siálico desde el núcleo al aparato de Golgi, donde tiene lugar la sialilación (Figura 3).[44,52,53]

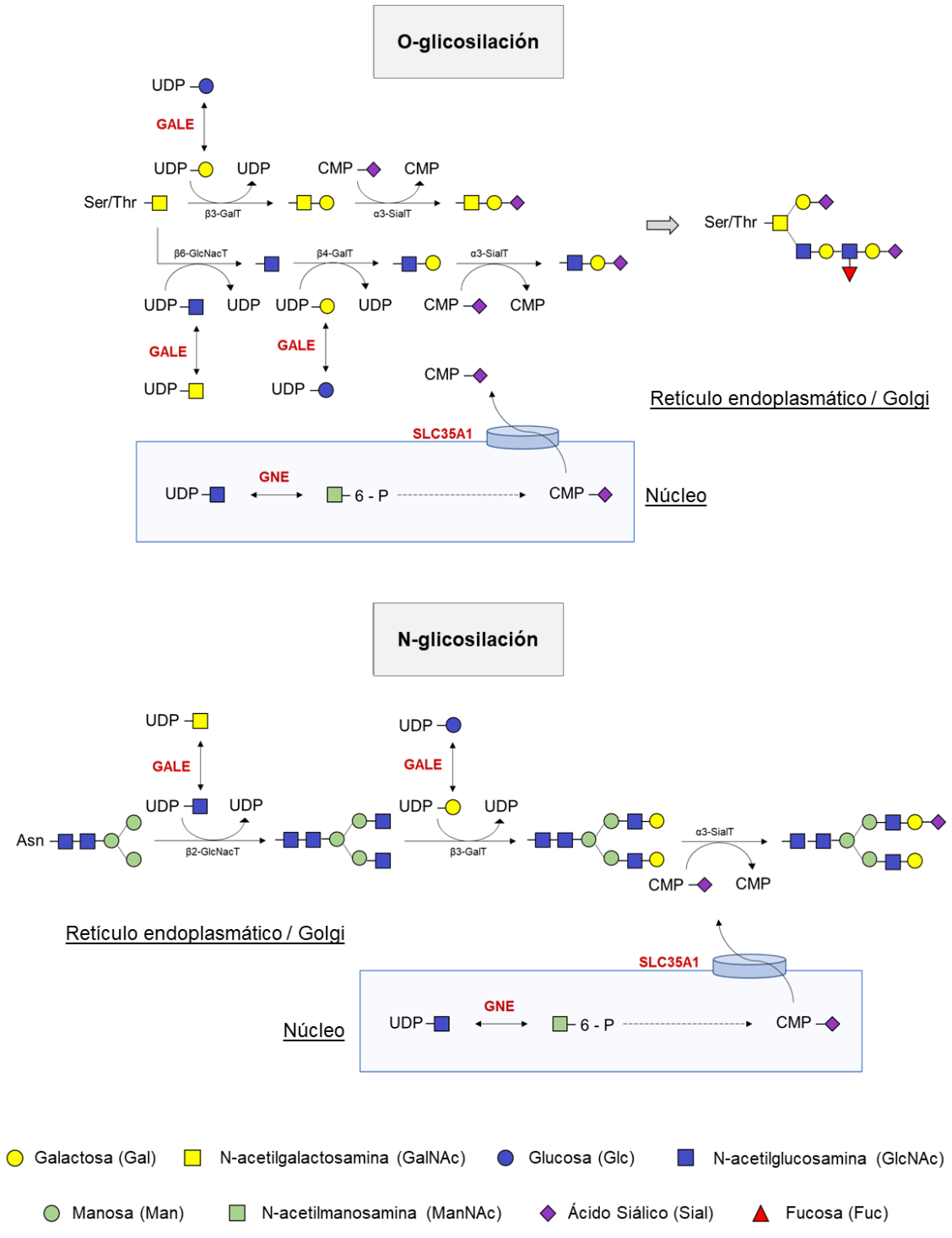

**Figura 3. O-glicosilación, N-glicosilación y sialilación de las plaquetas.** La proteína GALE permite la interconversión de cuatro moléculas esenciales en el proceso de glicosilación, al servir de sustrato para otras enzimas que incorporan los carbohidratos de interés y liberan UDP. Durante la glicosilación se producen ramificaciones de los hidratos de carbono. La unión del ácido siálico final previene del aclaramiento plaquetario. GNE y SLC35A1 participan en la vía que permite la incorporación de este ácido siálico en la plaqueta.

### 1.3 Función plaquetaria

En condiciones fisiológicas, las plaquetas circulan en la sangre en estado de quiescencia sin interactuar con el endotelio. Después de una lesión que compromete la integridad de la pared del vaso, las plaquetas interaccionan con los componentes de la matriz extracelular, durante el proceso denominado adhesión.[54,55] La adhesión implica principalmente al receptor de membrana tipo integrina, o a las glicoproteínas que se unen específicamente a componentes de la matriz extracelular, como el fibrinógeno, el colágeno, la fibronectina, la laminina y/o el factor von Willebrand [vWF], que activan las vías de señalización vinculadas a las quinasas Src.[56,57]

La inmunoglobulina GPVI y la integrina α2β1 son los dos principales receptores de la superficie plaquetaria que se unen al colágeno tras el daño vascular.[58,59] El vWF, que se encuentra en condiciones fisiológicas de forma soluble en la sangre para evitar la agregación, cambia su afinidad, interactuando así con el complejo GPIb-IX-V.[60–62] Por otro lado, las integrinas α5β1 y α6β1 se unen a la fibronectina y a la laminina, respectivamente, que también se exponen tras el daño vascular (Figura 4).[63,64]

Tras la adhesión de plaquetas en monocapa sobre las matrices expuestas, el siguiente paso necesario para la formación del trombo es el reclutamiento de plaquetas adicionales. Las plaquetas activadas secretan agonistas solubles, como el tromboxano A2 [TBXA2] o el difosfato de adenosina [ADP], en la circulación,[56,65] que estimulan a las plaquetas adyacentes, desencadenando su activación mediante la unión específica de las moléculas a su receptor específico, principalmente receptores transmembrana acoplados a proteínas G,

como la unión del ADP a los receptores P2Y1 y P2Y12, o la trombina que se une a los receptores PAR1 y PAR4, entre otros (Figura 4).[66–68]

Los componentes solubles, como el ADP o el vWF, se almacenan principalmente en los gránulos de las plaquetas. Los gránulos α son ricos en péptidos y proteínas, como el PF4, la P-selectina, el FvW o el fibrinógeno, mientras que los gránulos δ son ricos en moléculas solubles como el ADP, el ATP, el Ca2+ o la serotonina.[69–71] El último paso es la activación de la GPIIb/IIIa, también conocida como integrina αIIbβ3. El cambio conformacional producido tras la activación permite la unión del fibrinógeno, que da lugar a la formación de puentes estables entre las plaquetas (Figura 4). La interacción plaqueta-fibrinógeno-plaqueta inicia el proceso de agregación plaquetaria.[72–74]

La estimulación con agonistas provoca la activación secuencial de una o más isoformas de PLC, activando a PKC y produciendo un aumento del Ca2+ citosólico, que activa la vía de señalización de CalDAG-GEF1, lo que conduce a la reorganización y activación de las proteínas del citoesqueleto plaquetario, y promueve un cambio en la forma de la plaqueta. La activación de las vías de señalización PKC y CalDAG-GEF1 permiten la activación final de RAP1. Estos procesos se agrupan en la vía de señalización conocida como *outside-in*.[75,76] El último paso es la activación de la integrina αIIbβ3 por parte de RAP1, conocida como señalización *inside-out*, que desencadena procesos esenciales para el crecimiento y la estabilización del trombo, como la reorganización del citoesqueleto, la formación y estabilización de grandes agregados plaquetarios y la retracción final del coágulo (Figura 4).[70,77]

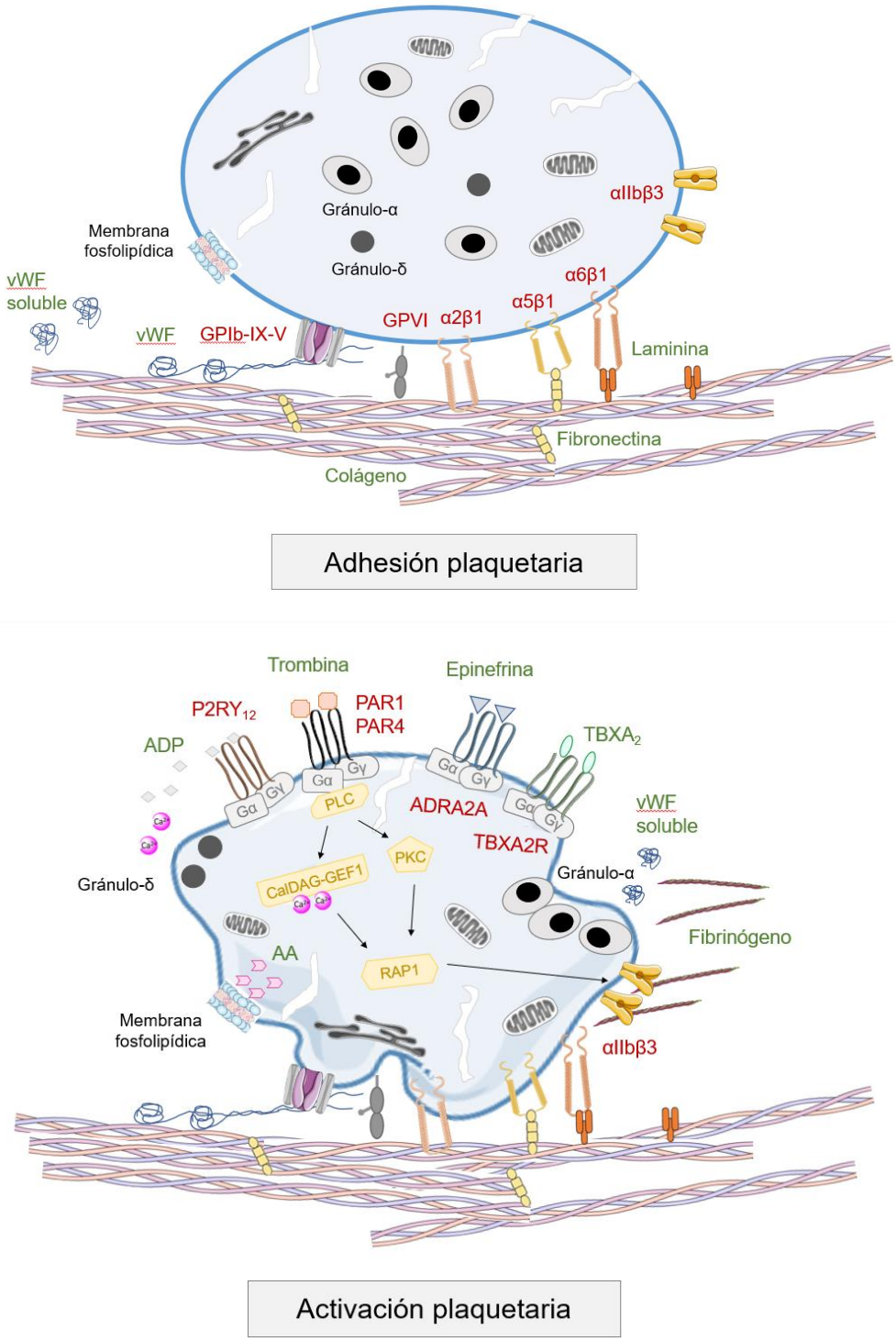


**Figura 4. Mecanismos de adhesión y activación de las plaquetas.** Durante la adhesión plaquetaria, las principales matrices extracelulares, como el colágeno, la fibronectina, la laminina y el FvW (verde) se unen a sus correspondientes receptores de membrana plaquetaria (rojo). Durante la activación plaquetaria, los principales agonistas solubles (verde) se unen a los receptores correspondientes (rojo). Se muestra la secreción de los gránulos y las principales proteínas implicadas en la vía de activación de las plaquetas. Creado con Servier Medical Art (https://smart.servier.com/).

## 2. TRASTORNOS PLAQUETARIOS CONGÉNITOS

Los Trastornos Plaquetarios Congénitos [CPDs] comprenden un grupo heterogéneo de enfermedades raras causadas por alteraciones moleculares en genes que son esenciales para la formación y/o función de las plaquetas.[78] La prevalencia de los CPDs es desconocida, pero se estima que afectan a un individuo entre 1.000-100.00, siendo reconocidas como más frecuentes en los últimos años.[79,80] Hasta la fecha, la Sociedad Internacional de Trombosis y Hemostasia [ISTH] ha establecido que los CPDs están causados por alteraciones moleculares en 66 genes diferentes, que se clasifican como genes *Tier1* (Figura 5).[81,82] Los genes se consideran *Tier1* si la asociación gen-enfermedad se ha notificado en al menos tres pedigríes independientes, o en menos de tres pedigríes pero con una gran asociación de segregación familiar en pedigríes grandes, y datos funcionales específicos o un modelo murino. De hecho, 7 genes se consideran *Tier2*, descubiertos recientemente en pequeños pedigríes individuales, y que aún requieren estudios de confirmación (Figura 5).[81,83]

En términos generales, los CPDs se clasifican en:

- Trombocitopenias Hereditarias [ITs]: trastornos relacionados con un bajo recuento de plaquetas (< 150 x $10^9$ plt/L) en sangre. Las ITs pueden asociarse a un tamaño de plaquetas disminuido, normal o aumentado, medido como volumen medio plaquetario [VPM], que da lugar a microtrombocitopenia (VPM < 7,2 fL), trombocitopenia (VPM: 7,2-11,1 fL) o macrotrombocitopenia (VPM > 11,1 fL), respectivamente. Las ITs están causadas principalmente por alteraciones en los genes que intervienen en la megacariopoyesis, la trombopoyesis y la liberación y aclaramiento de las plaquetas.[84–86]

- Trastornos Hereditarios en la Función de las Plaquetas [IPFDs]: trastornos caracterizados por la alteración de la funcionalidad de las plaquetas debido a defectos en los receptores de membrana, en las proteínas de señalización, en los gránulos alfa (α) y/o densos (δ), en el mantenimiento de la ultraestructura plaquetaria o en otras alteraciones implicadas en los mecanismos de activación de las plaquetas tras la estimulación con los agonistas.[87,88]

Múltiples trastornos se asocian a trombocitopenia con disfunción plaquetaria variable.[85] El aumento del riesgo de hemorragia es la característica principal y común de estos trastornos, y su relevancia depende del grado de trombocitopenia y de la asociación concomitante de una disfunción plaquetaria significativa.[89] La relevancia de las complicaciones clínicas es muy variable, incluso para el mismo trastorno, pudiendo causar desde una hemorragia casi insignificante hasta una que pone en peligro la vida.[90] Además, se sabe que muchos CPDs causan defectos congénitos graves que afectan a diferentes órganos o enfermedades adicionales, como las neoplasias hematológicas, la insuficiencia de la médula ósea o los defectos no hematológicos (Figura 5).[91,92]

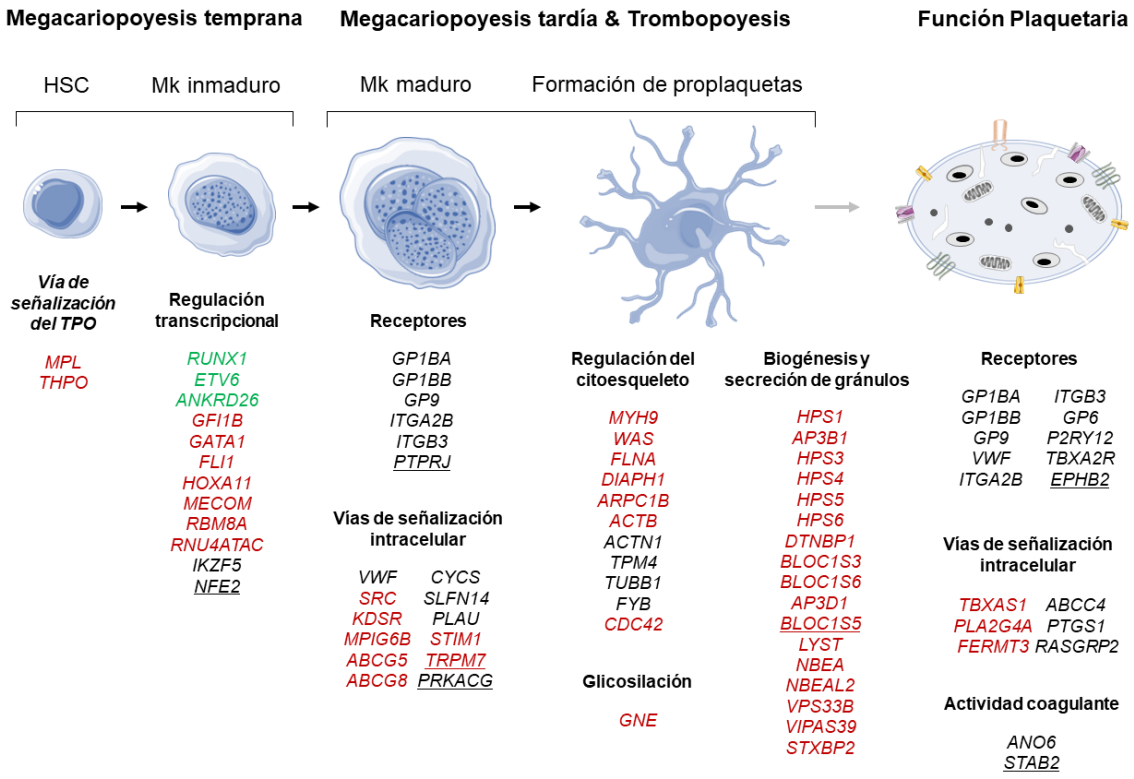


**Figura 5. Genes implicados en los Trastornos Plaquetarios Congénitos.** Clasificación de los genes *Tier1* y *Tier2* (subrayados) según la función del gen durante la megacariopoyesis, la trombopoyesis o las plaquetas en el torrente sanguíneo. El verde indica los genes con predisposición a desarrollar leucemias. El rojo indica genes asociados a manifestaciones sindrómicas. Adaptado de: [82,93] Creado con Servier Medical Art (https://smart.servier.com/).

## 3. ASPECTOS MOLECULARES Y CLÍNICOS DE LOS TRASTORNOS PLAQUETARIOS CONGÉNITOS

Los Trastornos Plaquetarios Congénitos [CPDs] se asocian a una amplia heterogeneidad de fenotipos clínicos, ya que los pacientes con alteraciones en diferentes genes pueden presentar el mismo fenotipo, mientras que otros individuos con alteraciones moleculares en el mismo gen pueden mostrar un fenotipo diferente. [89] Los CPDs suelen asociarse a hemorragias mucocutáneas leves o moderadas, como la epistaxis o la menorragia, y a la pérdida excesiva de sangre tras un traumatismo, una intervención quirúrgica, tratamientos farmacológicos o el parto. En los casos graves, se pueden diagnosticar diátesis importantes en el sistema nervioso central o hemorragias gastrointestinales.[94–96] Aunque las alteraciones en varios genes sólo se asocian clínicamente a un aumento del sangrado, otros CDPs predisponen a neoplasias hematológicas, o a trastornos multisistémicos, como la sordera neurosensorial, la insuficiencia renal o las cataratas, entre otros (Figura 5).[92,93,97]

A continuación, se describen brevemente algunos CPDs de relevancia clínica, entre los que se encuentran los trastornos con un alto grado de riesgo hemorrágico y trastornos sindrómicos.

### 3.1. Trastornos Plaquetarios Congénitos asociados a un incremento del riesgo de sangrado.

- <u>Trombastenia de Glanzmann</u>

La Trombastenia de Glanzmann es un trastorno autosómico recesivo causado por variantes patogénicas que afectan a los genes *ITGA2B* o *ITGB3*, que impiden la formación del complejo GPIIb/IIIa (integrina αIIbβ3). Este trastorno rara vez se asocia con trombocitopenia, pero los pacientes presentan hemorragias graves o potencialmente mortales. La función plaquetaria suele verse afectada debido a una activación deficiente de la integrina αIIbβ3, lo que provoca una reducción grave de la unión al fibrinógeno y de la agregación.[98,99]

Las variantes monoalélicas en estos genes causan la trombocitopenia relacionada [RT] con *ITGA2B / ITGB3*, un trastorno caracterizado por una

trombocitopenia y una tendencia a las hemorragias leves. La función plaquetaria rara vez se ve afectada.[100]

- Síndrome de Bernard Soulier

El síndrome de Bernard Soulier es causado por variantes patogénicas en *GP1BA, GP1BB* o *GP9*, interrumpiendo la formación del complejo GPIb-IX-V. Las formas generales del trastorno están relacionadas con la alteración bialélica de los genes, y el fenotipo se caracteriza por una tendencia grave a la hemorragia y una trombocitopenia moderada con plaquetas gigantes. La función plaquetaria está alterada tras la estimulación con FvW, así como la adhesión de las plaquetas y de los megacariocitos a esta matriz.[101–103]

Las variantes heterocigotas de los genes *GP1BA* y *GP1BB* causan una forma leve de la enfermedad, conocida como trombocitopenia mediterránea, y suele asociarse con una trombocitopenia leve y una diátesis hemorrágica casi ausente o leve.[104,105]

- Alteraciones en las proteínas del citoesqueleto

La trombocitopenia relacionada con *ACTN1, TUBB1* y *TPM4* son trastornos autosómicos dominantes con fenotipos similares. Suelen presentar una trombocitopenia leve con plaquetas grandes y una tendencia a la hemorragia que oscila entre moderada a casi nula. La disfunción plaquetaria no es frecuente, pero se asocian a alteraciones en la remodelación del citoesqueleto plaquetario tras la activación con varios agonistas.[26,34,106–109]

- Defectos en las vías de señalización plaquetarias

Las variantes de *P2RY12, TBXA2R* y *GP6* se asocian a un recuento y una morfología plaquetaria normales, y a una tendencia a la hemorragia leve o moderada, generalmente tras la administración de anticoagulantes. Las alteraciones de *P2RY12* y *TBXA2R* pueden heredarse tanto de forma autosómica dominante como recesiva, mientras que la de *GP6* tiene un patrón autosómico recesivo. La función plaquetaria se ve alterada tras la estimulación con ADP, TBXA2 y colágeno, respectivamente.[110–112]

*RASGPR2* codifica para CalDAG-GEF1, que participa en la vía de señalización de RAP1 durante la activación de las plaquetas (Figura 4). Las variantes patogénicas en homocigosis se asocian con hemorragias graves debido a una activación deficiente de la integrina αIIbβ3.[113]

### 3.2. Trastornos Plaquetarios Congénitos con predisposición a neoplasias

La clasificación de la Organización Mundial de la Salud (WHO) de 2016 incorporó las variantes germinales monoalélicas en los factores transcripcionales *RUNX1, ETV6* y *ANKRD26* como un nuevo subgrupo: Neoplasia mieloide hereditaria asociada a trastorno plaquetario.[114,115]

El trastorno relacionado [RD] con *RUNX1*, o trastorno plaquetario hereditario con predisposición a la leucemia mieloide aguda [FPD/AML] se asocia con una hemorragia de carácter leve a moderado, trombocitopenia variable con tamaño normal de las plaquetas, alteración de la función plaquetaria y mayor riesgo de desarrollar leucemias: 45% de riesgo a leucemia mieloide aguda [LMA] o síndrome mielodisplásico [SMD], y 1-3% a desarrollar leucemia linfoblástica aguda T [LLA]. La edad media es de 33 años (rango; 6-76 años).[116,117]

Los pacientes con *ETV6*-RD y *ANKRD26*-RD presentan una diátesis hemorrágica leve, trombocitopenia variable con morfología plaquetaria normal y, por lo general, una función plaquetaria normal. Alrededor del 25% de los pacientes con variantes patogénicas de *ETV6* desarrollan LLA durante la infancia, mientras que el 5-10% de los pacientes padecen LMA, SMD, mieloma múltiple o policitemia vera. Los pacientes con *ANKRD26*-RD desarrollan LMA o SMD a la edad media de 35 años (rango; 6-93) en el 5-10% de los casos.[118,119] Las variantes patogénicas en *ANKRD26* se encuentran principalmente en la región 5'UTR.[120]

### 3.3 Trastornos Plaquetarios Congénitos Sindrómicos

- Trombocitopenia amegacariocítica congénita

Este trastorno autosómico recesivo está causado por variantes bialélicas en el gen *MPL*, que codifica para el receptor de la TPO. Los pacientes con trombocitopenia amegacariocítica congénita presentan una trombocitopenia hipomegacariocítica de por vida, que progresa desde la citopenia durante los primeros años de vida hasta la aplasia medular. Los pacientes sufren con frecuencia diátesis hemorrágica grave.[121,122] En la actualidad, el tratamiento con análogos de la TPO se ha demostrado como una terapia prometedora para los pacientes.[123,124]

- Defectos en factores transcripcionales

En general, los trastornos plaquetarios congénitos sindrómicos se asocian a factores transcripcionales con funciones esenciales durante la diferenciación de las HSC a progenitores, y genes implicados en la megacariopoyesis temprana, como *GATA1* o *FLI1.*[85]

*GATA1*-RD es una enfermedad ligada al cromosoma X que se caracteriza por una trombocitopenia leve-moderada con megacariocitos displásicos, con grado variable de anemia, y frecuente β-talasemia, neutropenia y/o porfiria eritropoyética congénita. La diátesis hemorrágica suele ser moderada, asociada a un alteración funcional plaquetaria y defectos en los gránulos.[125,126]

*FLI1*-RD puede presentar un patrón de herencia autosómico dominante o recesivo. Los pacientes muestran trombocitopenia y tendencia a la hemorragia leves o moderadas, y malformaciones faciales, cardíacas y neurológicas.[127]

- Alteraciones en las proteínas del citoesqueleto

*MYH9* codifica la cadena pesada de miosina II-A no muscular. La trombocitopenia hereditaria causada por alteraciones en *MYH9* es la más común, ya que se han descrito más de 300 familias y hasta 100 variantes patogénicas diferentes en dicho gen. *MYH9*-RD se hereda de forma autosómica dominante, pero aproximadamente el 35% de los pacientes presentan una variante patogénica *de novo* durante la gestación en el utero.[128] El fenotipo

clínico se asocia con hemorragias leves o moderadas, macrotrombocitopenia grave e inclusiones neutrofílicas, conocidas como cuerpos de Döhle. Además, la mitad de los pacientes presentan sordera neurosensorial, y el 20-25% desarrollan nefropatías y/o cataratas.[129,130]

El síndrome de Wiskott-Aldrich [WAS] está causado por variantes patogénicas es *WAS*, que codifica para el WASP. Actualmente se han descrito más de 400 variantes diferentes en *WAS*, descubriendo una relación entre el curso clínico y el genotipo. Este trastorno ligado al cromosoma X se asocia con microtrombocitopenia moderada, hemorragias leves o moderadas, eczema e infecciones recurrentes. Además, se han observado síndromes autoinmunes en ~40% de los pacientes, que tienen un mayor riesgo de desarrollar tumores a cualquier edad.[131,132]

Las alteraciones de las proteínas FLNA, ACTB o ARPC1B son trastornos menos frecuentes. *FLNA*-RD se hereda como un trastorno ligado al cromosoma X y se asocia con una leve tendencia a las hemorragias y una macrotrombocitopenia de leve a moderada. Las manifestaciones sindrómicas pueden incluir heterotopía nodular periventricular, malformaciones esqueléticas, retraso mental, distrofia de las válvulas cardíacas, obstrucción intestinal o displasia medular.[133,134] La *ACTB*-RD es un trastorno autosómico dominante caracterizado por una macrotrombocitopenia leve-moderada, diátesis hemorrágica casi ausente, leucopenia o leucocitosis frecuentes con eosinofilia, microcefalia con retraso en el desarrollo y discapacidad intelectual leve.[135] *ARPC1B*-RD está causada por la pérdida bialélica de la función en ARP2/3, y las manifestaciones clínicas incluyen hemorragias leves-moderadas y trombocitopenia, normalmente con plaquetas pequeñas, y eosinofilia frecuente, enfermedad inflamatoria inmunomediada, eczema, linfadenopatía y hepatoesplenomegalia.[136]

- <u>Defectos en glicosilación y sialilación</u>

Hasta hace pocos años, los defectos de glicosilación no se relacionaban con los Trastornos Plaquetarios Congénitos.[44] De hecho, sólo *GNE* se considera un gen *Tier1* en la última revisión del ISTH 2021 (Figura 1).[83]

El trastorno relacionado con *GNE* se hereda de forma autosómica recesiva y se asocia a una macrotrombocitopenia y una tendencia hemorrágica graves. Los pacientes con pérdida biálica de la función de la UDP-N-acetilglucosamina 2-epimerasa presentan miopatía desde la infancia y un aumento del aclaramiento de plaquetas del torrente sanguíneo.[137,138]

Las variantes bialélicas en el gen del transportador siálico *SLC35A1* también se han relacionado con trombocitopenia y hemorragias de leves a moderadas.[47] Sin embargo, la diátesis hemorrágica encontrada en estos pacientes es menos agresiva que en los pacientes con *GNE*-RD, ya que el truncamiento del *SLC35A1* no está implicado en una megacariopoyesis alterada, y la reducción de plaquetas en sangre sólo se debe a un aumento del aclaramiento.[139] Además, estos pacientes padecen un desarrollo psicomotor alterado, epilepsia, ataxia, microcefalia.[47]

Por último, el trastorno relacionado con variantes en *GALE* presenta un patrón de herencia autosómico recesivo y suele asociarse a la galactosemia. La galactosemia periférica se asocia generalmente a formas no generalizadas o incluso a presentaciones asintomáticas,[140,141] mientras que la galactosemia clásica puede estar relacionada con complicaciones como trombocitopenia grave, neutropenia febril, dificultades de aprendizaje, retraso en el desarrollo, insuficiencia cardíaca o rasgos dismórficos.[142–145]

## 4. DIAGNÓSTICO DE TRASTORNOS PLAQUETARIOS CONGÉNITOS

El diagnóstico de los pacientes con Trastornos Plaquetarios Congénitos [CPDs] es un reto debido a la gran heterogeneidad clínica y de laboratorio, al escaso conocimiento del papel biológico de muchos genes implicados en los CPDs, y a la escasa reproducibilidad y especificidad de los ensayos de función plaquetaria.[146,147] En consecuencia, muchos CPDs son infradiagnosticados, lo que disminuye la calidad de vida de los pacientes y aumenta el riesgo de nuevos episodios hemorrágicos; o bien se diagnostican erróneamente, recibiendo un tratamiento inadecuado, incluso perjudicial e innecesariamente invasivo, como la esplenectomía, entre otros.[148,149] Además, suponen un gran reto económico,

debido al uso de métodos de diagnóstico lentos y costosos, y a la necesidad de volver a tratar de forma específica a aquellos pacientes.[150]

Muchas trombocitopenias hereditarias se asocian a una reducción moderada del recuento de plaquetas, a una disfunción plaquetaria leve y a una ligera tendencia a la hemorragia.[79] Por ello, es frecuente que las trombocitopenias asintomáticas se detecte de forma incidental en la edad adulta, en el contexto de un examen médico rutinario o al someterse a una intervención quirúrgica u otras alteraciones hemostáticas.[95,151]

En general, el diagnóstico de los Trastornos Plaquetarios Congénitos se basa en la combinación de: (Figura 6)

- Síntomas clínicos, basados en antecedentes familiares de hemorragias, neoplasias hematológicas, tumores sólidos, y/o manifestaciones sistémicas, como insuficiencia renal, miopatías, entre otras. Para la evaluación clínica del sangrado se recomienda el uso de cuestionarios estandarizados, como el ISTH-BAT.[152] En general, se establece una diátesis hemorrágica alterada cuando el ISTH-BAT>3 en hombres, y >5 en mujeres, y >2 puntos en niños.[152,153]

- Pruebas de rutina de laboratorio, incluyendo la coagulación y las pruebas bioquímicas de rutina, el hemograma, siendo particularmente importante el recuento de plaquetas y el MPV para el diagnóstico de la trombocitopenia hereditaria, y finalmente la evaluación de la morfología utilizando frotis de sangre con o sin tinción de inmunofluorescencia.[154,155]

- Fenotipo plaquetario. Estas pruebas son limitadas y suelen realizarse en laboratorios muy especializados, donde se realizan estudios específicos de las plaquetas, como la agregometría por transmisión de luz [LTA] y la citometría de flujo.[149,156] Además, el estudio funcional de las plaquetas debe realizarse en un tiempo limitado tras la extracción de sangre, con condiciones estándar, como reactivos, métodos, equipos e interpretación de datos, lo que dificulta el diagnóstico.[157]

- Confirmación del diagnóstico mediante el análisis molecular del gen afecto. Los criterios de inclusión se basan en al menos ≥1 criterio de fenotipo clínico y ≥1 de pruebas de laboratorio.[158] Hasta hace pocos años, la secuenciación

Sanger [SS] de genes candidatos se utilizaba como herramienta de diagnóstico. Sin embargo, este enfoque es, en la actualidad, costoso, requiere mucho tiempo y no es aplicable a los trastornos cuyo diagnóstico basado en el fenotipo no es sencillo y para los que no existe un gen candidato claro. La implementación de la secuenciación de alto rendimiento [HTS], ya sea la secuenciación de genes específicos, la secuenciación del exoma completo [WES] o la secuenciación del genoma completo [WGS], ha revolucionado el campo del diagnóstico genético y se ha establecido rápidamente como una herramienta para la práctica clínica.[97,159] A pesar de su evidente importancia, hasta hace poco, los estudios moleculares de los CPDs se han realizado como último paso en el flujo de trabajo del diagnóstico de estas enfermedades.[160,161] La principal limitación del análisis molecular es la clasificación de las variantes genéticas encontradas, ya que la mayoría de ellas son nuevas o de significado incierto. Por ello, la ACMG / AMP estableció recomendaciones internacionales estándares para clasificar la patogenicidad de las variantes genéticas encontradas en los pacientes.[162] Sin embargo, a pesar de estas guías, todavía existe una gran variabilidad en la clasificación de las variantes entre los laboratorios. La aparición del proyecto GoldVariant ha permitido compartir datos de variantes procedentes de diferentes grupos de investigación de todo el mundo,[83] que son curadas por paneles de expertos del Clinical Genome Resource [ClinGen] para determinar el papel del gen y el efecto de la variante detectada en una enfermedad concreta, lo que ha permitido elaborar recomendaciones específicas.[163–166]

- Caracterización funcional. La validación de posibles variantes nuevas o de significado incierto debe ir acompañada de pruebas funcionales, cuando sea posible, en modelos de líneas celulares, células primarias de muestras de pacientes, células madre pluripotentes inducidas [iPSC] y/o, en última instancia, modelos animales.[93]

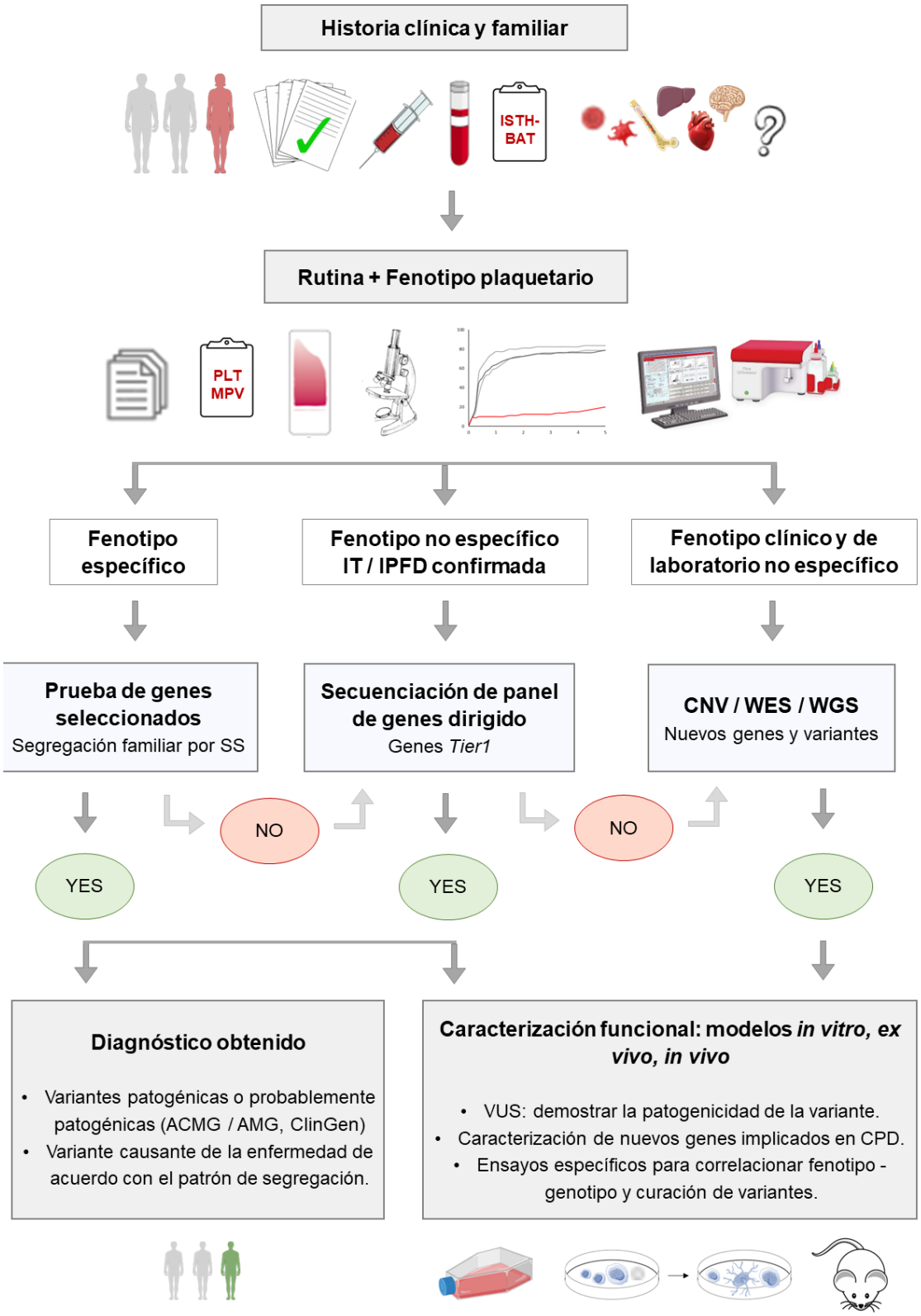


**Figura 6. Algoritmo del flujo de trabajo para el diagnóstico de los Trastornos Plaquetarios Congénitos**. Adaptado de: [97,167]

### 4.1 Estudios de fenotipado plaquetario

Las pruebas iniciales deben incluir un recuento sanguíneo completo y la evaluación de un frotis de sangre periférica: estos ensayos ayudan a detectar anomalías en el número y la estructura de las plaquetas que podrían guiar los estudios de laboratorio adicionales.[147,154] Los recuentos de plaquetas normales excluirán la trombocitopenia hereditaria [IT] como causa de la hemorragia, lo que sugiere un trastorno de la función plaquetaria. Sin embargo, un número reducido de plaquetas no excluye la realización de pruebas de función plaquetaria, ya que varias ITs están asociados a la disfunción plaquetaria. La evaluación del MPV es también un parámetro importante para el diagnóstico, pues las ITs se asocian frecuentemente a un tamaño anormal de las plaquetas.[78,88,168–170] Una trombocitopenia con alteración del MPV puede orientar el diagnóstico de varias ITs, especialmente, las asociadas a alteraciones de las proteínas del citoesqueleto.[169,171] Sin embargo, es importante señalar que se pueden observar características inusuales, como WAS asociado a la macrotrombocitopenia en lugar de las frecuentes microtrombocitopenias.[172]

La evaluación de frotis de sangre periférica permite evaluar el tamaño de las plaquetas, complementario a los valores de MPV, pero también la aglutinación, la morfología y la granularidad de las plaquetas, o las anomalías de los glóbulos blancos y/o rojos.[147] Las plaquetas grises y grandes centran el diagnóstico en la ausencia/reducción de gránulos plaquetarios, característico de las variantes en *NBEAL2*;[173] un reducido número de plaquetas de gran tamaño son características del Síndrome de Bernard Soulier;[174] las inclusiones leucocitarias (cuerpos de Döhle) sugieren el *MYH9*-RD,[175,176] las plaquetas grandes con estomatocitos orientan hacia alteraciones moleculares en *ABCG5* o *ABCG8*,[177,178] mientras que la morfología anormal de los glóbulos rojos centra el diagnóstico en el gen *GATA1*.[179] Además, un estudio reciente basado en la tinción del frotis sanguíneo con anticuerpos fluorescentes contra proteínas plaquetarias específicas ha aumentado la tasa de diagnóstico de forma fácil y rápida.[154,155]

Por otro lado, la prueba de cribado más utilizada para la hemostasia primaria es el analizador de la función plaquetaria (PFA-100®). A pesar de su amplio uso

en los laboratorios, el PFA-100® no se recomienda para el cribado inicial de laboratorio debido a su baja especificidad, sensibilidad y reproducibilidad. Sin embargo, podría orientar el diagnóstico de una hemostasia alterada.[180,181]

El método de referencia para el diagnóstico de la función plaquetaria es la agregometría por transmisión de luz [LTA].[182] Al añadir un agonista, las plaquetas se agregan, por lo que el plasma rico en plaquetas pierde turbidez y se vuelve más claro, aumentando la transmisión de luz detectada por la fotocélula. El tiempo necesario para conseguir este cambio se registra y se representa como la agregación en el tiempo.[183,184] Los agonistas habituales para el diagnóstico mediante LTA incluyen el ADP, el colágeno, el ácido araquidónico [AA] o la epinefrina en concentraciones estandarizadas (Figura 4). La activación mediada por la α-trombina se analiza utilizando péptidos específicos, como los péptidos activadores del receptor de trombina TRAP-6, PAR-4 y/o PAR-1. Para evaluar el complejo GPIb-IX-V, se utiliza frecuentemente el antibiótico ristocetina, que provoca la unión del vWF al complejo. Los agonistas específicos, como el péptido relacionado con el colágeno [CRP], la convulxina o el forbol-12-miristato-13-acetato [PMA], pueden utilizarse opcionalmente cuando se sospeche una alteración de estas vías específicas.[183,185,186]

La agregación plaquetaria también puede evaluarse mediante la agregometría de impedancia en sangre total. Este método se basa en la medición de la resistencia a la electricidad entre dos electrodos de platino. Cuando las plaquetas agregan, se unen a los electrodos produciendo cambios en la impedancia eléctrica que luego se transforman en un registro de la agregación. Sin embargo, este método se utiliza con menos frecuencia en la actualidad, ya que es poco sensible para detectar defectos leves de la función plaquetaria.[187,188]

Por otra parte, la citometría de flujo permite evaluar varios parámetros estructurales y funcionales de las plaquetas, como la expresión de los receptores de superficie, la unión de ligandos o la secreción del contenido de los gránulos, mediante el uso de anticuerpos específicos. Además, la técnica requiere bajas cantidades de sangre, siendo un ensayo muy útil para pacientes con trombocitopenia grave o pediátricos. La evaluación habitual incluye los

anticuerpos contra la GPIIb (anti-CD41), la GPIIIa (anti-CD61), la GPIbα (anti-CD42b) y la GPIX (anti-CD42a), y con menor frecuencia o como segundo paso, la GPIa/IIa (CD31 y CD49b), la GPIV (CD36) y la GPVI. La citometría de flujo también permite evaluar los defectos de la función plaquetaria midiendo la expresión superficial de marcadores de activación, como CD62P (α-granulos), CD63 (δ-granulos) o PAC-1 (integrina αIIbβ3 activa), tras la estimulación con agonistas.[189–191]

### 4.2 Molecular diagnosis in the genomic era

Hasta principios de 2010, la secuenciación del ADN se había limitado en gran medida al análisis de genes candidatos mediante la secuenciación Sanger. El diagnóstico basado en esta técnica era limitado debido a la selección de los genes candidatos, que requería un fenotipo clínico y de laboratorio bien definido. Por ello, se diagnosticaba a menos del 40% de los pacientes. La reciente aplicación de la secuenciación de alto rendimiento [HTS], especialmente utilizando paneles de un número variable de genes conocidos implicados en los trastornos hemorrágicos, ha revolucionado el diagnóstico molecular de los Trastornos Plaquetarios Congénitos, mejorando la eficacia diagnóstica en un 70%, y hasta en un 90% en los casos con una clara sospecha diagnóstica o con un fenotipo específico.[97,158,192–195] Por último, los costes cada vez más económicos y la progresión en la interpretación de exomas y genomas completos ha permitido el descubrimiento de nuevos genes implicados en la patología.[108,142,196,197]

#### *4.2.1 Secuenciación de Sanger*

La secuenciación de Sanger [SS] permitió mapear la totalidad del genoma humano,[198] siendo el método de referencia para el diagnóstico molecular de los trastornos hemorrágicos desde principios de los años 90.[149,192] Es útil para los Trastornos Plaquetarios Congénitos con un fenotipo clínico y de laboratorio bien definido, como el Síndrome de Bernard Soulier o la Trombastenia Glanzmann. Además, la SS asociado a otras técnicas como los estudios de asociación de todo el genoma permitió identificar los genes *MYH9* o *RUNX1*, entre otros.[97] Sin embargo, su principal limitación es la reducida eficacia diagnóstica para los

trastornos cuya relación fenotipo-genotipo es incierta y para los que no se puede seleccionar un gen candidato claro. De hecho, el hecho de que muchas enfermedades estén causadas por muchos genes, como el síndrome de Hermansky-Pudlak [HPS], o por genes con muchos exones, hace que el diagnóstico por SS sea costoso y requiera mucho tiempo. En la actualidad, la SS se utiliza cuando existe una fuerte evidencia fenotipo-genotipo, para la confirmación genética del diagnóstico y para la segregación familiar (Figura 7).[97,158,192,199,200]

*4.2.2 Secuenciación dirigida de genes candidatos*

En la última década, la HTS ha revolucionado la secuenciación del ADN y el diagnóstico de las enfermedades humanas, permitiendo la exploración simultánea de múltiples genes de forma rápida y económica. El uso de paneles de genes diana simplifica y acelera el diagnóstico global, permitiendo la secuenciación de regiones diana de interés a partir de un panel de genes candidatos preseleccionados (Figura 7).[97,201,202]

Varios grupos de investigación han introducido ya paneles de genes en la práctica clínica para el manejo y el diagnóstico de pacientes con Trastornos Plaquetarios Congénitos. El grupo *Genotyping and Phenotyping of Platelets Project* (GAPP) examinó hasta 329 genes, caracterizando nuevas variantes en genes como *FLI1* o *RUNX1*,[193,203] o el consorcio ThromboGenomics, surgido del consorcio BRIDGE-BPD, que desarrolló una plataforma HTS para secuenciar un panel de 63 genes implicados en trastornos hemorrágicos, trombóticos y plaquetarios hereditarios.[194,204] Por otra parte, un grupo australiano utilizó un panel de amplicones personalizados de 27 genes candidatos causantes de trombocitopenia hereditaria para investigar una gran cohorte de pacientes con macrotrombocitopenia.[175,205]

En cuanto al "Grupo Español de Alteraciones Plaquetarias Congénitas", se utilizó un panel dirigido de 72 genes para la práctica clínica, descubriendo nuevas variantes en genes poco frecuentes, como *DIAPH1, RASGRP2* o *PTGS1*.[113,158,206]

El uso de la secuenciación de genes diana ha mejorado el diagnóstico genético de los pacientes hasta en un 70%, mediante el uso de diferentes

paneles personalizados en distintos laboratorios de todo el mundo.[158,193,204,207] Sin embargo, todavía existen limitaciones, como una proporción considerable de pacientes que no son diagnosticados.[208] Sigue siendo difícil identificar grandes variaciones estructurales y cromosómicas, las inversiones, las translocaciones, las aneuploidías y las variaciones en el número de copias [CNVs] mediante esta técnica, además del hecho de que varios procesos de la megacariopoyesis y la función plaquetaria no están bien caracterizados, lo que explicará que un número considerable de trastornos esté causado por genes no descritos hasta la fecha.[97,161]

*4.2.3 Secuenciación de exoma completo*

WES permite secuenciar todas las regiones codificantes de las proteínas (exones), lo que representa aproximadamente el 1,5% del genoma humano, y justifica el 85% de los trastornos mendelianos (Figura 7).[209] En los últimos años, el uso de WES ha permitido identificar nuevos genes en los Trastornos Plaquetarios Congénitos, como *DIAPH1*, *GNE* o *TPM4*.[108,138,197] Además, los CNVs pueden identificarse con este enfoque. Sin embargo, la principal limitación de la técnica es el tiempo que requiere, la gran cantidad de datos generados y las dificultades en la interpretación de los genes.[97]

*4.2.4. Secuenciación de genoma completo*

WGS puede proporcionar información genómica completa, ya que se analizan todas las secuencias codificantes y no codificantes (Figura 7). Este método tiene cada vez más importancia, y el coste de esta tecnología ha descendido progresivamente.[210] Sin embargo, y de forma similar a WES, proporciona una gran cantidad de datos, lo que requiere un extenso y complejo flujo de trabajo bioinformático y la interpretación por parte de expertos para identificar las variantes causantes de la enfermedad.[211] Además, la interpretación de las variantes no codificantes ha demostrado ser extremadamente difícil y todavía no se realiza de forma rutinaria en la mayoría de los proyectos de investigación.[212,213]


**Figure 7. Los principales tipos de secuenciación del ADN utilizados para el diagnóstico de los Trastornos Plaquetarios Congénitos.**

### *4.2.5. Interpretación de variantes*

El diagnóstico genético de los Trastornos Plaquetarios Congénitos ayuda a conseguir un diagnóstico preciso, lo que permite mejorar la atención clínica, el pronóstico y los tratamientos preventivos, y posibilita el asesoramiento genético. Este último paso es esencial para los pacientes con riesgo de neoplasias y otras predisposiciones a patologías graves.[195] En este contexto, la secuenciación de alto rendimiento [HTS] proporciona, de forma rápida y cada vez más económica, una gran cantidad de información genética, facilitando la identificación de variantes genéticas, estableciéndose como el *gold standard* para identificar la patología molecular subyacente a las enfermedades monogénicas.[97,211] Sin embargo, a pesar de las ventajas diagnósticas de la HTS, persisten los dilemas éticos en el uso del cribado genético y la identificación de variantes de significado incierto.[208,214]

Para categorizar la gran cantidad de información genética obtenida a partir de la HTS, se han establecido unas normas para la interpretación de las variantes secuenciadas por parte del ACMG/AMP.[162] Sin embargo, estas normas no se aplican de forma universal en los diferentes genes o trastornos, lo que da lugar a diferentes interpretaciones de una misma variante por parte de diferentes laboratorios de todo el mundo y, por tanto, no se llega a una clasificación definitiva y uniforme. Para lograr un diagnóstico preciso de los pacientes, se ha creado recientemente el proyecto GoldVariant, que facilita el intercambio de datos entre diferentes laboratorios de todo el mundo, concretamente, 30 centros

expertos de 14 países.[83] Esta gran cantidad de información genética se envía rápida y fácilmente a ClinVar, y estas variantes serán reclasificadas y evaluadas por pequeños grupos de trabajo de expertos, los paneles de expertos en curación de variantes de ClinGen, proporcionando una modificación específica de las reglas generales de clasificación de variantes de la ACMG / AMP, basándose en la literatura publicada y en las bases de datos relativas al fenotipo clínico y de laboratorio encontrado en pacientes con un trastorno específico, modelos celulares o animales, o bases de datos poblacionales. Este enfoque permitirá determinar el papel de la variante en una enfermedad (asociación de la enfermedad) y proporcionar información sobre el modo de herencia y el mecanismo mutacional de la enfermedad, descartando las variantes incidentales en los genes causantes de la enfermedad que no están relacionadas con el motivo original de la prueba.[163–166]

## 5. CARACTERIZACIÓN FUNCIONAL DE LOS TRASTORNOS PLAQUETARIOS CONGÉNITOS

El paso final para la curación de una variante de significado incierto es la demostración de la patogénesis y el mecanismo subyacente a la variante, especialmente cuando no se encuentra ninguna evidencia de asociación con la enfermedad revisando la bibliografía.[215] De hecho, la creciente aplicación de WES y WGS en la práctica clínica rutinaria ha permitido la identificación de nuevos genes implicados en la patogénesis de los Trastornos Plaquetarios Congénitos, que requieren estudios funcionales para descubrir su papel e implicación en la enfermedad. Por lo tanto, la confirmación final de una variante como causante de la enfermedad debe estar ligada a la realización de un modelo experimental que demuestre la causalidad.[97,162,167]

### 5.1 Estudios *in vitro*

Las líneas celulares megacariocíticas humanas, derivadas de la sangre periférica o de la médula ósea de pacientes con leucemia, son una potente herramienta para evaluar la proliferación, diferenciación y maduración de los

megacariocitos. La disponibilidad de poblaciones homogéneas de células progenitoras hematopoyéticas ha facilitado la comprensión del mecanismo biológico y molecular de genes cruciales en la megacariopoyesis.[216–218]

Hasta la fecha, se han descrito en la literatura al menos 18 líneas celulares humanas con algunas propiedades megacariocíticas.[219] Estas líneas celulares en condiciones indiferenciadas expresan marcadores específicos de megacariocitos o eritrocitos (Tabla 1). El tratamiento con PMA o TPO estimula la diferenciación megacariocítica, permitiendo el estudio de las vías de señalización implicadas en el proceso. Comúnmente, las células son tratadas con PMA, ya que la inducción-diferenciación se acompaña de cambios en la morfología celular, detención del crecimiento celular, endomitosis y adquisición de marcadores megacariocíticos específicos, imitando el proceso fisiológico que tiene lugar en la médula ósea. Además, el tratamiento con PMA no requiere un receptor específico, ya que activa directamente la proteína PKC.[218,220,221] El tratamiento con TPO es fisiológicamente más similar a la megacariopoyesis que tiene lugar en la médula ósea humana, sin embargo, sólo la línea celular UT7 presenta el gen *MPL*. De hecho, UT7 es la única línea celular dependiente de factores hematopoyéticos, por lo que esta línea celular puede proporcionar un nuevo e importante modelo para el estudio de la diferenciación de megacariocitos inducida por TPO (Tabla 1).[222,223]

K562, HEL, MEG-01 y Dami son las líneas celulares más frecuentemente utilizadas para la caracterización *in vitro* de la megacariopoyesis, ya que tras el tratamiento con dosis bajas de PMA (10-30 nM), las células aumentan su tamaño y muestran maduración citoplasmática. Por lo tanto, la poliploidía puede medirse fácilmente por citometría de flujo. Además, también aumentan la expresión superficial de varias proteínas asociadas a los megacariocitos y a las plaquetas, como GPIIb-IIIa, GPIb, vWF y PF4. De hecho, la expresión de GPIb en las líneas K562 y MEG-01 en condiciones basales está ausente, por lo que la aparición de la expresión podría considerarse como una medida directa de la maduración inducida por PMA.[219,224–227]

| Línea celular | Origen | GPIIb-IIIa (CD41-61) expres. | GPIb (CD42b) expres. | vWF expres. | Diferenciación con PMA / TPO | Ref |
|---|---|---|---|---|---|---|
| **K562** | CML crisis blástica | +/- | - | - | PMA | [224] |
| **HEL** | AML M6 | + | + | - | PMA | [225] |
| **MEG-01** | CML crisis blástica | + | +/- | + | PMA | [226] |
| **EST-IU** | Tumor de centro germinal | + | N/A | + | PMA | [228] |
| **LAMA-84** | CML crisis blástica | + | - | - | PMA | [229] |
| **Dami** | AML M7 | + | + | + | PMA | [227] |
| **KOPM-28** | CML crisis blástica | + | N/A | N/A | PMA | [230] |
| **T-33** | CML crisis blástica | + | + | + | PMA | [231] |
| **M-07** | AML M7 | + | + | N/A | N/A | [232] |
| **OCIM1/ OCIM2** | AML M6 | +/- | - | - | PMA | [233] |
| **KU812** | CML crisis blástica | +/- | - | N/A | PMA | [234] |
| **CMK** | AML M7 | + | + | - | PMA | [235] |
| **CHRF-288-11** | AML M7 | + | N/A | + | PMA | [236] |
| **UT7** | AML M7 | + | + | N/A | PMA / TPO | [222, 223] |
| **MOLM-1** | CML crisis blástica | + | N/A | N/A | N/A | [237] |
| **MKPL-1** | AML M7 | + | - | - | N/A | [238] |
| **ELF-153** | AML M7 | + | + | + | PMA | [239] |
| **MEG-A2** | CML crisis blástica | + | - | - | PMA | [240] |

**Tabla 1. Características generales de las líneas celulares humanas que expresan propiedades megacariocíticas.** La expresión de GPIIa, IIIa, Ib y vWF se

refiere a condiciones indiferenciadas. + significa expresión positiva, +/- muy débilmente positiva, - negativa, N/A indica características no evaluadas en la línea celular. Adaptado de: [219].

### 5.2 Estudios *ex vivo*

La diferenciación y maduración de las Mk depende en gran medida del microambiente y de las citocinas.[5] Aunque las aproximaciones *in vitro* son útiles para la caracterización de las vías de señalización implicadas en la megacariopoyesis, no reproducen los procesos biológicos. En los últimos años, la generación *ex vivo* de plaquetas a partir de HSC ha mejorado la comprensión de la heterogeneidad que subyace al desarrollo de los Mks humanos.[241] Los Mks cultivados a partir de HSC y de células madre embrionarias humanas [ESC] o de células madre pluripotentes inducidas humanas [iPSC] han surgido como un modelo eficaz para el estudio de la megacariopoyesis en pacientes con trombocitopenia hereditaria o con disfunción plaquetaria, y es una fuente alternativa prometedora para satisfacer la demanda cada vez mayor de terapia plaquetaria.[241–243]

- Megacariocitos cultivados a partir de HSC y progenitores

Los megacariocitos [Mks] y las plaquetas humanas pueden generarse *in vitro* tras el aislamiento de células progenitoras CD34+ derivadas de la sangre periférica, la sangre del cordón umbilical, el hígado fetal o la médula ósea. Las células deben cultivarse durante 14 días en presencia de TPO o plasma humano (Figura 8). Se ha demostrado que la suplementación adicional con citoquinas aumenta las tasas de diferenciación en el cultivo. De hecho, como el microambiente hematopoyético depende de las células estromales para proporcionar muchas de las señales para la autorrenovación y proliferación de las HSC, los cultivos basados en células estromales podrían ser de gran interés.[4,244,245]

La caracterización de Mk a partir de células primarias es un procedimiento limitado, ya que el número de células que se obtiene al final del cultivo es bastante reducido y poco prolongado en el tiempo.[246]

- Células madre embrionarias humanas y células madre pluripotentes inducidas

En comparación con los Mks primarias, las ESC y las iPSC pueden ser células inmortalizadas y podrían proporcionar un número ilimitado de células CD34+ tras la manipulación de C-MYC, y uno de los cuatro factores de Yamanaka utilizados para inducir la pluripotencia en las células somáticas (SOX2, REX1, NANOG y OCT4) (Figura 8).[247,248]

Sin embargo, estos Mks son bastante diferentes de los fisiológicos, ya que no superan una ploidía de 32n y sólo alrededor de un 15% de estos Mks son CD41+ CD42b+. De hecho, la principal limitación es el bajo número de plaquetas que producen los Mks.[241,247]

Una de las principales razones de estas diferencias se debe al hecho de que la generación *ex vivo* se lleva a cabo en un cultivo estático y, por tanto, no imita las condiciones de flujo sanguíneo. Una estrategia emergente para conocer el papel fundamental del microambiente de la médula ósea en la regulación de la hematopoyesis es el uso de modelos tridimensionales (3D) de tejidos humanos mediante ingeniería de tejidos. Los modelos más recientes están fabricados con materiales biocompatibles que favorecen la función de los Mks. Una vez en contacto con el biomaterial, los Mk producen las proplaquetas en el medio de cultivo perfundido imitando las fuerzas de cizallamiento de la sangre. En los últimos 20 años se han logrado avances prometedores en la producción de plaquetas *ex vivo*, lo que sugiere que en un futuro próximo esta técnica podría utilizarse comúnmente para la investigación para diferenciar completamente a los Mks funcionales.[4,246,249–251]

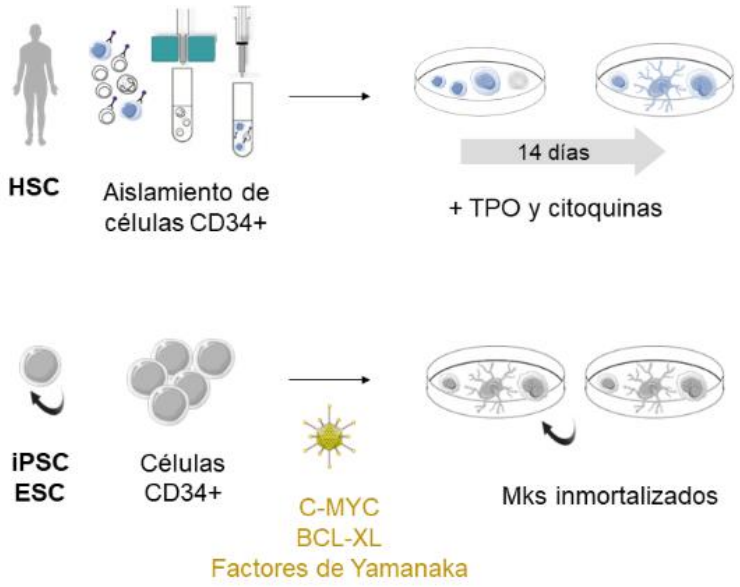


**Figura 8. Estrategias de megacariopoyesis *ex vivo*.** En la figura superior se representa el aislamiento y la expansión de células CD34+ a Mks. En la figura inferior, la generación de células madre pluripotentes inducidas (iPSCs) y células madre embrionarias (ESCs) mediante la activación de transgenes, que proporciona una fuente de Mks inmortalizados. Creadas con Servier Medical Art (https://smart.servier.com/).

### 5.3 Estudios *in vivo*

El desarrollo de la reprogramación genética de iPSC o de la diferenciación de megacariocitos ha permitido algunos avances, pero estos sistemas *in vitro* son imperfectos y no reproducen fielmente todos los pasos que conducen a la formación de las plaquetas. La mejora en las herramientas de estudio de los ratones modificados genéticamente ha permitido generar modelos *in vivo* que imitan las patologías y permiten evaluar el impacto de las variantes genéticas en la producción y la función de las plaquetas. Aunque son menos utilizados, los modelos de pez cebra también han demostrado ser un modelo animal potencialmente útil que reproduce los trastornos plaquetarios humanos.[252–254]

La mutagénesis dirigida y la transgénesis ofrecen una amplia posibilidad de modelos modificados genéticamente. Los *knock-out* [KO] se generan mediante la inactivación del gen en todo el organismo. Dada la condición de línea germinal de los Trastornos Plaquetarios Congénitos, estos modelos

animales son potencialmente útiles. Los ratones *knock-out* condicionales permiten la inactivación de un gen en un tejido concreto, o en una etapa específica del desarrollo bajo el control del promotor de interés. Por último, los ratones *knock-in* [KI] se generan mediante la mutación puntual o las inserciones/deleciones por recombinación homóloga en el locus de interés. Estos modelos reproducen fielmente las variantes *missense* presentes en humanos y representan la mejor aproximación para imitar la patología.[255,256] Hasta la fecha, se han generado modelos de ratón para el estudio de *MYH9*-RD, el Síndrome de Bernard Soulier, Síndrome de Wiskott Aldrich, trombocitopenia amegacariocítica congénita o *RUNX1*-RD, entre otros.[22,257–260]

### 5.4 Tecnologías de edición genética

En los últimos años, el desarrollo de las tecnologías de edición genómica ha revolucionado el campo de la ingeniería genética, permitiendo la modificación del genoma de forma rápida, específica y sencilla.[265,266]

Los sistemas de edición del genoma implementados hasta ahora incluyen las nucleasas de dedos de zinc [ZFN], las nucleasas efectoras similares al activador de la transcripción [TALEN] y las repeticiones palindrómicas cortas agrupadas y regularmente espaciadas [CRISPR] / Cas9. Las metodologías ZFN y TALENs se basan en la ingeniería de proteínas que constan de una región de reconocimiento de la secuencia objetivo a editar y una región catalítica responsable de generar roturas de doble cadena [DSB] en el ADN (Figura 9). Ambas metodologías tienen algunas limitaciones, ya que es necesario generar una proteína diferente para cada región del genoma a editar y, además, ambos sistemas son difíciles de introducir en las células debido a su gran tamaño, lo que reduce la eficiencia de la edición y compromete la capacidad de generar ediciones simultáneas de varias regiones genómicas en la misma célula.[267,268] Sin embargo, el sistema CRISPR/Cas9 es capaz de superar estas limitaciones, permitiendo la edición de secuencias de ADN de una forma más sencilla y eficiente.[269]

Para inducir cortes dirigidos en células humanas mediante este sistema, es necesario expresar dos componentes esenciales: la proteína Cas9 y una secuencia de ARN, que consta de 20 nucleótidos complementarios a la región

genómica diana y a la región de unión de la proteína Cas9, y que actúa como guía. Esta secuencia específica se denomina ARN de guía única [sgRNA]. El único requisito para editar la región genómica mediante la herramienta CRISPR/Cas9 es que la secuencia de 20 nucleótidos vaya seguida de una secuencia de tres nucleótidos, -NGG-, denominada PAM. Estos componentes se introducen en las células de mamíferos mediante plásmidos, lentivirus o ribonucleoproteínas. Una vez introducido el sistema en la célula, se producirá un corte de ADN de doble cadena mediado por la nucleasa Cas9 en la región complementaria a la guía, entre los nucleótidos 17 y 18 de la secuencia complementaria aguas arriba de la PAM.[270,271] Posteriormente, se activarán en la célula los mecanismos endógenos de reparación de la rotura de la doble cadena, que consisten en dos mecanismos principales. En la mayoría de los casos, la rotura se corrige mediante el mecanismo de unión de extremos no homólogos [NHEJ], basado en la unión de extremos romos mediante la incorporación o eliminación de nucleótidos al azar, generando inserciones o deleciones. Estas alteraciones pueden dar lugar a una alteración del marco de lectura, dando lugar a un codón de parada que puede truncar la proteína diana, generando así un KO.[272,273] Por otro lado, el mecanismo de recombinación homóloga [HR] utiliza una secuencia homóloga como plantilla [ssODN] para la reparación dirigida. De este modo, es posible generar o corregir mutaciones puntuales en una región genómica de interés, integrando un molde de reparación específico junto con los componentes del sistema CRISPR/Cas9 (Figura 9).[274,275]

Dado que la aplicación de CRISPR/Cas9 para la edición de células humanas es relativamente reciente, todavía existen varias limitaciones asociadas al uso de esta metodología. Uno de los principales puntos débiles es la aparición de efectos "off-target", es decir, mutaciones en regiones del genoma no seleccionadas por la nucleasa Cas9. El progreso y la mejora continuos del sistema CRISPR incluyen el uso de la Cas9 nicasa (Cas9n) en lugar de la Cas9, lo que ha permitido reducir los efectos "off-target", ya que esta nucleasa produce roturas de una sola hebra muy próximas entre sí, imitando una rotura de doble hebra.[253,276]

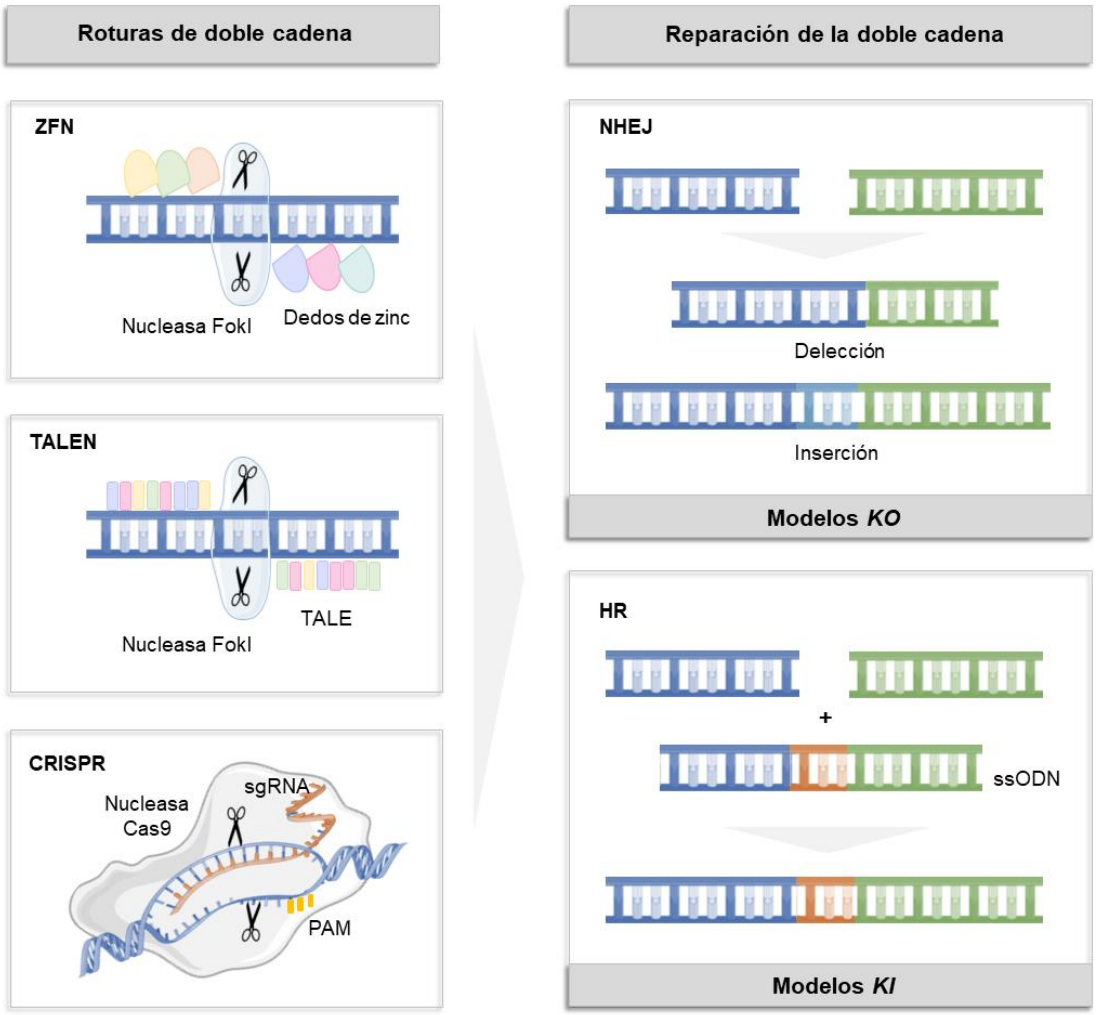


**Figura 9. Tecnologías de edición del genoma con nucleasas.** Los tres tipos de nucleasas más utilizados son los sistemas ZFN, TALEN y CRISPR, que pueden inducir roturas de doble cadena [DSB] en regiones diana, seguidas de la activación de los mecanismos de reparación del ADN. Estos DSB en las regiones diana pueden ser reparados por NHEJ o HR. NHEJ es un mecanismo de reparación propenso a errores, que generalmente da lugar a *indels* heterogéneos (deleciones e inserciones), mientras que HR es un método de reparación preciso en el que se utiliza una plantilla de ADN homóloga, llamada ssODN, para reparar el sitio diana de daño en el ADN. Creado con Servier Medical Art (https://smart.servier.com/).

El uso de CRISPR/Cas9 para la corrección de mutaciones puntuales en células de pacientes también presenta un reto importante porque la mayoría de los tipos celulares reparan preferentemente la rotura de la doble cadena por NHEJ en lugar de por HR, que es lo que se requiere para la corrección de la mutación. Actualmente se están investigando numerosas estrategias para

mejorar la eficacia de la HR modificando el molde necesario para la reparación, inhibiendo transitoriamente uno de los componentes del mecanismo NHEJ para promover la HR o mejorando los métodos de transfección.[277–279]

Hasta la fecha, han surgido varias estrategias en el campo de los Trastornos Plaquetarios Congénitos. Varios grupos han utilizado esta técnica de edición del genoma para generar mutaciones específicas con el fin de estudiar los mecanismos subyacentes de la patogénesis, como un modelo *KO* de PTPRJ,[254] que permitió determinar su papel en la megacariopoyesis, o un ratón *KI* portador de la variante ITGA2B c.2659C > T para establecer su efecto en la Trombastenia de Glanzmann.[280] Además, se ha desarrollado recientemente un sistema de megacariocitos editados con CRISPR para el cribado rápido de las funciones de los genes plaquetarios, surgiendo como una herramienta potencial para el estudio de variantes detectadas en pacientes.[281]

Por último, esta estrategia potencial no sólo se está utilizando para reproducir y caracterizar los mecanismos fisiopatológicos de las variantes detectadas en los pacientes, sino que también se está utilizando ya como una estrategia prometedora para abordar las enfermedades monogénicas. Recientemente, se ha desarrollado la corrección de alelos patogénicos de microduplicación para el Síndrome de Hermansky-Pudlak 1 (HPS1) a la secuencia de tipo salvaje en fibroblastos primarios derivados de pacientes,[282] lo que proporciona un futuro prometedor para la terapia génica en el campo de los Trastornos Plaquetarios Congénitos.

# HIPÓTESIS

Los Trastornos Plaquetarios Congénitos [TPC] comprenden un grupo amplio y heterogéneo de enfermedades raras que predisponen a los pacientes a la trombocitopenia y/o a las hemorragias, pero también, en algunos casos, a otras complicaciones, como las neoplasias hematológicas o las manifestaciones sindrómicas. El diagnóstico es difícil y requiere múltiples pruebas de laboratorio, así como una confirmación molecular final. La introducción de las herramientas de secuenciación de alto rendimiento [HTS] en la práctica clínica ha mejorado y simplificado significativamente el diagnóstico de los pacientes. Sin embargo, a pesar de la mejora sustancial que han aportado las herramientas de HTS, aún persisten dos grandes retos.

En primer lugar, la interpretación de las variantes encontradas por HTS y su clasificación según la ACMG / AMP. Por lo tanto, se recomienda encarecidamente que se compartan los datos. Por esta razón, el SSC-GinTH del ISTH desarrolló el proyecto GoldVariant para identificar la mayoría de las variantes reportadas en los trastornos plaquetarios para un envío rápido y fácil a ClinVar. Por lo tanto, estas variantes serán reclasificadas y curadas adecuadamente por pequeños grupos de trabajo de expertos. En ese contexto, los paneles de expertos de curación de variantes de ClinGen han desarrollado reglas específicas y adaptadas de la ACMG / AMP para los genes *ITGA2B* / *ITGB3* y *RUNX1*. No obstante, para la curación de las variantes, especialmente para las novedosas o de significado incierto, se recomienda el desarrollo de modelos funcionales para demostrar formalmente su papel en la patogénesis y el mecanismo subyacente a la enfermedad.

La variante *missense* c.167T>C; p.Leu56Ser previamente descrita en el factor transcripcional *RUNX1* ha suscitado una gran controversia sobre si se trata de una alteración que predispone a la leucemia o de un polimorfismo benigno. Esta variante se ha encontrado en algunos pacientes con sospecha clínica y de laboratorio de trastorno plaquetario familiar con predisposición a la leucemia mielógena aguda [FPD/AML]. Además, se ha descrito que esta variante está asociada a una activación transcripcional alterada de varios genes diana. Sin embargo, también es una variante relativamente frecuente en la población general, lo que lleva a su clasificación como benigna por ClinGen. Por lo tanto, la confirmación final del papel biológico y funcional de RUNX1 p.Leu56Ser en

FPD/AML requiere la generación de un modelo experimental que reproduzca la alteración humana, para desvelar los potenciales mecanismos de patogénesis.

El segundo reto que debemos afrontar es el hecho de que, a pesar del éxito en el diagnóstico y la caracterización fenotípica mediante un enfoque integrativo de los paneles de secuenciación dirigidos y los estudios funcionales, sigue habiendo pacientes y familias sin un diagnóstico final. Teniendo en cuenta la prevalencia desconocida y que los CPDs están infradiagnosticados, además del hecho de que varios procesos fisiológicos de la megacariopoyesis y de la función plaquetaria no están bien esclarecidos, es muy posible que un número importante de trastornos estén causados por variantes en genes que no han sido descritos o caracterizados hasta ahora.

En los últimos años, se han descrito nuevos genes relacionados con los CPD gracias al uso de WES y WGS. De hecho, la primera descripción en el mundo de una trombocitopenia asociada a variantes genéticas en *TPM4* se realizó utilizando estas tecnologías. *TPM4* codifica la tropomiosina-4, una proteína implicada en el citoesqueleto de actina, cuya alteración provoca macrotrombocitopenia. No obstante, es necesario profundizar en la caracterización del fenotipo asociado a las variantes de *TPM4*, así como realizar más investigaciones para evaluar el papel de esta proteína crucial en el remodelado del citoesqueleto de los megacariocitos y las plaquetas.

Asimismo, se describió la primera evidencia de alteraciones moleculares en *GALE* asociadas a trastornos hematológicos mediante el uso de WGS. La proteína UDP-Galactosa-4-Epimerasa está implicada tanto en el metabolismo de la galactosa como en la glicosilación de proteínas. A pesar de que se han descrito varios pacientes portadores de variantes patogénicas en *GALE* que presentan trombocitopenia, los mecanismos de patogenicidad siguen sin conocerse. Por lo tanto, un estudio en profundidad del papel de esta enzima en los procesos de megacariopoyesis y trombopoyesis, y la correlación con las reacciones de glicosilación que tienen lugar durante ambos procesos (que son esenciales para la correcta formación y función de las plaquetas) permitirá esclarecer los mecanismos moleculares subyacentes a este fenotipo.

Por lo tanto, la integración del análisis genómico mediante diferentes metodologías de secuenciación de alto rendimiento, junto con aproximaciones funcionales *in vitro, ex vivo* o *in vivo*, será útil para caracterizar y curar variantes de significado incierto en el factor transcripcional *RUNX1*, y para evaluar su papel en los trastornos plaquetarios y la progresión de la leucemia, así como para proporcionar nuevos descubrimientos sobre los procesos biológicos y fisiopatológicos desencadenados por variantes en dos nuevos genes implicados en los Trastornos Plaquetarios Congénitos: *TPM4* y *GALE*.

# OBJETIVOS

**Objetivo General**

Caracterizar el fenotipo clínico y plaquetario asociado a las alteraciones moleculares encontradas por secuenciación de alto rendimiento en genes implicados en los Trastornos Plaquetarios Congénitos, y demostrar el mecanismo relacionado con la patogenicidad utilizando cultivos de megacariocitos *in vitro* y *ex vivo*, y modelos de enfermedad *in vivo* generados por la tecnología CRISPR/Cas9.

**Objetivos Específicos**

- Caracterización funcional de la variante RUNX1 p.Leu56Ser, encontrada previamente por un panel de genes de diseño propio, utilizando una aproximación *in vivo*.
    - Generar un modelo murino *knock-in* portador de la variante RUNX1 p.Leu43Ser (que imita a la variante en línea germinal humana p.Leu56Ser) mediante CRISPR/Cas9, para establecer su implicación en el trastorno plaquetario.
    - Conocer las vías de señalización y los determinantes biológicos que subyacen a la progresión leucémica asociada a las variantes de *RUNX1*.

- Aplicación de la secuenciación del exoma completo para la identificación de nuevos genes implicados en los Trastornos Plaquetarios Congénitos, y evaluación de los mecanismos fisiopatológicos que originan la enfermedad mediante modelos funcionales *in vivo* y *ex vivo*.
    - Analizar el fenotipo clínico y de laboratorio de la tercera familia en el mundo con trombocitopenia asociada a variantes en *TPM4*, y caracterizar en profundidad su papel en la remodelación del citoesqueleto plaquetario.
    - Evaluar el fenotipo clínico y plaquetario de tres pacientes de dos familias no relacionadas con macrotrombocitopenia sindrómica asociada a variantes en heterocigosis compuesta en *GALE*.
    - Investigar el efecto funcional de las variantes genéticas identificadas en *GALE* durante la megacariopoyesis y la trombopoyesis, y su papel en la

glicosilación de los megacariocitos y las plaquetas utilizando un modelo de sobreexpresión *in vitro* y un cultivo *ex vivo* de megacariocitos de pacientes.

# RESULTADOS

Esta sección incluye el trabajo experimental realizado en esta tesis, incluyendo Material y Métodos, Resultados y Discusión. Esta sección se ha dividido en cuatro capítulos:

**Capítulo 1.** Marín-Quílez A, García-Tuñón I, Fernández-Infante C, Hernández-Cano L, Palma-Barqueros V, Vuelta E, Sánchez-Martín M, González-Porras JR, Guerrero C, Benito R, Rivera J, Hernández-Rivas JM, Bastida JM. **Characterization of the Platelet Phenotype Caused by a Germline *RUNX1* Variant in a CRISPR/Cas9-Generated Murine Model.** *Thrombosis and Haemostasis*. 2021;121(9):1193-1205. doi: 10.1055/s-0041-1723987. PMID: 33626581.

**Capítulo 2.** Marin-Quilez A, Sanz D, del Rey M, Ordoñez JL, Diaz-Ajenjo L, González-Porras JR, Guerrero C, Pérez-Losada J, Rivera J, Hernández-Rivas JM, Benito R, García-Tuñón I, Bastida JM. **Expanding the role of germline *RUNX1* variants in leukemogenesis in a murine model generated by CRISPR/Cas9.** *Manuscript in preparation.*

**Capítulo 3.** Marín-Quílez A, Vuelta E, Díaz-Ajenjo L, Fernández-Infante C, García-Tuñón I, Benito R, Palma-Barqueros V, Hernández-Rivas JM, González-Porras JR, Rivera J, Bastida JM**. A novel nonsense variant in *TPM4* caused dominant macrothrombocytopenia, mild bleeding tendency and disrupted cytoskeleton remodeling.** *Journal of Thrombosis and Haemostasis.* 2022;20(5):1248-1255. doi: 10.1111/jth.15672. PMID: 35170221

**Capítulo 4.** Marín-Quílez A, Di Buduo CA, Díaz-Ajenjo L, Abbonante V, Vuelta E, Soprano P, Miguel-García C, Santos-Mínguez S, Serramito-Gómez I, Ruiz-Sala P, Peñarrubia MJ, Pardal E, Hernández-Rivas JM, González-Porras JR, García-Tuñón I, Benito R, Rivera J, Balduini A, Bastida JM. **Novel variants in *GALE* cause syndromic macrothrombocytopenia by disrupting glycosylation and thrombopoiesis.** *Blood. Second revision.*

Todos ellos se han desarrollado para cumplir el objetivo general de este trabajo y dan título a la tesis doctoral: **"Caracterización de nuevos genes y variantes implicados en los Trastornos Plaquetarios Congénitos: de los datos genómicos a los estudios funcionales".**

Al final de cada capítulo se incluye el material suplementario correspondiente a cada uno de los apartados indicados.

Además, una Discusión General, con datos adicionales y que comprende toda la investigación, se aborda en una sección separada de esta tesis.

# CAPÍTULO 1

## Characterization of the Platelet Phenotype Caused by a Germline *RUNX1* Variant in a CRISPR/Cas9-Generated Murine Model.

Ana Marín-Quílez[1], Ignacio García-Tuñón[1], Cristina Fernández-Infante[1], Luis Hernández-Cano[1], Verónica Palma-Barqueros[2], Elena Vuelta[1,3], Manuel Sánchez-Martín[1,3], José Ramón González-Porras[4], Carmen Guerrero[1], Rocío Benito[1], José Rivera[2,5*], Jesús María Hernández-Rivas[1,4*] and José María Bastida[4,5*].

[1] Cancer Research Center - CSIC, University of Salamanca, Instituto de Investigación Biomédica de Salamanca (IBSAL), Spain; [2] Servicio de Hematología y Oncología Médica, Hospital Universitario Morales Meseguer, Centro Regional de Hemodonación, University of Murcia, IMIB - Arrixaca, CIBERER-U765, Murcia, Spain; [3] Transgenic Facility, Nucleus, University of Salamanca, Spain; [4] Department of Hematology - University Hospital of Salamanca - IBSAL, Spain; [5] On behalf of the "Grupo Español de Alteraciones Plaquetarias Congénitas, (GEAPC)"; Hemorrhagic Diathesis Working Group, SETH. *These authors share senior authorship.

*Thrombosis & Haemostasis*. 2021 Sep;121(9):1193-1205. doi: 10.1055/s-0041-1723987. PMID: 33626581

## Caracterización del fenotipo plaquetario causado por una variante germinal en *RUNX1* en un modelo murino generado por CRISPR/Cas9.

### Introducción

El trastorno plaquetario congénito con predisposición a leucemia mieloide aguda (FPD/AML) está causado por variantes germinales en *RUNX1*. Posee herencia autosómica dominante y suele cursar con trombocitopenia leve/moderada con volumen plaquetario normal y/o aumento de la clínica hemorrágica por disfunción plaquetaria, si bien los mecanismos de patogenicidad son muy heterogéneos. Además, los pacientes tienen riesgo de desarrollar hemopatía maligna. Dado que no hay un método diagnóstico definitivo, se emplea la secuenciación masiva para su diagnóstico genético. Sin embargo, es necesario definir la patogenicidad de las variantes encontradas y, para ello, se siguen las recomendaciones del Colegio Americano de Genética Molecular. No obstante, para demostrar la relación final de causalidad y los mecanismos subyacentes etiopatogénicos, los modelos celulares y/o animales pueden ser de gran utilidad.

### Objetivo

Generación de un modelo murino portador de la variante germinal p.Leu43Ser en RUNX1 (p.Leu56Ser en humanos) mediante la tecnología de edición genómica CRISPR/Cas9. Caracterización fenotípica y funcional del trastorno plaquetario, e identificación de los mecanismos de patogenicidad.

### Metodología

La generación del modelo murino *knock-in* se realizó mediante la tecnología de edición genómica CRISPR/Cas9 en su variante Cas9 doble-nickasa. Se diseñaron dos guías dirigidas frente al exón 2 de *RUNX1* flanqueando el sitio diana a mutar. Las guías, el RNA codificante para la nucleasa y el DNA molde con la mutación p.Leu43Ser fueron microinyectados en zigotos de la cepa C57BL/6J e implantados en hembras CD1 pseudopreñadas. Los ratones nacidos se secuenciaron para seleccionar los portadores de la variante. La función

plaquetaria se evaluó en un total de 75 ratones; 25 de cada genotipo ($RUNX1^{WT/WT}$, $RUNX1^{WT/L43S}$, $RUNX1^{L43S/L43S}$). El tiempo de sangrado se evaluó mediante cortes de cola. La caracterización fenotípica y funcional se realizó por citometría de flujo, y se determinó el recuento de plaquetas CD41+, la secreción de gránulos α y δ (CD62P, CD63); la activación de la integrina $\alpha_{IIb}\beta_3$ (JON/A, fibrinógeno); y agregación plaquetaria (CD9). Se empleó microscopía confocal para evaluar la adhesión, capacidad de *spreading*, y niveles de fosforilación de PKC. Los agonistas utilizados fueron: trombina (0,1-1U/mL), PMA (3µM) y ADP (30µM).

**Resultados**

En general, los ratones $RUNX1^{L43S/L43S}$ y $RUNX1^{WT/L43S}$ mostraron un tiempo de sangrado de la cola significativamente mayor que los ratones $RUNX1^{WT/WT}$, lo que indica que la variante juega un papel importante en la hemostasia. Sin embargo, sólo los ratones homocigotos mostraron una leve trombocitopenia. Los ratones $RUNX1^{L43S/L43S}$ y $RUNX1^{WT/L43S}$ presentaron una menor secreción de los gránulos α, sin diferencias en la liberación de los gránulos δ. Los niveles de activación de la integrina $\alpha_{IIb}\beta_3$, la unión del fibrinógeno y la agregación plaquetaria fueron significativamente más bajos en las plaquetas de $RUNX1^{L43S/L43S}$ y $RUNX1^{WT/L43S}$ que en $RUNX1^{WT/WT}$, tras la estimulación con los agonistas PMA, ADP y altas dosis de trombina. Sin embargo, no se encontraron diferencias en la agregación empleando bajas dosis de trombina y $CaCl_2$ 2mM. Estos resultados sugieren una alteración en la segunda ola de activación por trombina, dependiente de PKC, sin afectación de la primera ola de activación plaquetaria por trombina dependiente de calcio. Los niveles disminuidos de fosfo-PKC tras la activación con trombina 1U/mL y, principalmente, con PMA, en $RUNX1^{L43S/L43S}$ y $RUNX1^{WT/L43S}$ vs. $RUNX1^{WT/WT}$ confirmaron la alteración funcional en PKC. Por último, no se detectaron diferencias en la capacidad de adhesión plaquetaria entre ratones de los tres genotipos. Sin embargo, las plaquetas de los ratones $RUNX1^{L43S/L43S}$ y $RUNX1^{WT/L43S}$ presentaron una disminución de la capacidad de *spreading* tras 15 y 30 minutos de estímulo con trombina respecto a plaquetas control, demostrando una alteración de la vía de señalización plaquetaria *inside-out*, que justifica el retraso en la retracción del coágulo observada en los ratones $RUNX1^{L43S/L43S}$.

**Conclusiones**

Se ha realizado con éxito la edición genómica mediante CRISPR/Cas9 en línea germinal, generando el un modelo murino portador de la variante p.Leu43Ser en RUNX1, demostramos la viabilidad y utilidad de generar un modelo animal para evaluar la patogenicidad de variantes germinales en *RUNX1* identificadas en humanos. La disfunción plaquetaria causada por la variante p.Leu43Ser en RUNX1 se relaciona con hipo-activación de la integrina $\alpha_{IIb}\beta_3$, y una alteración funcional en la vía de señalización mediada por PKC. Ellos se refleja en un defecto de agregación, secreción de gránulos α y *spreading* plaquetario.

# CAPÍTULO 2

## Expanding the role of germline *RUNX1* variants in leukemogenesis in a murine model generated by CRISPR/Cas9

Marin-Quilez A[1], Sanz D[1], del Rey M[1], Ordoñez JL[1,2], Diaz-Ajenjo L[1], González-Porras JR[3], Guerrero C[1], Pérez-Losada J[1], Rivera J[4,#], Hernández-Rivas JM[1,3], Benito R[1], García-Tuñón I[1], Bastida JM[3,#].

[1] Cancer Research Center - CSIC, University of Salamanca, Instituto de Investigación Biomédica de Salamanca (IBSAL), Spain; [2] Laboratory of Pharmacology, Department of Physiology and Pharmacology, Faculty of Pharmacy, University of Salamanca, Salamanca, Spain; [3] Department of Hematology - University Hospital of Salamanca - IBSAL, Spain; [4] Servicio de Hematología y Oncología Médica, Hospital Universitario Morales Meseguer, Centro Regional de Hemodonación, University of Murcia, IMIB - Arrixaca, CIBERER-U765, Murcia, Spain; [#] On behalf of the "Grupo Español de Alteraciones Plaquetarias Congénitas, (GEAPC)".

*Manuscript in preparation.*

## Expandiendo el papel de las variantes germinales de *RUNX1* en la leucemogénesis en un modelo murino generado por CRISPR/Cas9.

### Introducción

Las variantes germinales en *RUNX1* provocan el Trastorno Plaquetario Congénito con Predisposición a Leucemia Mieloide (FPD/AML). Se estima que en el 40% de los casos desarrollan una hemopatía maligna al adquirir un segundo evento somático, aunque los mecanismos de leucemogénesis no están bien esclarecidos. Los modelos celulares y/o animales nos pueden ayudar para determinar la patogenicidad de las variantes en *RUNX1*, y su potencial mecanismo leucemogénico.

### Objetivos

Caracterización de la leucemogénesis en un modelo murino *knock-in* generado por CRISPR/Cas9 portador de la variante germinal p.Leu43Ser en RUNX1, e identificación de segundos eventos y genes transcripcionalmente desregulados.

### Metodología

Se estudiaron 75 ratones; 25 de cada genotipo ($RUNX1^{WT/WT}$, $RUNX1^{WT/L43S}$, $RUNX1^{L43S/L43S}$). Se analizaron las poblaciones maduras e inmaduras por citometría de flujo (CF) (Gr1*FITC, Mac1*PE, CD45*PerCPCy5.5, ckit*PECy7, CD3*APC, B220*APCH7, Sca1*PB) en sangre periférica (SP) cada 3 meses, en médula ósea (MO) y bazo. Los estudios de morfología/anatomía patológica se realizaron de muestras de MO y bazo al sacrificar los ratones (punto final: 22 meses, o por síntomas de enfermedad). Para detectar segundo eventos, se secuenciaron todos los exones de *RUNX1* y se analizaron genes desregulados en MO de 3 ratones / genotipo mediante RNA-seq. El análisis de la expresión diferencial entre los grupos experimentales se realizó con DESeq2 y goseq.

**Resultados**

Hemos detectado la presencia de células aberrantes mieloides Mac1+ Sca1+ ckit- en SP de dos ratones RUNX1$^{L43S/L43S}$: en *Hom1* un 15,3% a los 15 meses y; *Hom2* un 7,3% a los 20 meses, mientras que se detectaron un 2,4% de células aberrantes en sólo un ratón RUNX1$^{WT/L43S}$ (*Het1*) a los 21 meses de edad. Las células Mac1+ Sca1+ ckit- estaban presentes tanto en MO como en bazo en los tres ratones afectos. Además, la MO mostraba distribuciones anómalas de las diferentes series hematopoyéticas e hipercelularidad, mientras que el bazo de los ratones *Hom1* y *Hom2* mostró una desestructuración de la pulpa blanca/roja del bazo, con presencia de células apoptóticas, y esplenomegalia. No se detectaron células Mac1+ Sca1+ ckit- en ningún ratón RUNX1$^{WT/WT}$. Los análisis de DNA-seq no mostraron mutaciones somáticas adicionales en *RUNX1* en los tres ratones enfermos. Sin embargo, los estudios de RNA-seq mostraron 698 genes significativamente desregulados en los 3 ratones enfermos vs. 6 ratones RUNX1$^{WT/WT}$, RUNX1$^{WT/L43S}$ y RUNX1$^{L43S/L43S}$ sanos, destacando la sobrexpresión de *Rapgef1*, cuya alteración se ha relacionado previamente con leucemia mieloide crónica y tumores sólidos.

**Conclusión**

Hemos identificado células aberrantes en 2 ratones con la variante RUNX1 p.Leu43Ser en homocigosis y en un ratón heterocigoto. No se han identificado mutaciones somáticas en *RUNX1* adicionales. Estos ratones presentan una sobreexpresión de *Rapgef1*, lo que podría sugerir un nuevo mecanismo de progresión leucémica que requiere estudios adicionales.

# CAPÍTULO 3

## A novel nonsense variant in *TPM4* caused dominant macrothrombocytopenia, mild bleeding tendency and disrupted cytoskeleton remodeling.

Ana Marín-Quílez[1], Elena Vuelta[1,2], Lorena Díaz-Ajenjo[1], Cristina Fernández-Infante[1], Ignacio García-Tuñón[1], Rocío Benito[1], Verónica Palma-Barqueros[3], Jesús María Hernández-Rivas[1,4], José Ramón González-Porras[4], José Rivera[2,5*], and José María Bastida[4,5*].

[1] IBSAL, CIC, IBMCC, Universidad de Salamanca-CSIC, Salamanca, Spain; [2] Transgenic Facility, Nucleus, University of Salamanca, Salamanca, Spain; [3] Department of Hematology and Oncology, Hospital Universitario Morales Meseguer, Centro Regional de Hemodonación, Universidad de Murcia, IMIB-Arrixaca, CIBERER-U765, Spain; [4] Department of Hematology, Complejo Asistencial Universitario de Salamanca (CAUSA), Instituto de Investigación Biomédica de Salamanca (IBSAL), Universidad de Salamanca (USAL), Spain; [5] On behalf of "Grupo Español de Alteraciones Plaquetarias Congénitas (GEAPC)", SETH. *These authors share senior authorship.

*Journal of Thrombosis and Haemostasis*. 2022;20(5):1248-1255. doi: 10.1111/jth.15672. PMID: 35170221

## Una nueva variante de codón de parada en *TPM4* causa macrotrombocitopenia dominante, una leve tendencia a la hemorragia y una alteración de la remodelación del citoesqueleto.

### Introducción

Las macrotrombocitopenias congénitas (MCTP) son trastornos raros y heterogéneos causados por alteraciones en genes implicados en las diferentes fases de la megacariopoyesis, la trombopoyesis y/o la liberación de plaquetas. Su diagnóstico supone un reto debido a la escasa especificidad de los ensayos funcionales de caracterización plaquetaria, el gran número de genes involucrados en la enfermedad y la difícil evaluación de la patogenicidad de las nuevas variantes detectadas mediante el estudio molecular por secuenciación masiva.

### Objetivo

Caracterización del fenotipo clínico y de laboratorio, e identificación de la alteración molecular subyacente, en un pedigrí con trombocitopenia de etiología incierta.

### Metodología

Se estudió mediante secuenciación del exoma completo (WES) una familia con 5 miembros afectos de macrotrombocitopenia autosómica dominante y sangrado variable, dentro del Proyecto Español de Caracterización de Trastornos Plaquetarios Congénitos. El fenotipo hemorrágico (BS) se evaluó usando la escala ISTH-BAT. La caracterización funcional incluyó: hemograma y frotis de sangre periférica, agregometría (LTA), citometría de flujo (CMF) y Western-Blot (WB). Las proteínas del citoesqueleto y el *spreading* plaquetario se analizaron por inmunofluorescencia (IF) sobre fibrinógeno. Los niveles de mRNA de las tropomiosinas 1-3 se evaluaron mediante qPCR.

## Resultados

Las características de los pacientes se muestran en la Tabla 1. La *propositus* era una mujer de 40 años con macrotrombocitopenia leve crónica y sangrado moderado (II-2). Mediante WES identificamos una nueva variante *nonsense* (c.322C>T; p.Gln108*) en *TPM4* (NM_003290.3). La LTA mostró una moderada hipo-respuesta a bajas dosis de epinefrina y ADP. La CMF mostró una expresión normal de las glicoproteínas de superficie (GPIX, GPIb, GPVI, $\alpha_{IIb}\beta_3$) y de la secreción de gránulos α/δ. Mediante *inmunoblotting* detectamos niveles de TPM4 significativamente reducidos respecto a plaquetas control. Los niveles de mRNA de *TPM2* y *TPM3* en la enferma fueron 8 y 14 veces (respectivamente) más altos que en los controles, sugiriendo un posible mecanismo compensatorio. El *spreading* plaquetario de los afectos (II.2, II.4) estaba alterado respecto a controles y familiar no portador (II.3), con disminución en la formación de filipodios y lamelipodios tras la estimulación con TRAP-6 y CRP. La localización celular de TPM4 en las plaquetas activadas del paciente fue anómala, sin alteración de la de otras proteínas del citoesqueleto (actina, actinina-1, β-tubulina y miosina-9).

## Conclusión

Hemos identificado y caracterizado una nueva variante patogénica de tipo *nonsense* (p.Gln108*) en *TPM4* asociada a macrotrombocitopenia familiar con efecto deletéreo en la agregación y en el *spreading* plaquetario. Ello refuerza el papel funcional de TPM4 en la correcta remodelación del citoesqueleto. Nuestro estudio expande y consolida la patología *TPM4*-RT y apoya la inclusión de *TPM4* como gen Tier1 (criterios ISTH), relacionado con MCTP congénitas.

**Tabla 1: Caracteristicas clínicas de los miembros de la familia.**

| Paciente | Edad | Plaquetas ($x10^9$/L) | MPV (fL) | BS | Variante en TPM4 (p.Gln108*) |
|---|---|---|---|---|---|
| I-1 | 60 | 145 | 12.7 | 2 | Heterocigoto |
| I-2 | 64 | 121 | 13.5 | 2 | Heterocigoto |
| II-1 | 34 | 140 | 11.8 | 4 | Heterocigoto |
| II-2 | 40 | 111 | 14.7 | 6 | Heterocigoto |
| II-3 | 36 | 180 | 10.9 | 2 | WT |
| II-4 | 33 | 124 | 13.4 | 0 | Heterocigoto |

# CAPÍTULO 4

## Novel variants in *GALE* cause syndromic macrothrombocytopenia by disrupting glycosylation and thrombopoiesis.

Ana Marín-Quílez[1#], Christian Andrea Di Buduo[2#], Lorena Díaz-Ajenjo[1], Vittorio Abbonante[2], Elena Vuelta[1], Paolo María Soprano[2], Cristina Miguel-García[1], Sandra Santos-Mínguez[1], Inmaculada Serramito-Gómez[1], Pedro Ruiz-Sala[3], María Jesús Peñarrubia[4], Emilia Pardal[5], Jesús María Hernández-Rivas[1,6], José Ramón González-Porras[6], Ignacio García-Tuñón[1], Rocío Benito[1], José Rivera[7*#], Alessandra Balduini[2,8#], José María Bastida[6*#].

[1] IBSAL, CIC, IBMCC, Universidad de Salamanca-CSIC, Salamanca, Spain; [2] Department of Molecular Medicine, University of Pavia, Pavia, Italy; [3] Centro de Diagnóstico de Enfermedades Moleculares, Universidad Autónoma de Madrid, CIBERER, IdIPAZ, Madrid, Spain; [4] Department of Hematology, Hospital Clínico Universitario de Valladolid, Spain; [5] Department of Hematology, Hospital Virgen del Puerto, Plasencia, Spain; [6] Department of Hematology, Complejo Asistencial Universitario de Salamanca (CAUSA), Instituto de Investigación Biomédica de Salamanca (IBSAL), Universidad de Salamanca (USAL), Spain; [7] Department of Hematology and Oncology, Hospital Universitario Morales Meseguer, Centro Regional de Hemodonación, Universidad de Murcia, IMIB-Arrixaca, CIBERER-U765, Spain; [8] Department of Biomedical Engineering, Tufts University, Medford, MA, USA. *On behalf of “Grupo Español de Alteraciones Plaquetarias Congénitas (GEAPC)”, Sociedad Española de Trombosis y Hemostasia (SETH). # Equal authors´ contributions

*Blood. Second Revision.*

## Nuevas variantes en *GALE* causan macrotrombocitopenia sindrómica alterando la glicosilación y la trombopoyesis.

### Introducción

La glicosilación es un proceso clave para la correcta megacariopoyesis y la formación de las plaquetas. La enzima UDP-galactosa-4-epimerasa, codificada por *GALE*, está implicada en el metabolismo de la galactosa y en la glicosilación de glucoproteínas (GP). Se desconocen los mecanismos biológicos implicados en la trombocitopenia de pacientes con alteraciones genéticas en *GALE.*

### Objetivo

Evaluar el fenotipo clínico y plaquetario en tres pacientes con macrotrombocitopenia sindrómica asociada a variantes en *GALE*, e investigar el papel de *GALE* en la glicosilación y la trombopoyesis.

### Metodología

Secuenciamos el exoma completo (WES) en 3 pacientes con macrotrombocitopenia sindrómica grave, diátesis hemorrágica moderada, retraso mental, prolapso de válvula e insuficiencia mitrales, cataratas, ictericia y hepatomegalia, reclutados en el proyecto multicéntrico del Grupo Español de Alteraciones Plaquetarias Congénitas (GEAPC). La caracterización fenotípica plaquetaria incluyó recuento sanguíneo completo, frotis de sangre periférica, agregometría, análisis de citometría de flujo de las principales glucoproteínas de superficie y secreción de gránulos inducida por agonistas. La actividad enzimática de la UDP-galactosa-4-epimerasa se midió por HPLC/MS/MS. La megacariopoyesis se evaluó mediante el cultivo de megacariocitos (Mk) a partir de $CD34^+$ purificados de sangre de pacientes, de un control sano, y de $CD34^+$ de sangre de cordón umbilical. Los niveles de GALE, N-acetil-lactosamina (LacNac), Caspasa 8, GPIbα, integrina β1, integrina β3 y factor von Willebrand (FvW) se evaluaron por Western-blotting (WB) en lisados de plaquetas y Mks, y/o por inmunofluorescencia (IF).

**Resultados**

Identificamos en las familias 2 heterocigosis compuestas en *GALE:* Pedigrí A: p.Lys78ValfsX32 y p.Thr150Met; Pedigrí B: p.Val128Met y p.Leu223Pro. El estudio plaquetario de los tres pacientes mostró plaquetas gigantes y/o grises, alteración de la agregación plaquetaria con varios agonistas, reducción severa de la secreción de gránulos alfa (P-selectina) y densos (CD63), y una función normal de la integrina αIIbβ3. La actividad enzimática de GALE y sus niveles proteicos en plaquetas y Mks estaban reducidas significativamente en todos los pacientes. Además, los ensayos en Mks de cordón umbilical mostraron expresión de GALE en la fase tardía de la megacariopoyesis a nivel del retículo endoplasmático (RE).

El cultivo de Mks del paciente del pedigree B (B.II.2) mostró ploidía y maduración normal, así como niveles totales de integrina β3, GPIbα e integrina β1 similares a los Mk control. Sin embargo, la expresión en superficie de GPIbα y de β1 estaba reducida, sugiriendo una alteración en su externalización. Los WB revelaron bandas de GPIbα e integrina β1 de menor peso molecular en los Mk de B.II.2 vs. los del control sano, compatible con su hipoglicosilación. Los estudios de IF demostraron que ambas proteínas quedan retenidas en el RE. Además, observamos deslocalización del FvW en la membrana de los Mks. Estos hallazgos se relacionan con el defecto de formación de proplaquetas y la expresión reducida de GPIbα-IX-V y la integrina β1 en la superficie plaquetaria observada tanto por WB como por CMF. Finalmente, las plaquetas de los enfermos mostraron una disminución significativa de LacNAc, acorde con una hipoglicosilación plaquetaria, y niveles elevados de caspasa 8 activa, sugiriendo una apoptosis incrementada.

**Conclusiones**

Nuestro estudio confirma que *GALE* tiene un papel crítico en trombopoyesis. Por primera vez, demostramos que la trombocitopenia sindrómica asociada a *GALE* se debe a una glicosilación alterada de la integrina β1 y del complejo GPIb-IX-V, que impide su externalización y su participación crítica en la formación de proplaquetas. También se desvela el papel de un mayor aclaramiento plaquetario en esta enfermedad, debido a la hipoglicosilación de las plaquetas.

Por último, demostramos por primera vez el papel de las variantes en *GALE* con una alteración de la función plaquetaria, asociado a una severa reducción de la liberación de los gránulos α/δ, agregación alterada con múltiples agonistas, sin afectación de la función de la integrina. Estos nuevos hallazgos pueden tener implicaciones en el tratamiento de estos pacientes.

# DISCUSIÓN GENERAL

Los Trastornos Plaquetarios Congénitos [CPDs] son un amplio grupo de enfermedades raras asociados frecuentemente a trombocitopenia y/o hemorragias, pero que también predisponen a complicaciones severas, tales como neoplasias hematológicas o manifestaciones multisistémicas. Los pacientes con CPDs representan un reto diagnóstico debido a la gran heterogeneidad de los trastornos, con múltiples genes implicados en el desarrollo de la enfermedad que pueden dar lugar a fenotipos clínicos y de laboratorio diversos, pero a la vez coincidentes.[79,85,89] Sin embargo, actualmente nos encontramos ante una revolución en el diagnóstico genético y molecular debido al desarrollo de los métodos de secuenciación de alto rendimiento [HTS]. Esta tecnología proporciona de forma rápida y económica una gran cantidad de información genómica, facilitando la identificación de variantes genéticas subyacentes a enfermedades con base molecular, y que está sustituyendo potencialmente a las herramientas de secuenciación convencionales.[158,194,204,207]

En este contexto, nuestro grupo en Salamanca ha sido pionero en el uso de HTS para el estudio de pacientes con CPDs involucrados en el proyecto "Caracterización funcional y molecular de pacientes con Trastornos Plaquetarios Hereditarios", por parte del Grupo Español de Alteraciones Plaquetarias Congénitas (GEAPC) (https://www.seth.es/index.php/investigacion.html) mediante el uso de un panel diseñado y validado de 72 genes,[158] y posteriormente, una versión actualizada de 85 genes.[283] Este enfoque se ha visto reflejado en un beneficio directo en la eficacia diagnóstica, que ha pasado del 38% obtenido con las técnicas diagnósticas convencionales al 70% derivado del uso de herramientas HTS dirigidas a genes previamente descritos.[158,194,204,207] Por ello, este enfoque se ha incorporado a la práctica clínica habitual.[97,158]

Sin embargo, el amplio uso de la HTS en los laboratorios clínicos y de investigación ha llevado a un aumento de la detección de variantes en línea germinal de significado desconocido en genes implicados en hematopoyesis y diferenciación de linaje que contribuyen a las neoplasias mieloides.[163,164] Aunque se han establecido recomendaciones de la ACMG / AMP para clasificar las variantes,[162] existe una variabilidad interlaboratorio o interpretaciones alternativas para muchas variantes genéticas, especialmente para las variantes

nuevas. Por lo tanto, se clasifican como significado incierto o de forma discordante entre diferentes laboratorios.[208]

La curación de variantes genéticas asociadas a estas enfermedades es relevante, y se está llevando a cabo actualmente por el Clinical Genome Resource (ClinGen) mediante paneles de expertos en curación de variantes. Este enfoque permite clasificar una variante genómica en un espectro que va desde patogénico a benigno, en lo relativo a una enfermedad concreta y a un patrón de herencia.[81,83] Hasta la fecha, sólo se han reportado reglas específicamente adaptadas de la ACMG / AMP para *RUNX1*,[164,165] y para *ITGA2B* / *ITGB3* en la trombastenia de Glanzmann autosómica recesiva.[166] Gracias a este abordaje, se reclasificó la patogenicidad de varias variantes en *RUNX1* descritas en pacientes: entre las 80 variantes de significado incierto [VUS] descritas anteriormente, 30 se reclasifican ahora como variantes benignas o patogénicas.[164,165] Esta mejora en la clasificación de las variantes es esencial, ya que puede proporcionar dianas específicas para la detección temprana de la neoplasia mieloide o para futuras terapias.[164,284]

Sin embargo, siguen existiendo controversias en torno a las variantes *missense* germinales en *RUNX1*, especialmente fuera del *runt homology domain* (RHD).[285] De estas variantes, la variante c.167T>C [p. Leu56Ser], localizada en la región N-terminal de RUNX1,[286] suscita controversia sobre si se trata de un alelo que predispone a la leucemia o de un polimorfismo benigno.[287] Esta variante se ha encontrado en algunos pacientes con sospecha clínica y de laboratorio de FPD/AML, según han descrito varios grupos.[286,288,289] Pero también es una variante relativamente frecuente en la población general (MAF: 0,0127 en GnomAD), lo que centra su clasificación como benigna.[164,165,290] También se puede encontrar una clasificación de patogenicidad discrepante en varias bases de datos (COSMIC: Patogénica; dbSNP: Probablemente Benigna; ClinVar: Benigna), y según su predicción in-silico (MutationTaster: Causante de enfermedad; PROVEAN: Neutral; SIFT: Tolerada).

Recientemente, Decker et al. publicaron la caracterización funcional de nueve variantes VUS en *RUNX1* previamente reportadas, utilizando 6 variantes patogénicas conocidas y *RUNX1* normal como controles. Así, se describió que

p.Leu56Ser tiene una dimerización normal con CBFβ y una correcta fosforilación de RUNX1, pero una activación transcripcional reducida de genes como rETV1 y rCSF1R.[291] Además, Koh et. al describieron la inhabilidad de RUNX1 p.Leu56Ser para unirse a MLL, lo que sugiere un nuevo modelo de leucemogénesis relacionado con la variante.[288]

Para esclarecer definitivamente la controversia sobre la patogenicidad de la variante RUNX1 p.Leu56Ser, pero también para dilucidar los mecanismos de patogénesis molecular, desarrollamos mediante la herramienta de edición del genoma CRISPR/Cas9 un modelo murino *knock-in* portador de la variante p.Leu43Ser, imitando la alteración humana.[253]

En general, los recuentos de plaquetas en pacientes con FPD/AML suelen ser leve a moderadamente bajos (70-145 × $10^9$/L), pero también pueden ser muy bajos o estar dentro del rango bajo-normal en los pacientes.[292,293] En este contexto, observamos que los ratones RUNX1$^{L43S/L43S}$ tenían un recuento de plaquetas leve, pero significativamente más bajo que los ratones RUNX1$^{WT/L43S}$ y RUNX1$^{WT/WT}$. Los ratones RUNX1$^{WT/L43S}$ no presentaron trombocitopenia. Sin embargo, tanto los ratones RUNX1$^{L43S/L43S}$ como los RUNX1$^{WT/L43S}$ tuvieron tiempos de sangrado más largos que los RUNX1$^{WT/WT}$, lo que indica que la variante RUNX1 p.Leu43Ser tiene un efecto sobre la hemostasia. Los estudios funcionales de las plaquetas mostraron una reducción de la unión al fibrinógeno y de la agregación plaquetaria en RUNX1$^{L43S/L43S}$ y RUNX1$^{WT/L43S}$ en comparación con RUNX1$^{WT/WT}$ tras el tratamiento con trombina, PMA y ADP, sin diferencias tras la estimulación con CRP. Se observó una disminución de la respuesta plaquetaria similar en los ratones RUNX1$^{L43S/L43S}$ y RUNX1$^{WT/L43S}$ al evaluar los gránulos α, sin cambios en la secreción de gránulos δ. Estos hallazgos son bastante diferentes de los observados en muchos pacientes con FPD/AML, en los que se ha informado previamente tanto de la disfunción de la secreción de gránulos como de la activación anormal de la integrina αIIbβ3.[294–296] Sin embargo, pone de manifiesto la heterogeneidad de la disfunción plaquetaria en los portadores de variantes en *RUNX1*.

Además, observamos una correlación entre el genotipo y el fenotipo, ya que los ratones RUNX1$^{L43S/L43S}$ mostraban una función notablemente más disminuida

que el genotipo RUNX1$^{WT/L43S}$, de acuerdo con resultados anteriores que demostraban la importancia de la carga alélica y los niveles de *RUNX1* en la presentación de la enfermedad.[297]

La heterogeneidad fenotípica en las familias con variantes germinales en *RUNX1* implica que las alteraciones genómicas o epigenéticas adicionales pueden ser modificadores importantes tanto de la penetrancia como del fenotipo en relación con el desarrollo de una neoplasia hematológica.[298] *RUNX1* podría actuar como un evento desencadenante tardío de estados preleucémicos hereditarios, forzando la adquisición de diferentes alteraciones moleculares cooperantes.[299,300] Los portadores pueden presentar evidencias de alteraciones premalignas en la médula ósea, siendo la dismegacariopoyesis la más común;[40,301] o, en algunos casos, tienen una expresión aberrante de marcadores de superficie celular, como el CD123, que es un marcador caracterizado de las células madre leucémicas.[302]

Para descubrir el papel de la variante p.Leu56Ser en la progresión leucémica y el segundo evento que promueve la enfermedad, seguimos las poblaciones hematopoyéticas maduras e inmaduras en nuestro modelo de ratón durante toda la vida. Detectamos la presencia de una población mieloide aberrante Mac1$^{+}$ Sca1$^{+}$ ckit$^{-}$, descrita previamente como células leucémicas,[303] en la sangre periférica de dos ratones homocigotos: 15,3% en Hom#1 a los 15 meses, y 7,3% en Hom#2 a los 20 meses, mientras que sólo un ratón heterocigoto (Het#1) mostraba un 2,4% de células aberrantes a los 21 meses de edad. De hecho, las células Mac1$^{+}$ Sca1$^{+}$ ckit$^{-}$ estaban presentes tanto en la médula ósea como en el bazo de los tres ratones afectos, mientras que no se detectaron células Mac1$^{+}$ Sca1$^{+}$ ckit$^{-}$ en ninguno de los ratones RUNX1$^{WT/WT}$.

El segundo evento más frecuente es la alteración somática de *RUNX1* en lugar de otros remodeladores de la cromatina y reguladores transcripcionales diferentes, como *GATA2, BCOR, PHF6* y *WT1.*[117,293,304] No se han observado variantes somáticas en *RUNX1* en los portadores antes del desarrollo de la neoplasia, mientras que se han notificado variantes somáticas premalignas en *TET2, DNMT3A, KRAS* y *SRSF2*.[117,293] Las alteraciones en estos genes indican el potencial de la evolución de los estados preleucémicos a leucémicos de las

mutaciones genéticas somáticas. Mecánicamente, la adquisición de alteraciones somáticas patogénicas secundarias puede ser el resultado de un aumento de los procesos mutagénicos en los portadores de variantes germinales en *RUNX1,* caracterizados por una hematopoyesis clonal de inicio temprano, y como resultado de las vías de reparación del ADN desreguladas asociadas a las estas alteraciones de *RUNX1*.[298,299,305]

Nuestros análisis de secuenciación del ADN en los tres ratones afectados no mostraron variantes somáticas adicionales en *Runx1*. Sin embargo, los estudios de RNA-seq mostraron 698 genes significativamente desregulados en los 3 ratones $Mac1^{+}$ $Sca1^{+}$ $ckit^{-}$ frente a los 6 sanos $RUNX1^{WT/WT}$, $RUNX1^{WT/L43S}$ y $RUNX1^{L43S/L43S}$ sanos, destacando la sobreexpresión de *Rapgef1* (también conocido como *C3G*), que es un factor de intercambio de nucleótidos de guanina que activa a las GTPasas de Rap1 con una función relevante en la hemostasia plaquetaria,[306-308] y cuya alteración se ha relacionado previamente con la leucemia mieloide crónica y los tumores sólidos.[308-310] De hecho, hemos detectado en nuestros ratones afectos que el fenotipo más agresivo de la enfermedad se asocia con una mayor expresión de *Rapgef1*, ya que los ratones Hom#1 y Hom#2 presentaron una mayor sobreexpresión del gen que los ratones Het#1, que presentaron niveles similares a los ratones no afectos.

Anteriormente describimos en el modelo murino la disfunción de la vía de señalización PKC-α/β, sin alteraciones en los niveles transcripcionales, como el mecanismo implicado en el trastorno plaquetario. Curiosamente, nuestro RNA-seq reveló la sobreexpresión de *Rapgef1* en los ratones leucémicos, cuya función se ha descrito que está regulada por la PKC.[306,307]

Estos resultados sugieren que la variante murina p.Leu43Ser se asocia con un aumento de la hemorragia debido a una disfunción moderada de las plaquetas causada por la reducción de la activación de la integrina αIIbβ3, la secreción de gránulos α, la alteración de la capacidad de *spreading* sin alteraciones en la adhesión plaquetaria y la disminución de la retracción del coágulo, siendo más significativa en el estado homocigoto. De hecho, la variante en heterocigosis se asocia a una débil predisposición y a una aparición tardía de células aberrantes (4%, a los 21 meses), correlacionándose con el fenotipo benigno asociado a la

variante RUNX1 p.Leu56Ser en el ámbito clínico,*287* pero con un fenotipo más agresivo en los ratones homocigotos (8% de los ratones afectados, a los 15-20 meses), asociado a una mayor sobreexpresión de *Rapgef1*, y a una notable afectación de la médula ósea y el bazo. Estos datos sugieren un mecanismo novedoso de disfunción plaquetaria y progresión de neoplasias hematológicas. Sin embargo, estos resultados deben ampliarse y confirmarse mediante el estudio de pacientes y de más variantes en la línea germinal del gen *RUNX1*, ya que los modelos murinos no reproducen completamente la enfermedad humana.[252]

A pesar de la importante mejora en el diagnóstico de los Trastornos Plaquetarios Congénitos basado en la secuenciación por paneles de genes y en la caracterización funcional de variantes de significado incierto para establecer el vínculo causal genotipo-fenotipo, como demostramos en la Sección de Resultados - Capítulo 1 y Capítulo 2, muchos pacientes siguen sin conseguir un diagnóstico definitivo (el 30% en nuestra cohorte específica).[158,283] El principal problema de la secuenciación de paneles de genes es el limitado número de genes y regiones de interés que pueden analizarse, ya que requiere un diseño previo que incluya candidatos preespecíficos.[97,201,208] Además, varios procesos de la megacariopoyesis y de la función plaquetaria no están bien caracterizados, lo que podría explicar que un número importante de trastornos estén causados por genes no descritos o bien caracterizados hasta ahora.[97,161] Desde 2010, tanto los enfoques de WES como de WGS han permitido identificar más de 15 nuevos genes implicados en los IT.[9,25] Entre estos genes, encontramos el *GNE*, que se asoció con IT por primera vez en 2014,[52] y se estableció como un nuevo trastorno plaquetario en 2018, con la publicación y caracterización de dos pedigríes no relacionados.[137,138] Hasta la fecha, es el único gen *Tier1* asociado a alteraciones en la glicosilación.[81,82] De forma similar, *DIAPH1* se describió por primera vez en 2016 mediante WES en dos pedigríes no relacionados con IT.[197] En la actualidad, se han descrito más de cinco pedigríes y se incluye también como gen *Tier1* para trastornos plaquetarios.[311-313] En cambio, otros genes como *PTPRJ* o *PRKACG* requieren más estudios funcionales y la demostración del vínculo entre genotipo-fenotipo en más pedigríes para consolidar el trastorno plaquetario, por lo que ambos se clasifican como genes *Tier2*.[254,314]

El gen *TPM4*, que codifica para la tropomiosina 4, se describió por primera vez en 2017 mediante WES en cinco miembros de dos familias no relacionadas portadoras de la variante p.Arg69*. Dichos pacientes mostraban una leve tendencia a la hemorragia y un fenotipo plaquetario casi normal.[108] Hasta 2021, *TPM4* se consideraba un gen raro implicado en las IT y estaba clasificado como *Tier2* para los trastornos plaquetarios por el ISTH.[81,82] La identificación y la caracterización clínica, de laboratorio y molecular de un pedigrí español con trombocitopenia relacionada [RT] con *TPM4* (Sección de Resultados - Capítulo 3), hizo que el SSC-GinTH de la ISTH incluyera a *TPM4* entre los genes *Tier1*.[315] De hecho, la incorporación de este gen a la práctica clínica habitual permitió la identificación de otras variantes en diferentes pedigríes de todo el mundo.[316]

Identificamos mediante WES una nueva variante de codón de parada (c.322 C>T; p.Gln108*) en el dominio *coiled coil* de TPM4 en todos los miembros afectos de la familia, cuyo fenotipo se caracterizaba por una leve macrotrombocitopenia y tendencia a la hemorragia.[109] Los portadores de la variante mostraron una agregación plaquetaria normal con varios agonistas, incluyendo dosis bajas de TRAP-6 y colágeno, pero una leve alteración y retraso en la agregación plaquetaria a dosis bajas de ADP y epinefrina, con niveles normales de las principales glucoproteínas, y una unión al fibrinógeno y secreción de gránulos α y δ normales, similar al fenotipo plaquetario observado previamente en los portadores de la variante TPM4 p.Arg69*.[108] Por el contrario, se ha descrito recientemente que los portadores de las variantes *missense* p.Arg182Cys y p.Ala183Val presentan hemorragias relevantes, una secreción y agregación plaquetaria significativamente disminuida, y un recuento de plaquetas y niveles de TPM4 normales o ligeramente reducidos.*316* Las razones de estas diferencias en la hemorragia y el fenotipo plaquetario en estos pacientes con *TPM4*-RT son todavía desconocidas, y requieren más investigaciones. Podemos especular que las variantes heterocigotas de codón de parada en TPM4, como p.Arg69* y p.Gln108*, causan principalmente haploinsuficiencia, lo que se relaciona con la reducción de los niveles de tropomiosina-4, mientras que las variantes *missense* podrían presentar un efecto dominante negativo que exacerbe la disfunción de TPM4 y conduzca a un trastorno plaquetario importante. De hecho, la formación de plaquetas es dependiente de la dosis de

TPM4, lo que podría justificar que ambas variantes p.Arg69* y p.Gln108* se asocien con la trombocitopenia, mientras que las variantes *missense* no lo hacen.[108,109,316] Estos resultados sugieren que es importante no sólo la identificación de *TPM4* como la alteración molecular causante del trastorno, sino que también es importante detectar el tipo de variante, ya que puede tener una relación con el fenotipo.

Además, nuestro estudio expendió el papel funcional de TPM4 en la remodelación del citoesqueleto plaquetario. En primer lugar, observamos una reducción significativa en la formación de filipodios y lamelipodios, así como una reducción severa de las estructuras de *full spreading* en las plaquetas de los pacientes frente a las de control, lo que conduce a una función de *spreading* plaquetario alterada. Además, mostramos por primera vez que la TPM4 en las plaquetas de control está distribuida homogéneamente por todo el citoplasma junto con los filamentos de actina, mientras que la TPM4 Gln108* se acumula principalmente en el centro de las plaquetas del paciente, y la proteína está reducida en los filopodios/lamelipodios en las plaquetas en *spreading*. Así, esta alteración genética conduce a una leve reducción de la localización de TPM4 con otras proteínas del citoesqueleto. La reducción moderada de TPM4 en las estructuras de *spreading* podría explicar el defecto en la remodelación del citoesqueleto, aportando nuevos conocimientos sobre el mecanismo fisiológico subyacente al trastorno.

Nuestros hallazgos apoyan el papel clave de TPM4 en las plaquetas y amplían el fenotipo y el genotipo de *TPM4*-RT, reforzando la importancia de los enfoques funcionales para validar las variantes encontradas por las herramientas de secuenciación. De forma similar, describimos las características clínicas y de laboratorio de tres nuevos pacientes adultos con macrotrombocitopenia sindrómica debida a la heterocigosidad compuesta de cuatro variantes que afectan al gen *GALE*, encontradas por WES, y demostrando la correlación entre las alteraciones moleculares de *GALE* y la alteración de la glicosilación y la trombopoyesis de las plaquetas y los megacariocitos (Sección de Resultados - Capítulo 4).

La primera evidencia que relaciona los defectos de *GALE* y las alteraciones hematológicas fue en 2019, cuando Seo et al. reportaron seis pacientes de un pedigrí con trombocitopenia grave, neutropenia febril y anemia leve, que eran homocigotos para la variante GALE p.Arg51Trp.[142] En 2020, Febres-Aldana et al. describieron a un niño con fallo de la médula ósea y cardiopatía congénita compleja asociada a una heterocigosidad compuesta en GALE (p.Arg51Trp y p.Gly237Asp).[143] Por último, en 2021, Markovitz et al. reportaron un paciente con pancitopenia y desregulación inmunitaria debido a una variante de GALE homocigota (p.Thr150Met).[144] Aunque se han notificado tres pedigríes portadores de variantes en *GALE* asociadas a anomalías hematológicas y a diferentes fenotipos, no hay pruebas sobre el mecanismo que desencadena la enfermedad en los pacientes portadores de variantes en *GALE.*

En esta tesis, hemos estudiado las variantes en *GALE* desde una perspectiva funcional, para caracterizar los mecanismos moleculares subyacentes a la enfermedad. En primer lugar, demostramos que el patrón de glicosilación está alterado en las plaquetas de los pacientes portadores de las variantes identificadas en *GALE*, descubriendo la ausencia de integrina β1 glicosilada madura, y una severa reducción del complejo GPIb-IX-V. Se detectaron niveles normales de la integrina β3, lo que sugiere una conservación sustancial de esta proteína en la superficie de las plaquetas. Además, las plaquetas de los pacientes estaban hipoglucosiladas y eran más apoptóticas. A continuación, desarrollamos un modelo *in vitro* basado en la sobreexpresión de las variantes en *GALE* en la línea celular humana K652, que se diferenciaron a un fenotipo similar al de los megacariocitos. Además, realizamos experimentos adicionales utilizando Mks diferenciados *in vitro* a partir de la sangre periférica del paciente. Esta caracterización funcional nos permitió demostrar, por primera vez, que las variantes en *GALE* no alteran la maduración de las Mks, sino que interrumpen la trombopoyesis, afectando al proceso de formación de las proplaquetas. Observamos en las Mks de los pacientes niveles normales de la GPIbα total y de la integrina β1, pero una disminución significativa de su expresión en superficie, lo que sugiere una externalización alterada de las integrinas a la membrana plasmática en comparación con los controles sanos. De hecho, los niveles totales y en membrana de la integrina β3 eran comparables a los de los

controles sanos. Por último, los estudios de proteína de los lisados totales de Mk revelaron bandas de menor peso molecular para la integrina β1 y la GPIbα, lo que sugiere su hipoglucosilación. Por lo tanto, la disfunción de la GALE se asocia con una alteración de la glicosilación y la externalización de la GPIbα y la integrina β1, quedando retenidas en el retículo endoplásmico de las Mks, donde GALE tiene su papel principal durante la megacariopoyesis tardía. La ausencia de ambas proteínas, junto con la deslocalización del vWF, en la membrana de las Mks, justifica la alteración en la formación de proplaquetas, y la producción de plaquetas con morfología, función y viabilidad alteradas.

Nuestro estudio no sólo amplía el conocimiento del trastorno relacionado con *GALE* desvelando el papel esencial de GALE en la glicosilación, la formación, la función y la eliminación de las plaquetas, sino que también proporciona nuevas perspectivas para comprender los mecanismos biológicos que subyacen a la biología y la fisiopatología de la integrina β1 y el complejo GPIb-IX-V, que son proteínas clave en la producción y la función de las plaquetas. Además, consideramos que nuestras investigaciones demuestran la causalidad entre genotipo-fenotipo, y por lo tanto, *GALE* debería incluirse en los paneles de secuenciación para el cribado rutinario de los Trastornos Plaquetarios Congénitos.

En resumen, la presente investigación pone de manifiesto la utilidad de las técnicas de secuenciación de alto rendimiento para identificar las bases moleculares de un grupo de trastornos ultra-raros y heterogéneos, en combinación con enfoques funcionales para comprender los mecanismos biológicos que subyacen a la fisiopatología. La combinación de ambas metodologías se propone como una estrategia óptima para el correcto diagnóstico de los Trastornos Plaquetarios Congénitos, tanto para la secuenciación de paneles de genes dirigidos y la validación de las variantes novedosas, desconocidas, o alteraciones muy controvertidas, como para el estudio de nuevos genes con función y significado desconocidos detectados por WES / WGS. De hecho, la mejora en la interpretación de nuevos genes y variantes mediante técnicas automatizadas en los últimos años, basadas en bases de datos exhaustivas que integran el fenotipo-genotipo de amplias poblaciones, en combinación con consorcios de expertos en la materia, facilitará

el diagnóstico correcto de los pacientes, proporcionando no sólo una atención sanitaria adecuada sino también una terapia personalizada. Por último, la aplicación de la tecnología CRISPR/Cas9 no sólo permite generar modelos experimentales que reproduzcan las variantes genéticas seleccionadas que se encuentran en los pacientes, sino que establece la base técnica para su posible uso como herramienta terapéutica en el futuro.[317]

# CONCLUSIONES

1. La implementación integrativa de técnicas de secuenciación de alto rendimiento y abordajes funcionales para caracterizar variantes en genes ultra raros o clínicamente relevantes son de gran utilidad e importancia en los Trastornos Plaquetarios Congénitos.

2. El modelo murino *knock-in* portador de la variante RUNX1 p.Leu43Ser (que imita la variante humana RUNX1 p.Leu56Ser) permitió evaluar su efecto deletéreo en la hemostasia, basado en la hipoactivación de la integrina αIIbβ3, y una alteración funcional en la vía de señalización mediada por la PKC. Esto se refleja en un defecto de agregación, de secreción de gránulos α y de *spreading* de las plaquetas, que justifica los tiempos de sangrado incrementados. El fenotipo fue más notable en la homocigosis, reforzando la importancia de los niveles de *RUNX1* en el fenotipo de la enfermedad.

3. RUNX1 p.Leu43Ser en homocigosis se relaciona con la presencia de una población aberrante $Mac1^{+}$ $Sca1^{+}$ $ckit^{-}$, alteraciones morfológicas de la médula ósea y el bazo, y una notable sobreexpresión de *Rapgef1*, que se propone como un novedoso y potencial segundo evento en la progresión de la enfermedad, y que requiere futuros estudios.

4. La nueva variante de codón de parada en TPM4 p.Gln108* causó una leve hemorragia, una leve macrotrombocitopenia y una ligera reducción de la agregación plaquetaria con agonistas débiles, ampliando y consolidando el fenotipo clínico de la trombocitopenia relacionada con *TPM4*. El defecto en la remodelación del citoesqueleto plaquetario provocó la deslocalización de la tropomiosina-4 en las estructuras de *spreading*, lo que podría justificar el grave deterioro de la función de *spreading* plaquetario.

5. Se detectaron cuatro variantes en *GALE* en tres pacientes de dos familias no relacionadas, con macrotrombocitopenia grave congénita, tendencia moderada de sangrado, retraso mental, prolapso de la válvula mitral y aumento de los niveles de bilirrubina. Estas variantes en *GALE* reducían gravemente los niveles y la actividad enzimática de la UDP-galactosa-4-epimerasa en las plaquetas y los megacariocitos.

6. Las variantes de *GALE* causaron una reducción de la glicosilación de la GPIbα y de la integrina β1 y su externalización a la superficie de los megacariocitos, quedando ambas retenidas en el retículo endoplásmico, donde la UDP-galactosa-4-epimerasa tiene su papel principal durante la megacariopoyesis tardía. Esto se refleja en una disminución en la formación de plaquetas, y en la producción de plaquetas con morfología, función y viabilidad alteradas. Estos nuevos datos ponen de manifiesto el papel clave de la *GALE* en la glicosilación, producción, función y aclaramiento de las plaquetas.

# REFERENCES

1. Noetzli LJ, French SL, Machlus KR. New insights into the differentiation of megakaryocytes from hematopoietic progenitors. *Arterioscler. Thromb. Vasc. Biol.* 2019;39(7):1288–1300.
2. Vainchenker W, Raslova H. Megakaryocyte polyploidization: role in platelet production. *Platelets*. 2020;31(6):707–716.
3. Schulze H, Korpal M, Hurov J, et al. Characterization of the megakaryocyte demarcation membrane system and its role in thrombopoiesis. *Blood*. 2006;107(10):3868–3875.
4. Abbonante V, Di Buduo CA, Malara A, Laurent PA, Balduini A. Mechanisms of platelet release: in vivo studies and in vitro modeling. *Platelets*. 2020;31(6):717–723.
5. Behrens K, Alexander WS. Cytokine control of megakaryopoiesis. *Growth Factors*. 2018;36(3–4):89–103.
6. Yu M, Cantor AB. Megakaryopoiesis and thrombopoiesis: An update on cytokines and lineage surface markers. *Methods Mol. Biol.* 2012;788:291–303.
7. Deutsch VR, Tomer A. Megakaryocyte development and platelet production. *Br. J. Haematol.* 2006;134(5):453–466.
8. Worthington RE, Nakeff A, Micko S. Flow cytometric analysis of megakaryocyte differentiation. *Cytometry*. 1984;5(5):501–508.
9. Vainchenker W, Kieffer N. Human megakaryocytopoiesis: In vitro regulation and characterization of megakaryocytic precursor cells by differentiation markers. *Blood Rev.* 1988;2(2):102–107.
10. Majka M, Baj-Krzyworzeka M, Kijowski J, et al. In vitro expansion of human megakaryocytes as a tool for studying megakaryocytic development and function. *Platelets*. 2001;12(6):325–332.
11. Yamamoto R, Morita Y, Ooehara J, et al. Clonal analysis unveils self-renewing lineage-restricted progenitors generated directly from hematopoietic stem cells. *Cell*. 2013;154:1112–1126.
12. Notta F, Zandi S, Takayama N, et al. Distinct routes of lineage development reshape the human blood hierarchy across ontogeny. *Science.* 2016;351(6269):aab2116.
13. Rodriguez-Fraticelli AE, Wolock SL, Weinreb CS, et al. Clonal analysis of lineage fate in native haematopoiesis. *Nature*. 2018;553(7687):212–216.
14. Pietras EM, Reynaud D, Kang YA, et al. Functionally Distinct Subsets of Lineage-Biased Multipotent Progenitors Control Blood Production in Normal and Regenerative Conditions. *Cell Stem Cell*. 2015;17(1):35–46.

15. Pendaries C, Watson SP, Spalton JC. Methods for genetic modification of megakaryocytes and platelets. *Platelets*. 2007;18(6):393–408.
16. Noh JY. Megakaryopoiesis and platelet biology: Roles of transcription factors and emerging clinical implications. *Int. J. Mol. Sci.* 2021;22(17):9615.
17. Martin F, Prandini MH, Thevenon D, Marguerie G, Uzan G. The transcription factor GATA-1 regulates the promoter activity of the platelet glycoprotein IIb gene. *J. Biol. Chem.* 1993;268(29):21606–21612.
18. Kwiatkowskit BA, Bastian LS, Bauer TR, et al. The ets family member tel binds to the Fli-1 oncoprotein and inhibits its transcriptional activity. *J. Biol. Chem.* 1998;273(28):17525–17530.
19. Kurokawa M. AML1/Runx1 as a versatile regulator of hematopoiesis: Regulation of its function and a role in adult hematopoiesis. *Int. J. Hematol.* 2006;84(2):136–142.
20. Ichikawa M, Asai T, Saito T, et al. AML-1 is required for megakaryocytic maturation and lymphocytic differentiation, but not for maintenance of hematopoietic stem cells in adult hematopoiesis. *Nat. Med.* 2004;10(3):299–304.
21. Growney JD, Shigematsu H, Li Z, et al. Loss of Runx1 perturbs adult hematopoiesis and is associated with a myeloproliferative phenotype. *Blood*. 2005;106(2):494–504.
22. Wang Q, Stacy T, Binder M, et al. Disruption of the Cbfa2 gene causes necrosis and hemorrhaging in the central nervous system and blocks definitive hematopoiesis. *Proc. Natl. Acad. Sci. U. S. A.* 1996;93(8):3444–3449.
23. Geddis AE. The regulation of proplatelet production. *Haematologica*. 2009;94(6):756–759.
24. Mbiandjeu S, Balduini A, Malara A. Megakaryocyte Cytoskeletal Proteins in Platelet Biogenesis and Diseases. *Thromb. Haemost.* 2021;122(5):666–678.
25. Italiano JE, Lecine P, Shivdasani RA, Hartwig JH. Blood platelets are assembled principally at the ends of proplatelet processes produced by differentiated megakaryocytes. *J. Cell Biol.* 1999;147(6):1299–1312.
26. Palma-Barqueros V, Bury L, Kunissima S, et al. Expanding the genetic spectrum of TUBB1- related thrombocytopenia. *Blood Adv.* 2021;5(24):5453–5467.
27. Ghalloussi D, Dhenge A, Bergmeier W. New insights into cytoskeletal remodeling during platelet production. *J. Thromb. Haemost.* 2019;17(9):1430–1439.
28. Manstein DJ, Meiring JCM, Hardeman EC, Gunning PW. Actin–tropomyosin distribution in non-muscle cells. *J. Muscle Res. Cell Motil.* 2020;41(1):11–22.
29. Antkowiak A, Viaud J, Severin S, et al. Cdc42-dependent F-actin dynamics drive

structuration of the demarcation membrane system in megakaryocytes. *J. Thromb. Haemost.* 2016;14(6):1268–1284.

30. Patel SR, Richardson JL, Schulze H, et al. Differential roles of microtubule assembly and sliding in proplatelet formation by megakaryocytes. *Blood*. 2005;106(13):4076–4085.
31. Italiano JE, Shivdasani RA. Megakaryocytes and beyond: The birth of platelets. *J. Thromb. Haemost.* 2003;1(6):1174–1182.
32. Thomas SG, Poulter NS, Bem D, et al. The actin binding proteins cortactin and HS1 are dispensable for platelet actin nodule and megakaryocyte podosome formation. *Platelets*. 2017;28(4):372–379.
33. Poulter NS, Thomas SG. Cytoskeletal regulation of platelet formation: Coordination of F-actin and microtubules. *Int. J. Biochem. Cell Biol.* 2015;66:69–74.
34. O'sullivan LR, Cahill MR, Young PW. The importance of alpha-actinin proteins in platelet formation and function, and their causative role in congenital macrothrombocytopenia. *Int. J. Mol. Sci.* 2021;22(17):9363.
35. Lin JJC, Eppinga RD, Warren KS, McCrae KR. Human tropomyosin isoforms in the regulation of cytoskeleton functions. *Adv. Exp. Med. Biol.* 2008;644:201–222.
36. Rosa JP, Raslova H, Bryckaert M. Filamin A: Key actor in platelet biology. *Blood*. 2019;134(16):1279–1288.
37. Badirou I, Pan J, Souquere S, et al. Distinct localizations and roles of non-muscle myosin II during proplatelet formation and platelet release. *J. Thromb. Haemost.* 2015;13(5):851–859.
38. Chen Y, Boukour S, Milloud R, et al. The abnormal proplatelet formation in MYH9-related macrothrombocytopenia results from an increased actomyosin contractility and is rescued by myosin IIA inhibition. *J. Thromb. Haemost.* 2013;11(12):2163–2175.
39. Antony-Debré I, Bluteau D, Itzykson R, et al. MYH10 protein expression in platelets as a biomarker of RUNX1 and FLI1 alterations. *Blood*. 2012;120(13):2719–2722.
40. Bluteau D, Glembotsky AC, Raimbault A, et al. Dysmegakaryopoiesis of FPD/AML pedigrees with constitutional RUNX1 mutations is linked to myosin II deregulated expression. *Blood*. 2012;120(13):2708–2718.
41. Jalagadugula G, Mao G, Kaur G, et al. Regulation of platelet myosin light chain (MYL9) by RUNX1: Implications for thrombocytopenia and platelet dysfunction in RUNX1 haplodeficiency. *Blood*. 2010;116(26):6037–6045.

42. Li R, Hoffmeister KM, Falet H. Glycans and the platelet life cycle. *Platelets*. 2016;27(6):505–511.
43. Grozovsky R, Giannini S, Falet H, Hoffmeister KM. Regulating billions of blood platelets: Glycans and beyond. *Blood*. 2015;126(16):1877–1884.
44. Lee-Sundlov MM, Stowell SR, Hoffmeister KM. Multifaceted role of glycosylation in transfusion medicine, platelets, and red blood cells. *J. Thromb. Haemost.* 2020;18(7):1535–1547.
45. Lebois M, Josefsson EC. Regulation of platelet lifespan by apoptosis. *Platelets*. 2016;27(6):497–504.
46. Di Buduo CA, Giannini S, Abbonante V, et al. Increased B4GALT1 expression is associated with platelet surface galactosylation and thrombopoietin plasma levels in MPNs. *Blood*. 2021;137(15):2085–2089.
47. Ma X, Li Y, Kondo Y, et al. Slc35a1 deficiency causes thrombocytopenia due to impaired megakaryocytopoiesis and excessive platelet clearance in the liver. *Haematologica*. 2021;106(3):759–769.
48. Giannini S, Lee-Sundlov MM, Rivadeneyra L, et al. β4GALT1 controls β1 integrin function to govern thrombopoiesis and hematopoietic stem cell homeostasis. *Nat. Commun.* 2020;11(1):356–371.
49. Sørensen AL, Rumjantseva V, Nayeb-Hashemi S, et al. Role of sialic acid for platelet life span: Exposure of β-galactose results in the rapid clearance of platelets from the circulation by asialoglycoprotein receptor-expressing liver macrophages and hepatocytes. *Blood*. 2009;114(8):1645–1654.
50. Broussard A, Florwick A, Desbiens C, et al. Human UDP-galactose 4′-epimerase (GALE) is required for cell-surface glycome structure and function. *J. Biol. Chem.* 2020;295(5):1225–1239.
51. Openo KK, Schulz JM, Vargas CA, et al. Epimerase-deficiency galactosemia is not a binary condition. *Am. J. Hum. Genet.* 2006;78(1):89–102.
52. Izumi R, Niihori T, Suzuki N, et al. GNE myopathy associated with congenital thrombocytopenia: A report of two siblings. *Neuromuscul. Disord.* 2014;24(12):1068–1072.
53. Jones C, Denecke J, Strter R, et al. A novel type of macrothrombocytopenia associated with a defect in α2,3-sialylation. *Am. J. Pathol.* 2011;179(4):1969–1977.
54. Jurk K, Kehrel BE. Platelets: Physiology and biochemistry. *Semin. Thromb. Hemost.* 2005;31(4):381–392.
55. Gremmel T, Frelinger AL, Michelson AD. Platelet physiology. *Semin. Thromb.*

*Hemost.* 2016;42(3):191–204.

56. Rivera J, Lozano ML, Navarro-Núñez L, Vicente García V. Platelet receptors and signaling in the dynamics of thrombus formation. *Haematologica*. 2009;94(5):700–711.
57. Watson S. Platelet Activation by Extracellular Matrix Proteins in Haemostasis and Thrombosis. *Curr. Pharm. Des.* 2009;15(12):1358–1372.
58. Sarratt KL, Chen H, Zutter MM, et al. GPVI and α2β1 play independent critical roles during platelet adhesion and aggregate formation to collagen under flow. *Blood*. 2005;106(4):1268–1277.
59. Nuyttens BP, Thijs T, Deckmyn H, Broos K. Platelet adhesion to collagen. *Thromb. Res.* 2011;127(Suppl 2):26–29.
60. Siedlecki CA, Lestini BJ, Kottke-Marchant K, et al. Shear-dependent changes in the three-dimensional structure of human von Willebrand factor. *Blood*. 1996;88(8):2939–2950.
61. Rivera J, Lozano ML, Corral J, et al. Platelet GP Ib/IX/V complex: Physiological role. *J. Physiol. Biochem.* 2000;56(4):355–365.
62. Kanaji S, Fahs SA, Shi Q, Haberichter SL, Montgomery RR. Contribution of platelet vs. endothelial VWF to platelet adhesion and hemostasis. *J. Thromb. Haemost.* 2012;10(8):1646–1652.
63. Schaff M, Tang CJ, Maurer E, et al. Integrin α6β1 is the main receptor for vascular laminins and plays a role in platelet adhesion, activation, and arterial thrombosis. *Circulation*. 2013;128(5):541–552.
64. Schick PK, Wojenski CM, He X, et al. Integrins involved in the adhesion of megakaryocytes to fibronectin and fibrinogen. *Blood*. 1998;92(8):2650–2656.
65. Smyth SS, Mcever RP, Weyrich AS, et al. Platelet functions beyond hemostasis. *J. Thromb. Haemost.* 2009;7(11):1759–1766.
66. Brass LF, Hoxie JA, Manning DR. Signaling through G proteins and G protein-coupled receptors during platelet activation. *Thromb. Haemost.* 1993;70(1):217–223.
67. Kawabata A, Kuroda R. Protease-activated receptor (PAR), a novel family of G protein-coupled seven trans-membrane domain receptors: Activation mechanisms and physiological roles. *Jpn. J. Pharmacol.* 2000;82(3):171–174.
68. Bambace NM, Levis JE, Holmes CE. The effect of P2Y-mediated platelet activation on the release of VEGF and endostatin from platelets. *Platelets*. 2010;21(2):85–93.
69. Yadav S, Storrie B. The cellular basis of platelet secretion: Emerging

structure/function relationships. *Platelets*. 2017;28(2):108–118.

70. Chen Y, Yuan Y, Li W. Sorting machineries: How platelet-dense granules differ from α-granules. *Biosci. Rep.* 2018;38(5):BSR20180458.
71. Rendu F, Brohard-Bohn B. The platelet release reaction: Granules' constituents, secretion and functions. *Platelets*. 2001;12(5):261–273.
72. Yang H, Reheman A, Chen P, et al. Fibrinogen and von willebrand factor-independent platelet aggregation in vitro and in vivo. *J. Thromb. Haemost.* 2006;4(10):2230–2237.
73. Feng D, Lindpaintner K, Larson MG, et al. Platelet glycoprotein IIIa PlA polymorphism, fibrinogen, and platelet aggregability: The Framingham Heart Study. *Circulation*. 2001;104(2):140–144.
74. Bennett JS. Structure and function of the platelet integrin alphaIIbbeta3. *J. Clin. Invest.* 2005;115(12):3363–3369.
75. Stefanini L, Roden RC, Bergmeier W. CalDAG-GEFI is at the nexus of calcium-dependent platelet activation. *Blood*. 2009;114(12):2506–2514.
76. Franke B, van Triest M, de Bruijn KMT, et al. Sequential Regulation of the Small GTPase Rap1 in Human Platelets. *Mol. Cell. Biol.* 2000;20(3):779–785.
77. Harper MT, Poole AW. Diverse functions of protein kinase C isoforms in platelet activation and thrombus formation. *J. Thromb. Haemost.* 2010;8(3):454–462.
78. Nurden AT, Nurden P. Congenital platelet disorders and understanding of platelet function. *Br. J. Haematol.* 2014;165(2):165–178.
79. Palma-Barqueros V, Revilla N, Sánchez A, et al. Inherited platelet disorders: An updated overview. *Int. J. Mol. Sci.* 2021;22(9):1–31.
80. Oved JH, Lambert MP, Kowalska MA, Poncz M, Karczewski KJ. Population based frequency of naturally occurring loss-of-function variants in genes associated with platelet disorders. *J. Thromb. Haemost.* 2021;19(1):248–254.
81. Megy K, Downes K, Simeoni I, et al. Curated disease-causing genes for bleeding, thrombotic, and platelet disorders: Communication from the SSC of the ISTH. *J. Thromb. Haemost.* 2019;17(8):1253–1260.
82. Freson K. Hemostatic Phenotypes and Genetic Disorders. *Res Pr. Thromb Haemost.* 2021;5(5):e12532.
83. Megy K, Downes K, Morel-Kopp MC, et al. GoldVariants, a resource for sharing rare genetic variants detected in bleeding, thrombotic, and platelet disorders: Communication from the ISTH SSC Subcommittee on Genomics in Thrombosis and Hemostasis. *J. Thromb. Haemost.* 2021;19(10):2612–2617.
84. Noris P, Pecci A. Hereditary thrombocytopenias: A growing list of disorders.

*Hematology*. 2017;2017(1):385–399.

85. Nurden AT, Nurden P. Inherited thrombocytopenias: history, advances and perspectives. *Haematologica*. 2020;105(8):2004–2019.
86. Bury L, Falcinelli E, Gresele P. Learning the Ropes of Platelet Count Regulation: Inherited Thrombocytopenias. *J. Clin. Med.* 2021;10(3):533.
87. Gresele P, Falcinelli E, Bury L. Laboratory diagnosis of clinically relevant platelet function disorders. *Int. J. Lab. Hematol.* 2018;40(Suppl 1):34–45.
88. Nurden P, Stritt S, Favier R, Nurden AT. Inherited platelet diseases with normal platelet count: Phenotypes, genotypes and diagnostic strategy. *Haematologica*. 2021;106(2):337–350.
89. Balduini CL, Melazzini F, Pecci A. Inherited thrombocytopenias—recent advances in clinical and molecular aspects. *Platelets*. 2017;28(1):3–13.
90. Bolton-Maggs PHB, Chalmers EA, Collins PW, et al. A review of inherited platelet disorders with guidelines for their management on behalf of the UKHCDO. *Br. J. Haematol.* 2006;135(5):603–633.
91. Pecci A, Balduini CL. Inherited thrombocytopenias: an updated guide for clinicians. *Blood Rev.* 2021;48:100784.
92. Melazzini F, Zaninetti C, Balduini CL. Bleeding is not the main clinical issue in many patients with inherited thrombocytopaenias. *Haemophilia*. 2017;23(5):673–681.
93. Warren JT, Di Paola J. Genetics of Inherited thrombocytopenias. *Blood*. 2022;139(22):3264–3277.
94. Gresele P, Orsini S, Noris P, et al. Validation of the ISTH/SSC bleeding assessment tool for inherited platelet disorders: A communication from the Platelet Physiology SSC. *J. Thromb. Haemost.* 2020;18(3):732–739.
95. Almazni I, Stapley R, Morgan NV. Inherited Thrombocytopenia: Update on Genes and Genetic Variants Which may be Associated With Bleeding. *Front. Cardiovasc. Med.* 2019;6:80.
96. Peyvandi F, Menegatti M, Palla R. Rare bleeding disorders: Worldwide efforts for classification, diagnosis, and management. *Semin. Thromb. Hemost.* 2013;39(6):579–584.
97. Bastida JM, Benito R, Lozano ML, et al. Molecular Diagnosis of Inherited Coagulation and Bleeding Disorders. *Semin. Thromb. Hemost.* 2019;45(7):695–707.
98. Nurden AT, Pillois X. ITGA2B and ITGB3 gene mutations associated with Glanzmann thrombasthenia. *Platelets*. 2018;29(1):98–101.

99. Nurden AT, Pillois X, Fiore M, et al. Expanding the mutation spectrum affecting αIIbβ3 integrin in glanzmann thrombasthenia: Screening of the ITGA2B and ITGB3 genes in a large international cohort. *Hum. Mutat.* 2015;36(5):548–561.
100. Morais S, Oliveira J, Lau C, et al. αIIbβ3 variants in ten families with autosomal dominant macrothrombocytopenia: Expanding the mutational and clinical spectrum. *PLoS One*. 2020;15(12):e0235136.
101. Savoia A, Kunishima S, De Rocco D, et al. Spectrum of the mutations in bernard-soulier syndrome. *Hum. Mutat.* 2014;35(9):1033–1045.
102. Sivapalaratnam S, Westbury SK, Stephens JC, et al. Rare variants in GP1BB are responsible for autosomal dominant macrothrombocytopenia. *Blood*. 2017;129(4):520– 524.
103. Boeckelmann D, Hengartner H, Greinacher A, et al. Patients with Bernard-Soulier syndrome and different severity of the bleeding phenotype. *Blood Cells, Mol. Dis.* 2017;67:69–74.
104. Noris P, Perrotta S, Bottega R, et al. Clinical and laboratory features of 103 patients from 42 italian families with inherited thrombocytopenia derived from the monoallelic Ala156Val mutation of gpibα (Bolzano mutation). *Haematologica*. 2012;97(1):82–88.
105. Ferrari S, Lombardi AM, Cortella I, et al. New heterozygous variant in GP1BB gene is responsible for an inherited form of macrothrombocytopenia. *Br. J. Haematol.* 2019;184(5):855–858.
106. Westbury SK, Shoemark DK, Mumford AD. ACTN1 variants associated with thrombocytopenia. *Platelets*. 2017;28(6):625–627.
107. Burley K, Westbury SK, Mumford AD. TUBB1 variants and human platelet traits. *Platelets*. 2018;29(2):209–211.
108. Pleines I, Woods J, Chappaz S, et al. Mutations in tropomyosin 4 underlie a rare form of human macrothrombocytopenia. *J. Clin. Invest.* 2017;127(3):814–829.
109. Marín-Quílez A, Vuelta E, Díaz-Ajenjo L, et al. A novel nonsense variant in TPM4 caused dominant macrothrombocytopenia, mild bleeding tendency and disrupted cytoskeleton remodeling. *J Thromb Haemost*. 2022;20(5):1248–1255.
110. Cattaneo M. Bleeding manifestations of congenital and drug-induced defects of the platelet P2Y 12 receptor for adenosine diphosphate. *Thromb. Haemost.* 2011;105(Suppl 1):2102–2112.
111. Mundell SJ, Mumford A. TBXA2R gene variants associated with bleeding. *Platelets*. 2018;29(7):739–742.
112. Poulter NS, Pollitt AY, Owen DM, et al. Clustering of glycoprotein VI (GPVI) dimers

upon adhesion to collagen as a mechanism to regulate GPVI signaling in platelets. *J. Thromb. Haemost.* 2017;15(3):549–564.

113. Lozano ML, Cook A, Bastida JM, et al. Novel mutations in RASGRP2, which encodes CalDAG-GEFI, abrogate Rap1 activation, causing platelet dysfunction. *Blood*. 2016;128(9):1282–1289.
114. Arber DA, Orazi A, Hasserjian R, et al. The 2016 revision to the World Health Organization classification of myeloid neoplasms and acute leukemia. *Blood*. 2016;127(20):2391–2405.
115. Jung J, Cho BS, Kim HJ, et al. Reclassification of acute myeloid leukemia according to the 2016 who classification. *Ann. Lab. Med.* 2019;39(3):311–316.
116. Ichikawa M, Yoshimi A, Nakagawa M, et al. A role for RUNX1 in hematopoiesis and myeloid leukemia. *Int. J. Hematol.* 2013;97(6):726–734.
117. Schlegelberger B, Heller PG. RUNX1 deficiency (familial platelet disorder with predisposition to myeloid leukemia, FPDMM). *Semin. Hematol .* 2017;54(2):75–80.
118. Gao J, Gong S, Chen YH. Myeloid neoplasm with germline predisposition: A 2016 update for pathologists. *Arch. Pathol. Lab. Med.* 2019;143(1):13–22.
119. Porter CC. Germ line mutations associated with Leukemias. *Hematology*. 2016;2016(1):302–308.
120. Marconi C, Canobbio I, Bozzi V, et al. 5′UTR point substitutions and N-terminal truncating mutations of ANKRD26 in acute myeloid leukemia. *J. Hematol. Oncol.* 2017;10(1):18.
121. Ballmaier M, Germeshausen M. Congenital amegakaryocytic thrombocytopenia: Clinical presentation, diagnosis, and treatment. *Semin. Thromb. Hemost.* 2011;37(6):673–681.
122. Germeshausen M, Ballmaier M. Congenital amegakaryocytic thrombocytopenia – Not a single disease. *Best Pract. Res. Clin. Haematol.* 2021;34(2):101286.
123. Bastida JM, Gonzalez-Porras JR, Rivera J, Lozano ML. Role of thrombopoietin receptor agonists in inherited thrombocytopenia. *Int. J. Mol. Sci.* 2021;22(9):4330.
124. Gilreath J, Lo M, Bubalo J. Thrombopoietin Receptor Agonists (TPO-RAs): Drug Class Considerations for Pharmacists. *Drugs*. 2021;81(11):1285–1305.
125. Millikan PD, Balamohan SM, Raskind WH, Kacena MA. Inherited thrombocytopenia due to GATA-1 mutations. *Semin. Thromb. Hemost.* 2011;37(6):682–689.
126. Freson K, Wijgaerts A, Van Geet C. GATA1 gene variants associated with thrombocytopenia and anemia. *Platelets*. 2017;28(7):731–734.

127. Raslova H, Komura E, Le Couédic JP, et al. FLI1 monoallelic expression combined with its hemizygous loss underlies Paris-Trousseau/Jacobsen thrombopenia. *J. Clin. Invest.* 2004;114(1):77–84.
128. Savoia A, Pecci A. MYH9-Related Disease. *GeneReviews*. 2008;1–24.
129. Pecci A, Klersy C, Gresele P, et al. MYH9-related disease: A novel prognostic model to predict the clinical evolution of the disease based on genotype-phenotype correlations. *Hum. Mutat.* 2014;35(2):2236–247.
130. Bury L, Megy K, Stephens JC, et al. Next-generation sequencing for the diagnosis of MYH9-RD: Predicting pathogenic variants. *Hum. Mutat.* 2020;41(1):277–290.
131. Candotti F. Clinical Manifestations and Pathophysiological Mechanisms of the Wiskott-Aldrich Syndrome. *J. Clin. Immunol.* 2018;38(1):13–27.
132. Thrasher AJ. New insights into the biology of Wiskott-Aldrich syndrome (WAS). *Hematology Am. Soc. Hematol. Educ. Program*. 2009;132–138.
133. Nurden P, Debili N, Coupry I, et al. Thrombocytopenia resulting from mutations in filamin A can be expressed as an isolated syndrome. *Blood*. 2011;118(22):5928–5937.
134. Vassallo P, Westbury SK, Mumford AD. FLNA variants associated with disorders of platelet number or function. *Platelets*. 2020;31(8):1097–1100.
135. Latham SL, Ehmke N, Reinke PYA, et al. Variants in exons 5 and 6 of ACTB cause syndromic thrombocytopenia. *Nat. Commun.* 2018;9(1):4250.
136. Kahr WHA, Pluthero FG, Elkadri A, et al. Loss of the Arp2/3 complex component ARPC1B causes platelet abnormalities and predisposes to inflammatory disease. *Nat. Commun.* 2017;8:14816.
137. Futterer J, Dalby A, Lowe GC, et al. Mutation in GNE is associated with severe congenital thrombocytopenia. *Blood*. 2018;132(17):1855–1858.
138. Revel-Vilk S, Shai E, Turro E, et al. GNE variants causing autosomal recessive macrothrombocytopenia without associated muscle wasting. *Blood*. 2018;132(17):1851–1854.
139. Kauskot A, Pascreau T, Adam F, et al. A mutation in the gene coding for the sialic acid transporter SLC35A1 is required for platelet life span but not proplatelet formation. *Haematologica*. 2018;103(12):e613–e617.
140. Bang YL, Nguyen TTT, Trinh TTB, et al. Functional analysis of mutations in UDP-galactose-4-epimerase (GALE) associated with galactosemia in Korean patients using mammalian GALE-null cells. *FEBS J.* 2009;276(7):1952–1961.
141. Timson DJ. Functional analysis of disease-causing mutations in human UDP-galactose 4-epimerase. *FEBS J.* 2005;272(23):6170–6177.

142. Seo A, Gulsuner S, Pierce S, et al. Inherited thrombocytopenia associated with mutation of UDP-galactose-4-epimerase (GALE). *Hum. Mol. Genet.* 2019;28(1):133–142.
143. Febres-Aldana CA, Pelaez L, Wright MS, et al. A Case of udp-galactose 4′-epimerase deficiency associated with dyshematopoiesis and atrioventricular valve malformations: An exceptional clinical phenotype explained by altered n-glycosylation with relative preservation of the leloir pathway. *Mol. Syndromol.* 2020;11(5–6):320–330.
144. Markovitz R, Owen N, Satter LF, et al. Expansion of the clinical phenotype of GALE deficiency. *Am. J. Med. Genet. Part A*. 2021;185(10):3118–3121.
145. Dias Costa F, Ferdinandusse S, Pinto C, et al. Galactose epimerase deficiency: Expanding the phenotype. *JIMD Rep.* 2017;37:19–25.
146. Dovlatova N. Current status and future prospects for platelet function testing in the diagnosis of inherited bleeding disorders. *Br. J. Haematol.* 2015;170(2):150–161.
147. Gresele P, Bury L, Mezzasoma AM, Falcinelli E. Platelet function assays in diagnosis: an update. *Expert Rev. Hematol.* 2019;12(1):29–46.
148. Harrison P, Mumford A. Screening tests of platelet function: Update on their appropriate uses for diagnostic testing. *Semin. Thromb. Hemost.* 2009;35(2):150–157.
149. Sánchez-Guiu I, Antón AI, Padilla J, et al. Functional and molecular characterization of inherited platelet disorders in the Iberian Peninsula: Results from a collaborative study. *Orphanet J. Rare Dis.* 2014;24(9):213.
150. Hayward CPM, Moffat KA, Brunet J, et al. Update on diagnostic testing for platelet function disorders: What is practical and useful? *Int. J. Lab. Hematol.* 2019;41(Suppl 1):26–32.
151. Balduini CL, Savoia A, Seri M. Inherited thrombocytopenias frequently diagnosed in adults. *J. Thromb. Haemost.* 2013;11(6):1006–1019.
152. Rodeghiero F, Tosetto A, Abshire T, et al. ISTH/SSC bleeding assessment tool: A standardized questionnaire and a proposal for a new bleeding score for inherited bleeding disorders. *J. Thromb. Haemost.* 2010;8(9):2063–2065.
153. Elbatarny M, Mollah S, Grabell J, et al. Normal range of bleeding scores for the ISTH-BAT: Adult and pediatric data from the merging project. *Haemophilia*. 2014;20(6):831–835.
154. Greinacher A, Pecci A, Kunishima S, et al. Diagnosis of inherited platelet disorders on a blood smear: a tool to facilitate worldwide diagnosis of platelet disorders. *J.*

*Thromb. Haemost.* 2017;15(7):1511–1521.

155. Zaninetti C, Greinacher A. Diagnosis of inherited platelet disorders on a blood smear. *J. Clin. Med.* 2020;9(2):539.
156. Greinacher A, Eekels JJM. Simplifying the diagnosis of inherited platelet disorders? The new tools do not make it any easier. *Blood*. 2019;133(23):2478–2483.
157. Frelinger AL, Rivera J, Connor DE, et al. Consensus recommendations on flow cytometry for the assessment of inherited and acquired disorders of platelet number and function: Communication from the ISTH SSC Subcommittee on Platelet Physiology. *J. Thromb. Haemost.* 2021;19(12):3193–3202.
158. Bastida JM, Lozano ML, Benito R, et al. Introducing high-throughput sequencing into mainstream genetic diagnosis practice in inherited platelet disorders. *Haematologica*. 2018;103(1):148–162.
159. Bastida JM, Hernández-Rivas JM, González-Porras JR. Novel approaches for diagnosing inherited platelet disorders. *Med. Clin. (Barc).* 2017;148(2):71–77.
160. Depristo MA, Banks E, Poplin R, et al. A framework for variation discovery and genotyping using next-generation DNA sequencing data. *Nat. Genet.* 2011;43(5):491–498.
161. Feng Y, Chen D, Wang GL, Zhang VW, Wong LJC. Improved molecular diagnosis by the detection of exonic deletions with target gene capture and deep sequencing. *Genet. Med.* 2015;17(2):99–107.
162. Richards S, Aziz N, Bale S, et al. Standards and guidelines for the interpretation of sequence variants: A joint consensus recommendation of the American College of Medical Genetics and Genomics and the Association for Molecular Pathology. *Genet. Med.* 2015;17(5):405–424.
163. Preston CG, Wright MW, Madhavrao R, et al. ClinGen Variant Curation Interface: a variant classification platform for the application of evidence criteria from ACMG/AMP guidelines. *Genome Med.* 2022;14(1):6.
164. Wu D, Luo X, Feurstein S, et al. How I curate: Applying American Society of Hematology-Clinical Genome Resource Myeloid Malignancy Variant Curation Expert Panel rules for RUNX1 variant curation for germline predisposition to myeloid malignancies. *Haematologica*. 2020;105(4):870–887.
165. Luo X, Feurstein S, Mohan S, et al. ClinGen Myeloid Malignancy Variant Curation Expert Panel recommendations for germline RUNX1 variants. *Blood Adv.* 2019;3(20):2962–2979.
166. Ross JE, Zhang BM, Lee K, et al. Specifications of the variant curation guidelines

for ITGA2B/ITGB3: ClinGen Platelet Disorder Variant Curation Panel. *Blood Adv.* 2021;5(2):414–431.

167. Perez Botero J, Di Paola J. Diagnostic approach to the patient with a suspected inherited platelet disorder: Who and how to test. *J. Thromb. Haemost.* 2021;19(9):2127–2136.
168. Balduini CL, Pecci A, Noris P. Inherited thrombocytopenias: The evolving spectrum. *Hamostaseologie*. 2012;32(4):259–270.
169. Collins J, Astle WJ, Megy K, Mumford AD, Vuckovic D. Advances in understanding the pathogenesis of hereditary macrothrombocytopenia. *Br. J. Haematol.* 2021;1–21.
170. D'Andrea G, Chetta M, Margaglione M. Inherited platelet disorders: Thrombocytopenias and thrombocytopathies. *Blood Transfus.* 2009;7(4):278–292.
171. Thon JN, Italiano JE. Does size matter in platelet production? *Blood*. 2012;120(8):1552–1561.
172. Bastida JM, Del Rey M, Revilla N, et al. Wiskott–Aldrich syndrome in a child presenting with macrothrombocytopenia. *Platelets*. 2017;28(4):417–420.
173. Tariq H, Perez Botero J, Higgins RA, Medina EA. Gray Platelet Syndrome Presenting with Pancytopenia, Splenomegaly, and Bone Marrow Fibrosis. *Am. J. Clin. Pathol.* 2021;156(2):253–258.
174. Andrews RK, Berndt MC. Bernard-soulier syndrome: An update. *Semin. Thromb. Hemost.* 2013;39(6):656–662.
175. Rabbolini DJ, Chun Y, Latimer M, et al. Diagnosis and treatment of MYH9-RD in an Australasian cohort with thrombocytopenia. *Platelets*. 2018;29(8):793–800.
176. Natesirinilkul R, Sosothikul D, Komwilaisak P, et al. MYH9 disorder: Identification and a novel mutation in patients with macrothrombocytopenia. *Pediatr. Blood Cancer*. 2021;68(7):e29055.
177. Bastida JM, Benito R, González-Porras JR, Rivera J. ABCG5 and ABCG8 gene variations associated with sitosterolemia and platelet dysfunction. *Platelets*. 2021;32(4):573–577.
178. Bastida JM, Benito R, Janusz K, et al. Two novel variants of the ABCG5 gene cause xanthelasmas and macrothrombocytopenia: a brief review of hematologic abnormalities of sitosterolemia. *J. Thromb. Haemost.* 2017;15(9):1859–1866.
179. Meinders M, Hoogenboezem M, Scheenstra MR, et al. Repercussion of megakaryocyte-specific Gata1 Loss on megakaryopoiesis and the hematopoietic precursor compartment. *PLoS One*. 2016;11(5):e0154342.

180. Favaloro EJ. Clinical utility of the PFA-100. *Semin. Thromb. Hemost.* 2008;34(8):709–733.
181. Lassila R. Platelet function tests in bleeding disorders. *Semin. Thromb. Hemost.* 2016;42(3):185–190.
182. Cattaneo M, Cerletti C, Harrison P, et al. Recommendations for the standardization of light transmission aggregometry: A consensus of the working party from the platelet physiology subcommittee of SSC/ISTH. *J. Thromb. Haemost.* 2013;11(6):1183–1189.
183. Cattaneo M. Light transmission aggregometry and ATP release for the diagnostic assessment of platelet function. *Semin. Thromb. Hemost.* 2009;35(2):158–167.
184. Chan MV, Armstrong PC, Warner TD. 96-well plate-based aggregometry. *Platelets*. 2018;29(7):650–655.
185. Munnix ICA, Van Oerle R, Verhezen P, et al. Harmonizing light transmission aggregometry in the Netherlands by implementation of the SSC-ISTH guideline. *Platelets*. 2021;32(4):516–523.
186. Alessi MC, Sié P, Payrastre B. Strengths and weaknesses of light transmission aggregometry in diagnosing hereditary platelet function disorders. *J. Clin. Med.* 2020;9(3):763.
187. Cardinal DC, Flower RJ. The electronic aggregometer: A novel device for assessing platelet behavior in blood. *J. Pharmacol. Methods*. 1980;3(2):135–158.
188. Wadowski PP, Pultar J, Weikert C, et al. Comparison of Light Transmission Aggregometry With Impedance Aggregometry in Patients on Potent P2Y12 Inhibitors. *J. Cardiovasc. Pharmacol. Ther.* 2021;26(3):260–268.
189. Rubak P, Nissen PH, Kristensen SD, Hvas AM. Investigation of platelet function and platelet disorders using flow cytometry. *Platelets*. 2016;27(1):66–74.
190. Van Velzen JF, Laros-Van Gorkom BAP, Pop GAM, Van Heerde WL. Multicolor flow cytometry for evaluation of platelet surface antigens and activation markers. *Thromb. Res.* 2012;130(1):92–98.
191. Andres O, Henning K, Strauß G, et al. Diagnosis of platelet function disorders: A standardized, rational, and modular flow cytometric approach. *Platelets*. 2018;29(4):347–356.
192. Watson SP, Lowe GC, Lordkipanidzé M, Morgan NV. Genotyping and phenotyping of platelet function disorders. *J. Thromb. Haemost.* 2013;11(suppl 1):351–363.
193. Leo VC, Morgan NV, Bem D, et al. Use of next-generation sequencing and candidate gene analysis to identify underlying defects in patients with inherited

platelet function disorders. *J. Thromb. Haemost.* 2015;13(4):643–650.

194. Freson K, Turro E. High-throughput sequencing approaches for diagnosing hereditary bleeding and platelet disorders. *J. Thromb. Haemost.* 2017;15(7):1262–1272.
195. Gresele P, Bury L, Falcinelli E. Inherited platelet function disorders: Algorithms for phenotypic and genetic investigation. *Semin. Thromb. Hemost.* 2016;42(3):292–305.
196. Germeshausen M, Ancliff P, Estrada J, et al. MECOM-associated syndrome: A heterogeneous inherited bone marrow failure syndrome with amegakaryocytic thrombocytopenia. *Blood Adv.* 2018;2(6):586–596.
197. Stritt S, Nurden P, Turro E, et al. A gain-of-function variant in DIAPH1 causes dominant macrothrombocytopenia and hearing loss. *Blood*. 2016;127(23):2903–2914.
198. Craig Venter J, Adams MD, Myers EW, et al. The sequence of the human genome. *Science*. 2001;291(5507):1304–1351.
199. Bastida JM, Palma-Barqueros V, Lozano ML, et al. A Modern Approach to the Molecular Diagnosis of Inherited Bleeding Disorders. *J. Mol. Genet. Med.* 2018;12(1):471–487.
200. Heremans J, Freson K. High-throughput sequencing for diagnosing platelet disorders: lessons learned from exploring the causes of bleeding disorders. *Int. J. Lab. Hematol.* 2018;40(Suppl 1):89–96.
201. Westbury SK, Mumford AD. Genomics of platelet disorders. *Haemophilia*. 2016;22(Suppl 5):20–24.
202. Sivapalaratnam S, Collins J, Gomez K. Diagnosis of inherited bleeding disorders in the genomic era. *Br. J. Haematol.* 2017;179(3):363–376.
203. Maclachlan A, Watson SP, Morgan NV. Inherited platelet disorders: Insight from platelet genomics using next-generation sequencing. *Platelets*. 2017;28(1):14–19.
204. Simeoni I, Stephens JC, Hu F, et al. A high-throughput sequencing test for diagnosing inherited bleeding, thrombotic, and platelet disorders. *Blood*. 2016;127(23):2791–2803.
205. Rabbolini DJ, Ward CM, Stevenson WS. Thrombocytopenia caused by inherited haematopoietic transcription factor mutation: clinical phenotypes and diagnostic considerations. *EMJ Hematol*. 2016;4(1):100–109.
206. Palma-Barqueros V, Crescente M, de la Morena ME, et al. A novel genetic variant in PTGS1 affects N-glycosylation of cyclooxygenase-1 causing a dominant-

negative effect on platelet function and bleeding diathesis. *Am. J. Hematol.* 2021;96(3):E83–E88.

207. Nurden AT, Nurden P. High-throughput sequencing for rapid diagnosis of inherited platelet disorders: A case for a European consensus. *Haematologica*. 2018;103(1):6–8.
208. Ver Donck F, Downes K, Freson K. Strengths and limitations of high-throughput sequencing for the diagnosis of inherited bleeding and platelet disorders. *J. Thromb. Haemost.* 2020;18(8):1839–1845.
209. Yang Y, Muzny DM, Reid JG, et al. Clinical Whole-Exome Sequencing for the Diagnosis of Mendelian Disorders. *N. Engl. J. Med.* 2013;369(16):1502–1511.
210. Prokop JW, May T, Strong K, et al. Genome sequencing in the clinic: The past, present, and future of genomic medicine. *Physiol. Genomics*. 2018;50(8):563–579.
211. Biesecker LG, Green RC. Diagnostic Clinical Genome and Exome Sequencing. *N. Engl. J. Med.* 2014;371(12):1170.
212. Petersen BS, Fredrich B, Hoeppner MP, Ellinghaus D, Franke A. Opportunities and challenges of whole-genome and -exome sequencing. *BMC Genet.* 2017;18(1):14.
213. Laffan M. A whole genome approach to platelet and bleeding disorders. *Hamostaseologie*. 2016;36(3):161–166.
214. Downes K, Borry P, Ericson K, et al. Clinical management, ethics and informed consent related to multi-gene panel-based high throughput sequencing testing for platelet disorders: Communication from the SSC of the ISTH. *J. Thromb. Haemost.* 2020;18(10):2751–2758.
215. Megy K, Downes K, Simeoni I, et al. Curated disease-causing genes for bleeding, thrombotic, and platelet disorders: Communication from the SSC of the ISTH. *J. Thromb. Haemost.* 2019;17(8):1253–1260.
216. Jacquel A, Herrant M, Defamie V, et al. A survey of the signaling pathways involved in megakaryocytic differentiation of the human K562 leukemia cell line by molecular and c-DNA array analysis. *Oncogene*. 2006;25(5):781–794.
217. Conde I, Pabón D, Jayo A, Lastres P, Gonzalez-Manchon C. Involvement of ERK1/2, p38 and PI3K in megakaryocytic differentiation of K562 cells. *Eur. J. Haematol.* 2010;84(5):430–440.
218. Ortiz-Rivero S, Baquero C, Hernández-Cano L, et al. C3G, through its GEF activity, induces megakaryocytic differentiation and proplatelet formation. *Cell Commun. Signal.* 2018;16(1):101–117.

219. Saito H. Megakaryocytic cell lines. *Baillieres. Clin. Haematol.* 1997;10(1):47–63.
220. Herrera R, Hubbell S, Decker S, Petruzzelli L. A role for the MEK/MAPK pathway in PMA-induced cell cycle arrest: Modulation of megakaryocytic differentiation of K562 cells. *Exp. Cell Res.* 1998;238(2):407–414.
221. Sardina JL, López-Ruano G, Sánchez-Abarca LI, et al. P22phox-dependent NADPH oxidase activity is required for megakaryocytic differentiation. *Cell Death Differ.* 2010;17(12):1842–1854.
222. Komatsu N, Nakauchi H, Miwa A, et al. Establishment and characterization of a human leukemic cell line with megakaryocytic features. *Cancer Res.* 1991;51(1):341–348.
223. Komatsu N, Kunitama M, Yamada M, et al. Establishment and characterization of the thrombopoietin-dependent megakaryocytic cell line, UT-7/TPO. *Blood*. 1996;87(11):4552–4560.
224. Gewirtz AM, Burger D, Rado TA, Benz EJ, Hoffman R. Constitutive expression of platelet glycoproteins by the human leukemia cell line K562. *Blood*. 1982;60(3):785–789.
225. Martin P, Papayannopoulou T. HEL cells: A new human erythroleukemia cell line with spontaneous and induced globin expression. *Science (80-. ).* 1982;216(4551):1233–1235.
226. Ogura M, Morishima Y, Ohno R, et al. Establishment of a novel human megakaryoblastic leukemia cell line, MEG-01, with positive Philadelphia chromosome. *Blood*. 1985;66(6):1384–1392.
227. Greenberg SM, Rosenthal DS, Greeley TA, Tantravahi R, Handin RI. Characterization of a new megakaryocytic cell line: The Dami cell. *Blood*. 1988;72(6):1968–1977.
228. Sledge GW, Giant M, Jansen J, et al. Establishment in Long Term Culture of Megakaryocytic Leukemia Cells (EST-IU) from the Marrow of a Patient with Leukemia and a Mediastinal Germ Cell Neoplasm. *Cancer Res.* 1986;46:155-2159.
229. Seigneurin D, Champelovier P, Mouchiroud G, et al. Human chronic myeloid leukemic cell line with positive Philadelphia chromosome exhibits megakaryocytic and erythroid characteristics. *Exp. Hematol.* 1987;15(8):822–832.
230. Tsuda H, Sakaguchi M, Kawakita M, et al. Alteration of cell cycle progression in human leukemia cell line (KOPM-28) induced by 12-o-tetradecanoylphorbol-13-acetate. *Int. J. Cell Cloning*. 1988;6(3):209–220.
231. Tange T, Nakahara K, Mitani K, et al. Establishment of a Human Megakaryoblastic

Cell Line (T-33) from Chronic Myelogenous Leukemia in Megakaryoblastic Crisis. *Cancer Res.* 1988;48(21):6137–6144.

232. Avanzi GC, Lista P, Giovinazzo B, et al. Selective growth response to IL-3 of a human leukaemic cell line with megakaryoblastic features. *Br. J. Haematol.* 1988;69(3):359–366.
233. Papayannopoulou T, Nakamoto B, Kurachi S, Tweeddale M, Messner H. Surface antigenic profile and globin phenotype of two new human erythroleukemia lines: Characterization and interpretations. *Blood*. 1988;72(3):1029–1038.
234. Nakazawa M, Mitjavila MT, Debili N, et al. KU 812: A pluripotent human cell line with spontaneous erythroid terminal maturation. *Blood*. 1989;73(7):2003–2013.
235. Sato T, Fuse A, Eguchi M, et al. Establishment of a human leukaemic cell line (CMK) with megakaryocytic characteristics from a Down's syndrome patient with acute megakaryoblastic leukaemia. *Br. J. Haematol.* 1989;72(2):184–190.
236. Fugman D, Witte D, Jones C, Aronow B, Lieberman M. In vitro establishment and characterization of a human megakaryoblastic cell line. *Blood*. 1990;75(6):1252–1261.
237. Matsuo Y, Adachi T, Tsubota T, Imanishi J, Minowada J. Establishment and characterization of a novel megakaryoblastic cell line, MOLM-1, from a patient with chronic myelogenous leukemia. *Hum. Cell*. 1991;4(3):261–264.
238. Takeuchi S, Sugito S, Uemura Y, et al. Acute megakaryoblastic leukemia: Establishment of a new cell line (MKPL-1) in vitro and in vivo. *Leukemia*. 1992;6(6):588–594.
239. Mouthon MA, Freund M, Titeux M, et al. Growth and differentiation of the human megakaryoblastic cell line (ELF- 153): A model for early stages of megakaryocytopoiesis. *Blood*. 1994;84(4):1085–1097.
240. Abe A, Emi N, Kato H, et al. Establishment and characterization of an immature human megakaryoblastic cell line, MEG-A2. *Leukemia*. 1995;9(2):341–349.
241. Liu C, Huang B, Wang H, Zhou J. The heterogeneity of megakaryocytes and platelets and implications for ex vivo platelet generation. *Stem Cells Transl. Med.* 2021;10(12):1614–1620.
242. Wang B, Zheng J. Platelet generation in vivo and in vitro. *Springerplus*. 2016;5(1):787.
243. Smith BW, Murphy GJ. Stem cells, megakaryocytes, and platelets. *Curr. Opin. Hematol.* 2014;21(5):430–437.
244. Avanzi MP, Mitchell WB. Ex Vivo production of platelets from stem cells. *Br. J. Haematol.* 2014;165(2):237–247.

245. Di Buduo CA, Soprano PM, Miguel CP, et al. A Gold Standard Protocol for Human Megakaryocyte Culture Based on the Analysis of 1,500 Umbilical Cord Blood Samples. *Thromb. Haemost.* 2021;121(4):538–542.
246. Balduini A, Di Buduo CA, Kaplan DL. Translational approaches to functional platelet production ex vivo. *Thromb. Haemost.* 2016;115(2):250–256.
247. Karagiannis P, Eto K. Manipulating megakaryocytes to manufacture platelets ex vivo. *J. Thromb. Haemost.* 2015;13(Suppl 1):S47–S53.
248. Huang J, Chen T, Liu X, et al. More synergetic cooperation of Yamanaka factors in induced pluripotent stem cells than in embryonic stem cells. *Cell Res.* 2009;19(10):1127–1138.
249. Di Buduo CA, Kaplan DL, Balduini A. In vitro generation of platelets: Where do we stand? *Transfus. Clin. Biol.* 2017;24(3):273–276.
250. Di Buduo CA, Aguilar A, Soprano PM, et al. Latest culture techniques: Cracking the secrets of bone marrow to mass-produce erythrocytes and platelets ex vivo. *Haematologica*. 2021;106(4):947–957.
251. Di Buduo CA, Laurent PA, Zaninetti C, et al. Miniaturized 3d bone marrow tissue model to assess response to thrombopoietin-receptor agonists in patients. *Elife*. 2021;10:1–30.
252. Jagadeeswaran P, Cooley BC, Gross PL, Mackman N. Animal Models of Thrombosis From Zebrafish to Nonhuman Primates. *Circ. Res.* 2016;118(9):1363–1379.
253. Marín-Quílez A, García-Tuñón I, Fernández-Infante C, et al. Characterization of the Platelet Phenotype Caused by a Germline RUNX1 Variant in a CRISPR/Cas9-Generated Murine Model. *Thromb. Haemost.* 2021;121(9):1193–1205.
254. Marconi C, DI Buduo CA, LeVine K, et al. Loss-of-function mutations in PTPRJ cause a new form of inherited thrombocytopenia. *Blood*. 2019;133(12):1346–1357.
255. Léon C, Dupuis A, Gachet C, Lanza F. The contribution of mouse models to the understanding of constitutional thrombocytopenia. *Haematologica*. 2016;101(8):896–908.
256. Petazzi P, Menéndez P, Sevilla A. CRISPR/Cas9–Mediated Gene Knockout and Knockin Human iPSCs. *Methods Mol Biol*. 2020;
257. Alexander WS, Roberts AW, Maurer AB, et al. Studies of the c-Mpl thrombopoietin receptor through gene disruption and activation. *Stem Cells*. 1996;14(Suppl 1):124–132.
258. Blundell MP, Bouma G, Calle Y, et al. Improvement of migratory defects in a

murine model of Wiskott-Aldrich syndrome gene therapy. *Mol. Ther.* 2008;16(5):836–844.

259. Ware J, Russell S, Ruggeri ZM. Generation and rescue of a murine model of platelet dysfunction: The Bernard-Soulier syndrome. *Proc. Natl. Acad. Sci. U. S. A.* 2000;97(6):2803–2808.
260. Matsushita T, Hayashi H, Kunishima S, et al. Targeted disruption of mouse ortholog of the human MYH9 responsible for macrothrombocytopenia with different organ involvement: Hematological, nephrological, and otological studies of heterozygous KO mice. *Biochem. Biophys. Res. Commun.* 2004;325(4):1163–1171.
261. García-Tuñón I, Hernández-Sánchez M, Ordoñez JL, et al. The CRISPR/Cas9 system efficiently reverts the tumorigenic ability of BCR/ABL in vitro and in a xenograft model of chronic myeloid leukemia. *Oncotarget*. 2017;8(16):26027–26040.
262. Montaño A, Ordoñez JL, Alonso-Pérez V, et al. ETV6/RUNX1 Fusion Gene Abrogation Decreases the Oncogenicity of Tumour Cells in a Preclinical Model of Acute Lymphoblastic Leukaemia. *Cells*. 2020;9(1):215–231.
263. Quijada-Álamo M, Hernández-Sánchez M, Rodríguez-Vicente AE, et al. Biological significance of monoallelic and biallelic BIRC3 loss in del(11q) chronic lymphocytic leukemia progression. *Blood Cancer J.* 2021;11(7):127–138.
264. Connolly MR, Kuravi K, Burdorf L, et al. Humanized von Willebrand factor reduces platelet sequestration in ex vivo and in vivo xenotransplant models. *Xenotransplantation*. 2021;28(6):e12712.
265. Montaño A, Forero-Castro M, Hernández-Rivas JM, García-Tuñón I, Benito R. Targeted genome editing in acute lymphoblastic leukemia: A review. *BMC Biotechnol.* 2018;18(1):45–55.
266. Gaj T, Gersbach CA, Barbas CF. ZFN, TALEN, and CRISPR/Cas-based methods for genome engineering. *Trends Biotechnol.* 2013;31(7):397–405.
267. Urnov FD, Rebar EJ, Holmes MC, Zhang HS, Gregory PD. Genome editing with engineered zinc finger nucleases. *Nat. Rev. Genet.* 2010;11(9):636–646.
268. Sun N, Zhao H. Transcription activator-like effector nucleases (TALENs): a highly efficient and versatile tool for genome editing. *Biotechnol. Bioeng.* 2013;110(7):1811–1821.
269. Lander ES. The Heroes of CRISPR. *Cell*. 2016;164(1–2):18–28.
270. Ran FA, Hsu PD, Wright J, et al. Genome engineering using the CRISPR-Cas9 system. *Nat. Protoc.* 2013;8(11):2281–2308.

271. Hsu PD, Lander ES, Zhang F. Development and applications of CRISPR-Cas9 for genome engineering. *Cell*. 2014;157(6):1262–1278.

272. Chiruvella KK, Liang Z, Wilson TE. Repair of double-strand breaks by end joining. *Cold Spring Harb. Perspect. Biol.* 2013;5(5):1–21.

273. Jasin M, Haber JE. The democratization of gene editing: Insights from site-specific cleavage and double-strand break repair. *DNA Repair (Amst).* 2016;44:6–16.

274. Choi PS, Meyerson M. Targeted genomic rearrangements using CRISPR/Cas technology. *Nat. Commun.* 2014;5:3728.

275. Banan M. Recent advances in CRISPR/Cas9-mediated knock-ins in mammalian cells. *J. Biotechnol.* 2020;308:1–9.

276. Trevino AE, Zhang F. Genome editing using cas9 nickases. *Methods Enzym.* 2014;546:161–174.

277. Yin H, Xue W, Chen S, et al. Genome editing with Cas9 in adult mice corrects a disease mutation and phenotype. *Nat. Biotechnol.* 2014;32(6):551–553.

278. Richardson CD, Ray GJ, DeWitt MA, Curie GL, Corn JE. Enhancing homology-directed genome editing by catalytically active and inactive CRISPR-Cas9 using asymmetric donor DNA. *Nat. Biotechnol.* 2016;34(3):339–344.

279. Maruyama T, Dougan SK, Truttmann MC, et al. Increasing the efficiency of precise genome editing with CRISPR-Cas9 by inhibition of nonhomologous end joining. *Nat. Biotechnol.* 2015;33(5):538–542.

280. Xie Z, Jiang J, Cao L, et al. Nonsense-mediated mRNA decay efficiency influences bleeding severity in ITGA2B c.2659C > T (p.Q887X) knock-in mice. *Clin. Genet.* 2021;100(2):213–218.

281. Montenont E, Bhatlekar S, Jacob S, et al. CRISPR-edited megakaryocytes for rapid screening of platelet gene functions. *Blood Adv.* 2021;5(9):2362–2374.

282. Shen MW, Arbab M, Hsu JY, et al. Predictable and precise template-free CRISPR editing of pathogenic variants. *Nature*. 2018;563(7733):646–651.

283. Bastida JM, L Lozano M, Benito R, et al. High Throughput Sequencing for the Molecular Diagnosis of Inherited Platelet Disorders in Spain. Experience of the GEAPC Group. *Res Pr. Thromb Haemost.* 2021;5(Suppl 2):1.

284. Brown AL, Hahn C, Hiwase D, Godley LA, Scott HS. Correct application of variant classification guidelines in germline RUNX1 mutated disorders to assist clinical diagnosis. *Leuk. Lymphoma*. 2019;61(1):246–247.

285. Feurstein S, Zhang L, DiNardo CD. Accurate germline RUNX1 variant interpretation and its clinical significance. *Blood Adv.* 2020;4(24):6199–6203.

286. Garcia JS, Madzo J, Cooper D, et al. Pre-Donor Evaluation of an HLA Matched

Sibling Identifies a Novel Inherited RUNX1 Mutation Encoding a Missense Mutation Found Outside of the RUNT Domain in Familial Platelet Disorder. *Blood*. 2010;116(21):2709.

287. Duployez N, Fenwarth L. Controversies about germline RUNX1 missense variants. *Leuk. Lymphoma*. 2020;61(2):497–499.
288. Koh CP, Wang CQ, Ng CE, et al. RUNX1 meets MLL: epigenetic regulation of hematopoiesis by two leukemia genes. *Leukemia*. 2013;27(9):1793–1802.
289. Prieto-Conde MI, Labrador J, Hermida G, et al. Genomic analysis of a familial myelodysplasia/acute myeloid leukemia and inherited RUNX1 mutations without a pre-existing platelet disorder. *Leuk. Lymphoma*. 2019;61(1):181–184.
290. Palmer D, Nacheva E. An analysis of the RUNX1p.(Leu56Ser) variant in a cohort of individuals with myeloid neoplasms; suggests it is a benign germline variant. *Leuk. Lymphoma*. 2021;62(5):1255–1258.
291. Decker M, Lammens T, Ferster A, et al. Functional classification of RUNX1 variants in familial platelet disorder with associated myeloid malignancies. *Leukemia*. 2021;35(11):3304–3308.
292. Latger-Cannard V, Philippe C, Bouquet A, et al. Haematological spectrum and genotype-phenotype correlations in nine unrelated families with RUNX1 mutations from the French network on inherited platelet disorders. *Orphanet J. Rare Dis.* 2016;11(1):49.
293. Brown AL, Hahn CN, Scott HS. Secondary leukemia in patients with germline transcription factor mutations (RUNX1, GATA2, CEBPA). *Blood*. 2020;136(1):24–35.
294. Glembotsky AC, Bluteau D, Espasandin YR, et al. Mechanisms underlying platelet function defect in a pedigree with familial platelet disorder with a predisposition to acute myelogenous leukemia: Potential role for candidate RUNX1 targets. *J. Thromb. Haemost.* 2014;12(5):761–772.
295. Gabbeta J, Yang X, Sun L, et al. Abnormal inside-out signal transduction-dependent activation of glycoprotein IIb-IIIa in a patient with impaired pleckstrin phosphorylation. *Blood*. 1996;87(4):1368-1376.
296. Sood R, Kamikubo Y, Liu P. Role of RUNX1 in hematological malignancies. *Blood*. 2017;129(15):2070–2082.
297. Antony-Debré I, Manchev VT, Balayn N, et al. Level of RUNX1 activity is critical for leukemic predisposition but not for thrombocytopenia. *Blood*. 2015;125(6):930–940.
298. Yokota A, Huo L, Lan F, Wu J, Huang G. The Clinical, Molecular, and Mechanistic

Basis of RUNX1 Mutations Identified in Hematological Malignancies. *Mol. Cells*. 2020;43(2):145–152.

299. Ng IK, Lee J, Ng C, et al. Preleukemic and second-hit mutational events in an acute myeloid leukemia patient with a novel germline RUNX1 mutation. *Biomark. Res.* 2018;11(6):16.
300. Sakurai M, Kasahara H, Yoshida K, et al. Genetic basis of myeloid transformation in familial platelet disorder/acute myeloid leukemia patients with haploinsufficient RUNX1 allele. *Blood Cancer J.* 2016;6(2):e392.
301. Kanagal-Shamanna R, Loghavi S, Dinardo CD, et al. Bone marrow pathologic abnormalities in familial platelet disorder with propensity for myeloid malignancy and germline RUNX1 mutation. *Haematologica*. 2017;102(10):1661–1670.
302. Ok CY, Leventaki V, Wang SA, et al. Detection of an abnormal myeloid clone by flow cytometry in familial platelet disorder with propensity to myeloid malignancy. *Am. J. Clin. Pathol.* 2016;145(2):271–276.
303. Campbell KJ, Bath ML, Turner ML, et al. Elevated Mcl-1 perturbs lymphopoiesis, promotes transformation of hematopoietic stem/progenitor cells, and enhances drug resistance. *Blood*. 2010;116(17):3197–3207.
304. Preudhomme C, Renneville A, Bourdon V, et al. High frequency of RUNX1 biallelic alteration in acute myeloid leukemia secondary to familial platelet disorder. *Blood*. 2009;113(22):5583–5587.
305. Hayashi Y, Harada Y, Huang G, Harada H. Myeloid neoplasms with germ line RUNX1 mutation. *Int. J. Hematol.* 2017;106(2):183–188.
306. Gutiérrez-Herrero S, Maia V, Gutiérrez-Berzal J, et al. C3G transgenic mouse models with specific expression in platelets reveal a new role for C3G in platelet clotting through its GEF activity. *Biochim. Biophys. Acta*. 2012;1823(8):1366–1377.
307. Gutiérrez-Herrero S, Fernández-Infante C, Hernández-Cano L, et al. C3G contributes to platelet activation and aggregation by regulating major signaling pathways. *Signal Transduct. Target Ther.* 2020;5(1):29.
308. Martín-Granado V, Ortiz-Rivero S, Carmona R, et al. C3G promotes a selective release of angiogenic factors from activated mouse platelets to regulate angiogenesis and tumor metastasis. *Oncotarget*. 2017;8(67):110994–111011.
309. Carabias A, Guerrero C, de Pereda JM. C3G self-regulatory mechanism revealed: implications for hematopoietic malignancies. *Mol. Cell. Oncol.* 2021;8(1):1837581.
310. Gutiérrez-Berzal J, Castellano E, Martín-Encabo S, et al. Characterization of p87C3G, a novel, truncated C3G isoform that is overexpressed in chronic myeloid

leukemia and interacts with Bcr-Abl. *Exp. Cell Res.* 2006;312(6):938–948.

311. Neuhaus C, Lang-Roth R, Zimmermann U, et al. Extension of the clinical and molecular phenotype of DIAPH1-associated autosomal dominant hearing loss (DFNA1). *Clin. Genet.* 2017;91(6):892–901.
312. Kundishora AJ, Peters ST, Pinard A, et al. DIAPH1 Variants in Non-East Asian Patients with Sporadic Moyamoya Disease. *JAMA Neurol.* 2021;78(8):993–1003.
313. Karki NR, Ajebo G, Savage N, Kutlar A. DIAPH1 Mutation as a Novel Cause of Autosomal Dominant Macrothrombocytopenia and Hearing Loss. *Acta Haematol.* 2021;144(1):91–94.
314. Manchev VT, Hilpert M, Berrou E, et al. A new form of macrothrombocytopenia induced by a germ-line mutation in the PRKACG gene. *Blood*. 2014;124(16):2554–2563.
315. Marín-Quílez A, Fernández-Infante C, Manrique Gonzalo MÁ, et al. Characterization of a New Family with Lifelong Macrothrombocytopenia Caused by a Novel Nonsense Variant in TPM4. *Res Pr. Thromb Haemost.* 2021;5(suppl 2):1.
316. Stapley RJ, Poulter NS, Khan AO, et al. Rare missense variants in Tropomyosin-4 (TPM4) are associated with platelet dysfunction, cytoskeletal defects and excessive bleeding. *J Thromb Haemost*. 2021;20(2):478–485.
317. García-Tuñón I, Hernández-Sánchez M, Ordoñez JL, et al. The CRISPR-Cas9 system efficiently reverts the tumorigenic ability of BCR/ABL in vitro and in a xenograft model of Chronic Myeloid Leukemia. *Oncotarget*. 2017;18(8):26027–26040.

# SUPPLEMENTARY INFORMATION

**TPO signaling pathway + Transcriptional Factors**

| Disorder (OMIM) | Gene | Inheritance | Bleeding / Thrombocytopenia / Platelet dysfunction | Other manifestations | Ref |
|---|---|---|---|---|---|
| Congenital amegakaryocytic thrombocytopenia (CAMT) (604498) | *MPL* | AR | Severe<br>Severe<br>No | Cytopenia<br>Medullar aplasia | 1 |
| *THPO*-RT | *TPHO* | AD/AR | Severe<br>Mild (AD) to Severe (AR)<br>No | Cytopenia<br>Medullar aplasia (AR) | 2,3 |
| Familial platelet disorder with propensity to acute myeloid leukemia (FPD/AML) (601399) | *RUNX1* | AD | Absent to moderate<br>Mild to moderate<br>Platelet granule deficiency and αIIbβ3 integrin dysfunction | 45% AML / MDS<br>1-3% T-ALL, solid tumor | 4 |
| *ETV6*-RT / thrombocytopenia Type-5 (616216) | *ETV6* | AD | Absent to mild<br>Mild to moderate<br>Slight, altered α-granules<br>Circulating CD34 + cells | 25% ALL during the childhood, 5-10% AML, MDS, multiple myeloma, or polycythemia vera | 5 |
| *ANKRD26*-RT / thrombocytopenia Type-2 (188000) | *ANKRD26* | AD | Absent to mild<br>Mild to moderate<br>No | 5-10% AML / MDS<br>High levels of hemoglobin and/or leukocytosis | 6 |
| *GFI1b*-RT (187900) | *GFI1B* | AD/AR | Absent to severe<br>Mild to severe + macro<br>α/β-granule deficiency and aggregation defect.<br>CD34+ abnormal expression | Red blood cells with anisopoikilocytosis, dysplastic Mks, emperipolesis | 7,8 |
| *GATA1*-RD (314050;300367) | *GATA1* | XL | Mild to severe<br>Mild to severe + macro<br>Granule deficiency and functional defect | Dyserythropoiesis +/- anemia, β-thalassemia, neutropenia, splenomegaly, congenital erythropoietic porphyria. Dysplastic Mks | 9 |

| | | | | | |
|---|---|---|---|---|---|
| *FLI1*-RT (61744) | *FLI1* | AD/AR | Absent to moderate<br>Mild to moderate + macro<br>Enlarged granules | Facial, cardiac, and neurological malformation | 10,11 |
| Radioulnar synostosis with amegakaryocytic thrombocytopenia 1 (RUSAT1, 605432) | *HOXA11* | AD | Severe<br>Severe<br>No | Aplastic anemia; radius and ulna synostosis +/- other skeletal alterations; sensorineural hearing loss | 12 |
| *MECOM*-RT (including amegakaryocytic thrombocytopenia 2 with Radioulnar synostosis) (RUSAT2) (616738) | *MECOM* | AD | Severe<br>Severe<br>No | Hyporegenerative anemia. Radius and ulna synostosis +/- other skeletal alterations; B-cell deficiency. Renal or cardiac malformations and sensorineural hearing loss | 13 |
| Thrombocytopenia with absent radii (TAR) (274000) | *RBM8A* | AR | Severe<br>Moderate to severe<br>No | Bilateral absence of radius +/- other skeletal abnormalities. Kidney, cardiac, or central nervous system anomalies | 14 |
| Roifman syndrome (616651) | *RNU4ATAC* | AR | Absent to mild<br>Mild to moderate + macro<br>increased α-granule and dense granule levels | Spondyloepiphyseal dysplasia, growth retardation, cognitive delay, hypogammaglobulinemia, reduction in B-cell numbers | 15 |
| *IKZF5*-RT | *IKZF5* | AD | No<br>Mild to moderate<br>Fewer α and δ granules | No | 16 |

**Megakaryocyte and platelet receptors**

| Disorder (OMIM) | Gene | Inheritance | Bleeding / Thrombocytopenia / Platelet dysfunction | Other manifestations | Ref |
|---|---|---|---|---|---|
| Bernard-Soulier syndrome (BSS) (231200) | *GP1BA, GP1BB, GP9* | AR | Severe<br>Moderate to severe + macro<br>Severe dysfunction of receptor GPIbα/IX. Absence aggregation with ristocetin<br>Normal/reduced response to other agonists. Adhesion defect to FVW | No | 17,18 |
| Bernard-Soulier syndrome, monoallelic form (mBSS) (153670) Or Mediterranean thrombocytopenia | *GP1BA, GP1BB* | AD | Absent to mild<br>Mild to moderate<br>No | No | 19 |
| Platelet-type von Willebrand disease (PTvWD) (177820) | *GP1BA* | AD | Absent to mild<br>Absent to severe.<br>Abnormally high platelet VWF binding and hyperaggregation with low-dose ristocetin due to gain of function variants in GPIbα. | No | 20 |
| Glanzmann Thrombasthenia (GT) (273800) | *ITGA2B, ITGB3* | AR | Severe<br>No<br>Absent or severely reduced aggregation with all agonists.<br>Absence or decreased αIIbβ3 integrin.<br>Absence or severely reduced clot retraction | No | 21,22 |
| *ITGA2B/ITGB3*-RT (187800) | *ITGA2B, ITGB3* | AD | Moderate<br>Mild to severe<br>Defective expression and αIIbβ3 activation | No | 23 |

| | | | | | |
|---|---|---|---|---|---|
| Von Willebrand disease - type 2B (VWD2) (613554) | *VWF* | AD | Mild<br>Mild + macro.<br>Increased affinity for GPIb and enhanced ristocetin-induced platelet aggregation.<br>Decreased numbers of Vwf. | No | [24] |
| GPVI collagen receptor defect (614201) | *GP6* | AR | Mild to moderate<br>No<br>Absent or severely reduced LTA with collagen or GPVI agonists. Defective platelet secretion | No | [25] |
| ADP receptor deficiency (609821) | *P2RY12* | AD/AR | Mild to moderate<br>No<br>Aggregation decreased with ADP | No | [26] |
| $TxA_2$ receptor deficiency (614009) | *TBXA2R* | AD/AR | Mild to moderate<br>No<br>Absence or severely reduced aggregation with arachidonic acid or $TxA_2$ analogs | No | [27] |

**Intracellular Signaling Pathways**

| Disorder (OMIM) | Gene | Inheritance | Bleeding / Thrombocytopenia / Platelet dysfunction | Other manifestations | Ref |
|---|---|---|---|---|---|
| *SRC*-RT (thrombocytopenia type-6) (616937) | *SRC* | AD | Mild to severe<br>Mild to severe + macro<br>Granule defect | Myelofibrosis and early edentulism, facila dysmorphia. Mks with immature features (hypolobulated nuclei) | 28 |
| *KDSR*-RT | *KDSR* | AR | Moderate to severe<br>Severe<br>Secretion and activation defect | Hyperkeratosis from pamoplantar and anogenital hyperkeratosis /erythema to a Harlequin ichthyosis | 29 |
| *G6b*-B-RT (617441) | *MPIG6B* | AR | Mild to moderate<br>Mild to severe + macro<br>No | Atypical Mks<br>Microcytic anemia, leukocytosis, myelofibrosis | 30 |
| Thrombocytopenia associated with sitosterolemia | *ABCG5, ABCG8* | AR | Mild to moderate<br>Mild to moderate + macro<br>No | Elevated plasma levels of plant sterols. Xanthomas in tendoms and xanthelasmas. Premature atherosclerosis, hemolytic anemia with stomatocytosis | 31,32 |
| *CYCS*-RT (thrombocytopenia type-4) (612004) | *CYCS* | AD | No<br>Mild to moderate<br>No | No | 33 |
| *SLFN14*-RT (616913) | *SLFN14* | AD | Moderate to severe<br>Mild to moderate + macro<br>δ granule secretion defect. | No | 34 |

| | | | | | |
|---|---|---|---|---|---|
| Quebec Syndrome (QS) (601709) | *PLAU* | AD | Mild to moderate<br>Moderate<br>Absent or reduced aggregation with epinephrine. α granule protein defect. Defect of procoagulant platelet activity and increased fibrinolytic activity | No | 35 |
| Stormorken syndrome (185070) | *STIM1* | AD | Mild<br>Moderate<br>Abnormal clot formation and retraction | Asplenia, mild anemia, myopathy with tubular aggregates, congenital miosis, ichthyosis, short stature, migraine and mild cognitive impairment. | 36 |
| York platelet syndrome | *STIM1* | AD | Mild<br>Moderate to severe<br>Fewer α and δ granules, giant dense bodies | Myopathy with rimmed vacuoles | 37 |
| Defect in TxA2 pathway (176805, 231095, 600522) | *TBXAS1, PLA2G4A, PTGS1* | AR/AD | Absent or moderate<br>No<br>Reduced aggregation with arachidonic acid. Reduced with low dose of several agonists | Osteoporosis (*TBXAS1* defect); recurrent gastrointestinal ulceration (*PLA2G4A* defect) | 38,39 |
| Leukocyte adhesion deficiency syndrome type 3 (Kindlin-3 deficiency) (612840) | *FERMT3* | AR | Severe<br>No<br>No | Infections, poor healing, osteopetrosis | 40 |
| *ABCC4*-RD | *ABCC4* | AR | Mild<br>No<br>platelet δ-storage pool deficiency and impaired aggregation | No | 41 |
| CalDAG-GEF1 defect (615888) | *RASGRP2* | AR | Moderate to severe<br>No<br>Impaired aggregation, αIIbβ3 integrin activation with weak agonists. | No | 42 |

**Cytoskeleton regulation**

| Disorder (OMIM) | Gene | Inheritance | Bleeding / Thrombocytopenia / Platelet dysfunction | Other manifestations | Ref |
|---|---|---|---|---|---|
| *MYH9*-RD (155100) | *MYH9* | AD | Absent to mild<br>Mild to severe + macro<br>No | Basophilic neutrophilic inclusions (Döhle bodies). Hearing loss, kidney disease, liver disease, cataracts | 43,44 |
| Wiskott-Aldrich syndrome (WAS) (301000) | *WAS* | XL | Severe<br>Severe + micro<br>No | Immunodeficiency, eczema, lymphoproliferative and autoimmune disorders | 45 |
| X-linked thrombocytopenia (XLT or thrombocytopenia type-1) (313900) | *WAS* | XL | Absent to moderate<br>Moderate to severe + micro<br>No | Possible immunodeficiency and mild eczema. Increased risk of malignancy and autoimmune disorders | 45 |
| *FLNA*-RT | *FLNA* | XL | Mild<br>Moderate + macro<br>No | Nodular periventricular heterotopia; skeletal malformations, mental retardation, heart valve dystrophy, intestinal obstruction, bone dysplasia | 46 |
| *DIAPH1-RT* | *DIAPH1* | AD | Absent to mild<br>Mild + macro<br>No | Moderate fluctuating neutropenia with low to moderate infectious risk; early sensorineural deafness | 47 |

| | | | | | |
|---|---|---|---|---|---|
| *ARPC1B*-RT (617718) | *ARPC1B* | AR | Moderate<br>Moderate to severe+ micro<br>No | Eosinophilia, immune-mediated inflammatory disease, lymphadenopathy, eczema, hepato-splenomegaly. Impaired growth | 48 |
| *ACTB*-RT | *ACTB* | AD | No<br>Mild to moderate + macro<br>No | Leucocytosis with eosinophilia or leukopenia. Microcephaly, minor facial anomalies, developmental delay and mild intellectural disability | 49 |
| *ACTN1-RT (615193)* | *ACTN1* | AD | Absent to mild<br>Mild to moderate + macro<br>Moderate | No | 50 |
| *TPM4*-RT | *TPM4* | AD | Absent to mild<br>Mild + macro<br>No | No | 51,52 |
| *TUBB1*-RT (613112) | *TUBB1* | AD | Absent to mild<br>Mild to moderate + macro<br>No | No | 53 |
| *FYB*-RT (ADAP-RT or thrombocytopenia type-3) (273900) | *FYB* | AR | Mild to moderate<br>Moderate to severe + micro<br>Baseline platelet hyperactivation. Impaired activation of αIIbβ3 | No | 54 |
| Takenouchi-Kosaki syndrome with macrothrombocytopenia (616737) | *CDC42* | AD | No<br>Moderate + macro<br>No | Defective intellectual, growth and psychomotor development. Brain, facial, mucle, skeleta abnormalities. Immunodeficiency, eczema, hearing/visual disability, lymphedema and cardiac or | 55 |

| | | | | | |
|---|---|---|---|---|---|
| | | | | genitourinary malformations | |

## Glycosylation

| Disorder (OMIM) | Gene | Inheritance | Bleeding / Thrombocytopenia / Platelet dysfunction | Other manifestations | Ref |
|---|---|---|---|---|---|
| *GNE*-RD | *GNE* | AR | Mild to severe<br>Severe + macro<br>Increased reticulated platelets<br>Unknown | Myopathy with rimmed vacuoles since early adulthood | 56 |

**Granule biogenesis & trafficking**

| Disorder (OMIM) | Gene | Inheritance | Bleeding / Thrombocytopenia / Platelet dysfunction | Other manifestations | Ref |
|---|---|---|---|---|---|
| Hermansky-Pudlak Syndrome (HPS) (203300, 608233, 614072, 614073, 614074, 614075, 614076, 614077, 614071, 617050, 619172) | *HPS1, AP3B1, HPS3, HPS4, HPS5, HPS6, DTNBP1, BLOC1S3, BLOC1S6 AP3D1* | AR | Mild to moderate<br>No<br>Selective δ granule defect.<br>Reduced aggregation or absence of second wave with weak/low dose agonists | Oculocutaneous albinism, neutropenia, immunodeficiency, pulmonary fibrosis, granulomatorus colitis | 57,58 |
| Chediak-Higashi Syndrome (CHS) (214500) | *LYST* | AR | Mild to moderate<br>No<br>δ-granule defect.<br>Reduced aggregation or absence of second wave with weak/low dose agonists | Oculocutaneous albinism; Immunodeficiency with predisposition to recurrent infections. Hemophagocytic lymphohistiocytosis with an accelerated phase | 59 |
| *NBEA* - RD | *NBEA* | AD | Absent to mil<br>No<br>Decreased platelet ATP dense granule secretion. Increased serotonin plasma levels. | Autism | 60 |
| Gray platelet syndrome (GPS) (139090) | *NBEAL2* | AR | Moderate to severe<br>Moderate to severe<br>Absence of α granules Impaired platelet function with weak agonists. Selective defects of GPVI and activation by collagen | Elevated vitamin B12 serum level. Early myelofibrosis; occasional splenomegaly; predisposition to autoimmune diseases | 61,62 |
| Cholestasis 1 (208085) | *VPS33B VIPAS39* | AR | Mild<br>No<br>Reduced α granules | Arthrogryposis, renal dysfunction, and cholestasis. | 63 |
| Hemophagocytic lymphohistiocytosis (613101) | *STXBP2* | AR | Absent to mild<br>No<br>Absence of granules and reduced secretion | Hepatosplenomegaly, pancytopenia, Neurologic inflammation. | 64 |

## Coagulant activity

| Disorder (OMIM) | Gene | Inheritance | Bleeding / Thrombocytopenia / Platelet dysfunction | Other manifestations | Ref |
|---|---|---|---|---|---|
| Scott Syndrome (262890) | *ANO6* | AR | Moderate to severe<br>No<br>Abnormal clot formation and retraction | No | [65] |

**Supplemental Table 1. Clinical presentation of *Tier1* genes variants**. Adapted from:[66]

## Supplemental References


1. Ballmaier M, Germeshausen M. Congenital amegakaryocytic thrombocytopenia: Clinical presentation, diagnosis, and treatment. *Semin. Thromb. Hemost.* 2011;37(6):673–681.

2. Noris P, Marconi C, De Rocco D, et al. A new form of inherited thrombocytopenia due to monoallelic loss of function mutation in the thrombopoietin gene. *Br. J. Haematol.* 2018;181(5):698–701.

3. Cornish N, Aungraheeta MR, FitzGibbon L, et al. Monoallelic loss-of-function THPO variants cause heritable thrombocytopenia. *Blood Adv.* 2020;4(5):920–924.

4. Schlegelberger B, Heller PG. RUNX1 deficiency (familial platelet disorder with predisposition to myeloid leukemia, FPDMM). *Semin. Hematol .* 2017;54(2):75–80.

5. Hock H, Shimamura A. ETV6 in hematopoiesis and leukemia predisposition. *Semin. Hematol.* 2017;54(2):98–104.

6. Noris P, Perrotta S, Seri M, et al. Mutations in ANKRD26 are responsible for a frequent form of inherited thrombocytopenia: Analysis of 78 patients from 21 families. *Blood*. 2011;117(24):6673–6680.

7. Rabbolini DJ, Morel-Kopp MC, Ward CM, Stevenson WS. GFI1B variants associated with thrombocytopenia. *Platelets*. 2017;28(5):525–527.

8. Marneth AE, Van Heerde WL, Hebeda KM, et al. Platelet CD34 expression and

a/d-granule abnormalities in GFI1B- and RUNX1-related familial bleeding disorders. *Blood*. 2017;129(12):1733–1736.

9. Freson K, Wijgaerts A, Van Geet C. GATA1 gene variants associated with thrombocytopenia and anemia. *Platelets*. 2017;28(7):731–734.

10. Raslova H, Komura E, Le Couédic JP, et al. FLI1 monoallelic expression combined with its hemizygous loss underlies Paris-Trousseau/Jacobsen thrombopenia. *J. Clin. Invest.* 2004;114(1):77–84.

11. Stevenson WS, Rabbolini DJ, Beutler L, et al. Paris-Trousseau thrombocytopenia is phenocopied by the autosomal recessive inheritance of a DNA-binding domain mutation in FLI1. *Blood*. 2015;126(17):2027–2030.

12. Thompson AA, Woodruff K, Feig SA, Nguyen LT, Carolyn Schanen N. Congenital thrombocytopenia and radio-ulnar synostosis: A new familial syndrome. *Br. J. Haematol.* 2001;113(4):866–870.

13. Germeshausen M, Ancliff P, Estrada J, et al. MECOM-associated syndrome: A heterogeneous inherited bone marrow failure syndrome with amegakaryocytic thrombocytopenia. *Blood Adv.* 2018;2(6):586–596.

14. Albers CA, Paul DS, Schulze H, et al. Compound inheritance of a low-frequency regulatory SNP and a rare null mutation in exon-junction complex subunit RBM8A causes TAR syndrome. *Nat. Genet.* 2012;44(4):435–439.

15. Heremans J, Garcia-Perez JE, Turro E, et al. Abnormal differentiation of B cells and megakaryocytes in patients with Roifman syndrome. *J. Allergy Clin. Immunol.* 2018;142(2):630–646.

16. Lentaigne C, Greene D, Sivapalaratnam S, et al. Germline mutations in the transcription factor IKZF5 cause thrombocytopenia. *Blood*. 2019;134(23):2070–2081.

17. Savoia A, Kunishima S, De Rocco D, et al. Spectrum of the mutations in bernard-soulier syndrome. *Hum. Mutat.* 2014;35(9):1033–1045.

18. Boeckelmann D, Hengartner H, Greinacher A, et al. Patients with Bernard-Soulier syndrome and different severity of the bleeding phenotype. *Blood Cells, Mol. Dis.* 2017;67:69–74.

19. Sivapalaratnam S, Westbury SK, Stephens JC, et al. Rare variants in GP1BB are responsible for autosomal dominant macrothrombocytopenia. *Blood*.

2017;129(4):520– 524.

20. Othman M, Gresele P. Guidance on the diagnosis and management of platelet-type von Willebrand disease: A communication from the Platelet Physiology Subcommittee of the ISTH. *J. Thromb. Haemost.* 2020;18(8):1855–1858.

21. Perez-Botero J, Lee K, Branchford BR, et al. Glanzmann thrombasthenia: Genetic basis and clinical correlates. *Haematologica*. 2020;105(4):888–894.

22. Nurden AT, Pillois X. ITGA2B and ITGB3 gene mutations associated with Glanzmann thrombasthenia. *Platelets*. 2018;29(1):98–101.

23. Morais S, Oliveira J, Lau C, et al. αIIbβ3 variants in ten families with autosomal dominant macrothrombocytopenia: Expanding the mutational and clinical spectrum. *PLoS One*. 2020;15(12):e0235136.

24. Seidizadeh O, Peyvandi F, Mannucci PM. Von Willebrand disease type 2N: An update. *J. Thromb. Haemost.* 2021;19(4):909–916.

25. Jandrot-Perrus M, Hermans C, Mezzano D. Platelet glycoprotein VI genetic quantitative and qualitative defects. *Platelets*. 2019;30(6):708–713.

26. Scavone M, Femia EA, Cattaneo M. P2Y12 receptor gene mutations associated with bleeding. *Platelets*. 2017;28(4):421–423.

27. Mundell SJ, Mumford A. TBXA2R gene variants associated with bleeding. *Platelets*. 2018;29(7):739–742.

28. Turro E, Greene D, Wijgaerts A, et al. A dominant gain-of-function mutation in universal tyrosine kinase SRC causes thrombocytopenia, myelofibrosis, bleeding, and bone pathologies. *Sci. Transl. Med.* 2016;8(328):328ra330.

29. Takeichi T, Torrelo A, Lee JYW, et al. Biallelic Mutations in KDSR Disrupt Ceramide Synthesis and Result in a Spectrum of Keratinization Disorders Associated with Thrombocytopenia. *J. Invest. Dermatol.* 2017;137(11):2344–2353.

30. Hofmann I, Geer MJ, Vögtle T, et al. Congenital macrothrombocytopenia with focal myelofibrosis due to mutations in human G6b-B is rescued in humanized mice. *Blood*. 2018;132(13):1399–1412.

31. Bastida JM, Benito R, Janusz K, et al. Two novel variants of the ABCG5 gene cause xanthelasmas and macrothrombocytopenia: a brief review of hematologic abnormalities of sitosterolemia. *J. Thromb. Haemost.* 2017;15(9):1859–1866.

32. Bastida JM, Benito R, González-Porras JR, Rivera J. ABCG5 and ABCG8 gene variations associated with sitosterolemia and platelet dysfunction. *Platelets*. 2021;32(4):573–577.

33. Morison IM, Cramer Bordé EM, Cheesman EJ, et al. A mutation of human cytochrome c enhances the intrinsic apoptotic pathway but causes only thrombocytopenia. *Nat. Genet.* 2008;40(4):387–389.

34. Fletcher SJ, Johnson B, Lowe GC, et al. SLFN14 mutations underlie thrombocytopenia with excessive bleeding and platelet secretion defects. *J. Clin. Invest.* 2015;125(9):3600–3605.

35. Liang M, Soomro A, Tasneem S, et al. Enhancer-gene rewiring in the pathogenesis of Quebec platelet disorder. *Blood*. 2020;136(23):2679–2690.

36. Ticci C, Cassandrini D, Rubegni A, et al. Expanding the clinical and genetic spectrum of pathogenic variants in STIM1. *Muscle and Nerve*. 2021;64(5):567–575.

37. Markello T, Chen D, Kwan JY, et al. York platelet syndrome is a CRAC channelopathy due to gain-of-function mutations in STIM1. *Mol. Genet. Metab.* 2015;114(3):474–482.

38. Palma-Barqueros V, Bohdan N, Revilla N, et al. PTGS1 gene variations associated with bleeding and platelet dysfunction. *Platelets*. 2021;32(5):1–7.

39. Palma-Barqueros V, Crescente M, de la Morena ME, et al. A novel genetic variant in PTGS1 affects N-glycosylation of cyclooxygenase-1 causing a dominant-negative effect on platelet function and bleeding diathesis. *Am. J. Hematol.* 2021;96(3):E83–E88.

40. Rognoni E, Ruppert R, Fässler R. The kindlin family: Functions, signaling properties and implications for human disease. *J. Cell Sci.* 2016;129(1):17–27.

41. Cheepala SB, Pitre A, Fukuda Y, et al. The ABCC4 membrane transporter modulates platelet aggregation. *Blood*. 2015;126(20):2307–2319.

42. Lozano ML, Cook A, Bastida JM, et al. Novel mutations in RASGRP2, which encodes CalDAG-GEFI, abrogate Rap1 activation, causing platelet dysfunction. *Blood*. 2016;128(9):1282–1289.

43. Savoia A, Pecci A. MYH9-Related Disease. *GeneReviews*. 2008;1–24.

44. Natesirinilkul R, Sosothikul D, Komwilaisak P, et al. MYH9 disorder: Identification

and a novel mutation in patients with macrothrombocytopenia. *Pediatr. Blood Cancer*. 2021;68(7):e29055.

45. Thrasher AJ. New insights into the biology of Wiskott-Aldrich syndrome (WAS). *Hematology Am. Soc. Hematol. Educ. Program*. 2009;132–138.

46. Vassallo P, Westbury SK, Mumford AD. FLNA variants associated with disorders of platelet number or function. *Platelets*. 2020;31(8):1097–1100.

47. Stritt S, Nurden P, Turro E, et al. A gain-of-function variant in DIAPH1 causes dominant macrothrombocytopenia and hearing loss. *Blood*. 2016;127(23):2903–2914.

48. Kahr WHA, Pluthero FG, Elkadri A, et al. Loss of the Arp2/3 complex component ARPC1B causes platelet abnormalities and predisposes to inflammatory disease. *Nat. Commun.* 2017;8:14816.

49. Latham SL, Ehmke N, Reinke PYA, et al. Variants in exons 5 and 6 of ACTB cause syndromic thrombocytopenia. *Nat. Commun.* 2018;9(1):4250.

50. Kunishima S, Okuno Y, Yoshida K, et al. ACTN1 mutations cause congenital macrothrombocytopenia. *Am. J. Hum. Genet.* 2013;92(3):431–438.

51. Pleines I, Woods J, Chappaz S, et al. Mutations in tropomyosin 4 underlie a rare form of human macrothrombocytopenia. *J. Clin. Invest.* 2017;127(3):814–829.

52. Marín-Quílez A, Vuelta E, Díaz-Ajenjo L, et al. A novel nonsense variant in TPM4 caused dominant macrothrombocytopenia, mild bleeding tendency and disrupted cytoskeleton remodeling. *J Thromb Haemost*. 2022;20(5):1248–1255.

53. Palma-Barqueros V, Bury L, Kunissima S, et al. Expanding the genetic spectrum of TUBB1- related thrombocytopenia. *Blood Adv.* 2021;5(24):5453–5467.

54. Levin C, Koren A, Pretorius E, et al. Deleterious mutation in the FYB gene is associated with congenital autosomal recessive small-platelet thrombocytopenia. *J. Thromb. Haemost.* 2015;13(7):1285–1292.

55. Martinelli S, Krumbach OHF, Pantaleoni F, et al. Functional Dysregulation of CDC42 Causes Diverse Developmental Phenotypes. *Am. J. Hum. Genet.* 2018;102(2):309–320.

56. Izumi R, Niihori T, Suzuki N, et al. GNE myopathy associated with congenital thrombocytopenia: A report of two siblings. *Neuromuscul. Disord.* 2014;24(12):1068–1072.

57. Bastida JM, Morais S, Palma-Barqueros V, et al. Identification of novel variants in ten patients with Hermansky-Pudlak syndrome by high-throughput sequencing. *Ann. Med.* 2019;51(2):141–148.

58. Huizing M, Malicdan MCV, Wang JA, et al. Hermansky–Pudlak syndrome: Mutation update. *Hum. Mutat.* 2020;41(3):543–580.

59. Lozano ML, Rivera J, Sánchez-Guiu I, Vicente V. Towards the targeted management of Chediak-Higashi syndrome. *Orphanet J. Rare Dis.* 2014;9(1):132.

60. Bijl N, Thys C, Wittevrongel C, et al. Platelet studies in autism spectrum disorder patients and first-degree relatives. *Mol. Autism*. 2015;6(1):57.

61. Pluthero FG, Di Paola J, Carcao MD, Kahr WHA. NBEAL2 mutations and bleeding in patients with gray platelet syndrome. *Platelets*. 2018;29(6):632–635.

62. Tariq H, Perez Botero J, Higgins RA, Medina EA. Gray Platelet Syndrome Presenting with Pancytopenia, Splenomegaly, and Bone Marrow Fibrosis. *Am. J. Clin. Pathol.* 2021;156(2):253–258.

63. Ambrosio AL, Di Pietro SM. Mechanism of platelet a-granule biogenesis: Study of cargo transport and the VPS33B-VPS16B complex in a model system. *Blood Adv.* 2019;3(17):2617–2626.

64. Al Hawas R, Ren Q, Ye S, et al. Munc18b/STXBP2 is required for platelet secretion. *Blood*. 2012;120(12):2493–2500.

65. Millington-Burgess SL, Harper MT. Gene of the issue: ANO6 and Scott Syndrome. *Platelets*. 2020;31(7):964–967.

66. Palma-Barqueros V, Revilla N, Sánchez A, et al. Inherited platelet disorders: An updated overview. *Int. J. Mol. Sci.* 2021;22(9):1–31.